ADVANCED PLANETARY PROBE

FINAL TECHNICAL REPORT

TO THE JET PROPULSION LABORATORY

VOLUME 3

ALTERNATE SPACECRAFT AND MISSIONS

TRW SYSTEMS

Rpt 4112-6001

4547-6006-R0000

ADVANCED PLANETARY PROBE STUDY

FINAL TECHNICAL REPORT

27 July 1966

Prepared for the Jet Propulsion Laboratory
under Contract 951311

Volume 3

Alternate Spacecraft and Missions

This work was performed for the Jet Propulsion Laboratory, California Institute of Technology, sponsored by the National Aeronautics and Space Administration under Contract NAS7-100.

TRW SYSTEMS
1 Space Park
Redondo Beach, California

CONTENTS

CONTENTS (Continued)

CONTENTS (Continued)

CONTENTS (Continued)

ILLUSTRATIONS

ILLUSTRATIONS (Continued)

ILLUSTRATIONS (Continued)

ILLUSTRATIONS (Continued)

ILLUSTRATIONS (Continued)

ILLUSTRATIONS (Continued)

ILLUSTRATIONS (Continued)

TABLES

TABLES (Continued)

1. INTRODUCTION

This volume discusses a 3-axis stabilized, 50-pound science payload spacecraft which is to be compared directly with the spin-stabilized version of Volume 2. In addition, three alternate spacecraft configurations which carry 12-, 100-, and 250-pound science payloads are considered.

Because all of the material of Volumes 1 and 2 has concentrated on the year 1972 for the flyby mission, Section 4 of this volume discusses the implication for Jupiter flyby missions in the years 1973 to 1980. The effects of the changed requirements during these years upon the spacecraft design are analyzed.

Section 5 of this volume discusses flyby missions to the planets beyond Jupiter and Section 6 discusses orbiter missions about Jupiter. The possibilities and problems centering on capsule entry mission are briefly reviewed in Section 7. The volume concludes with a review of the cost effectiveness of all of these missions and a brief presentation of alternate spacecraft configurations.

2. THREE-AXIS STABILIZED 50-POUND PAYLOAD SPACECRAFT

The spacecraft system discussed in this section is, so far as possible, the same as the configuration discussed in Volume 2, except that it is controlled in three axes rather than spin stabilized. It shares with the spinner the following ground rules:

- A 50-pound science payload
- A highly directional, body-mounted, earth-pointing antenna
- The use of RTG power
- A given stable of boosters

In addition it has the same guidance and encounter geometry requirements. The analysis was done, as in the spin-stabilized version, for a 1972 launch.

The change to a 3-axis system for an otherwise comparable spacecraft appears to be a reasonably optimum approach and further, it allows a close comparison of most of the effectiveness criteria. The overall configuration of the spacecraft is the same since the 16-foot deployable antenna is used. The communication capability, the data handling subsystem, thermal control, power, etc., can all be compared directly and the advantages and disadvantages in such critical areas as accuracy and science scanning can be readily evaluated.

The addition of the weight for the control system itself and the weight associated with increased power requirements presses the capability of the minimum launch vehicle, the SLV3X/Centaur/TE364; however, the weight is well within the capability of the larger TE-364-4 motor and, therefore, an adequate comparison is possible.

To maximize allowable spacecraft weight, spin stabilization is used during the firing of the third stage solid propellant. This adds a despin requirement to the 3-axis controlled system. Thermal and radiation shielding requirements lead to the selection of three remotely-mounted RTG units, but, since the ratio of moments is not critical, the RTG's need not be deployable.

The basic conclusions of this study are that the 3-axis system for a Jupiter mission in 1972 is feasible and that it has both advantages and

disadvantages when compared with the spin-stabilized version. Perhaps the most important consideration is the matter of reliability, which is higher for the spin-stabilized version, 0.79 as compared with 0.70. However, such reliability estimates involve many assumptions and the difference may not be as large (or it may be larger).

The 3-axis version improves some of the planetary science experiments, in particular the TV, but it is not perhaps quite as effective as the spin-stabilized version for interplanetary experiments. A scan platform must be added, however, to realize this improvement.

Although difficult to evaluate numerically, an important difference lies in passive versus active attitude hold during DSIF off periods. Nothing except a catastrophic meteoroid impact could cause the spinner to appreciably change its attitude, while the 3-axis version is subject to electronic failures and possible loss of Canopus lock due to debris from the spacecraft in its field of view. Automatic reacquisition is of course possible but only at the expense of more complication.

2.1 FUNCTIONAL REQUIREMENTS

The functional requirements for the 3-axis 50-pound payload spacecraft are the same as those for the spin-stabilized configuration. These requirements are given in Volume 1. The same science payload and requirements have also been retained.

There are three basic spacecraft constraints in this study; 1) use of RTG power, 2) a large body-fixed antenna dish, and 3) earth-pointing antenna. The implication of 3-axis control upon these three constraints are not as severe as they are for a spin-stabilized configuration.

The RTG's need not be mounted so the spacecraft has disc-like moments of inertia. The effect of 3-axis control upon a large body-fixed antenna is not critical since the size of the antenna tends to make a gimballed approach unattractive. The essential effect is to require that either multiple electronically offsettable or gimballed reference sensors be used. The third requirement of earth pointing is irrelevant to the 3-axis system once a body-mounted antenna has been selected because in any event the antenna must point toward the earth.

Additional requirements on the 3-axis system arise from the science payload. The TV system must be mounted on a scan platform and retain the tippable mirror for the second degree of freedom. The auroral detector and the infrared radiometer must have a scan mode of at least 1 degree of freedom. In addition, the plasma probe and possibly the solar cosmic ray counter will require either a scan mode or multiple sensors to observe a fairly large region of the sky in the direction of the sun.

2.2 SPACECRAFT SYSTEM CONCEPT

The major questions to be answered in generating a concept for a 3-axis controlled spacecraft comparable with the spin-stabilized concept are: 1) what external references are to be used and what is the design concept of the appropriate sensors for an earth-pointed, 3-axis stabilized spacecraft? 2) Are one or more experiment scan platforms required or can the spacecraft be rolled to provide scan? 3) What is the weight increase associated with the shift to 3-axis stabilization and what are the launch vehicle implications?

2.2.1 Error Sensors to Maintain the Earth-Pointing Attitude

Three types of sensors for earth pointing have been considered: optical earth tracker, RF earth tracker, and sun/Canopus trackers suitably gimballed so that the spacecraft antenna points to the earth.

An optical earth tracker, which was found to be suitable in the TRW Phase 1A, Task A, Voyager study for a possible earth-pointing spacecraft concept was rejected in this application because the earth passes between the spacecraft and the sun during a flight to Jupiter.

RF earth trackers were rejected primarily because it is anticipated there will be periods of the order of a week during which there will be no DSIF contact. During such a period, gyro drift would definitely cause loss of angle lock. Of course, a sun/Canopus orientation could be maintained between DSIF contacts, but this would mean a reacquisition sequence before every contact. Further, RF tracking is quite complicated on a nonspinner, involving monopulse reception and multiple RF channels. Boresight inaccuracy problems are also significant, particularly with the narrow downlink beamwidth considered here.

This leaves offsettable sun/Canopus trackers. Again there is a critical accuracy problem; however, for these trackers the problem is one of angular resolution (granularity) rather than a bias error control problem. Based on ground received signal level, sensor offsets can be commanded which lead to the maximum received power. Therefore, in effect, bias errors can be completely removed. Such a technique has been extremely successful with Pioneer 6, allowing positioning of the spacecraft spin axis within 1/50th of a beamwidth from the position of maximum gain. Of course, in this application, with changing earth-spacecraft-sun angles, such an end-to-end calibration will be required several times.

A significant question is whether to roll the spacecraft to provide a scanning motion for the science payload during encounter or whether to mount the applicable portion of the science payload on a scan platform. This is really a question of whether to gimbal a scan platform or to add an additional degree of freedom (gimbal) to the sun and Canopus sensors. It also involves scan rate requirements and attitude control gas consumption. The disadvantage of a scan platform is that it involves the mechanical rotation of a large package involving many electrical leads. A scan platform has, however, been successfully used on Mariner. A scan platform does allow more rapid and controllable scanning than does rolling the spacecraft. The disadvantage of an additional gimbal each for the sun and Canopus sensors is a mechanical drive albeit of a smaller package. Another disadvantage is that the sensor error is no longer in the spacecraft gas jet coordinate system, leading at best to serious crosstalk terms and at worst to the requirement for a coordinate transformation of the error signals into spacecraft coordinates. Rotating the spacecraft about a nonprincipal axis is also difficult and may not give the desired response rates.

On the basis of these factors, and relying on the JPL Mariner decision to use a scan platform in a simpler sun pointing case where only the Canopus sensor would have to be gimballed and no crosstalk terms are present, the decision was made to use a scan platform.

Figure 1 shows cone angle versus clock angle* of the sun relative to earth-Canopus body axes for trajectory F of the earth-Jupiter 1972 opportunity. Figure 2 gives the correlated variation of the cone angle of Canopus as a function of time after launch. These figures suggest that a body-fixed, Mariner-type Canopus sensor combined with a sun sensor which has a small pitch and a large yaw offset capability is appropriate. To keep the body (and antenna) axis pointed at the earth through earth-spacecraft oppositions and conjunctions, a sun sensor with no pitch offset capability would require a Canopus sensor with a rotation capability of more than ± 90 degrees about the roll axis; however, giving the sun sensor a pitch offset of only about ± 5 degrees permits the Canopus sensor to be ungimballed in roll. (The pitch requirement of the Canopus sensor, indicated by Figure 2, is that its field of view encompass the range of cone angles of Canopus, or 12 degrees.)

The possible sun sensor concepts involve a single two-axis sensor, mechanically double gimballed, mechanically yaw gimballed with electronic pitch offset, or discrete-position mechanically yaw gimballed with electronic fine offset control for pitch and yaw. Another possibility involves separate single-axis pitch and yaw sensors. An electronic offset pitch sensor with a wide transverse field, ± 5 degrees, could be combined with a narrow transverse field yaw sensor which is either mechanically single gimballed, discrete-position mechanically gimballed with electronic fine yaw offset control, or a multiple set of overlapping electronically offset yaw sensors.

Overall pointing accuracy requirements are about ± 0.5 degree, to be spread between limit cycle motion and sensor instability and granularity, presuming bias errors are removed periodically by ground monitoring of signal strength versus sensor offset as discussed earlier. A reasonable sensor accuracy goal, in the above sense, appears to be ± 0.25 degree. This accuracy is required only for yaw offsets less than 27 degrees since

*The definition of these angles is analogous to their definition in the case of a sun-oriented spacecraft. Relative to earth-Canopus spacecraft axes, the cone angle of an object is the earth-spacecraft object angle, and the clock angle is measured from the earth-spacecraft-Canopus plane to the earth-spacecraft-object plane.

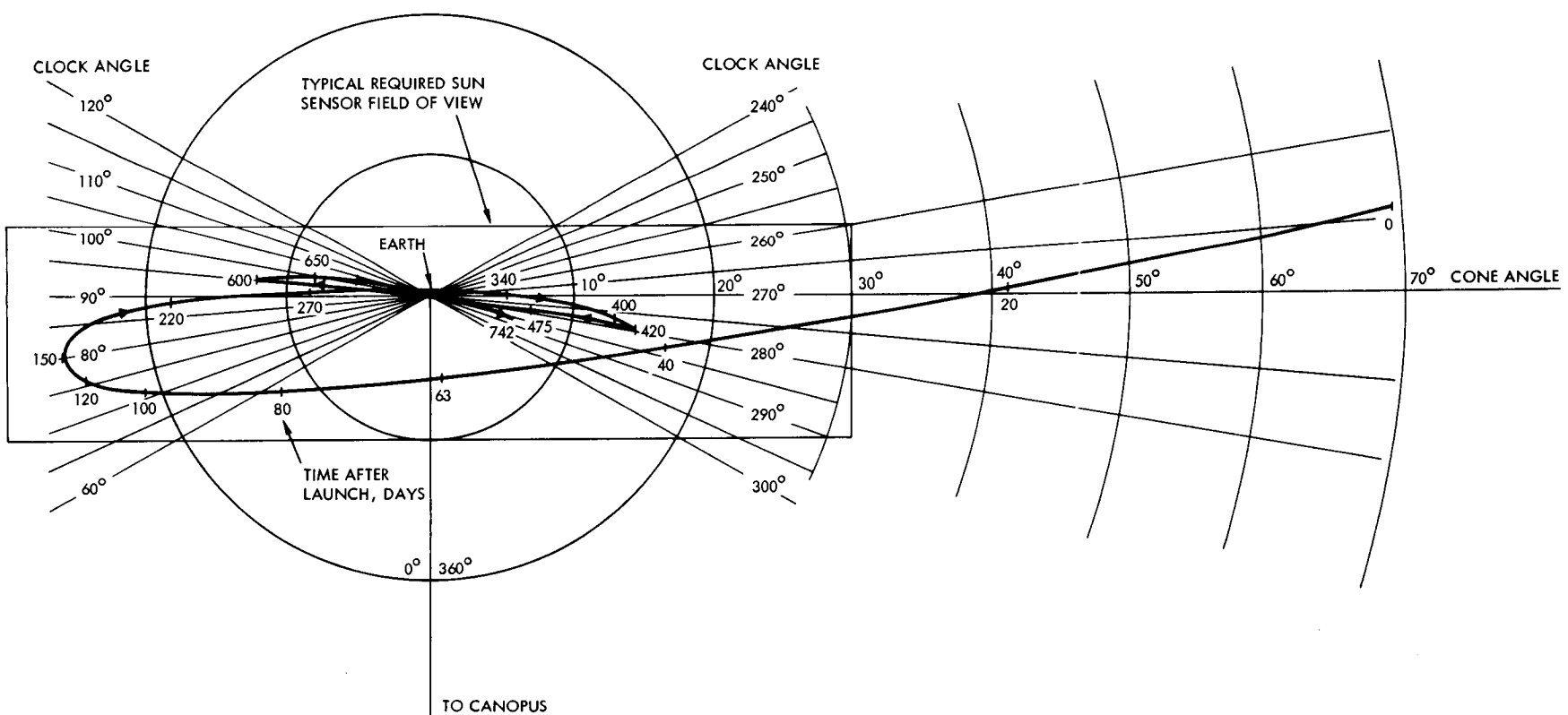

Figure 1. Cone Angle Versus Clock Angle of the Sun Relating to Earth-Canopus Axes, Trajectory F (1972 Earth-Jupiter)

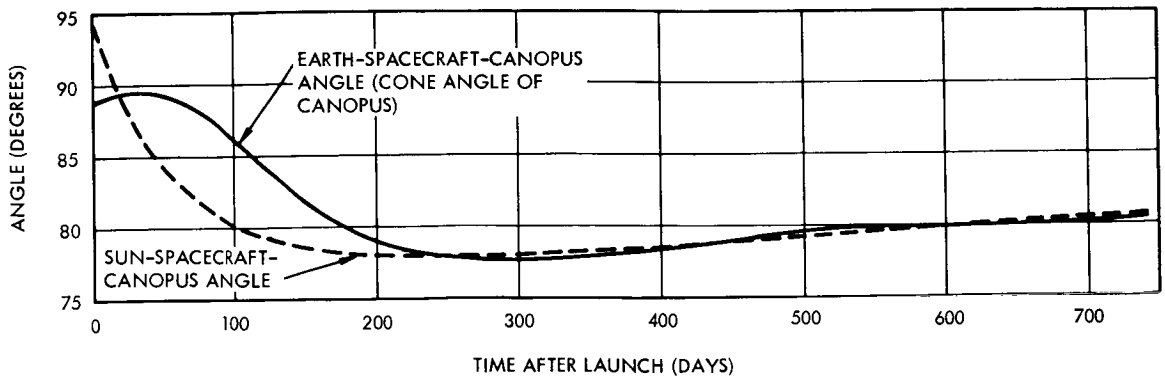

Figure 2. Cone Angle of Canopus (Earth-Spacecraft-Canopus Angle) Versus Time After Launch. 1972 Earth-Jupiter Trajectory F

prior to that time downlink communications can be by the 25-degree beamwidth medium-gain antenna or by the omni-antenna.

Considering the omni-antenna downlink capability, it follows that the spacecraft need not point at the earth during the early part of the flight. Thus, rather than point at the earth during this time, it is only necessary to point away from the sun towards the earth within about 30 degrees. For this case, the omni-antenna would allow a bit rate of well over 256 bits/sec at 20 days (spacecraft axis 12 degrees from the earth) at which time the helix antenna can be used to provide 700 bits/sec or more until the earth can be accurately tracked.

This solution conveniently circumvents large yaw offsets which would involve significant crosstalk in the pitch channel from roll errors. Further, it means that an electronically offset sun sensor may be a real possibility since the controllable offset field-of-view need be no larger than the rectangle shown in Figure 1. Two or three overlapping yaw sun sensors and a single pitch electronically offsettable sun sensor appear to provide adequate accuracy.

Typically, the output of such sensors is proportional to the solar brightness, but it is desirable, for a Jupiter mission where the brightness changes by a factor of 25, that this dependence be removed. Further, at Jupiter ranges, amplification of the sensor output is necessary. Both of these factors can be accommodated by controlling the gain of an amplifier

which amplifies the two frequency chopped outputs of a standard solar cell and the sun sensor such that the amplified and filtered output of the standard solar cell controls the amplifier gains. The mechanization of such a system is essentially the same as an AGC loop wherein the amplified carrier voltage is kept constant and then the information-carrying side bands are processed.

Such a system is described in Section 2.5. While it is clear that there are many possibilities for sensor selection and it is not clear that the system described is optimum for weight, power, or reliability, it is apparent that offset sun tracking obtained by biasing such sun sensors offers a reasonable solution when it is possible to remove bias errors by a ground controlled end-to-end calibration.

In addition to these offsettable tracking sun sensors, Mariner-type omni-coverage acquisition sun sensors would of course be required. It is even probable that reacquisition is possible without the aid of gyros. Such derived rate damping systems have been studied by JPL in detail and were incorporated as a backup in Mariner. They also have been discussed in detail in the TRW Phase B, Task A, Voyager study.

2.2.2 Midcourse Guidance

The program for midcourse guidance technique will be the same as for the spin-stabilized configuration except that a Mariner type of attitude control will be used during the maneuver. Gyros will control the cold gas system to point the spacecraft in the correct attitude for the midcourse correction. During thrusting, gyro controlled jet vanes will control pitch and yaw and cold gas will control roll. There will be one engine rather than two as in the spinner since the pointing maneuver under gyro control is more accurate than the open-loop procession mode used for the spinner. The engine will be mounted as on the spinner at the end of the antenna tripod. This selection provides a long moment arm, making jet vanes a very effective technique. Accelerometer cutoff has not been provided since the previous analysis of a timed firing of a blowdown system indicates it has adequate accuracy and results in a simpler system.

This system, because of the gyros and additional power, is somewhat heavier than the spin-stabilized control system. In addition, the

gyros must be capable of operating during the solar occultation by Jupiter. This long life requirement imposes a considerable reliability penalty using existing gyros. It is, however, probable that long life gyros will be available in the near future. Since an earth occultation is highly desirable it appears unlikely that a solar occultation can be avoided.

2.2.3 Science Sensors

The basic coverage of the science sensors described in Section 4.12 in Volume 2 is retained. For an attitude stabilized vehicle, this leads to the following location changes:

1) Solar Cosmic Ray Sensor. The removal of dynamic balance considerations allows the solar cosmic ray sensor to be removed from a boom and to be placed in forward equipment compartment.

2) TV and Infrared Radiometer. Three-axis stabilization involves the addition of a single-gimballed scan platform, similar to that used on Mariner, to provide comparable coverage to that obtained with the spinner. As before, the TV has an additional degree of freedom through the use of a tippable mirror, allowing Jupiter observations during approach and flyby. The removal of spin allows an increase in TV exposure time, which can be translated into improved resolution with a longer focal length system. The infrared radiometer experiment still looks sideways, giving multiple scans of Jupiter as the spacecraft flies by.

3) Aurora Sensors. An additional single gimbal platform is required on the forward side of the equipment compartment for the aurora sensors to give equivalent scan coverage to that obtained on the spinner.

4) Plasma Probe. Additional sensing apertures are required to obtain angular coverage equivalent to that which can be obtained from an arc of sensing apertures on the spinner.

2.2.4 Weight Implications

The weight of the 3-axis stabilized spacecraft is increased over the spinner largely as the result of the addition of the following components:

- Gyro package, Canopus tracker, increased electronics and associated increased weight for power
- Planetary scan platform, associated meteoroid protection and weight for power for drive

- Proportionate increase in propulsion and contingency weights

The net weight increase over the spinner totals about 70 pounds. A detailed weight breakdown is given in Section 2.5.

2.2.5 Thermal Control

Because of the similarity between the three-axis stabilized and spin-stabilized configuration, the same technique of thermal control has been chosen. This involves an insulated equipment compartment and the use of fiberglass for members which penetrate the insulation. Thermal switches are used to conduct excess heat to a radiating plate.

The slightly higher power level and the use of fixed RTG units which radiate some heat to the spacecraft allow an even higher margin for heat leaks on this spacecraft.

One problem which is unique to this version is asymmetric heating and resultant distortion of the antenna because the effect of oblique illumination by the sun is not averaged out through spin. Near Jupiter, where gain is critical, this effect is minimal because the illumination is at most only about 11 degrees from the spacecraft axis. For this angle, the temperature difference from one edge of the dish to the other is about 12 degrees. It has been estimated that the distortion from this temperature gradient is two orders of magnitude below the level of significance. Asymmetric heating of the feed tripod support results in a motion of the feed just slightly below the level of significance. However, the bias error introduced can be compensated for by the technique of ground command of the sun sensor tracking offset as discussed in Section 2.5.

2.2.6 RTG Location and Interactions

The two attractive solutions to the location of the RTG are:

- Far from the equipment and, particularly, the sensitive science sensors to reduce shielding weight requirements
- Close to the thermal mounting plate so that thermal energy from the RTG's provides additional heat, reducing the required control of heat leaks.

As discussed in Sections 4.9, 4.11, 8.2, and 8.8 of Volume 2, an adequate, light-weight solution to the problem of heat leaks from the

spacecraft is to use fiberglass for main structural members which penetrate the compartment insulation blanket, combined with thermal switches which have a large difference between closed and open thermal conductivities. The switches provide adequate heat rejection while solar heating is important, but establish an adequate thermal barrier when the spacecraft is far from the sun.

The result was the decision, as for the spinner, to favor physical separation of the RTG units because of the significant saving in weight otherwise needed for radiation shielding. In this case, however, deployment of the RTG's is not necessary to achieve a desired inertia ratio. The selected solution, then, utilizes fixed RTG units mounted on arms which place the units in a position corresponding to partial deployment for the spin-stabilized case. This position allows staging of the TE-364 without interference with the RTG units. Only about two pounds of radiation shielding is required.

Since spin is the simplest and lightest way of stabilizing during the TE-364 burn, this feature is retained. After firing, however, the spacecraft is completely despun and sun and Canopus acquisition is initiated. Three RTG units are again required for spin symmetry.

2.2.7 Configuration Design Considerations

The system design considerations not discussed elsewhere in Section 2.2 are presented here in the form of guidelines which have been employed in the development of the 3-axis stabilized spacecraft selected to carry a 50-pound science payload on the Jupiter flyby mission. These objectives and requirements are satisfied by the spacecraft configuration.

The several subsystem guidelines listed earlier in Section 4.13.1 of Volume 2, which apply to a spin stabilized spacecraft, apply to the 3-axis stabilized spacecraft except as noted below.

Propulsion System Guidelines

- Use jet vanes for thrust vector control
- Locate engine so as to provide thrust vector control at a maximum distance from the spacecraft c.g.

Attitude Control System Guidelines

- Nozzles for precession and the conical scan system are not required
- Provide pairs of pitch, yaw, and roll nozzles located as far as possible from the spacecraft c.g. to minimize gas requirements.
- Control axes are to coincide with or are to be close to the mass moment of inertia principal axes.
- Minimize control axes shift from the mass moment of inertia principal axes.

2.3 PROBLEM AREAS

The 3-axis 50-pound payload spacecraft has in common with the spin stabilized version the following problems: RTG's, Pu 238 development, large deployable antenna development, and thermal control problems. But as is maintained in Section 3.4, Volume 2, these are not feasibility questions so much as detailed engineering problems. The 3-axis system, like the spin-stabilized version, has an attitude reference problem since sun pointing, while more familiar than an earth pointing RF technique, has not yet been used over so large a distance nor with accurately offset-table sun sensors. This represents a standard engineering development and does not raise questions of feasibility.

Like the spin-stabilized version, the 3-axis system has a long life reliability problem which is accentuated by the requirement that the gyros operate during the sun-earth occultation period at Jupiter encounter. Tests at JPL show that gyros can have a long life capability; nevertheless, available historical reliability estimates for gyros over such a long life are low. On the other hand, the gyros required during this period are for the success only of the earth occultation and the auroral detector experiment since the spacecraft can reacquire the sun and Canopus without the use of the gyro assembly. Therefore, in the event of gyro failure the only data that would be lost would be from these two experiments, and the rest of the science could be transmitted back after a reacquisition.

Another problem area relates to the overall weight of the 3-axis spacecraft in view of booster capability. As pointed out in Section 7.7 of

Volume 2, the Atlas SLV 3C/Centaur/TE-364-3, based on Convair and Boeing data, has the capability to launch about 590 pounds to Jupiter. Making allowances for special launch window characteristics and the use of the Atlas SLV 3X increase this to over 600 pounds. A suitable margin over and above spacecraft weight should be at least 25 pounds. The estimated weight for the 3-axis system with a 45-pound contingency is 564. This margin then seems adequate. Moreover, there is always the alternate of using the TE-364-4 motor, which would provide another 50 pounds of capability.

2.4 COMPARISON WITH MARINER MARS

The 3-axis stabilized spacecraft has more in common with Mariner than has the spinner. The attitude control system is directly derived from Mariner and could include the use of the same gyro package, Canopus sensor and broad acquisition sun sensors, and similar electronics and pneumatics, provided that advances in the state of the art in these areas, as for example are being developed for Mariner 1969, would not dictate the use of improved components. In this regard, the Autonetics G-6 gyro, a miniaturized version of the Minuteman G-10 gyro, is touted as being ultra-reliable. Claims of 10^6 hours mean time between failure have been made which, if true, would remove the gyro reliability problem. The use of accurate, electronically offsettable sun sensors over a large range of solar distances is new and represents a significant development problem as does the requirement for decreased limit cycle amplitude and improved pointing accuracy.

Monopropellant midcourse propulsion using jet vanes for attitude control is comparable to that of Mariner, although a simpler blowdown system is proposed.

This 3-axis system also has in common with Mariner Mars the use of a planetary scan platform for the TV and infrared radiometer experiments. This scan platform is based upon the Mariner 4 configuration although the TV has a tippable mirror to supply one more degree of freedom. The requirement for a scanning auroral detector is new. Of course, the basic configuration is different from Mariner as is the power supply, thermal control, and structure.

While fundamentally different from Pioneer 6, the 3-axis configuration has similar subsystem elements. The communication subsystem is perhaps more closely related to Pioneer than to Mariner Mars as is the data handling subsystem except for the tape recorder. The command distribution system is related to Pioneer but the sequencing functions are more closely related to Mariner Mars.

2.5 SPACECRAFT SYSTEM

This section describes the 3-axis stabilized, 50-pound size payload spacecraft, principally by pointing out the differences between it and the spin-stabilized spacecraft of Volume 2. The basic configuration described in this section is in fact the same as that of the spin-stabilized version.

2.5.1 Configuration

Overall configuration is shown in Figure 3. The spacecraft is housed within a "B" fairing with a 16-inch extension. The interstage and adaptor assembly structures are the same as those on the spin-stabilized version, but no RTG tie-downs are required since the RGS's are body-fixed. They are supported by tubular struts attached to fixed hard points on the high-gain antenna hinge ring and the corner fittings of the main compartment. The high-gain antenna is identical with that on the spin-stabilized version. Since the spacecraft has 3-axis control, no wobble dampers are needed. The three solid-propellant spin rockets are mounted to the RTG support structure in the same way as for the spin-stabilized version. A single deployable boom separates the magnetometer from the spacecraft and is deployed after initial acquisition. The solar cosmic ray sensor, mounted on the deployed boom on the spin stabilized version, is located in the antenna feed assembly in this version. The 12 attitude control jets are mounted on the periphery of the fixed portion on the high-gain antenna. The equipment compartment is the same as on the spin stabilized version but the equipment mounting details are different as shown in Figure 3. Since only one midcourse engine is used, and it is mounted on the antenna feed assembly, there is no aft-pointing engine in the equipment compartment. A single gimballed scan platform is mounted at the base of the compartment for the television and infrared radiometer experiments. The TV camera retains its tippable mirror, giving the TV two degrees of

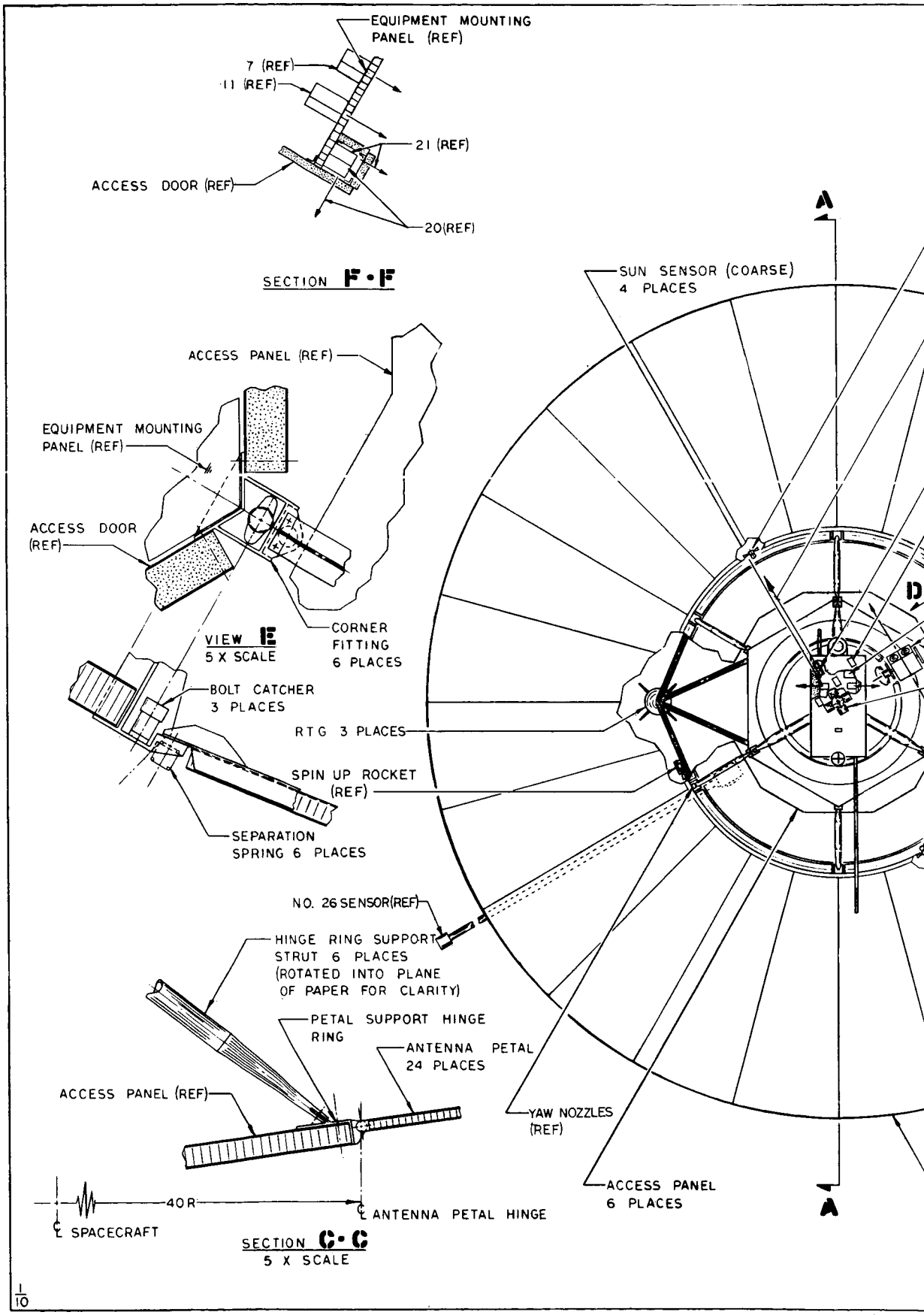
EQUIPMENT MOUNTING PANEL (REF)
7 (REF)
11 (REF)
21 (REF)
ACCESS DOOR (REF)
20(REF)
SECTION F • F
SUN SENSOR (COARSE) 4 PLACES
ACCESS PANEL (REF)
EQUIPMENT MOUNTING PANEL (REF)
ACCESS DOOR (REF)
CORNER FITTING 6 PLACES
VIEW E 5 X SCALE
BOLT CATCHER 3 PLACES
RTG 3 PLACES
SPIN UP ROCKET (REF)
SEPARATION SPRING 6 PLACES
NO. 26 SENSOR(REF)
HINGE RING SUPPORT STRUT 6 PLACES (ROTATED INTO PLANE OF PAPER FOR CLARITY)
PETAL SUPPORT HINGE RING
ANTENNA PETAL 24 PLACES
ACCESS PANEL (REF)
YAW NOZZLES (REF)
ACCESS PANEL 6 PLACES
40R
℄ SPACECRAFT
℄ ANTENNA PETAL HINGE
SECTION C • C 5 X SCALE
A
A
D

1/10

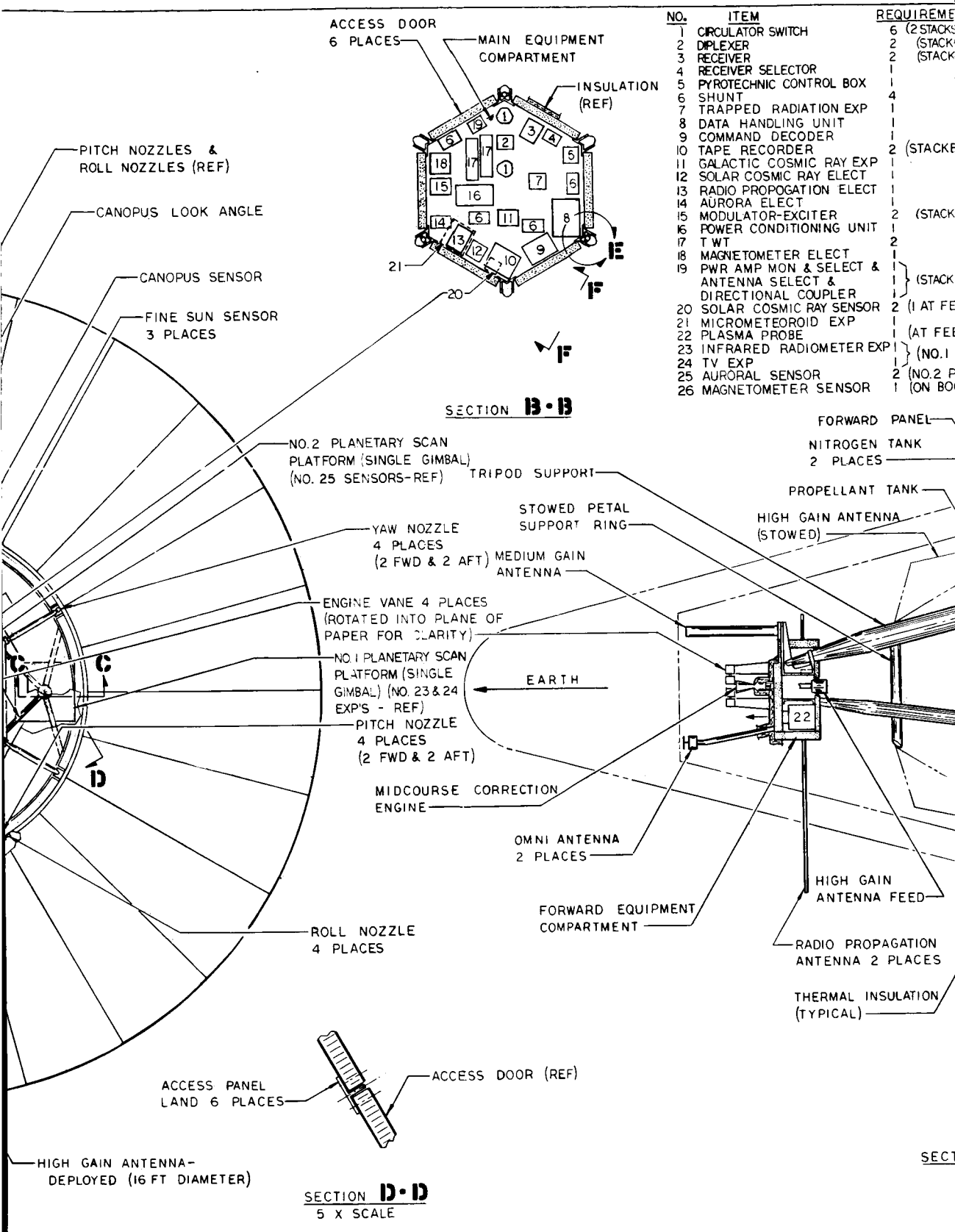
ACCESS DOOR
6 PLACES
MAIN EQUIPMENT
COMPARTMENT
INSULATION
(REF)
PITCH NOZZLES &
ROLL NOZZLES (REF)
CANOPUS LOOK ANGLE
CANOPUS SENSOR
FINE SUN SENSOR
3 PLACES
21
20
E
F
F
SECTION B-B
NO. ITEM REQUIREME
1 CIRCULATOR SWITCH 6 (2 STACKS
2 DIPLEXER 2 (STACK
3 RECEIVER 2 (STACK
4 RECEIVER SELECTOR 1
5 PYROTECHNIC CONTROL BOX 1
6 SHUNT 4
7 TRAPPED RADIATION EXP 1
8 DATA HANDLING UNIT 1
9 COMMAND DECODER 1
10 TAPE RECORDER 2 (STACKE
11 GALACTIC COSMIC RAY EXP 1
12 SOLAR COSMIC RAY ELECT 1
13 RADIO PROPOGATION ELECT 1
14 AURORA ELECT 1
15 MODULATOR-EXCITER 2 (STACK
16 POWER CONDITIONING UNIT 1
17 T WT 2
18 MAGNETOMETER ELECT 1
19 PWR AMP MON & SELECT & 1
ANTENNA SELECT & 1 (STACK
DIRECTIONAL COUPLER 1
20 SOLAR COSMIC RAY SENSOR 2 (1 AT FE
21 MICROMETEOROID EXP 1
22 PLASMA PROBE 1 (AT FE
23 INFRARED RADIOMETER EXP 1 (NO. 1
24 TV EXP 1
25 AURORAL SENSOR 2 (NO. 2 P
26 MAGNETOMETER SENSOR 1 (ON BO
FORWARD PANEL
NITROGEN TANK
2 PLACES
NO. 2 PLANETARY SCAN
PLATFORM (SINGLE GIMBAL)
(NO. 25 SENSORS-REF)
TRIPOD SUPPORT
PROPELLANT TANK
STOWED PETAL
SUPPORT RING
HIGH GAIN ANTENNA
(STOWED)
YAW NOZZLE
4 PLACES
(2 FWD & 2 AFT)
MEDIUM GAIN
ANTENNA
ENGINE VANE 4 PLACES
(ROTATED INTO PLANE OF
PAPER FOR CLARITY)
NO. 1 PLANETARY SCAN
PLATFORM (SINGLE
GIMBAL) (NO. 23 & 24
EXP'S - REF)
EARTH
PITCH NOZZLE
4 PLACES
(2 FWD & 2 AFT)
C
C
D
H
22
MIDCOURSE CORRECTION
ENGINE
OMNI ANTENNA
2 PLACES
HIGH GAIN
ANTENNA FEED
FORWARD EQUIPMENT
COMPARTMENT
RADIO PROPAGATION
ANTENNA 2 PLACES
THERMAL INSULATION
(TYPICAL)
ROLL NOZZLE
4 PLACES
ACCESS PANEL
LAND 6 PLACES
ACCESS DOOR (REF)
HIGH GAIN ANTENNA-
DEPLOYED (16 FT DIAMETER)
SECTION D-D
5 X SCALE
SECT

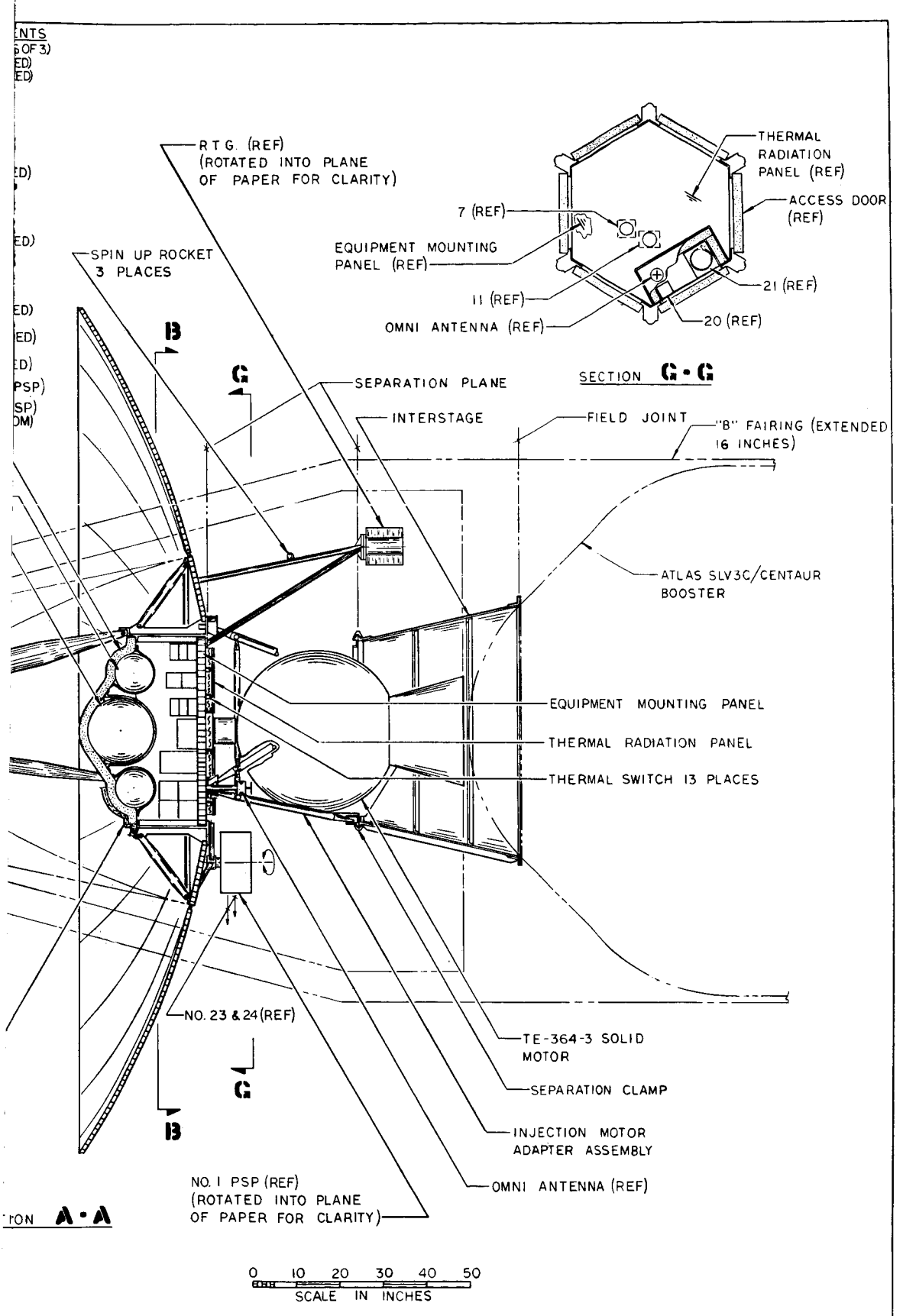

Figure 3. Jupiter Flyby, 50-Pound Science Payload, Three-Axis Stabilized In-Board Profile

freedom and allowing any part of Jupiter to be observed during approach and flyby. A single gimballed scan platform is located in the forward end of the compartment for the aurora sensors. As with the spin stabilized version, the antenna feed assembly houses the midcourse engine but jet vanes for thrust vector control have been added. It also houses the solar plasma probe and the solar cosmic ray sensors, a Canopus sensor has been added. Since no RF signals are required for earth tracking, the high-gain antenna feed is not articulated and the medium-gain (helix) antenna is aimed along the spin axis.

Table 1 gives the power requirements for the 3-axis stabilized 50-pound science payload spacecraft. The maximum load is 113.9 watts at encounter as compared with 99 watts for the spin-stabilized version. The increase results from the added control system requirements (see Section 7.1, Volume 2).

Table 2 presents detailed weight estimates. Gross weight is 564 pounds including 44.5 pounds of contingency. Most of the weights are identical to those given for the spin-stabilized version. The differences between the two versions are described here.

Structure and thermal control are essentially the same as for the spin-stabilized version but there is a small increase in thermal insulation and meteorite protection for the planet scan platform. The attitude control subsystem is considerably heavier since the gyro reference system and Canopus tracker have been added. The weight of the gyro package is based upon the Mariner 4 gyros, but if the gas-bearing gyro is used this weight will be at least 5 pounds less. As with the gyros, the weights of the other attitude control components are based on Mariner 4. The nitrogen gas supply is completely redundant, and three times the required gas is carried. The propulsion subsystem is reduced in weight since one engine and associated plumbing have been eliminated. A planet scan platform of 7 pounds has been added for the television and radiometer experiments. The weight is based on the Mariner 4 platform.

Centroidal moments of inertia and center-of-gravity estimates for the spacecraft are listed in Table 3, beginning at separation from the

Table 1. Power Requirements for the 3-Axis Stabilized Spacecraft, in Watts

Subsystem	Element	Mode	Input Power	Conversion Efficiency (%)	Midcourse Maneuver: Sun Sensor Turn-On	Midcourse Maneuver: Canopus Sensor Turn-On	Midcourse Maneuver: Propulsion	Midcourse Maneuver: Acquisition	Cruise Inter-Planetary	Cruise Early Encounter	Light Side Encounter	Dark Side Encounter
ACS	Electronics	Thrust	12	69			17.4					
		Other	5.0	69	7.2	7.2		7.2	7.2	7.2	7.2	7.2
	Valves	Acquisition	14	99				14.1				
		Other	14									
	Sun Sensor	Peak	5.0	69	7.2							
		Average	1.0	69		1.5	1.5	1.5	1.5	1.5	1.5	1.5
	Canopus Sensor	Peak	5.0	69		7.2						
		Average	1.8	69			2.6	2.6	2.6	2.6	2.6	2.6
	Gyros	Heater	5.5	99	5.5	5.5	5.5	5.5		14*		5.5
		Motor	12.0	91	14.3	14.3	14.3	14.3			14.3**	14.3**
	Thrust Control	Peak	5.0	84			6.0					
		Average	1.0	84								
	Accelerometer	All	2.0	69	2.4	2.4	2.4					
Thermal Control	Heaters	All	11.0		11.1	11.1		11.1	11.1	11.1	11.1	11.1
Science	All	Cruise	9.1	73					12.4			
		Light Side	19.5	73						26.7	26.7	
		Dark Side	10.1	73								13.9
Communications	TWTA	All	26.7	87	30.7	30.7	30.7	30.7	30.7	30.7	30.7	30.7
	Ancillary	All	4.6	69	6.7	6.7	6.7	6.7	6.7	6.7	6.7	6.7
Command Dist.	All	All	4.0	69	5.8	5.8	5.8	5.8	5.8	5.8	5.8	5.8
Data Handling	All	All	5.0	69	7.3	7.3	7.3	7.3	7.3	7.3	7.3	7.3
Totals					98.2	98.7	100.2	106.8	83.3	113.6	113.9	106.6

*Auxiliary warmup heater

**Note gyro heater power requirements may be lower

Table 2. Weight Estimate: 3-Axis Stabilized Spacecraft for the Basic Mission

		Weight (lb)
Structure and Thermal Control		90.0
Equipment platform (1)		9.7
Side panels (6)		3.0
Top cover (1)		2.2
Frames and longerons		9.7
Tank supports		1.8
Forward compartment		4.5
Experiment boom installation (2)		3.2
Planetary scan platform		7.0
Miscellaneous attachments		3.8
Meteoroid protection		33.1
Radiation protection		2.0
Thermal control		10.0
Thermal switches (13)	3.3	
Radiative panel	0.9	
Paint	2.2	
Insulation	3.6	
Power Supply		97.5
RTG installation		86.2
RTG units (3)	77.0	
Fixed boom installation (3)	9.2	
Power control unit		8.3
Shunt elements (4)		3.0
Integration		33.5
Command distribution unit (1)		7.0
Umbilical (1)		2.0
Pyrotechnic control box (1)		5.5
Cabling and connectors		19.0
Data Handling		35.4
Data handling unit (1)		11.0
Tape recorder (2)		15.9
Integrated decoder and sequencer (1)		8.5
Communications (2)		89.7
Receiver (2)		6.6
Modulator/exciter (2)		3.0
TWT (2)		2.0
Circulator switch (6)		1.8
Diplexer (2)		2.0
Antenna selector (1)		0.5
Receiver selector (1)		0.5
Power amplifier monitor and selector (1)		1.0
Directional coupler (1)		0.5
Omni-antenna installation (2)		1.5
Helical antenna installation (1)		2.8

Table 2. Weight Estimate: 3-Axis Stabilized Spacecraft for the Basic Mission (Continued)

		Weight (lb)
High-gain antenna installation (1)		67.5
Parabolic dish	49.2	
Tripod, including support ring and release mechanism	15.8	
Antenna feed including harness	2.5	
Attitude Control		82.8
Orientation system		73.1
Gyro reference assembly (1)	10.0	
Guidance and control electronics (1)	6.0	
Canopus tracker (1)	6.0	
Coarse sun sensor (1)	0.2	
Fine sun sensor (1)	1.9	
Gimbal for fine sun sensor (1)	2.0	
Sun sensor electronics (2)	0.3	
TVC (vane and actuator)(2)	3.5	
Regulator-relief valve (2)	2.6	
Solenoid valve (12)	6.0	
Fill valves (2)	0.6	
High-pressure transducer (2)	0.4	
Low-pressure transducer (2)	0.6	
Nozzles (12)	1.2	
Lines and fittings	3.0	
Nitrogen	12.0	
Nitrogen tanks and residuals (2)	16.8	
Despin system		5.5
Thrusters (2)	0.2	
Explosive valves (12)	3.0	
Electrical	0.8	
Lines and fittings	0.5	
N_2H_4 filter (2)	1.0	
Spinup system		4.2
Motor installation (3)	3.6	
Electrical	0.6	
Propulsion		36.6
Nitrogen fill valve (1)		0.2
N_2H_4 fill and drain valve (1)		0.2
Explosive valves (4)		1.0
N_2H_4 filter (1)		0.5
Electrical		0.5
Lines and fittings		0.5
Motor (1)		1.5
Instrumentation		0.6
Usable propellant		26.8
Tank, residuals and pressurization		4.8
Dynamic Balance Weights		4.0
Scientific Payload		50.0
Contingency		44.5
Spacecraft Weight		564.0

Table 3. Spacecraft Moments of Inertia and Center-of-Gravity

Condition	Weight (lb.)	$\bar{Z}$* (in.)	Moments of Inertia (slug ft^2) I_x	I_y	I_z	Inertia Ratio (I_z/I_x)
Gross SLV-3C payload	2204.1	54.1	328.8	326.8	134.7	.41
Vehicle at TE-364-3 ignition	2158.6	54.9	309.7	307.7	128.4	.41
Vehicle at TE-364-3 burnout	704.4	72.1	203.1	201.1	87.6	.43
Spacecraft-antenna deployed	564.0	79.9	158.1	156.1	122.6	.77
Spacecraft in cruise mode	564.0	79.9	188.0	156.1	152.5	.81

* Reference Station 0.0 is the Centaur/TE-364-3 adapter field joints.

Centaur. Mass properties of the adapters and injection stage were assumed identical to those of the spin-stabilized version.

2.5.2 Flight Sequence

The abbreviated flight sequence which follows is largely self-explanatory. Major differences between this and the Mariner sequence are:

- Spin stabilization of the solid rocket injection stage is required to obtain adequate payload on the Atlas SLV (3C or 3X)/Centaur/TE-364-3 launch vehicle. Thus additional spinup and despin steps are required in the flight sequence.
- Offsetable sun sensors are used to allow earth pointing after 30 days when the earth is within 30 degrees of the sun.
- The large antenna has a deployment step and communications can be switched between three instead of two antennas.
- Less reliance is placed on a computer and sequencer and more on real-time command capability.

- A real-time television mode is used until late in encounter. Only high resolution pictures during the last five hours are taken at rates which exceed the real-time transmission capabilities of the system.

Flight Sequence

Event	Timing	Comments
1. Prelaunch checkout	T-	Gyro heaters on
2. Liftoff	T + 0	
3. Shroud separation	350, 000 ft alt	
4. Atlas booster cutoff	T + 143 sec	
5. Atlas sustainer cutoff and staging	T + 237 sec	
6. Start first Centaur burn	T + 246 sec	
7. Centaur cutoff	T + 570 sec	
8. Centaur parking orbit	(1 to 25 min coast)	
9. Start Centaur second burn	I + 0	
10. Centaur cutoff	I + 100 sec	
11. Spacecraft and third stage separation	J = I + 170 sec	Springs impart 1 deg/sec 3σ tipoff rate. Centaur backed away and tumbled.
12. Spinup start	J + 1/4 sec	
13. Spinup end TE-364 ignition	J + 1 1/4 sec	
14. TE-364 burnout	J + 41 1/4 sec	
15. High power transmitter on	J + 1 min	Omni-antenna

Event	Timing	Comments
16. Start despin	J + 2 min	Despin to nominal zero speed as soon as TE364 tailoff complete.
17. Stop despin	J + 2 min, 26.2 sec	
18. Start gyros	J + 3 min	
19. Turn on attitude control system	J + 10 min	
20. Sun acquisition complete	J + 10 to 30 min	
21. Separate third stage	C - 10 min	Ground command
22. Deploy antenna	C - 7 min	Ground command
23. Deploy magnetometer boom	C + 5	Ground command
24. Turn on Canopus sensor and initiate roll search	C + 0	Ground command
25. Canopus acquisition	C + 1 hr max.	
26. Switch attitude control to derived rate mode, gyros off		
27. Turn on cruise science		Ground command
28. Initiate maneuver sequence	M = T + 5 to 20 days	
29. Turn off cruise science	M + 0	Ground command
30. Turn on gyros for warmup	M + 1 min	Ground command
31. Switch to autopilot mode	M + 1 hr	
32. Start roll turn		Ground command
33. Stop roll turn		Sequencer
34. Start pitch turn		Ground command

Event	Timing	Comments
35. Stop pitch turn		Sequencer
36. Start midcourse motor		Ground command
37. Stop midcourse motor		Sequencer
38. Start sun acquisition		Sequencer
39. Sun acquisition complete		
40. Initiate roll search for Canopus		Ground command
41. Canopus acquisition complete		
42. Offset sun sensor null		Ground command - sun sensors offset 30 degrees to position where earth will be acquired later.
43. Switch to helix antenna	Approx T + 20 days	When earth is within 12 degrees of spacecraft axis
44. Switch to high-gain antenna	Approx T + 30 days	When spacecraft points at earth. Can be delayed until T + 80 days and still keep maximum bit rate
45. Update sun sensor offset		As required
46. Gyro heaters on	E-300 hr	
47. Start encounter sequence	E-300 hr	Ground command at 150 Jupiter radii
Trapped radiation on		150 Jupiter radii
TV enable	E-170 hr	100 Jupiter radii
TV gimbal angles		100 Jupiter radii
TV exposure setting		100 Jupiter radii

Event	Timing	Comments
TV picture sequence		Sequencer and Jupiter presence sensor
Solar cosmic ray off		100 Jupiter radii
Solar plasma off		100 Jupiter radii
TV switched to storage	E-5 hr	
Infrared scanner		During flyby
48. TV and infrared off. Gyros on. Switch to autopilot mode		Before occultation
Science switched to storage Auroral sensor on		Scans during occultation
49. Post encounter Reacquire sun-Canopus Switch to cruise science Transmit stored data		

2.5.3 Trajectory Accuracy

This section describes briefly the differences between trajectory accuracy capabilities for the 3-axis and spin-stabilized spacecraft.

The midcourse guidance technique for the 3-axis stabilized system is identical with that for the spin-stabilized version, except that there is only a single engine, and orientation of the vehicle for a correction is achieved by gyro-controlled turns. Like the spin-stabilized version, the engine thrust is pointed so that a single velocity increment removes the target errors. Three components of target errors may be corrected, such as two miss components and time of flight, or a critical plane correction may be performed where two miss components only are removed with a minimum velocity increment. Time of flight may be changed with very nearly the same velocity increment as a critical plane correction to control the time of arrival on the day of encounter. See Volume 2, Section 7.4.

The launch vehicle injection accuracy, trajectory characteristics, tracking accuracies, and the effects of astrophysical constant uncertainties and ephemeris errors are not a function of the spacecraft. Therefore the midcourse correction velocity requirements are identical with the arbitrary pointing spin-stabilized version reported in Volume 2, Section 4.2. The gyro controlled orientation scheme, however, provides greater pointing accuracy than the open loop maneuver, which enables the midcourse correction to be performed with more precision. Estimates of the pointing errors and their contribution to the miss dispersion at Jupiter are presented below.

The autopilot subsystem which controls the thrust vector direction during engine firing is comparable in accuracy to the spin-stabilized spacecraft. Initial start up transients which cause an error perpendicular to the engine thrust direction are considered small and have not been estimated.

2.5.3.1 Pointing Errors

The desired orientation for midcourse correction is obtained by means of a sequence of roll and pitch rotations. These rotations are obtained by commanding the appropriate gyros to be torqued for a certain time. Midcourse correction pointing errors are caused by:

- Uncertainties in the initial orientation
- Inaccuracies in the gyro torquing process and gyro drift
- Execution errors, including center of gravity offset

The following errors have been assumed in computing uncertainties in the initial orientation:

Sun sensor electrical null offset	±0.1 deg, 3σ
Sun sensor mechanical misalignment	±0.1 deg, 3σ
Deadzone error	±0.25 deg
Electrical offsets	±0.1 deg, 3σ
RSS total	±0.304 deg. 3σ

The same value has been assumed for both pitch and roll initial orientation errors.

Gyro torquing accuracy and gyro drift were assumed to be 0.1 percent and 0.3 deg/hour, respectively. Contributing sources and the corresponding errors are listed below:

Initial roll orientation uncertainty	±0.304 deg, 3σ
Roll gyro drift	±0.3 deg, 3σ
Gyro alignment error (in roll)	±0.2 deg, 3σ
Gyro torquing error (in roll)	±0.2 deg, 3σ
Timing error	+0.2 deg, 3σ
Initial pitch orientation uncertainty	±0.304 deg, 3σ
Pitch gyro drift	±0.3 deg, 3σ
Gyro alignment error (in pitch)	±0.2 deg, 3σ
Gyro torquing error (in pitch)	±0.2 deg, 3σ
Timing error (pitch)	±0.2 deg, 3σ
Thrust vector limit cycle error (pitch)	±0.25 deg
CG location error (pitch component)	±0.554 deg, 3σ
Thrust vector limit cycle error (yaw)	±0.25 deg
CG location error (yaw component)	±0.57 deg, 3σ
Total RSS error	= ±1.17 deg, 3σ

The gyro reference unit has been assumed to consist of three single-degree-of-freedom gyros operating in the rate mode, which can be rotated by application of a constant current to a torquing device. Position errors are obtained by integration of the rate signals by means of series capacitors. Errors produced by capacitor leakage are neglected on the assumption that the spacecraft control system will follow the commanded position with a very small error.

2.5.3.2 Thrust Magnitude Errors

Engine thrust anomalies are identical to those summarized in Appendix H. Thrust magnitude errors are independent of the method of engine thrust vector control.

2.5.3.3 Midcourse Correction Covariance Matrix

In order to accurately compute the effects of pointing and thrust magnitude errors, a Monte Carlo simulation should be employed to account for the system nonlinearities. The only error source significantly different, however, from the spin version is the pointing error, which is approximately half as large. This error dominates the accuracy of the correction, and therefore the post-midcourse miss ellipse at Jupiter will be approximately half as large. Dividing the dimensions of the post-midcourse 99 percent probability ellipse of the spin version by 2 gives semimajor and minor axes of 12,000 and 9,000 kilometers respectively. This ellipse is more than adequate for satisfaction of the flyby mission scientific objectives.

2.5.3.4 Nongravitational Perturbations

The perturbations resulting from micro-accelerations from other than gravitational forces acting on the spacecraft have been evaluated in detail for the spin-stabilized configuration in Section 7.4 of Volume 2 and Appendix K. The effects are essentially the same in the case of the three-axis stabilized configuration with the few exceptions listed below.

Source of Perturbation	Spin-Stabilized Spacecraft	3-Axis Stabilized Spacecraft
Solar radiation pressure	Same	
Micrometeoroid pressure	Same	
Unbalanced attitude control	a) Compensation of asymmetric solar pressure	Cancels due to jet force symmetry
	b) Earth tracking torque	
Gas leakage	Cancels due to spin	Can produce small perturbations
Miscellaneous other sources, e.g., plasma forces, etc.	Neglected	

The effects of small gas leakage out of one or more of the clustered 12 attitude control nozzles do not cancel as in the case of the spin stabilized configuration. A typical arrangement of nozzle positions is sketched in Figure 4.

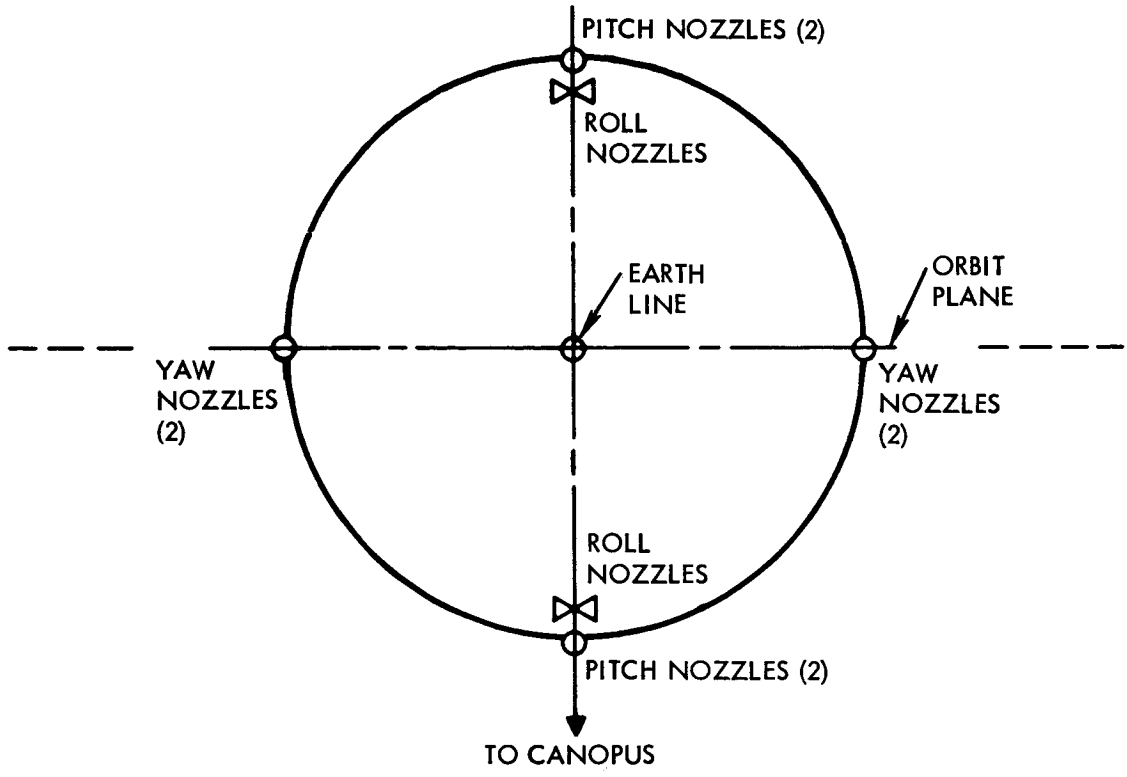

Figure 4. Arrangement of Attitude Control Nozzles

A precise description of the gas leakage and its effects on the trajectory would lead to a complex mathematical model. However, since the results of the worst-case analysis presented below indicate that the trajectory uncertainties do not exceed a few thousand kilometers at Jupiter encounter, the following (conservative) assumptions which serve to simplify the analysis appear to be justified:

1) It is assumed that leakage occurring in some of the solenoid valves remains constant throughout the mission, at the rate of 2 cc of gas per hour each.

2) The perturbation effects of reaction forces in three principal directions, radial to and from the sun, transverse, and normal to the orbit plane, will be considered.

However, no forces normal to the orbit plane occur in the typical nozzle arrangement shown in Figure 4.

3) The simplifying assumption is made that on the average the line of action of the pitch and yaw nozzles (total of eight)is in radial orientation, to or from the sun, although the spacecraft is actually oriented toward the earth. The four roll nozzles, contribute forces acting in the orbit plane, perpendicular to the sun line.

4) It is assumed that most probably not more than two out of eight pitch and yaw nozzles are leaking gas in the same direction at the rate of 2 cc/hour each, without cancellation by gas leakage in opposite directions. Similarly not more than one out of four roll nozzles produce leakage forces without cancellation.

5) The total mass leaking from one nozzle during a 650-day mission, for an assumed nitrogen gas density (at standard pressure and temperature) of 0.0727 lb/ft^3, will be 0.08 pound.

6) The specific impulse of the leaking gas is estimated as $I'_{sp} = 24$ sec. This reflects (a) a reduction from the nominal value $I_{sp} = 60$ sec by 1/1.7 for gas flow from an orifice rather than an expansion nozzle, and (b) a reduction by 33 percent which is obtained under the assumption of a uniform flow of the gas particles in all directions of a hemisphere rather than along the nozzle axis.

The above assumptions yield a total accrued velocity increment

$$\Delta V = I_{sp}\, \delta \frac{\Delta M}{M} = 0.124 \text{ ft/sec}$$

due to expenditure of 0.08 pound of gas over a period of 650 days.

The sensitivities of aphelion distance V_a with respect to incremental velocity changes in radial and transverse directions are integrated for uniform rate of change of ΔV due to leakage. This yields, for transverse velocity components ΔV_t,

$$\Delta r_{a_1} = \frac{H}{V_{ca}^2 - V_a^2} \frac{\Delta V_t}{T_F} \int_0^{T_F} \left(\frac{r_a}{r_i} - \frac{r_i}{r_a} \right) dt = 0.144 \times 10^3 \text{ km}$$

and for radial velocity components ΔV_r,

$$\Delta r_{a_2} = \frac{r_a}{V_{ca}^2 - V_a^2} \frac{\Delta V_r}{T_F} \int_o^{T_F} V_i \sin \theta_i \, dt = 3.41 \times 10^3 \text{ km}$$

where the integral terms were obtained from the characteristics of the 650 day sample trajectory given in Section 7.4 of Volume 2, namely

$$\int_o^{T_F} \left(\frac{r_a}{r_i} - \frac{r_i}{r_a} \right) dt = 0.069 \, T_F \text{ days}$$

$$\int_o^{T_F} V_i \sin \theta_i \, dt = 35 \times 10^3 \, T_F \text{ ft/sec x days}$$

The combined aphelion perturbation for leakage of two pitch or yaw nozzles and one roll nozzle is $\Delta r_a = 6.82 \times 10^3$ km. Transforming this distance into an equivalent miss perturbation ΔB at Jupiter encounter (using the ratio $\Delta B / \Delta r_a = 0.337$, which was derived for the radial solar pressure effects in Section 7.4 of Volume 2 we obtain

$$\Delta B = 2.5 \times 10^3 \text{ km}$$

As discussed previously out-of-plane perturbation effects do not occur for the nozzle arrangement considered here. However if the roll nozzle could exert forces normal to the orbit plane the effect could be integrated on the basis of the analysis of Section 7.4 of Volume 2.

The above computations show that even under most conservative assumptions the miss uncertainty ΔB due to gas leakage does not exceed the 3σ estimate of other perturbation uncertainties which affect the three-axis stabilized spacecraft. Those perturbation uncertainties are largely

due to solar pressure and yield 3.1×10^3 km for a black dish and 5.5×10^3 km for a white dish.

2.5.4 Reliability

The redundancy incorporated in the 3-axis version is the same as that on the spin-stabilized version except that because of volume constraints redundant gyros are not used. Although the failure rates claimed for the air bearing gyros are sufficiently good to make the system reliability satisfactory, a genuine item of improvement would be to incorporate redundant gyros. Neither is the Canopus tracker redundant, and, while the Mariner 4 experiment would suggest that it need not be redundant, another possible improvement would be partial redundancy in this unit. Mariner pneumatic redundancy is used.

2.5.5 Science Objectives

The 3-axis stabilized spacecraft provides a very good environment for the scientific platform. The magnetometer will sense spacecraft fields of about 0.1 gamma. The plasma probe will require additional sensing elements to get the same overall field of view as it does on the spin-stabilized version but with that modification it is completely adequate. The other interplanetary experiments (galactic, solar cosmic ray, micrometeoroid, and radio propagation and occultation), perform equally well on both spacecraft. The planetary experiments are improved because of the addition of the planetary scan platform which allows increased resolution since the spin rate does not contribute to smear. The requirement for a gimballed platform, while introducing some unreliability, more than compensates in science improvements. The trapped radiation counter performs equally well from the spin and the 3-axis control.

2.5.6 Booster Implications

For a 50-pound science payload, a 3-axis attitude controlled spacecraft weighs about 70 pounds more than a comparable spinner (564 versus 493 pounds). Counting an additional 18-pound adapter, this amounts to the difference between a narrow and a comfortable margin on the Atlas SLV3X/Centaur/TE-364-3 whose capability is approximately 600 pounds. Actually there appears to be some uncertainty as to the capability of this launch vehicle, since General Dynamics, Convair Division, and Boeing

(Burner II) data give a capability of about 540 pounds for the Atlas SLV3C/2 burn Centaur/spin table version of Burner II-3 (an injection stage incorporating the TE-364-3 solid rocket) and a corresponding capability of over 590 pounds with the lighter weight (separate-spin up) interstage as discussed in Section 7.7 of Volume 2. This performance was calculated for a 20-minute coast in a 90 nautical mile parking orbit as compared to a 25-minute coast in a 100 nautical mile parking orbit for the Atlas SLV3X/Centaur/TE-364-3.

In either case, there appears to be a minimal margin for the 3-axis spacecraft. If a greater margin is desired without resorting to the High Energy Kick Stage or the Titan, the alternative is to use a cylindrically extended version of the TE-364 denoted by -4. This version, although not yet qualified, would add an additional 50-pound capability, which should provide an adequate margin. It appears that the suitability of such comparatively minor launch vehicle improvement, if necessary, allows a better comparison between the 3-axis and spinner spacecraft than would be obtained by considering the HEKS or Titan.

The performance of the three-axis stabilized version of the Burner II-3 is degraded so much that it cannot be considered, and, in the above framework of comparison, a spin-stabilized injection is required for both the 3-axis and spinner spacecraft. The same solid rocket spinup and hydrazine monopropellant despin would be used for both versions.

2.6 SUBSYSTEM DESIGNS

This section summarizes the subsystem designs for the 3-axis, 50-pound payload spacecraft, concentrating upon the differences between it and the spinner.

2.6.1 Structure and Mechanisms

The basic structural configuration of the 3-axis system is essentially the same as the spin-stabilized version. The compartment, antenna, micrometeoroid protection, and interstage are the same as are materials. There are two basic structural differences. First, the RTG units, since they do not need to be near the roll plane, are not deployed. Fixed struts hold the RTG's in a position corresponding

to partial deployment on the spinner. At the location, the RTG's are the same distance from the payload as on the spin-stabilized version, which minimizes radiation effects upon the experiments; they are further away from the magnetometer, reducing possible magnetic interference. The second major difference is the requirement for a planetary scan platform to mount the infrared radiometer and the TV experiment. This device mounted at the base of the spacecraft has a scan capability of ±90 degrees which will permit a scan of the full planet during flyby. The TV is mounted on the scan platform and has an additional degree of freedom provided by a tippable mirror allowing coverage from the rear to the side of the spacecraft. These two degrees of freedom allow the TV to look at any part of Jupiter during the approach and flyby phases. In addition, a single degree of freedom scan technique is required for the auroral detector, which must point out from the front end of the spacecraft so that detection can be carried on during solar occultation. This detector is mounted in the feed assembly and can move ± 60 degrees to assure detection in all reasonable trajectories. Because the conical scan technique is not used, the two position feed on the parabolic antenna is not required. Also only the magnetometer need be boom mounted since spin symmetry is not required after injection.

2.6.2 Electric Power

Power requirements have increased by about 15 watts from the spin stabilized version to satisfy the requirements of the attitude control system and the planetary scan platform. Since the two planetary scan mechanisms are not required at the same time, the TV platform and the attitude control system power requirements size the system. The power shunts are the same but some additional power conversion equipment is required to satisfy the needs of the gyro assembly. See Section 8.2 of Volume 2.

2.6.3 Attitude Control Subsystem

The attitude control subsystem provides stabilization during injection motor firing and 3-axis attitude control at all times after

separation from the solid injection motor. It also controls the orientation of the high-gain and medium-gain body-fixed antennas on the basis of commands received from the earth. In addition, it controls the velocity increments executed during midcourse propulsion operations.

Stabilization during the injection phase will be maintained by spinning the spacecraft about its roll axis. Requirements and constraints during spinup and despin are similar to those outlined for the spin-stabilized configuration. A spin rate of 60 rpm is used to obtain the desired degree of injection accuracy. Because of the unfavorable ratio of moments of inertia and to limit the attitude errors originated by initial tipoff rates (imparted by the separation mechanism) and misalignments of the thrust vector, the spinup maneuver must be completed in about one second. Solid rocket thrusters are preferred for this operation and ignition will be initiated by the command subsystem immediately after separation from the launch vehicle. A set of three 67-pound thrusters will be used to minimize the wobble produced by misalignments. The despin phase will consist of a single operation in which the roll component of angular momentum will be reduced slowly to minimize the wobble buildup. A set of two 1-pound hydrazine-thrusters will be used as described in Section 8.3, Volume 2.

For the remaining phases of the mission the attitude control subsystem must provide the following modes of operation, which make use of various combinations of sensors and actuators.

Acquisition Mode

An acquisition configuration is required for nulling the large rates about each axis following the despin maneuver and locking on the selected references for attitude control. This configuration must be designed to minimize gas consumption and to obtain acquisition times compatible with thermal control constraints. The sun and Canopus have been selected to provide attitude control references. Coarse sun sensors will be required for sun acquisition. Rate information can be obtained by means of rate gyros or derived-rate schemes. Gyros are preferable to derived-rate feedback during coarse acquisition because they provide better acquisition performance.

It may be possible to develop a derived-rate which could be used to provide a capability of acquiring in case of gyro failure. The same gyros provided for the inertial mode can be used for acquisition by switching them to the rate mode. The yaw and pitch sun acquisition configuration will bring the sun within the field of view of a fine sun sensor which will control the acquisition process until the cruising limit cycle operation is reached. Torquing is accomplished by means of the same pneumatic system used for the cruise mode.

Because of the narrow field of view of the Canopus sensor and the high initial roll rate expected, the roll gyro is used to provide a search mode for Canopus acquisition. The roll rate is reduced to a low value and acquisition of Canopus terminates the roll search and switching is made to the cruise mode.

Following acquisition, the spacecraft roll axis will be pointed to the sun and the star sensor will be locked on Canopus.

Earth-Pointing Cruise Mode

One of the requirements of the cruise mode is to point the paraboloidal antenna to the earth, maintaining the downlink gain within 1 db of the nominal value. This is equivalent to specifying a maximum pointing error of 0.5 degree. The earth-pointing attitude will be achieved by appropriate biasing of the fine sun sensor. Bias levels will be controlled from the earth by means of quantitative commands until the downlink signal level is maximized. Since the greatest part of the mission time is spent in the cruise mode, it is essential that this mode combine the maximum possible reliability with the minimum control gas consumption. In order to satisfy the pointing accuracy requirements, the limit cycle amplitude must be no greater than $\pm$ 0.25 degree. The limit cycle rates are determined by the minimum impulse obtainable from the pneumatic system. The following alternatives were considered for mechanization of the cruise mode:

- On-off controller with lead compensation
- Fixed pulse controller
- Pulse modulated controller

The first approach was discarded because the large lead-lag ratios required are difficult to mechanize and generate noise problems as a consequence of the associated gain reduction. Fixed pulse controllers were eliminated because of the complexity required to insure satisfactory performance under disturbances. There are several pulse modulation techniques available: pulse width, pulse frequency, and pulse ratio modulation. Pulse ratio modulation was preferred because of its greater control range. This technique combines both pulse width and pulse frequency modulation and has been proven successfully in the Ranger and Mariner.

Some form of backup must be provided to maintain attitude references during solar eclipse conditions or eventual loss of Canopus lock during planet encounter. The attitude gyros provided for the inertial mode can be used to implement an inertial attitude hold mode under these circumstances.

Inertial Mode

The inertial mode is required to establish any arbitrary orientation for midcourse velocity corrections and provide attitude reference during eclipse, in the event of loss of Canopus reference and during midcourse velocity corrections. Reorientations are obtained by gyro torquing. Any desired attitude can be held within the tolerance imposed by gyro drift by disconnecting the torquing current generators. The following techniques are available for reorientation control system damping: a) derived-rate feedback, b) rate gyro feedback and c) lead-lag compensation. Derived rate feedback was selected to simplify the switching logic and because of its superior performance.

Thrust Vector Control Mode

Attitude stabilization during midcourse propulsion can be obtained by means of the following techniques:

- Cold gas mass expulsion
- Engine gimballing
- Spin stabilization
- Jet-vane thrust vector control

Disturbance torques are produced by thrust vector misalignments and transversal offsets of the center of mass. Attitude reference is provided by the gyros operating in the inertial attitude hold mode. Jet vane thrust vector control has been selected for pitch and yaw stabilization because of the low thrust levels available from the pneumatic control system.

The attitude control system concept proposed for the three-axis stabilized configurations of the Advanced Planetary Probe is basically similar to the Mariner design. Therefore, the only areas to be discussed in the following section are those where significant departures from the Mariner design are made to satisfy some of the new mission requirements or design constraints.

2.6.3.1 Sun Sensor

The coarse sun sensors to be used for acquisition must have a field of view of 4π steradians. Preliminary studies of the Voyager spacecraft have shown there may be an advantage in having saturation of the sun sensor output for large attitude errors. This would result in full rate commands for any attitude errors outside of a small linear region. The resulting bang-bang operation would give a fast response time and some economy of gas. One of the disadvantages of this sun sensor characteristic is the consequent degradation of acquisition performance with derived rate feedback. A typical coarse sun sensor characteristic for the yaw and pitch axes is shown in Figure 5. The scale factors are selected to match

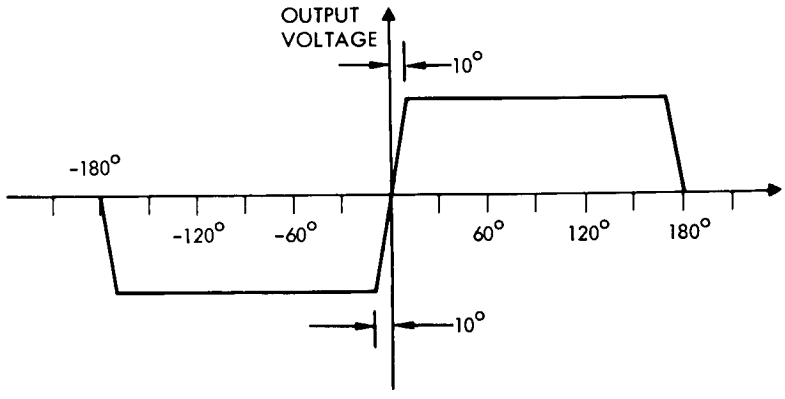

Figure 5. Pitch and Yaw Coarse Sun Sensor Characteristics

those of the respective fine sun sensors to prevent signal discontinuities when switching from coarse to fine sensors.

The pitch fine sun sensor must have a minimum operating range of the order of ± 7.5 degrees to allow for variations in the sun's clock angle relative to earth-Canopus axes. The selected characteristic is shown in Figure 6. The operating range has been extended to ± 10 degrees

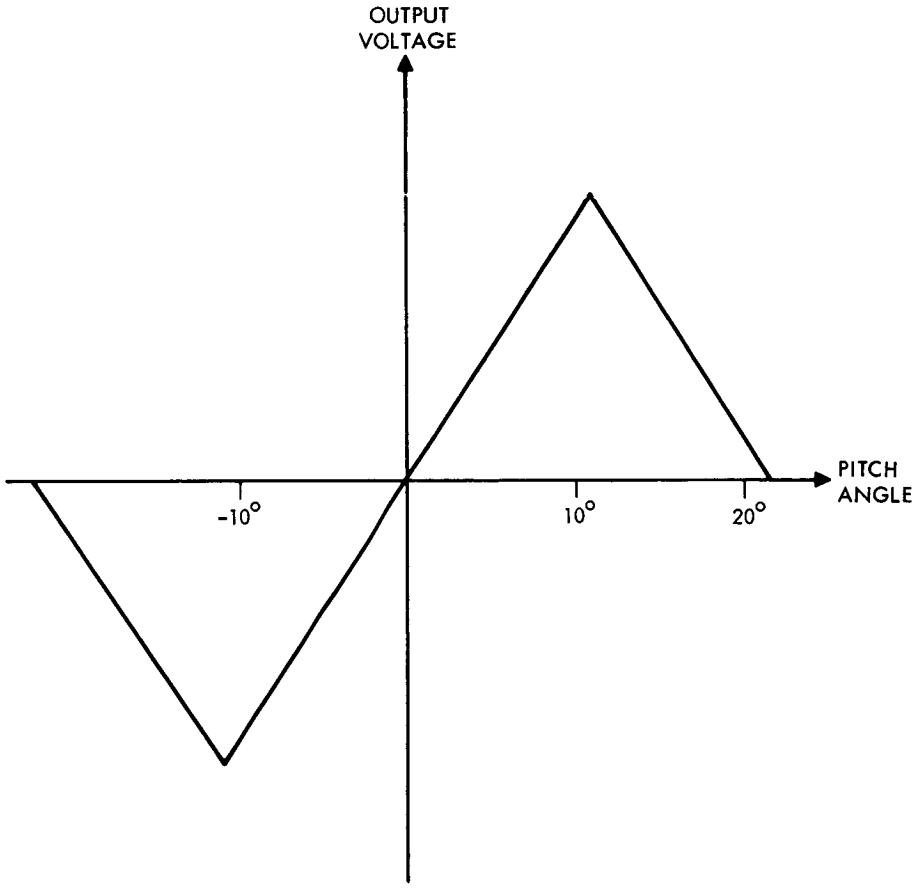

Figure 6. Pitch Fine Sensor Characteristics

to make the pitch fine sun sensor characteristic compatible with those of the coarse sun sensors as well as with that of the yaw fine sun sensor. The required yaw operating range of ± 30 degrees presents a difficult mechanization problem. To achieve an accuracy of ± 0.1 degree it is desirable to have a range no greater than ± 10 degrees. In this case the error is 1 percent of the maximum range, which is feasible on the basis of present technology. The 30-degree yaw sensor requirement

can be accommodated by using a set of three overlapping sun sensors to cover the whole range, as shown in Figure 7. A block diagram of a system for the mechanization of this characteristic is given in Figure 8.

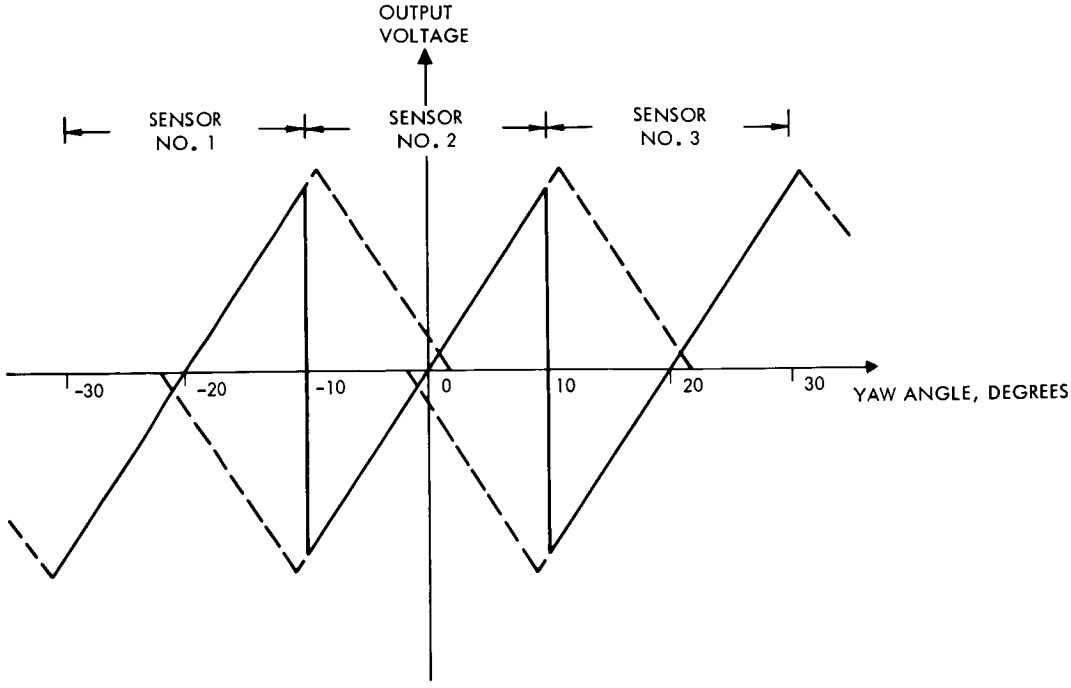

Figure 7. Yaw Fine Sensor Characteristics

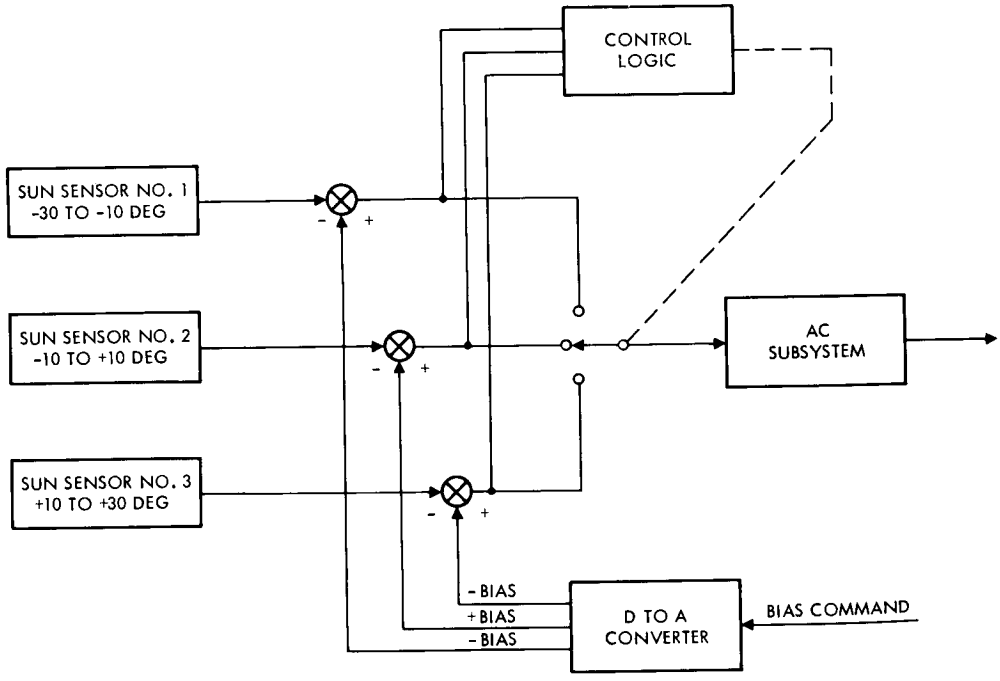

Figure 8. Block Diagram of Overlapping Sun Sensors

Theoretically, switching occurs when the error signals developed at the summing junctions corresponding to adjacent sensors become zero simultaneously. This approach has the advantage of minimizing disturbances as a consequence of switching with non-zero error signals. Provisions must be made at the control unit to prevent switching back during limit cycling in the vicinity of the switching points.

The principle of operation of the fine sun sensors is illustrated in Figure 9. Each cell has an area $A_i = a^2$ and the distance between the window and the sensitive surface is d such that

$$\frac{a}{d} = \tan 10 \text{ deg}$$

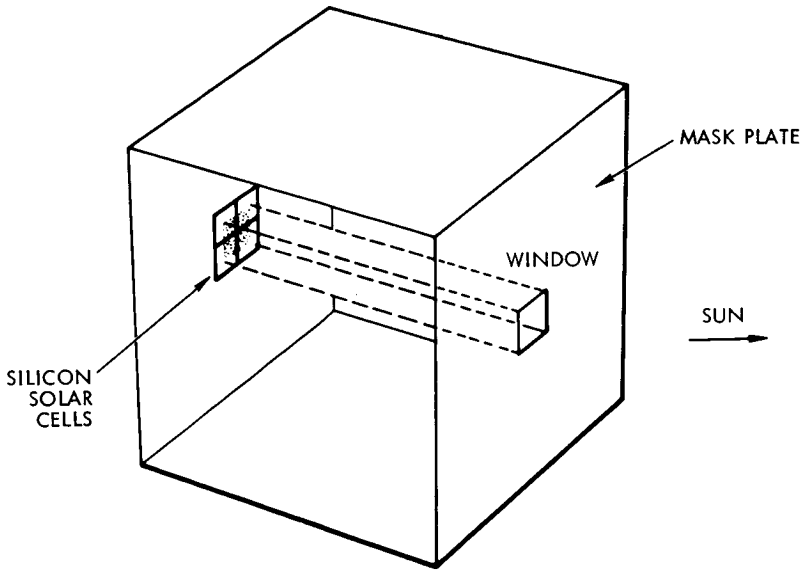

Figure 9. Principle of Operation of the Fine Sun Sensor

Letting x, y be the coordinates of the center of the light spot with respect to the coordinate axes shown in Figure 10, the illuminated areas are

$$A_1 = \left(\frac{a}{2} - x\right)\left(\frac{a}{2} + y\right) = \frac{a^2}{4} + \frac{a}{2}(y-x) - xy$$

$$A_2 = \left(\frac{a}{2} + x\right)\left(\frac{a}{2} + y\right) = \frac{a^2}{4} + \frac{a}{2}(x + y) + xy$$

$$A_3 = \left(\frac{a}{2}\uparrow + x\right)\left(\frac{a}{2}\uparrow - y\right) = \frac{a^2}{4} + \frac{a}{2}\downarrow(x - y) - xy$$

$$A_4 = \left(\frac{a}{2}\uparrow - x\right)\left(\frac{a}{2}\uparrow - y\right) = \frac{a^2}{4} - \frac{a}{2}\downarrow(x + y) + xy$$

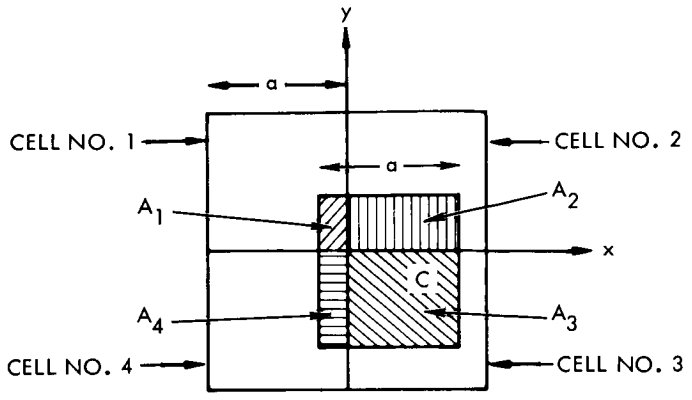

Figure 10. Geometry of Sun Sensor Operation

If the cells are operated in the "short circuit current" mode, the signal from each cell will be directly proportional to the corresponding illuminated area. Denoting the proportionality constant by K and the differential voltages between cells by V_{ij}

$$V_{13} = Ka\ (y - x)$$

$$V_{24} = Ka\ (x + y)$$

Therefore

$$V_{24} - V_{13} = 2\ Kax = 2\ Kad \tan\theta$$

where θ is the yaw angle.

Similarly,

$$V_{13} + V_{24} = 2\ Kay = 2\ Kad \tan\psi$$

in which ψ is the pitch angle. These last two expressions show that the output signals are proportional to the tangents of the respective angles, but they also indicate direct dependence on the solar cell constant K as well as on the window dimensions and distance between this window and the solar cell quad. Additional errors will be introduced by variations of the solar radiation energy with distance and preamplifier drift. The scale factors of the combined solar cell and preamplifier assemblies can be maintained fairly constant by means of an automatic gain control system operating with a calibrated reference. A block diagram of the proposed AGC preamplifier configuration for the APP sun sensors is shown in Figure 11. The reference solar cell and its field of view should be equal to the sun sensor's. The reference solar cell

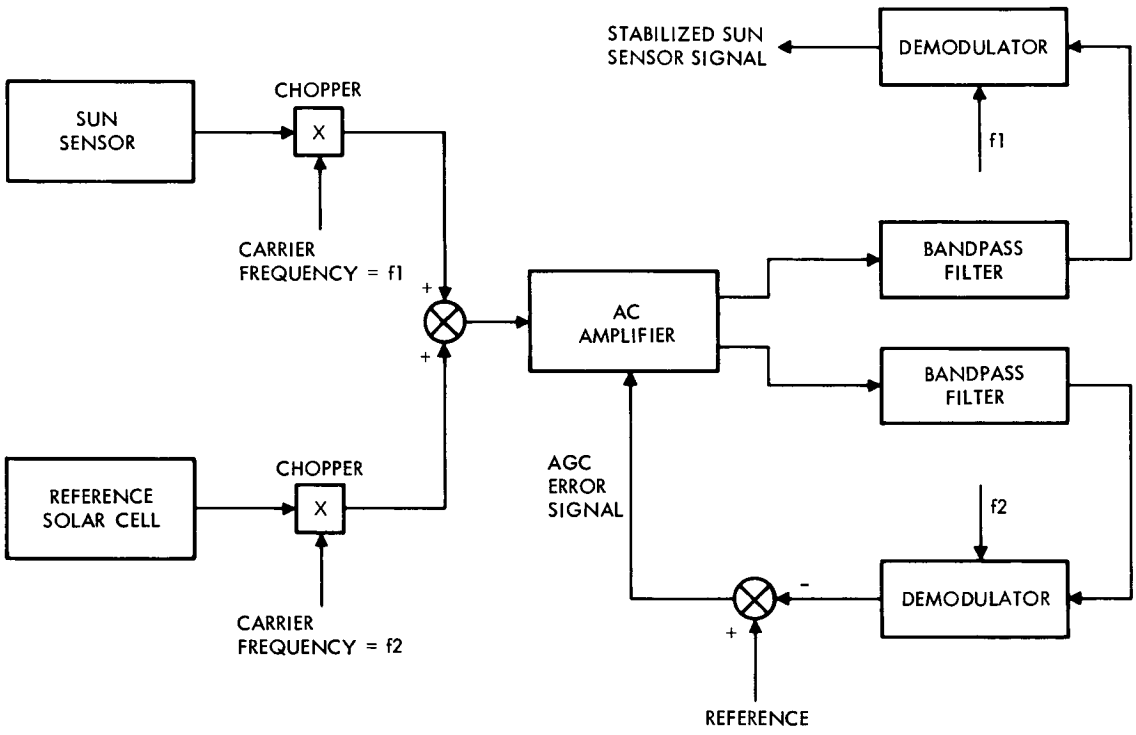

Figure 11. AGC Preamplifier System for APP Sun Sensors

output will vary with distance from the sun, temperature, incidence angle of the light, aging, etc. Instead of using a DC amplifier, the corresponding signal is modulated, AC-amplified and demodulated to minimize the effects of drift. The demodulator output is proportional to the cell constant and to the amplifier gain also. Comparing this signal with a fixed

reference, an error signal is obtained to control the preamplifier gain. By using a different carrier frequency the sun sensor output is processed by the same AC amplifier. Separation of the two signals is accomplished by means of bandpass filters.

2.6.3.2 Earth-Pointing Cruise Mode

This section describes a preliminary analysis of the cruise mode, during which the roll axis must be pointed to the earth with a maximum error of 0.5 degree. The maximum error per axis (yaw and pitch) must be no greater than 0.354 degree if the two channels are assumed to be similar. The primary error sources are:

a)	Attitude reference accuracy:	±0.1 degree, 3σ
b)	Limit cycle error: assume	±0.25 degree
c)	Sun sensor bias drift and command quantization:	±0.1 degree
d)	Antenna boresight error:	±0.2 degree, 3σ
e)	Antenna misalignment:	±0.2 degree, 3σ

If the errors contributed by b) and c) are assumed to be 3σ values, the RSS total will be ±0.403 degree, 3σ. This result is slightly greater than the allowable error of 0.354 degree per channel but this does not mean the desired accuracy cannot be achieved, because by appropriate biasing of the sun sensors the effects of antenna misalignments and boresight errors can be cancelled almost completely. The sun sensors is biased under closed-loop control from the ground by sensing the downlink signal strength and commanding that bias amplitude which maximizes the signal strength. Assuming a residual misalignment of 0.1 degree as a consequence of improper biasing, the RSS total becomes ±0.304 degree. Consequently, the assumed limit cycle amplitude of ±0.25 degree is compatible with the pointing accuracy requirements.

The selected configuration for the cruise mode consists of three overlapping two-axis sun sensors with electrical gimballing, a Canopus sensor, and an electronic switching amplifier with derived rate feedback. A block diagram of this configuration for a single axis is shown in Figure 12. A minimum on-time switching amplifier may be more desirable

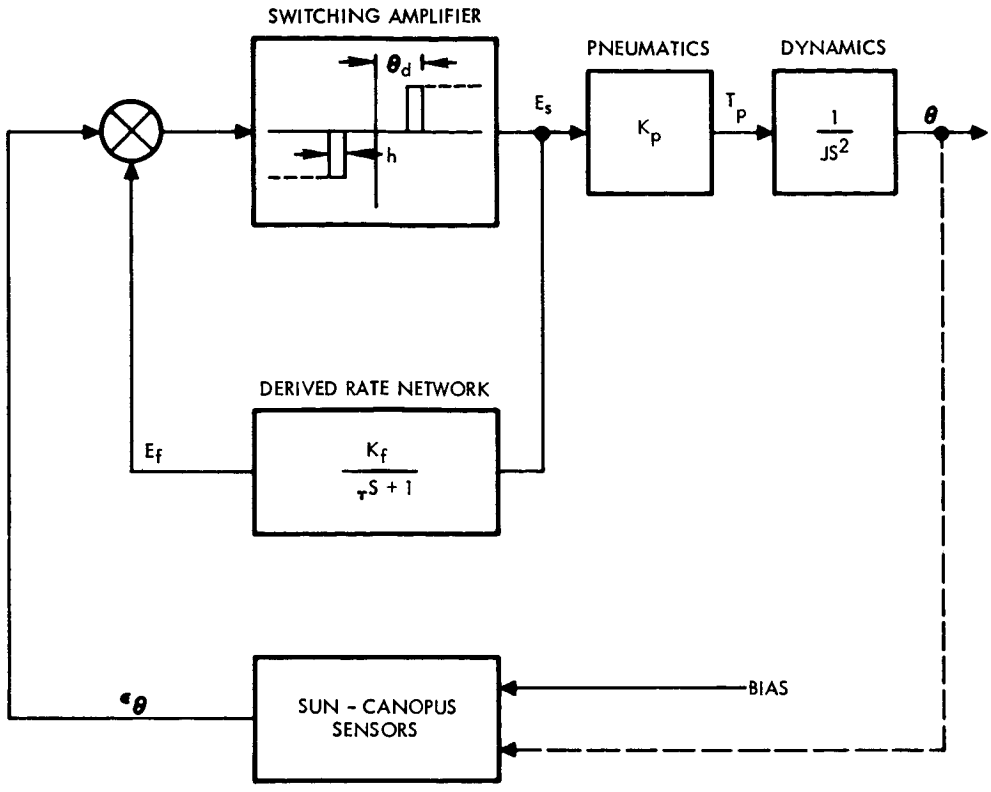

Figure 12. Block Diagram of the Cruise Mode Configuration for a Single Axis

than the hysteresis switching amplifier shown based on Mariner experience. The following terms are used in the figure:

E_s = switching amplifier output voltage

K_f = derived rate filter gain

τ_f = derived rate time constant

E_f = derived rate feedback voltage

K_p = pneumatic system constant

J = spacecraft moment of inertia about the corresponding axis

T_p = torque produced by the pneumatic system

θ = spacecraft attitude

ϵ_o = attitude error voltage

e_d = switching amplifier threshold

h = switching amplifier hysteresis

For a preliminary estimation of the cruise-mode performance characteristics the following system parameter values have been assumed:

J_1 = pitch moment of inertia = 180 ft-lb-sec^2

J_2 = yaw moment of inertia = 160 ft-lb-sec^2

J_3 = roll moment of inertia = 150 ft-lb-sec^2

ℓ = distance between thrusters = 6 ft

θ_{LC} = nominal limit cycle amplitude = $\pm$ 0.25 deg

t_{fmin} = minimum limit cycle firing time = 0.015 sec

F = pneumatic thrust = $\pm$0.02 lb

The limit cycle rates are given by

$$\dot{\theta}_{LC} = \frac{F l \, t_{fmin}}{2J}$$

Substitution of the parameter values given above gives

$\dot{\theta}_{LC1}$ = pitch limit cycle rate = 0.5×10^{-5} rad/sec
= 1.03 deg/hr

$\dot{\theta}_{LC2}$ = yaw limit cycle rate = 0.563×10^{-5} rad/sec
= 1.16 deg/hr

$\dot{\theta}_{LC3}$ = roll limit cycle rate = 0.6×10^{-5} rad/sec
= 1.24 deg/hr

The gas consumption per axis corresponding to the cruise mode is given by

$$W = \frac{\dot{\theta}_{LC} F t_m t_{fmin}}{\theta_{LC} I_{sp}}$$

where t_m = mission duration

I_{sp} = specific impulse for nitrogen

Assuming a specific impulse of 60 seconds and mission durations of 600 and 750 days, the gas consumption per axis will be given in Table 4.

For these calculations the pneumatic system has been assumed to consist of four gas jets per axis. Each gas jet develops 0.02 pound of thrust, and the distance between thrusters is 6 feet. The objective of this approach is to provide redundancy since pure couples are not required as a consequence of the cyclical nature of limit cycle thrusting. The pneumatic system is discussed further in Section 2.6.3.4.

Table 4. Gas Consumptions per Axis for the Cruise Mode, in Pounds

	Mission Duration	
	650 Days	720 Days
Pitch	0.33	0.36
Yaw	0.36	0.40
Roll	0.39	0.43
Totals	1.08	1.19

2.6.3.3. Acquisition Mode

This section is devoted to a preliminary analysis of the acquisition mode. The configuration selected for the acquisition mode is similar to the scheme proposed for the cruise mode, the only difference being the use of the coarse sun sensors and rate gyros to provide attitude and rate information respectively. A block diagram of the selected configuration for the pitch and yaw axes is shown in Figure 13. As indicated the coarse sun sensor has a saturating characteristic to give a controlled slewing rate for large attitude errors.

The sequence of operations for yaw and pitch acquisition will be as follows:

1) Reduction of initial rates. If the initial rates are greater than a searching rate of the order of 0.1 to 0.2 deg/sec, the corresponding gas jets are turned on until these rates are reduced to the desired values.

2) Sun sensor switching. Searching continues at the nominal rate until the pointing error of the corresponding channel becomes less than a nominal angle

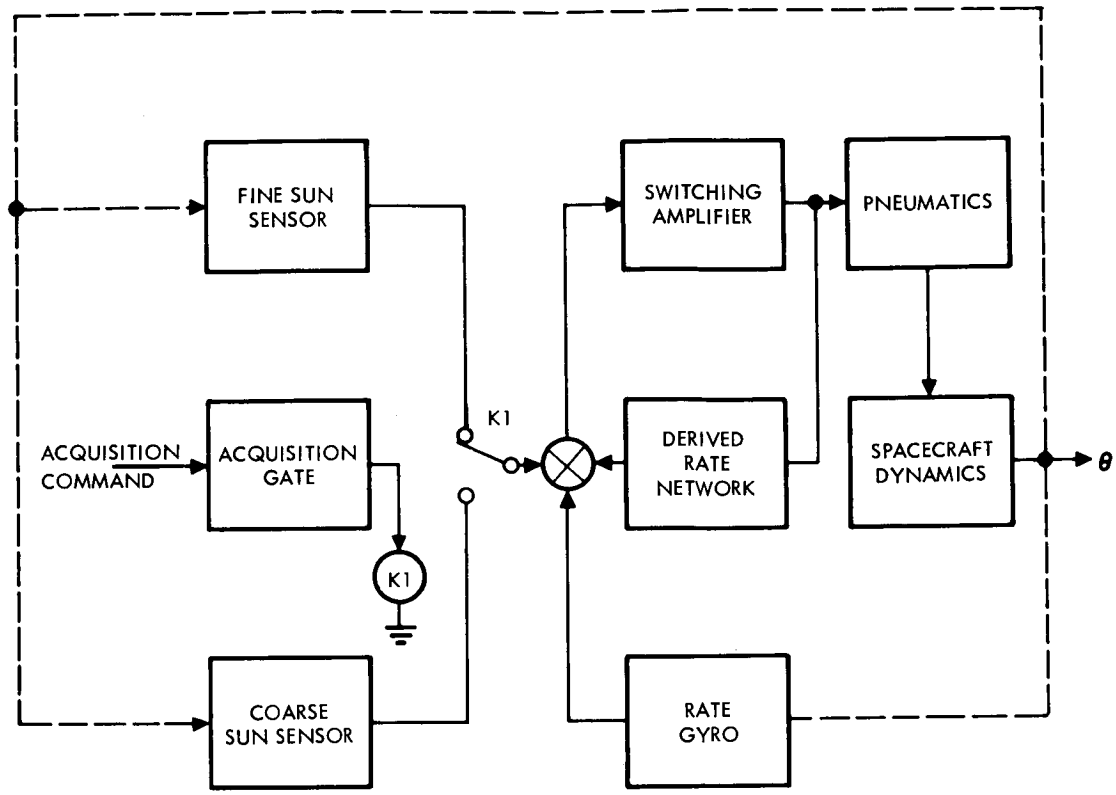

Figure 13. Typical Acquisition Configuration for the Yaw and Pitch Axes

of the order of 10 degrees. The fine sun sensors are switched in and both yaw and pitch errors are reduced to the limit cycle values.

After sun acquistion is completed Canopus acquisition is accomplished as follows:

1) The roll rate is reduced to about 0.1 deg/sec and is maintained under rate gyro control until a star of the Canopus magnitude comes within the sensor field of view.

2) When the Canopus sensor indicates lock onto a star, the roll rate bias is removed, the gyros are turned off and the system is switched to the cruise mode.

3) The acquisition process is monitored on the ground and roll over-ride commands can be sent if it appears that lock is being established on the wrong star.

A block diagram of the control system configuration for Canopus acquisition is shown in Figure 14. An integrator is provided to prevent excessive roll rates in case of a rate gyro failure.

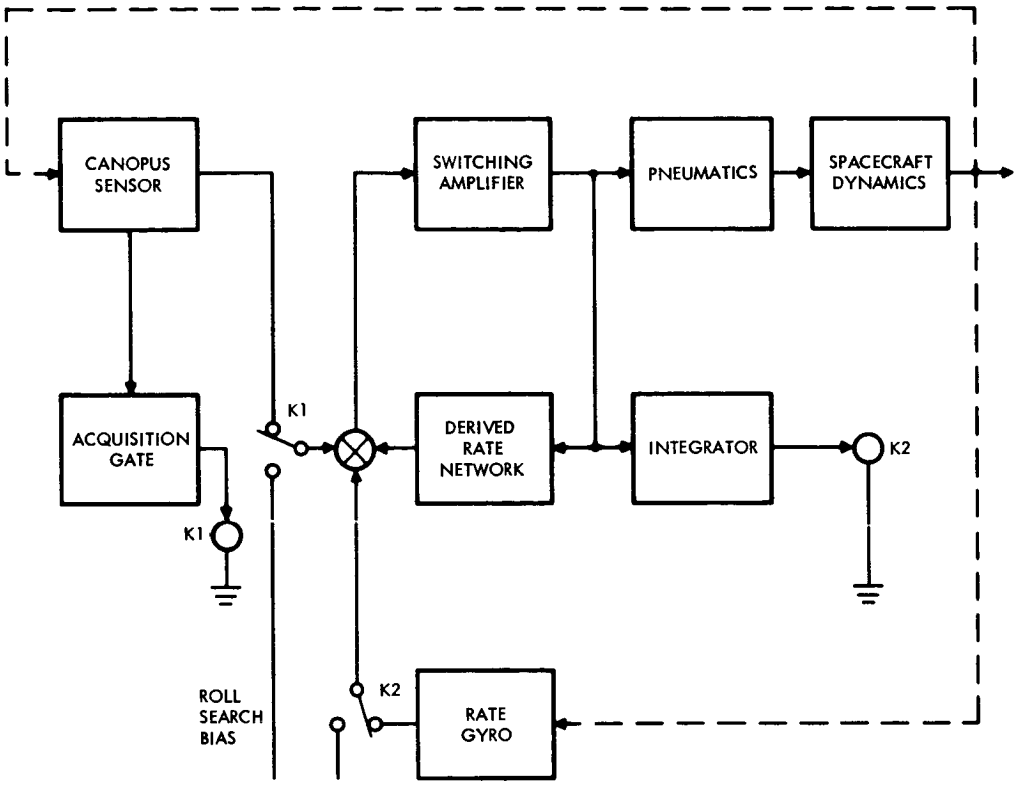

Figure 14. Typical Canopus Acquisition Configuration

The gas consumption during acquisition can be estimated by neglecting the effects of cross coupling terms, overshoots and limit cycling. Thus, the problem is reduced to computing the gas weight required for nulling angular momenta. After injection motor burnout the spin rate about the roll axis will be of the order of 60 rpm. If the roll moment of inertia is about 90 slug-ft^2, the angular momentum will be about 566 ft-lb-sec. Assuming a wobble angle of 2.5 degrees, the transverse component of angular momentum will be 24.7 ft-lb-sec. If the yaw and pitch moments of inertia are of the order of 200 slug-ft^2 the transverse component of rotation will be about 0.1234 rad/sec or 7.08 deg/sec. The gas weight required to null a rate of 7.08 deg/sec if it were only in one axis is given by

$$W = \frac{2J\omega}{\ell I_{sp}} = 0.137 \text{ lb}$$

where the moment arm ℓ and the specific impulse I_{sp} have been assumed to be 6 feet and 60 seconds respectively. In the worst case, this rate is divided between pitch and yaw and the square root of two more gas is required or 0. 194 pound.

Assuming a roll rate of about 2 rpm, the gas weight required for nulling the roll angular momentum will be of the order of 0. 10 pound. The total gas consumption for initial acquisition will be 0. 29 pound.

The sun acquisition time can be estimated by assuming it is equal to the time required for reducing the rate of one axis to the search value, plus the search time, plus the time to decelerate to zero rate. The longest possible thrusting time is obtained when the initial rate of 5 deg/sec is reduced to zero and then the system is accelerated to the search rate and finally it is returned to zero. Assuming a search rate of 0. 2 deg/sec, the total speed change is 5. 4 deg/sec. The acceleration produced by thrusting is

$$\dot{\omega} = \frac{T}{J} = 6 \times 10^{-4} \text{ rad/sec}^2$$

where J = moment of inertia = 200 ft lb

T = torque = 0. 02 lb x 6 ft = 0. 12 ft-lb

Consequently, the time to reduce the total 5. 4 deg/sec rate to zero is 146 seconds. The search time is estimated by assuming a maximum search angle of 180 degrees. At a search rate of 0. 2 deg/sec the maximum time that could be spent in this maneuver is 900 seconds. Therefore, sun acquisition might take approximately 15 minutes. Canopus acquisition consists of the time for reducing the roll rate to the search value of 0. 1 deg/sec, plus the time to find Canopus, plus the time to acquire it. Finding Canopus might take up to 360 degrees rotation in the worst case. Consequently, the roll acquisition process will take 60 minutes approximately.

2.6.3.4 Pneumatic System

The configuration selected for the Advanced Planetary Probe employs a total of 12 nozzles, with one solenoid valve for each nozzle. The nozzles

produce pure couples. There are two independent nitrogen supply systems and each gas jet in a coupled pair is supplied by one of these separate systems to insure the attitude control system will be operative in the event of a single failure. If a valve fails to open, the only effect will be a reduction of torque, because the resulting unbalanced forces alternate in sign during limit cycle operation and therefore the linear impulse imparted to the spacecraft tends to have zero average value. If a valve fails to close, the disturbance torque it applies to the spacecraft will be counteracted by the opposite coupled pair. The control system will be spending additional gas to maintain the desired attitude against this disturbance until the gas supply for the failed valve is exhausted. Therefore, to be able to complete the mission even when such a failure has occurred, three times the required gas weight must be carried in the two redundant tanks. The system also protects against regulator failures in the same way it protects against valve failures. The effects of a completely open regulator failure will be minimized by proper placement of the relief valve vent so that the disturbance torque is within the capability of the remaining half of the system. To provide protection against leakage failures, redundant seating techniques are used in the solenoid valves as well as in the pressure regulators.

Gas weights for mission durations of 650 and 720 days have been estimated as indicated in Table 5. Because of the gas redundancy, in a normal mission the gas supply should be adequate for 6-7 years after encounter.

2.6.4 Communication

The communication subsystem is identical with that of the spin-stabilized version. The modulator exciters, power amplifiers, and receivers are the same as are the antennas, diplexers and switches. The two position feed on the high gain antenna is not required and the helix antenna has 3 db more axial gain since it need not be canted as on the spinner.

2.6.5 Data Handling

The data handling system is basically the same as for the spin-stabilized version. The same digital telemetry unit and tape recorders

Table 5. Gas Weights (lb)

	Mission Duration	
	650 Days	720 Days
Cruise Mode	1.08	1.19
Initial Acquisition	0.29	0.29
Subsequent Acquisition	0.60	0.72
Solar Radiation Pressure	0.33	0.35
Leakage	0.88	1.11
Maneuvers	0.36	0.36
Totals Required	3.54	4.02
Redundancy	7.08	8.04
Totals	10.6	12.1

are used, but the logic for the integrated decoder and sequencer has been increased to account for the addition of 14 commands and the attitude acquisition sequencer.

2.6.6 Command Distribution

Command distribution equipment is essentially the same except for the addition of switching for 14 more commands and the additional cabling and connectors associated with the gyro assembly. See Section 8.6 of Volume 2.

2.6.7 Propulsion

The propulsion system for the 3-axis stabilized spacecraft with a 50-pound payload is essentially the same as that used for the 50-pound payload, spin-stabilized vehicle. The changes involve some additional propellant since the spacecraft is 73 pounds heavier, the removal of the aft thruster, and the incorporation of jet vanes in the forward thruster to insure that the thrust vector passes through the vehicle center of gravity at all times during operation. The jet vane assembly will be very similar to the unit used on Ranger and Mariner.

The amount of propellant required is 24.5 pounds for the 565-pound spacecraft to impart a velocity increment of 100 m/sec. The blowdown feed system tankage would be 0.5 pound heavier than the spinning configuration due to the increase in tank size for the additional 6.6 pounds of propellant. The removal of one thruster, valves, lines and sensor resulted in a reduction of 2.8 pounds. As on the spinner, additional propellant is supplied by this system for the design following the TE-364-3 spin stabilized injection.

2.6.8 Thermal Control

The thermal control subsystem is again essentially identical with that of the spin stabilized version. Thermal switches to a radiating panel are used with insulation to provide the required thermal environment. See Section 8.8 of Volume 2. The slightly increased heat leaks associated with the addition of the scan platform are compensated by the increased power dissipation of this spacecraft. A detailed analysis of the effects of transverse thermal gradients upon the large antenna structure when the sun is off axis will also be required.

2.7 SPACECRAFT RELIABILITY

The reliability analysis for the 3-axis stabilized, 50-pound payload configuration is basically the same as for the spin-stabilized version except for the attitude control system modifications and some of the separation and deployment requirements.

The critical difference is in the attitude control system. A gyro assembly is needed during midcourse firing to provide a reference and controls. This requirement for the use of a gyro package early in the mission would not reduce the estimated system reliability much below that needed for the spin-stabilized version. However, during the Jupiter encounter there will be a solar occultation to satisfy experiment objectives. Since the sun reference will be lost and since it is necessary to maintain body attitude during occultation the gyro package will again be in line. Using gyros, even such highly reliable ones as those developed for Mariner 4, would lead to a completely unsatisfactory reliability estimate if the gyro were to run the full duration of the mission. On the other hand, there appears to be no clear way of determining whether or not a gyro

will start up again in the spacecraft environment after it has been shut down for two years. Either approach then leads to unsatisfactory results.

For this reason an air bearing gyro of the Autonetics G10 type has been assumed for this reliability estimate, and it is also assumed that it is run in a low speed, low power mode throughout the life of the mission. This device has an estimated failure rate of 2000 bits. Since two gyros are required for all three axes, the estimated reliability for 750 days is 0.922. An alternate gyro being investigated at JPL is the Honeywell GG159. Since this also has a gas bearing, its reliability may also be satisfactory. In addition, the 3 axis control system has 12 jets where the spin-stabilized system has only two, and, although these jets are redundant in both cases, the reliability of the pneumatic system is reduced by about a factor of six for the main failure mode of a leaky solenoid valve. However, since the failure rate for a single valve is 200 bits, the effect is small.

The electronics for both systems are estimated to have about equal reliability. There are also some additional commands required which reduce slightly the reliability of the integrated decoder sequencer and the command distribution unit. Also the addition of jet vanes to the propulsion system reduce the reliability by a small factor. There is also additional power conversion needed for the gyro assembly and hence the reliability of the power control unit is reduced. The overall estimated reliability of the 3-axis spacecraft is estimated to be approximately 0.7, as shown in Figure 15.

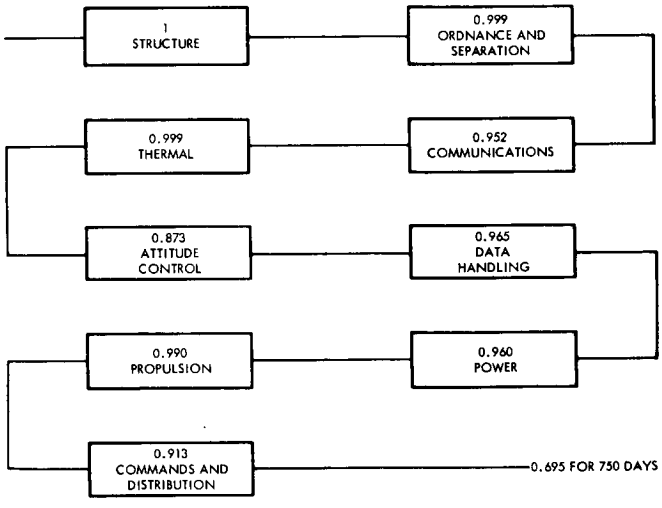

Figure 15. Reliability Block Diagram, Three-Axis Stabilized 50-Pound Science Payload

The critical item in the estimate is the failure rate of the gyros. This failure rate remains a relatively unreliable estimate since the proposed gyros are not yet fully developed. However, if they perform as a larger G-6 version has performed on the Minuteman, the estimate is reasonable.

2.8 SCHEDULE

The schedule given for the spin-stabilized version in Section 11 of Volume 2 appears to be completely compatible with the 3-axis system. However, to insure that the reliability objectives are achieved, it would be desirable to begin gyros work during Phase C and insure that a complete test program could be carried out within the entire program schedule without any possible schedule problem.

2.9 COST ESTIMATE

The cost estimate for this 3-axis, 50-pound payload spacecraft, given in Table 6, differs from the cost estimate for the spin-stabilized version in the following ways:

1) Program management, system engineering data management, are assumed to be essentially unchanged since it is primarily program duration which governs these costs. The somewhat increased complexity of the spacecraft should not have any significant effect upon these elements.

2) The structural subsystems are similar but the alignment tolerances are less stringent and the RTG's do not need to be deployed. The movable feed on the high-gain antenna is not required.

3) The thermal subsystem is essentially identical, although there will be additional cost associated with the analysis and test of the behavior of the deployable antenna under off-axis solar illumination which can be as high as 30 degrees. The effect does not occur on the spinner since the spinning causes transverse thermal gradients to be averaged out.

4) The electrical integration equipment is more complex because of the addition of items to the attitude control system and the additional commands.

5) The power subsystem (which does not include the RTG costs) is again somewhat more complex because of the added power requirements for attitude control.

Table 6. Estimated Costs for the 50-Pound Payload 3-Axis Stabilized Spacecraft (29-Month Program)

	Nonrecurring*	Recurring**	Total
Program management	1.6	1.0	2.6
System engineering	1.6	0.4	2.0
Data management	0.7	-	0.7
Structure	1.9	0.3	2.2
Thermal	0.9	0.1	1.0
Electrical integration equipment	0.9	0.1	1.0
Power (RTG interface and power conversion)	0.8	0.1	0.9
Data handling and command	1.6	0.5	2.1
Tape recorder	1.5	1.0	2.5
Communication	1.4	0.4	1.8
Deployable antenna	1.4	0.1	1.5
Attitude control	3.0	0.5	3.5
Midcourse and despin	1.9	0.2	2.2
Spacecraft integration and test	2.8	1.6	4.4
Reliability	0.9	0.6	1.5
Quality assurance	1.9	1.7	3.6
Electronic GSE	2.1	-	2.1
Mechanical GSE	0.7	-	0.7
TRW launch support	-	0.5	0.5
Planetary scan platform	0.8	0.2	1.0
	28.4	9.4	37.8

*(1 set qual units, 1 prototype)
**2 flight units and selected spares

6) Data handling and commands are almost the same except for a small factor for a few additional commands.

7) Tape recorder costs are the same.

8) The communication subsystem is essentially the same, but eliminating the requirement for conical scan will reduce antenna testing requirements.

9) Midcourse propulsion will be increased by the addition of the jet vanes and the associated test requirements.

10) The attitude control system is entirely different, using sun and Canopus sensors, a gyro package, and different electronics. In addition the attitude control system requires more pneumatics. However, the cost of the spin-stabilized version included the development of a conical scan technique which has not yet been proven. Hence the development cost for the spin-stabilized attitude control subsystem was significant and the cost difference is not as large as the increased equipment might indicate.

11) Spacecraft integration and test is estimated to have the same cost as the spinner because the added complexity in the attitude control system is offset by the somewhat simplified test requirements for the 3-axis system.

12) Reliability and quality assurance cost will be increased somewhat because of the added components, and considerable effort must be given to assure adequate reliability of the gyro assemblies.

13) Electrical GSE cost will again be increased somewhat to take care of the additional requirements of the attitude control system. Cost for mechanical GSE will be about the same as will be the cost of launch support.

2.10 COST EFFECTIVENESS

Cost effectiveness of the 3-axis stabilized spacecraft configuration can be evaluated by applying the criteria previously adopted for the spin-stabilized version (Section 12, Vol. 2), since the major design concepts, system constraints, and functional requirements remain unchanged. However, design differences affect the following spacecraft characteristics.

- Weight
- Complexity of design and operation
- Reliability

- Payload capability
- Choice of primary and backup modes of operation.

The slight weight increase of the 3-axis stabilized over the spin-stabilized spacecraft (70 pounds) may demand a launch vehicle with improved upper stage performance to achieve an adequate weight margin. The cost of the uprated launch vehicle and its availability at an early mission date must therefore be considered. This section will, however, be concerned with the cost-effectiveness implications of the altered spacecraft itself.

Table 7 lists design characteristics and other factors by which the two configurations differ significantly. The table facilitates a comparative evaluation of these characteristics for the purpose of deriving cost-effectiveness criteria. The most prominent differences are noted in two areas: (1) the sensor and actuator complements required to perform the attitude control functions, and (2) the constraints imposed on payload sensor arrangement and the extent to which payload sensing functions are facilitated by the stabilization technique employed.

These differences appreciably affect spacecraft design complexity, operational complexity, system and subsystem interfaces and constraints, and hence system reliability, hardware cost, development engineering, test requirements, etc.

On first glance, it would appear that the lower complexity of attitude control implementation, and hence the somewhat higher reliability, the smaller development risk, and the lower cost inherent in the spin-stabilized model give a clear preference to this design versus the three-axis configuration. However, in order to arrive at a fair comparison of the merits of each configuration in achieving the mission objectives a careful evaluation of the effects of attitude control on payload operation is required. In general, a greater flexibility of payload utilization is achieved by three-axis stabilization at the price of somewhat higher complexity and cost. Sections 2.7 and 2.9 have presented cost and reliability data in detail. The following additional factors must be considered in the comparison:

- Use of a one-gimbal scan platform and tippable mirror on the three-axis configuration yields higher-resolution TV images because of reduced body motion smear and avoids critical TV exposure timing problems.

Table 7. Comparison of Spin-Stabilized and 3-Axis Stabilized Spacecraft Systems

	Spin-Stabilized	Three-Axis Stabilized
Attitude Control	• RF earth tracking	• Sun/Canopus references
	*• Simpler implementation	• Offsetable sun sensor null
		• More complex sensor complement; more weight and power required.
		• More complex acquisition sequence
	• Midcourse maneuver orientation by open-loop precession demands accurate timing of precession sequence and calibration of gas jet forces.	*• Midcourse maneuver orientation under gyro control, more precise
	• Attitude perturbation on micrometeoroid impact averages out	• Continuous gas expenditure (limit cycles)
	• Either system capable of automatic reacquisition if requisite logic sequence is programmed into command and sequence unit	
	*• Sun occultation is no concern	• Sun occultation presents orientation and reacquisition problems (gyro lifetime)
Payload Operation	*• Automatic scan capability	*• Improved TV resolution
	• Constraints on payload arrangement and performance	• Gimbaled scan platform(s)
		• Greater flexibility of payload utilization.
Launch Vehicle	*• Lowest cost launch vehicle SLV 3X/Centaur/TE-364-3	• 70 pound weight increase may require uprated third stage (TE-364-4)
		• Cost increase
DSIF and Ground Support Interfaces	• RF tracking uses DSIF signal, hence some DSIF station tieup before maximum gain achieved	• Requires updated sensor bias commands from ground (or more complex on-board programming) hence some DSIF station tieup before maximum gain achieved
	• Two position high gain feed removes critical boresight error problems	*• Can remove boresight and sun sensor offset errors on basis of ground-received signal strengths
	• For both configurations DSIF tie-up only prior to and during infrequent telemetry sessions.	
Trajectory Accuracy	• Uncertainties due to unbalanced attitude control forces (e.g., earth tracking, balancing of solar pressure torques) (could be removed by doubling number of jets and gas requirements)	*• No unbalance in normal operation (Gas requirements could be reduced by using single jets but uncertainties would then be added)
	*• Gas leakage cancels out	• Gas leakage may produce appreciable miss uncertainty
Spacecraft Configuration	• RTG must be deployed	*• RTG in fixed position
	*• No movable scan platform, etc.	• Scan platform and other gimbaled sensor support (see Payload Operation)
Thermal Control, Power, Electrical Integration	• Spin rate averages thermal influences	• Since greater power margin greater tolerance for heat leaks
		• More power, more power conditioning
	* Simpler electrical integration	• More complex electrical integration (attitude control electronics, flex leads on gimbaled packages, etc.)

*Indicates significant advantage

- Preferred orientations of sensor axes during interplanetary cruise and Jupiter flyby can be obtained more easily by body-mounted sensors on the nonspinning spacecraft

- Flexibility of sensor orientation in primary or backup modes of payload operation may be obtained by spacecraft reorientation, e.g., a limited roll excursion; this flexibility can be incorporated into the three-axis controlled spacecraft concept more readily than into the spinner. This would be desirable for coverage of unexpected physical phenomena in the interplanetary or planetary environment

- On the other hand, continuous 360-degree scan coverage is automatically provided by the spinner as compared to the required multiple-aperture arrangement or gimbal-mounting of sensors in the nonspinning configuration

- Attitude control jets in greater numbers, operating at frequent intervals, and mounted in close proximity to the payload instruments may present problems of undesirable interaction with the sensors in the three-axis stabilized version. This problem requires further study.

Comparison of the respective advantages of each configuration in regard to payload arrangement and operation does not lead to a clearly defined preference. It is further seen that neither the slight cost increase nor the reliability reduction of the more complex three-axis configuration is sufficient ground for preference of the simpler spin-stabilized configuration. However, for the purpose of achieving precursor missions to Jupiter and the outer planets, the reduction in spacecraft complexity achievable by the spinner is of greatest concern. The more sophisticated payloads and greater system flexibility required for subsequent missions make the use of three-axis stabilization more appropriate for these.

In summary, the somewhat higher calculated reliability for the spinner of 0.79 versus 0.70 for the three axis, the lower weight by about 14 percent, and the lower cost of approximately 14 percent, reflect the lower complexity for the spinner. In view of all the imponderables involved in a Jupiter mission such as meteoroid flux and possible subsequent changes in meteoroid protection weight, difficulty of achieving asymptotic reliability and a presumed desire for minimum cost and maximum schedule confidence, it seems appropriate to favor the simpler

system which also has the greatest margin for weight increase or flight time decrease. But the differences are small and the three-axis spacecraft promises improved TV resolution and possibly better aural and infrared data because of the removal of the spin scan.

In any case, the fundamental conclusion is that either will provide an inexpensive, high capability, Jupiter mission for 1972 and, as will be seen in Section 3, for Jupiter missions for all launch opportunities. In Section 4, it is shown that using the Titan 3CX/Centaur/TE-364-3, either spacecraft is suitable for both direct and Jupiter swingby missions to any of the outer planets except direct flights to Pluto.

3. SPACECRAFT FOR THREE ALTERNATE SCIENCE PAYLOADS

This section discusses three spacecraft configurations designed around science payloads of 12, 100, and 250 pounds. The objective of this portion of the study was to determine the effects of varying payload sizes upon mission characteristics, science objectives, and spacecraft design. For comparison, the spin-stabilized configuration carrying a 50-pound payload is illustrated in Figure 16.

The basic conclusions are that the spacecraft carrying a 12-pound science payload does not perform as effective a mission as the spacecraft carrying a 50-pound payload for two reasons: first, the payload is not in itself comparable with the 50-pound payload since the experiment objectives are greatly limited. Second, although this spacecraft weighs only 287 pounds there is no lighter weight, lower cost booster than the SLV 3C/Centaur/TE-364-3 which can place the spacecraft of this weight to Jupiter. Since the 50-pound payload also uses the same booster the only saving is in flight time. The 50-pound payload spacecraft can make the transfer in a minimum of about 600 days while the 12-pound payload spacecraft can make it in a minimum of 470 days. This savings in flight time will increase spacecraft reliability but this improvement does not outweigh the enhanced science capability of the 50-pound spacecraft.

On the other hand, the spacecraft with 100- and 250-pound science payloads perform a greater depth of science but only of Jupiter and only at the expense of requiring a larger, more expensive launch vehicle. The interplanetary science is essentially complete in the 50-pound payload and additional weight does not seem useful for increased interplanetary science capability. Both these large science payloads would substantially increase the planetary data, particularly the TV data. To take best advantage of this increase in encounter science it is recommended that such large payloads be used with the 3-axis stabilized system.

The encounter time at Jupiter is largely a function of the resolution of the planetary observing instruments; that is, the higher the resolution, the earlier the observations may begin with a corresponding increase in the total amount of data gathered. Both an increase in optics size and an

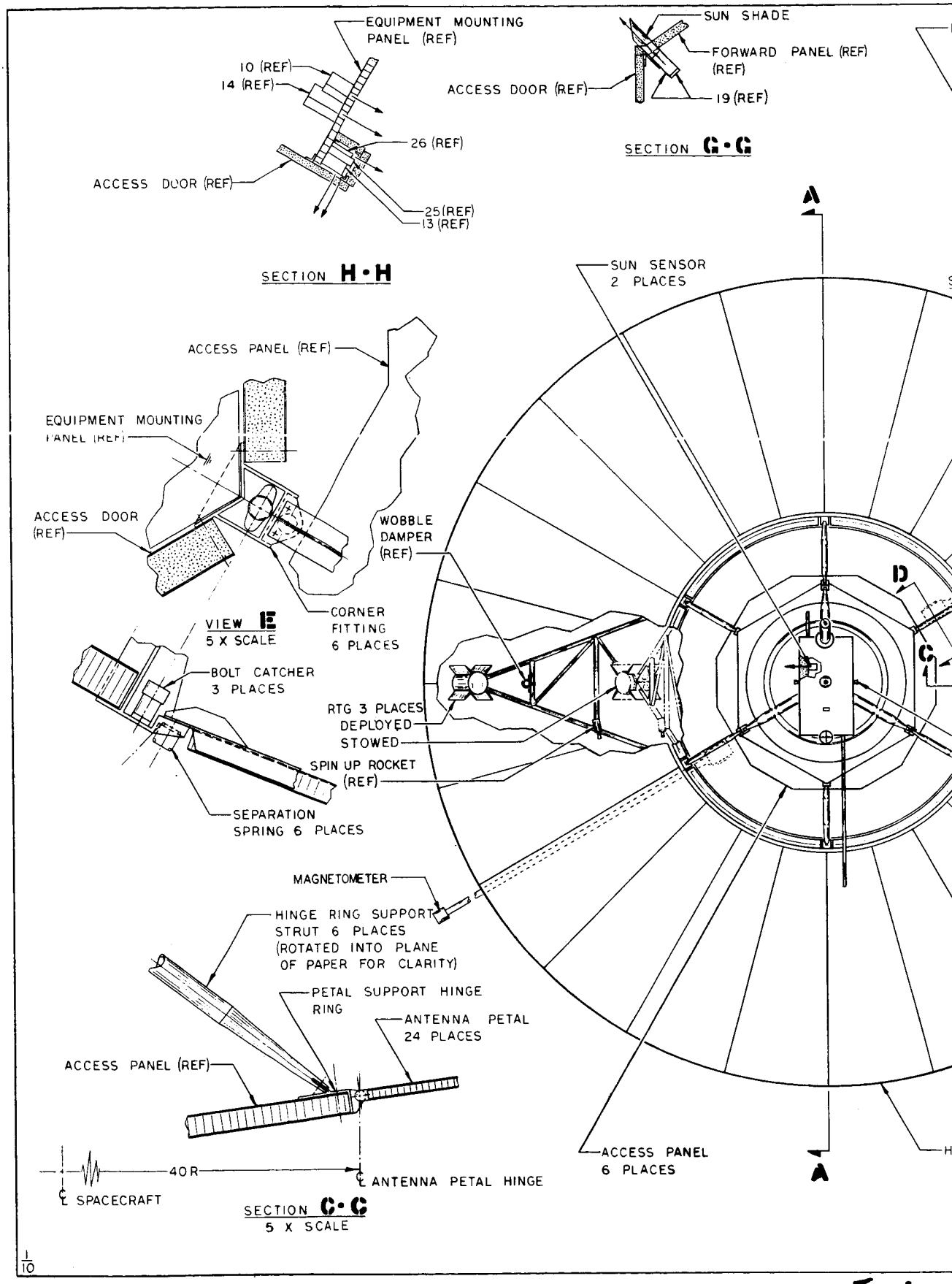
EQUIPMENT MOUNTING PANEL (REF)
10 (REF)
14 (REF)
26 (REF)
ACCESS DOOR (REF)
25 (REF)
13 (REF)
SECTION H•H
SUN SHADE
FORWARD PANEL (REF) (REF)
ACCESS DOOR (REF)
19 (REF)
SECTION G•G
SUN SENSOR 2 PLACES
ACCESS PANEL (REF)
EQUIPMENT MOUNTING PANEL (REF)
ACCESS DOOR (REF)
WOBBLE DAMPER (REF)
CORNER FITTING 6 PLACES
VIEW E 5 X SCALE
BOLT CATCHER 3 PLACES
RTG 3 PLACES
DEPLOYED
STOWED
SPIN UP ROCKET (REF)
SEPARATION SPRING 6 PLACES
MAGNETOMETER
HINGE RING SUPPORT STRUT 6 PLACES (ROTATED INTO PLANE OF PAPER FOR CLARITY)
PETAL SUPPORT HINGE RING
ANTENNA PETAL 24 PLACES
ACCESS PANEL (REF)
40R
℄ SPACECRAFT
℄ ANTENNA PETAL HINGE
SECTION C•C 5 X SCALE
ACCESS PANEL 6 PLACES
A
A
D
G
H

1/10

65-1

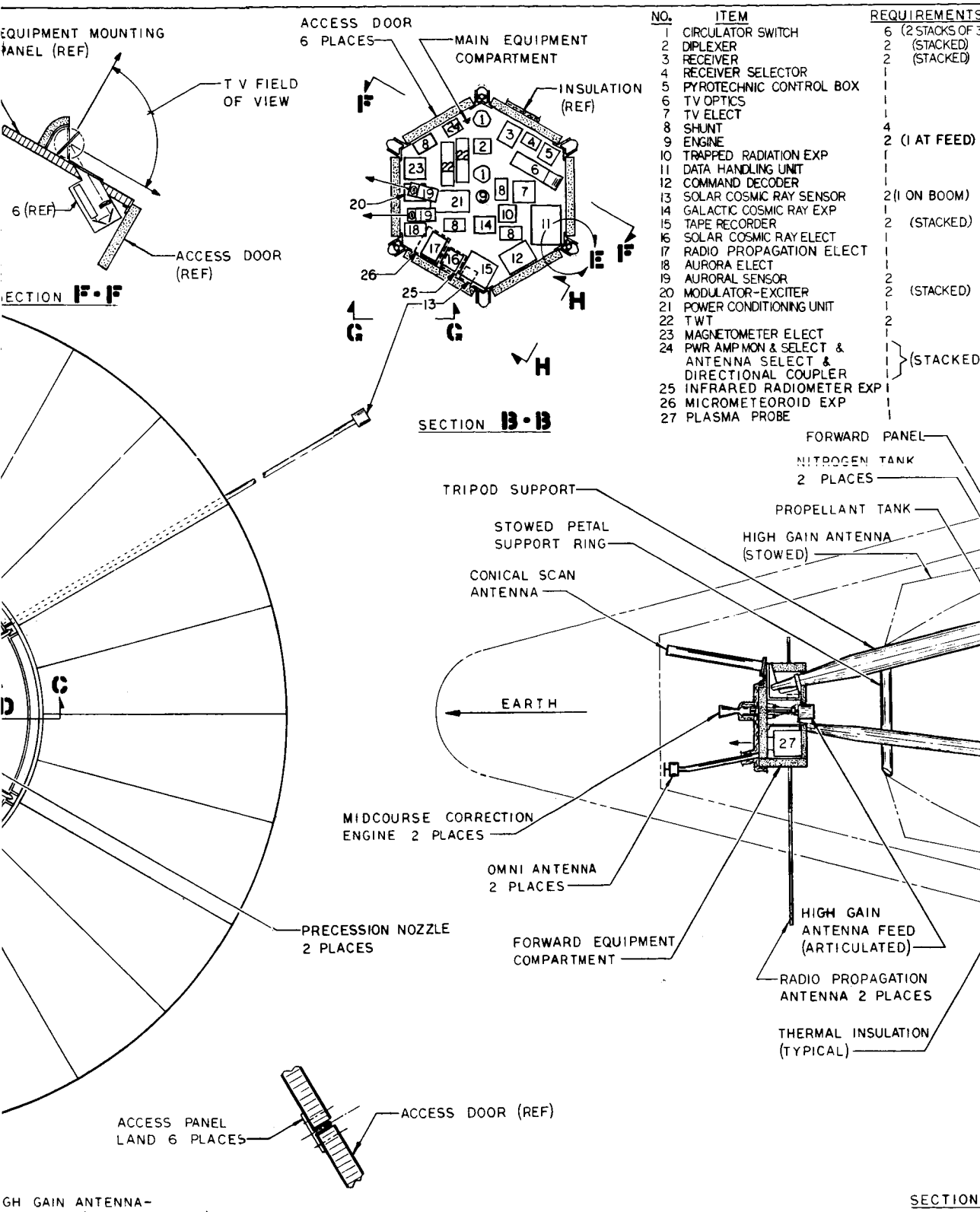

NO.	ITEM	REQUIREMENTS
1	CIRCULATOR SWITCH	6 (2 STACKS OF 3)
2	DIPLEXER	2 (STACKED)
3	RECEIVER	2 (STACKED)
4	RECEIVER SELECTOR	1
5	PYROTECHNIC CONTROL BOX	1
6	TV OPTICS	1
7	TV ELECT	1
8	SHUNT	4
9	ENGINE	2 (1 AT FEED)
10	TRAPPED RADIATION EXP	1
11	DATA HANDLING UNIT	1
12	COMMAND DECODER	1
13	SOLAR COSMIC RAY SENSOR	2 (1 ON BOOM)
14	GALACTIC COSMIC RAY EXP	1
15	TAPE RECORDER	2 (STACKED)
16	SOLAR COSMIC RAY ELECT	1
17	RADIO PROPAGATION ELECT	1
18	AURORA ELECT	1
19	AURORAL SENSOR	2
20	MODULATOR-EXCITER	2 (STACKED)
21	POWER CONDITIONING UNIT	1
22	TWT	2
23	MAGNETOMETER ELECT	1
24	PWR AMP MON & SELECT & ANTENNA SELECT & DIRECTIONAL COUPLER	1 (STACKED)
25	INFRARED RADIOMETER EXP	1
26	MICROMETEOROID EXP	1
27	PLASMA PROBE	1

GH GAIN ANTENNA-
DEPLOYED (16 FT DIAMETER)

SECTION

65-2

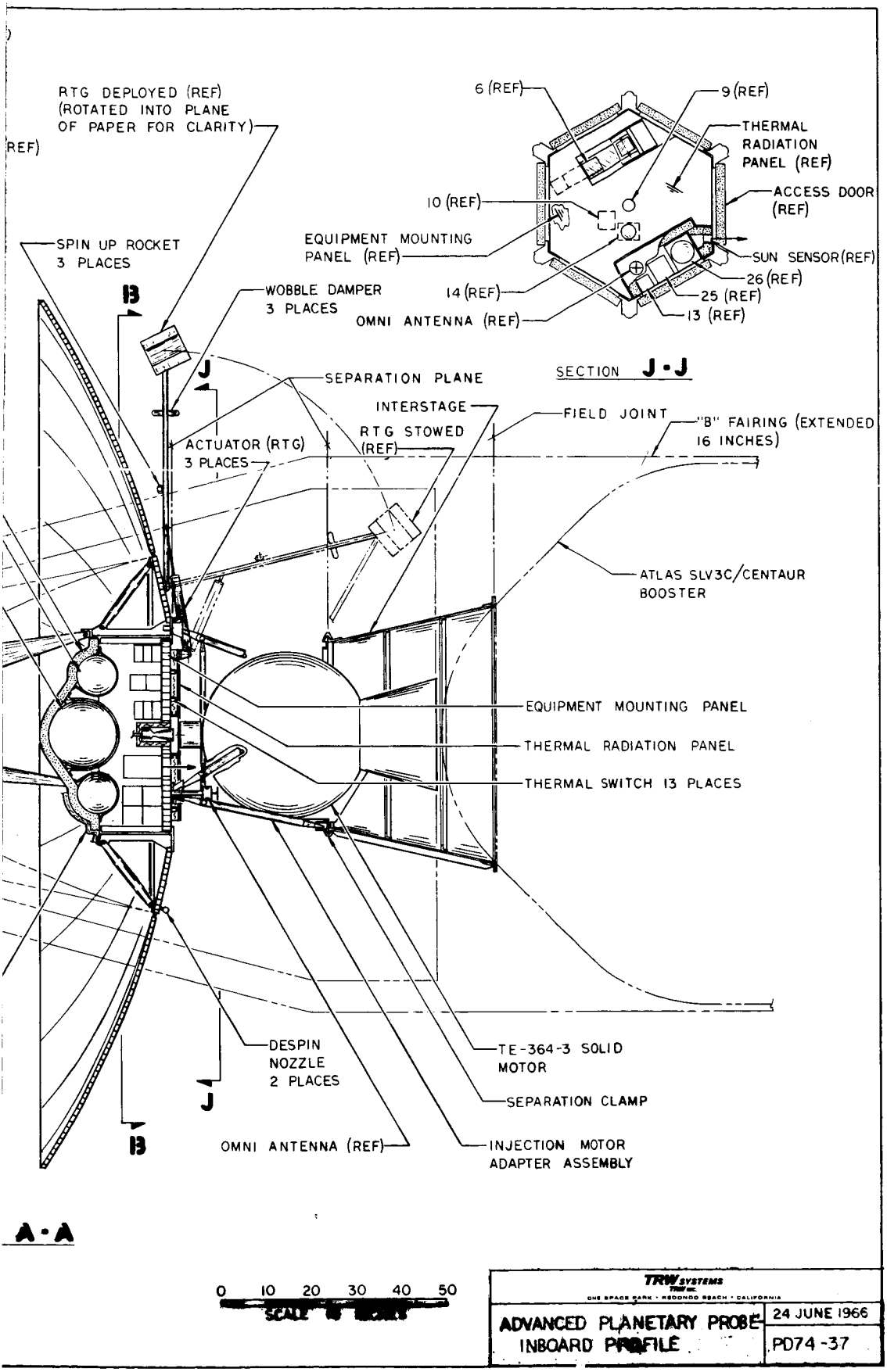

Figure 16. Advanced Planetary Probe In-Board Profile

improvement due to the removal of image smear due to spin scan can be used. The 100-pound science payload spacecraft resolution should be increased by about a factor of 10 over the 50-pound science, 3-axis stabilized system, which means that picture taking can begin at about 1000 Jupiter radii with a picture transmitted back in real time about once every 25 minutes. With the 250-pound science payload picture taking could begin even earlier with still larger TV optics. This combined with improved communications data rate commensurate with a larger spacecraft system would allow perhaps two orders of magnitude increase in total pictorial data over the 50-pound science 3-axis stabilized system. Additional tape storage would be added for these larger payloads which means that more very high resolution pictures could be taken at close approach and transmitted back after encounter. But in general both the pre-encounter and post-encounter overall data gathering capabilities dominate flyby missions, and therefore such data must be given some priority. As discussed in Section 7, it is the transitory nature of the encounter for a flyby mission which makes orbiters appear very attractive for these larger payload classes which stress encounter science.

3.1 FUNCTIONAL REQUIREMENTS

The functional requirements for the 12-pound science payload are basically the same as those for the 50-pound science payload. However, only three experiments are carried:

- Magnetometer
- Micrometeoroid detector
- Trapped radiation detector

Since none of these experiments require direct planetary observation, the encounter mode of the mission is considerably simplified, and since these experiments have no requirement for 3-axis orientation a spin-stabilized configuration with its inherent simplicity and reliability is most suitable.

The functional requirements for the 100- and 250-pound science payloads grow out of the increased planetary science data to be gathered, and of particular importance is the desire for higher resolution television data. Although the resolution of a spin-stabilized television system can

be increased by decreasing the spin rate, the additional payload capability of these larger spacecraft encourage the use of narrower field of view optics, which in turn require longer exposure times. For the spinner described earlier, the exposure time was limited to 0.5 millisecond, but with a 3-axis controlled system the exposure time would be limited to the body rates which would allow exposure time on the order of 2 seconds. Such long exposure times are not necessary, but resolution could be clearly increased by perhaps two orders of magnitude with the limit being controlled by factors other than exposure time such as the difficulty of keeping Jupiter in the field of view at longer ranges. For these reasons it is recommended that both these spacecraft be 3-axis controlled.

3.2 12-POUND SCIENCE PAYLOAD

This section describes a spacecraft design concept for a 12-pound science payload consisting of a magnetometer, micrometeoroid detector, and a trapped radiation counter. The basic approach in this section has been to use the spin stabilized design presented in Volume 2, but appropriately lightened for the reduced power requirements and data rate requirements. The boost vehicle proposed is the Atlas SLV3C/Centaur/TE-364-3. The spacecraft weight is 287.5 pounds including 24 pounds of contingency but not including the 27 pound injection motor adapter assembly. The proposed boost vehicle can inject the spacecraft to Jupiter with a C_3 of about 122 which will give a nominal flight time over a 20 day launch of about 470 days to Jupiter.

3.2.1 Configuration

An in-board profile of the configuration, Figure 17, shows the spacecraft housed within a "B" fairing lengthened 16 inches. The general configuration of the interstage and the spacecraft adapter are generally the same as for the 50-pound, spin-stabilized configuration. Changes from that configuration include: 1) gauge and size of structure components for reduced loads, 2) since the spacecraft is well separated from the 42-inch diameter V-band clamp assembly, no bracketry is required to protect the spacecraft, 3) separation springs are reduced to match the reduced spacecraft size, and 4) since the RTG's are body fixed, no interstage support structure is required.

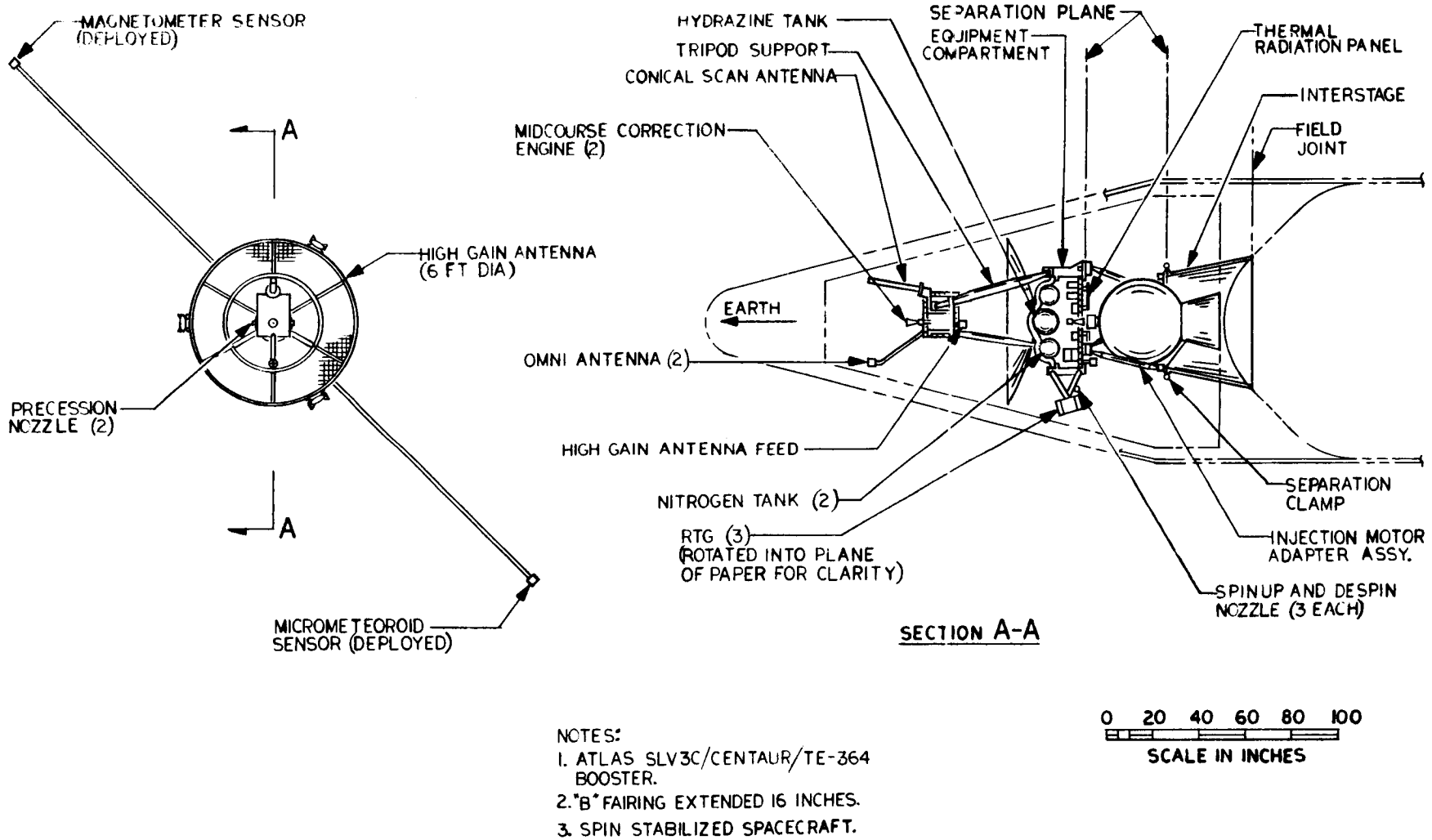

1/40

Figure 17. In-Board Profile of 12-Pound Science Payload Jupiter Flyby

The equipment compartment is similar to that of the 50-pound payload spacecraft except as follows: 1) the diameter is reduced to 34 inches and the average height to 12 inches since this accommodates all equipment, 2) trapped radiation experiment is located near the center of the compartment to minimize contamination from the RTG's, and 3) the midcourse propellant has been appropriately reduced in size as have the nitrogen supply for the orientation subsystem. The RTG units are body mounted for design simplicity and supply 63 watts of raw power. The spinup solid rocket motors, the despin nozzles, and three wobble dampers are mounted to the RTG titanium support struts.

The feed assembly is similar to that used in the 50-pound payload spacecraft but has been reduced in size since the solar plasma and radio propagation experiments are removed. The fixed high gain antenna feed is offset from the focal point to provide accurate earth tracking signals when the spacecraft is beyond Jupiter. For a Jupiter mission only, the offset helix will provide more than adequate signal from pointing the spacecraft. The high-gain antenna has been reduced in size to 6 feet and is a rigid nondeployable structure fabricated from wire mesh and aluminum tubular rings and radial members.

3.2.2 Mass Properties

A weight estimate of this spacecraft is given in Table 8. As can be seen, about the same micrometeoroid protection for this spacecraft is provided as for the 50-pound payload spacecraft. The weight of the communication system is the same as that for the 50-pound payload system except for the reduction in the high gain antenna weight. The command distribution unit has been reduced in size to match the reduced number of commands as has the data handling unit and the integrated decoder and sequencer. Only one tape recorder is carried. The cold gas supply, the hydrazine supply, cabling and connectors have all been reduced proportionally to satisfy system requirements. A contingency of 10 percent of all weights except for the scientific payload and propellants has been added. Table 9 gives the spacecraft moments of inertia and characteristics.

Table 8. Spin Stabilized Jupiter Fly-By Mission
12 Pound Science Payload

Item		Weight (lb.)
Structure and Thermal Control		61.8
Structure		28.2
Thermal control		6.7
Meteoroid protection		26.1
Radiation protection		0.8
Power Supply		57.4
RTG installation		47.1
RTG units (3)	43.0	
Boom assemblies (3)	4.1	
Power control unit (1)		8.0
Shunt elements (3)		2.3
Integration		22.0
Command distribution unit (1)		6.0
Umbilical (1)		1.5
Pyrotechnic control box (1)		4.5
Cabling and connectors		10.0
Data Handling		24.1
Data handling unit (1)		8.5
Tape recorder (1)		8.0
Integrated decoder and sequencer		7.6
Communications		33.6
Receiver (2)		7.0
Modulator/exciter (2)		3.0
TWT (2)		2.0
Circulator switch (6)		1.8
Diplexer (2)		2.0
Antenna selector (1)		0.5
Receiver selector (1)		0.5
Power Amp. monitor and selector (1)		1.0
Directional coupler (1)		0.5
Omni-antenna installation (2)		1.5
Helical antenna installation (1)		2.8
High-gain antenna installation (1)	(6 ft)	11.0

Table 8. Spin Stabilized Jupiter Fly-By Mission
12 Pound Science Payload (Continued)

Item		Weight (lb.)
Attitude Control		25.2
Reorientation system		16.1
Electronics assembly (1)	3.6	
Sun sensors (2)	1.5	
Nozzles, valves and plumbing	6.4	
Nitrogen	1.9	
Nitrogen tanks and residuals (2)	2.7	
Despin system		5.5
Spinup system		3.6
Propulsion		24.0
Nozzles, valves and plumbing		8.4
Usable propellant (100 m/sec)		12.8
Tank, residuals and pressurization		2.8
Dynamic Balance Weights		3.5
Scientific Payload		12.0
Contingency (10 percent, except science and propellant)		23.9
Spacecraft Weight		287.5

Table 9. Spacecraft Moments of Inertia and
Center-of-Gravity

Condition	Weight (lb)	$\overline{Z}$ (in.)	Moments of Inertia (slug ft.^{2}) I_x	I_y	I_z	Inertia Ratio I_z/I_x
Spacecraft prior to deployment of experiment booms	287.5	84.0	21.6	21.8	23.3	1.07
Spacecraft in cruise mode	287.5	84.0	28.7	39.0	47.8	1.23

3.2.3 System Characteristics

The operational sequence for this spacecraft will be similar to that for the 50-pound payload spacecraft except that neither RTG's nor the antenna need be deployed. The solid-propellant motors provide third stage and spacecraft spinup. After TE-364 firing, a hydrazine despin system will be used to bring the spacecraft down to an appropriate spin rate, which need not be as low as that for the 50-pound payload since there is no TV experiment. The booms with the magnotometer and the micrometeoroid detector will again be deployed after the first midcourse correction to minimize wobble during the midcourse reorientation maneuver. The spacecraft will acquire the earth in the same open loop maneuver, and fine pointing to the earth will be accomplished with the helix antenna; the offset feed of the high-gain antenna will provide earth pointing at very long ranges and serve as a backup for the helix. The same amount of redundancy allowing for the reduced size of the components is carried except that there will be only one tape recorder, which raises the importance of the backup real time mode of operation for the spacecraft. Such a mode is compatible with the limited data requirements for this spacecraft if a variable data rate for these experiments such as 8, 16, 32 and 64 bits/sec can be used. The spacecraft can transmit 70 bits/sec out to 4.3 AU and 35 bits/sec at 6 AU. If higher resolution is required, the tape recorder could be used to store such data intermittently.

3.2.4 Subsystem Characteristics

The structure of the spacecraft is basically that of the 50-pound payload spacecraft except that it is smaller and the design has been simplified.

The power supply has been sized to supply 63 watts of raw power to meet the following requirements:

- Communications, 20 watts
- Electrical integration, 5.8 watts
- Data handling, 5.3 watts
- Attitude control, 6.5 watts
- Heaters, 10 watts
- Science, 9 watts
- Contingency, 6.4 watts

System degradation is allowed for and conversion losses are included in each subsystem requirement. The power control unit is a scaled down version of that for the 50-pound payload system as are the shunt elements. The attitude control system is again a scaled version of the 50-pound system except that the beamwidth of the high gain antenna is 5.2 rather than 1.9 degrees. A two position feed on the high-gain antenna does not seem justified since adequate tracking can be obtained with less than 1.0 db scan loss without any beam accuracy problems even well beyond the orbit of Jupiter. The cold gas torquing system and the electronics are the same except for thrust level sizing.

The communication subsystem for this spacecraft has been modified in two ways. First the antenna has been reduced to 6 feet in diameter providing about a 30-db gain rather than 38 db and the transmitter has been reduced from 10 to 4 watts reducing the overall effective radiated power by about 13 db considering scan loss. The effect of these reductions has been to reduce the possible bit rate by a factor of 20 which means that maximum bit rate at 6 AU is 35 bits/sec. The switching functions and the omni and helix antennas and the exciter are the same.

The data handling subsystem is also similar although the digital telemetry has been reduced since it need only process housekeeping data and data from three experiments. Similarly the decoder and sequencer have been simplified since there are fewer commands and sequencing. The reduced bit rate requirements of the experiments makes the inclusion of a tape recorder necessary but only to minimize ground station on time. With one tape recorder storing 6 million bits, an average data acquisition rate of 8 bits/sec is appropriate for the experiments. This means that the spacecraft can accumulate stored data for about 1.5 days, transmitting it back in eight hours at 6 AU and faster at shorter ranges. Earth pointing requirement, even early in the mission, will not require more frequent ground station on time than this since, when angular rates are high, the omni or helix antennas can be used.

The command distribution equipment including the command distribution unit and the cabling and connectors have been appropriately reduced in weight and size to match the desired spacecraft size. The

pyrotechnic subsystem is the same except for the removal of dish and RTG deployment functions.

The propulsion system is again the same as on the 50-pound payload spacecraft, with the amount of hydrazine and pressurant reduced. Two engines are provided at each end of the spacecraft to simplify the midcourse maneuvers and to allow for an earth line correction late in the mission in the event it is desired.

The thermal subsystem is a scaled version. To some extent the thermal control problem is more difficult since it is probable that the heat leaks have not reduced in proportion to the reduction in power dissipated in the compartment, even though the number of experiment apertures is reduced.

3.2.5 Reliability

A separate computer analyses of the reliability of this 12-pound payload spacecraft has not been made, but a hand calculation, using the data from the computer analysis to determine the reliability of this system, has been completed. Since the communications and altitude control subsystems are unchanged and the improvements in the digital telemetry unit, the integrated decoder and sequencer, and the command distribution unit, have only a small effect, the overall system reliability has increased only slightly. It is estimated that the reliability of this spacecraft is 0.81 for a 750-day lifetime.

Past flight experience with the types of experiments carried in this spacecraft indicate that their lifetime is very high and hence it appears that a balanced system is possible.

3.2.6 Cost and Schedule

It has been estimated that the cost of this spacecraft can be reduced a little more than 20 percent and the schedule shortened by about 3 months as compared to the 50-pound science class spinner discussed in Volume 2.

3.3 100-POUND SCIENCE PAYLOAD

This section and the next describe two spacecraft configurations which are versions of the configurations described previously. However,

they have been increased in size and capability to match an increased science payload. This section deals with a spacecraft matched to a 100-pound science payload.

3.3.1 Functional Requirements

The functional requirements for this 100-pound science payload spacecraft are generally the same as for the spin stabilized spacecraft discussed in Volume 2, except that additional experiments have been added. The interplanetary experiments are:

- Magnetometer
- Galactic cosmic ray
- Solar cosmic ray
- Solar plasma
- Micrometeoroid
- Radio propagation and occultation

The specifically planetary experiments are:

- Trapped radiation
- Microwave radiometer
- Low energy proton monitor
- Visual solar occultation
- Auroral detector
- A special magnetometer designed for high resolution of the very large magnetic fields at Jupiter
- A substantially improved television system whose resolution should be about two orders of magnitude better than that discussed under the television system for the spin stabilized configuration.

All of the requirements and their implications are the same as discussed for the spin-stabilized configuration except for the requirements imposed by the television. To achieve the high resolution requires that the camera have long exposure times, which means that the configuration must either be 3-axis controlled with a scan platform or a despun platform must be provided in the spin stabilized version. For simplicity, a 3-axis control system has been used.

The gross weight of this spacecraft is estimated to be 774 pounds including 59 pounds of contingency. To achieve a Jupiter flyby mission with this gross weight requires the use of the SLV3C/Centaur/HEKS or the Titan III CX/Centaur booster. The boost vehicle selected was the Titan III C/Centaur. A third stage is not required with the Titan. However, a third stage could be used to shorten flight time if so desired. As shown in Section 4, the use of the Titan III CX/Centaur/TE-364-3 boost vehicle allows the spacecraft to be used for direct or swingby missions to all of the outer planets with the exception of direct flights to Pluto, whose orbit is highly inclined to the ecliptic.

3.3.2 Spacecraft System Design

A drawing of this configuration is shown in Figure 18. As can be seen it is similar to the configurations previously discussed, with the following differences: the spacecraft is launched with a "B" fairing which has been extended 48 inches. The launch vehicle is the Titan III CX/Centaur and the spacecraft is shown attached to the Centaur stage. The interstage is a 54-inch truncated cone whose aft end mates with the 58.5-inch diameter bolt circle on the Centaur forward tank dome. This connection is the field joint between the booster and the spacecraft. The upper end of the interstage mates with the six corner fittings of the spacecraft. This mating point is the in-flight separation plane; the separation is the same as that given in Volume 2, Section 7.1. The interstage has aluminum rings and longerons and a magnesium skin. It provides a uniformly distributed structural load path around the Centaur field joint.

The equipment compartment is the same as that described in Volume 2, Section 7.1, except that the area has been doubled (53-inch diameter) and the height increased by 2 inches to accommodate the increased scientific payload and supporting equipment.

In addition a doubled gimbaled scan platform for the television and microwave radiometer experiment is mounted on the aft end.

The three RTG units are body fixed like those carried on the 3-axis stabilized 50-pound science payload spacecraft. Wobble dampers and third stage spin-up motors have been eliminated. The two magnetometers are deployed on DeHavilland booms similar to those used in the spin-stabilized version.

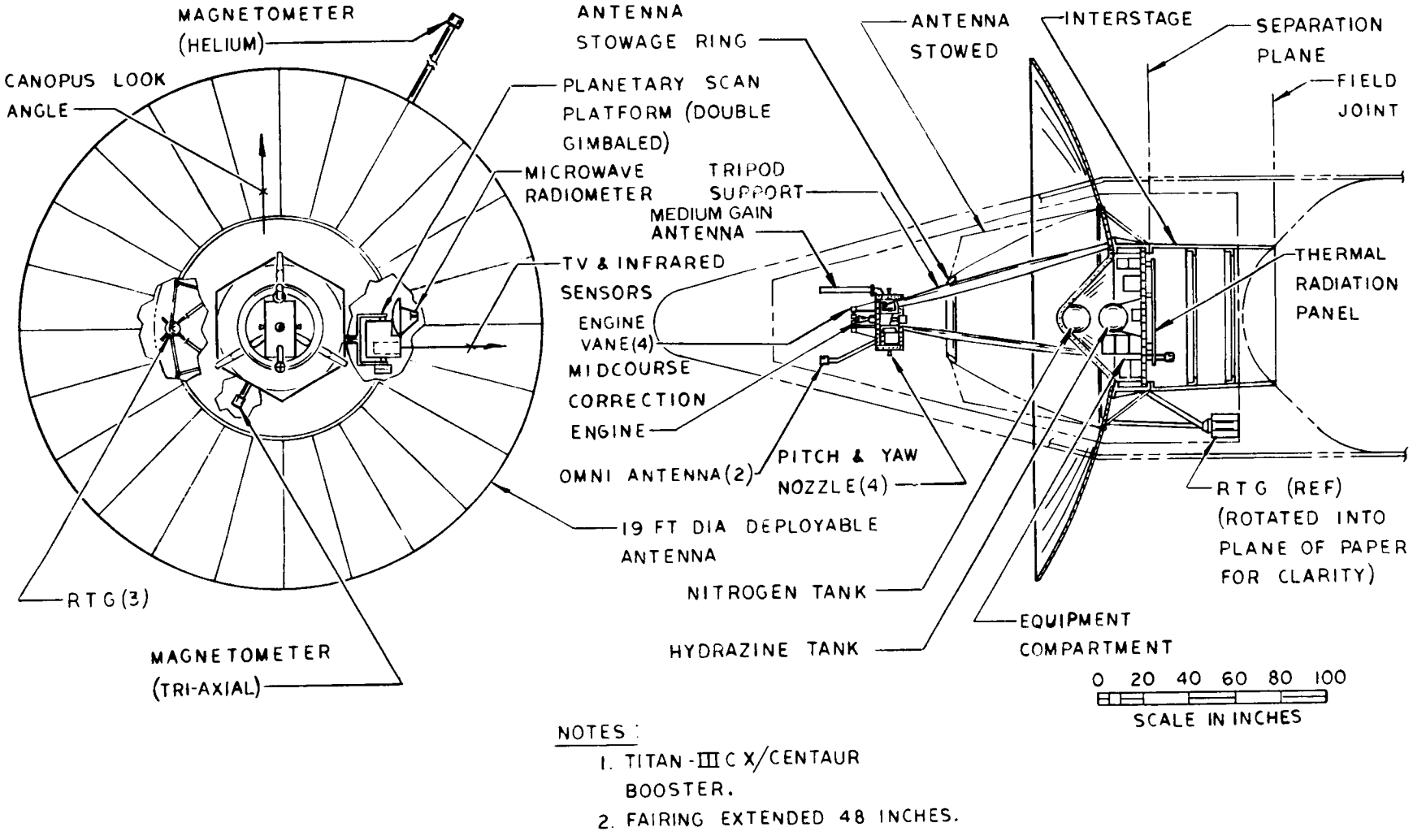

NOTES:

1. TITAN-IIIC X/CENTAUR BOOSTER.
2. FAIRING EXTENDED 48 INCHES.

1/40

Figure 18. Jupiter Flyby, 100-Pound Payload, Three-Axis Stabilized

The high gain antenna is similar in structural detail and geometry to that described in Volume 2 but the antenna has been increased to 19 feet in diameter. The feed assembly is the same as the 3-axis stabilized, 50-pound science payload. To increase reliability and total stored data three tape recorders are carried. Increased weight for command, sequencing, and data handling has been added. Since the vehicle is 3-axis controlled, only one midcourse engine is carried, located in the antenna feed assembly.

A weight estimate for this spacecraft is given in Table 10. As shown, the structure and thermal control and meteoroid protection have been increased in weight because of the increased compartment diameter and height and the increased diameter of the antenna feed assembly. The weight of the planetary scan platform is a scaled-up version of the Mariner Mars configuration.

The RTG units were increased to provide 141 watts of raw power and there are three additional shunt elements.

The attitude control subsystem is essentially identical to the 3-axis stabilized, 50-pound science payload configuration except for sizing. The gas requirements are based upon a 750-day mission, including limit cycling, acquisition, four reacquisitions, solar radiation pressure, and gas leakage. A safety factor of 3 was used, which gave total gas weight of 13.4 pounds.

The propellants for the midcourse propulsion have been reduced from 100 to 75 m/sec, since the injection accuracy of the Centaur stage alone is better than when a solid propellant spin-stabilized third stage is used.

Centroidal moments of inertia and center-of-gravity estimates were made for the spacecraft, prior to deployment of the antenna and before and after deployment of the experiment booms. These values are presented in Table 11.

3.3.3 System Performance

The basic performance of the spacecraft system is similar to that of the 3-axis, 50-pound science payload. However, the antenna diameter

Table 10. Weight Estimate — 3-Axis Stabilized Spacecraft with a 100 Pound Science Payload, Jupiter Flyby Mission

Item		Weight (lb.)
Structure and Thermal Control		160.2
Structure		59.7
Planetary scan platform		12.6
Thermal control		23.7
Meteoroid protection		62.2
Radiation protection		2.0
Power Supply		117.7
RTG installation		104.2
RTG units (3)	94.0	
Boom assemblies (3)	10.2	
Power control unit (1)		9.0
Shunt elements (6)		4.5
Integration		57.0
Command distribution unit (1)		7.5
Umbilical (1)		2.5
Pyrotechnic control box (1)		6.0
Cabling and connectors		41.0
Data Handling		46.4
Data handling unit (1)		12.7
Tape recorder (3)		23.9
Integrated decoder and sequencer (1)		9.8
Communications		121.4
Receiver (2)		6.6
Modulator/exciter (2)		3.0
TWT (2)		2.0
Circulator switch (6)		1.8
Diplexer (2)		2.0
Antenna selector (1)		0.5
Receiver selector (1)		0.5
Power amplifier monitor and selector (1)		1.0
Directional coupler (1)		0.5
Omni-antenna installation (2)		1.5
Helical antenna installation (1)		2.8
High-gain antenna installation (1)		99.2

Table 10. Weight Estimate — 3-Axis Stabilized Spacecraft with a 100 Pound Science Payload, Jupiter Flyby Mission (Continued)

Item		Weight (lb.)
Attitude Control		77.7
Orientation system		
Gyro reference assembly (1)	10.0	
Accelerometer (1)	1.0	
Guidance and control electronics (1)	6.0	
Canopus tracker (1)	6.0	
Coarse sun sensor (i)	0.2	
Fine sun sensor (1)	1.9	
Gimbal for fine sun sensor (1)	2.0	
Sun sensor electronics (2)	0.3	
TVC (vane and actuator) (2)	3.5	
Regulator/relief valve (2)	2.6	
Solenoid valves (12)	6.0	
Fill valves (2)	0.6	
High-pressure transducer (2)	0.4	
Low-pressure transducer (2)	0.6	
Nozzles (12)	1.2	
Lines and fittings	3.2	
Nitrogen	13.4	
Nitrogen tanks and residuals (2)	18.8	
Propulsion		34.8
Nitrogen fill valve (1)		0.2
N_2H_4 fill and drain valve (1)		0.2
Explosive valves (4)		1.0
N_2H_4 filter (1)		0.5
Electrical		0.5
Lines and fittings		0.6
Motor (1)		1.5
Instrumentation		0.6
Usable propellant		25.5
Tank, residuals, and pressurization		4.2
Scientific Payload		100.0
Contingency		59.0
Spacecraft Weight		774.2

Table 11. Moments of Inertia for 774-Pound Spacecraft

Condition	$\bar{Z}$ (in.)	Moments of Inertia (slug ft^2)		
		I_x	I_y	I_z
Spacecraft prior to deployment of experiment booms and antenna	72.6	270.7	284.5	131.2
Spacecraft with antenna deployed	71.2	298.9	312.6	215.8
Spacecraft in cruise mode	71.2	308.8	315.9	228.8

has been increased by 6 feet and the transmitted power by 4 watts. The net effect is to double the data transmission capability at Jupiter's orbit, raising it to 1400 bits/sec. This increase in bit rate was chosen as being commensurate with doubling the science payload.

Because the television system has better resolution, the picture taking sequence may begin earlier in the encounter for the same resolution. Since about 1000 bits/sec can be allocated to the television experiment, pictures can be transmitted back to earth once every 25 minutes and thus permit greatly increased television coverage. In addition, since three tape recorders are carried for a total storage capability of 1.8×10^8 bits, pictures may be taken near encounter as frequently as once every three minutes. Additional data storage required by the added planetary encounter experiments is only a small percent of the total storage capability.

After encounter the entire 1.8×10^8 bits can be read out in two days and repeated if desired. The increased bit rate will also require fewer ground station acquisition times.

The power requirements for this spacecraft are as follows:

- Communications: 50 watts
- Electrical integration: 8 watts
- Data handling: 9 watts

- Attitude control: 21 watts
- Heaters: 16 watts
- Science: 37 watts

Of these power requirements, the most problematic is the required heater power. If the science sensors can be thermally separated from their electronics and if the sensors can be allowed to fall to a very low temperature, experiment heaters will not be required. Although it appears at this time that this technique is possible for many of the experiments, a substantial contingency in heater power has been allowed in the event that this is not possible for all experiments.

In general all of the other system characteristics of this spacecraft are the same as for the 3-axis stabilized, 50-pound science payload spacecraft described in Section 2 of this volume. Flight sequence, accuracy and compatibility with scientific experiments are the same.

The reliability of the spacecraft is also estimated to be the same. However, the schedule and estimated cost would have to be slightly increased. It appears that an additional three months should be added to the schedule primarily to assure adequate time for experiment integration and that the cost should be increased by 20 to 25 percent.

3.4 250-POUND SCIENCE PAYLOAD

This section describes briefly the conceptual design of a spacecraft capable of carrying a 250-pound science payload on a Jupiter flyby mission. This spacecraft is simply a scaled-up version of that described in Section 3.3 and illustrated in Figure 18. It is a 3-axis stabilized spacecraft weighing 1136 pounds, including a 77-pound contingency. Table 12 gives a weight estimate of the configuration of the spacecraft and Table 13 gives the mass properties.

This spacecraft can be launched on a Jupiter flyby mission using the Titan III/Centaur configuration; however for a good payload margin, the TE-364-4 third stage could be used. The "B" fairing with a 108-inch extension would be required.

Table 12. Weight Estimate — 3-Axis Stabilized Spacecraft with a 250-Pound Science Payload

Item		Weight (lb.)
Structure and Thermal Control		219.3
Structure		82.8
Planetary scan platform		18.0
Thermal control		34.8
Meteoroid protection		80.7
Radiation protection		3.0
Power Supply		156.5
RTG installation		138.6
RTG units (3)	126.0	
Boom assemblies (3)	12.6	
Power control unit (1)		10.4
Shunt elements (10)		7.5
Integration		103.5
Command distribution unit (1)		8.5
Umbilical (1)		3.0
Pyrotechnic control box (1)		7.0
Cabling and connectors		85.0
Data Handling		50.9
Data handling unit (1)		15.0
Tape recorder (3)		23.9
Integrated decoder and sequencer (1)		12.0
Communications		145.2
Receiver (2)		6.6
Modulator/exciter (2)		3.0
TWT (2)		2.0
Circulator switch (6)		1.8
Diplexer (2)		2.0
Antenna selector (1)		0.5
Receiver selector (1)		0.5
Power amplifier monitor and selector (1)		1.0
Directional coupler (1)		0.5
Omni-antenna installation (2)		1.5
Helical antenna installation (1)		2.8
High-gain antenna installation (1)		123.0

Table 12. Weight Estimate — 3-Axis Stabilized Spacecraft with a 250-Pound Science Payload (Continued)

Item		Weight (lb.)
Attitude Control		85.4
Orientation system		85.4
Gyro reference assembly (1)	10.0	
Accelerometer (1)	1.0	
Guidance and control electronics (1)	6.0	
Canopus tracker (1)	6.0	
Coarse sun sensor (1)	0.2	
Fine sun sensor (1)	1.9	
Gimbal for fine sun sensor (1)	2.0	
Sun sensor electronics (2)	0.3	
TVC (vane and actuator) (2)	3.5	
Regulator/relief valve (2)	2.6	
Solenoid valves (12)	6.0	
Fill valves (2)	0.6	
High-pressure transducer (2)	0.4	
Low-pressure transducer (2)	0.6	
Nozzles (12)	1.2	
Lines and fittings	3.5	
Nitrogen	16.5	
Nitrogen tank and residual (1)	23.1	
Propulsion		48.7
Nitrogen fill valve (1)		0.2
N_2H_4 fill and drain valve (1)		0.2
Explosive valves (4)		1.0
N_2H_4 filter (1)		0.5
Electrical		0.6
Lines and fittings		0.8
Motor (1)		1.5
Instrumentation		0.6
Usable propellant		37.5
Tank, residuals, and pressurization		5.8
Scientific Payload		250.0
Contingency		77.2
	Spacecraft Weight	1,136.7

Table 13. Mass Properties

Condition	Weight (lb)	$\overline{Z}$ (in.)	Moments of Inertia (slug ft.^{2})		
			I_x	I_y	I_z
Spacecraft prior to deployment of experiment booms and antenna	774.2	72.6	270.7	284.5	131.2
Spacecraft with antenna deployed	774.2	71.2	298.9	312.6	215.8
Spacecraft in cruise mode	774.2	71.2	308.8	315.9	228.8

All of the experiments carried in the 100-pound payload are also carried in this payload, but the following four planetary encounter experiments have been added:

- Top side sounder
- Visual spectrometer
- VLF detector
- Infrared radiometer

Antennas are provided for the top side sounder. The VLF sensor must be boom-mounted for separation from the spacecraft. Windows must be provided for the infrared radiometer and visual spectrometer sensors. The main equipment compartment is again hexagonal but is 65 inches in diameter and 18 inches in height. The antenna is 23 feet in diameter and the antenna feed assembly has been enlarged to house any additional experiment. The planetary scan platform is 18 x 18 x 12 inches and has 3 square feet of frontal area available for the experiments which wish to observe the sunlit portion of Jupiter. The power supply requirements are as follows:

- Communications: 67 watts
- Integration: 9 watts
- Data handling: 10 watts
- Attitude control: 25 watts
- Heaters: 22 watts
- Science: 56 watts

The total raw power is then 189 watts. Ten shunt elements are provided for power dissipation. The communication system uses a 20-watt TWT transmitter which with the 23 foot antenna provides a bit rate of 2800 bits/sec at Jupiter's orbit.

As in the 100-pound payload spacecraft, three tape recorders are carried. With the increased bit rate, a television picture can be transmitted back every 12 minutes during the "real time" mode. The ground station required on time during cruise will be reduced proportionally to the increased bit rate.

This spacecraft configuration is not optimum since with the same booster a 100-pound science payload could be placed in orbit about Jupiter (see Section 6). Our knowledge of Jupiter could be greatly increased, even though the payload is reduced by 150 pounds, since prolonged study of the planet even with less scientific instruments will doubtless be more effective than a short duration flyby with improved instrumentation.

In general all of the other system characteristics of this spacecraft similar to the 3-axis stabilized, 50-pound science payload spacecraft described in Section 2 of this volume. Limit cycle amplitude will be reduced to ±0.175 degree and the double gimbaled planet sensor package allows other experiments in addition to the TV to observe Jupiter at any time during approach and flyby. Two different sizes of TV camera will probably be used. Flight sequence, trajectory accuracy, and compatability are otherwise the same.

The reliability of the spacecraft is also estimated to be the same although some improvements are possible through the use of additional redundancy. It appears that six months should be added to the schedule primarily for experiment integration and integration and test and that the cost should be increased by about 60 percent over the 50-pound science payload, 3-axis controlled spacecraft.

4. JUPITER FLYBY MISSIONS, 1970-1980

4.1 INTRODUCTION AND CONCLUSIONS

The preceding sections of this report pertain to the design of spacecraft for Jupiter flyby missions in the 1972 launch opportunity. The extension of these results to apply during the entire decade 1970 to 1980 is treated in this section.

The actual extent of the time period to be treated warrants some attention. The 1972 earth-Jupiter mission has been emphasized as the topic of this study of greatest immediate value. Indeed, the schedules generated for that mission in Volume 2 indicate that launch opportunities before 1972 can be met only by compressing the normal schedule of events leading from the mission definition phase to the launch. Thus the practical interest is in extending 1972 characteristics to the range 1972 to 1980. However, the 1970 to 1980 period is specified by the work statement. Furthermore, there is value in treating a series of launch opportunities which encompass an entire Jovian year, 11.9 terrestrial years. After the pattern of characteristics of one such cycle is studied, predictions of the nature of earth-Jupiter opportunities of other cycles can be generated by almost self-evident extension.

In this section we examine 12 launch opportunities encompassing the 12-year Jovian year cycle, starting with the 1968 to 1969 launch opportunity (December, 1968) and ending with the 1980 to 1981 launch opportunity (December, 1980). This examination is not detailed but serves to illustrate the regular trends acting over the Jovian cycle. The opportunities 1974 and 1978 are examined in greater detail, with "pork chop" curves produced to compare with the 1972 data of Volume 2. The 1978 opportunity is significant, since the best opportunities for Jupiter swingby trajectories to the outer planets occur during the 1977, 1978, and 1979 Jupiter opportunities.

The principal effects arising from the extension of the 1972 earth-Jupiter mission analysis and spacecraft conceptual design to other opportunities are the following:

a) Schedule Implications. The 1972 and later earth-Jupiter missions can be scheduled with adequate marging allowing a normal time interval for all intermediate phases and events from the present until launch. A mission in 1971 is feasible, but only if the normal schedule were compressed several months, by converting some series events to parallel events. A mission during the 1969 to 1970 opportunity cannot be practically scheduled. These conclusions are obvious from previous material, and are not discussed further.

b) Solar Cycle. The solar activity cycle, almost synchronous with the Jovian year, undergoes a cycle from maximum about 1969 to 1970 to minimum in 1975 to maximum in 1980 to 1981. The alternations of this cycle permeate the interplanetary particles and fields environment. Sine the 1972 spacecraft design of Volume 2 is adequate for even the maximum environment (from the viewpoint of adequate science instrumentation to study this environment and from the viewpoint of the ability of spacecraft subsystems and components to withstand it), the solar cycle has negligible effect. It is not discussed further.

c) Parking Orbit Coast Time. Because of the variation in the Declination of the Launch Asymptote (DLA) for Type I trajectories over the Jovian 12-year cycle, the 2 to 25 minute parking orbit coast time range of the Centaur launch vehicle stage, acceptable in 1972, must be extended to permit reasonably efficient exploitation of other opportunities in the cycle. In particular, earth-Jupiter missions from 1975 to 1982 require an increase in the maximum coast time.

d) Launch Azimuth. Because of the same variation in DLA, an increase in launch azimuth range from the 71 to 108 degree range assumed for 1972 is desirable for other years, particularly for 1973 and 1978. Although this change is not vital to missions conducted during those opportunities, it would decrease the injection energy requirement by about 5 km^2/sec^2.

e) Injection Energy. There is a substantial variation in the injection energy (C_3) necessary for earth-Jupiter trajectories over the full 12-year cycle. On the basis of a 20-day launch period with variable arrival date, the range of values of required C_3 for Type I trajectories is 81 to 97 km^2/sec^2 if the azimuth extension suggested in (d) is implemented, or 81 to 104 if it is not. The 87 km^2/sec^2 requirement of 1972 is exceeded in 7 of the other 10 opportunities of a complete cycle. Only the 1969 to 1970, 1971, and 1975 opportunities have a lower C_3 requirement than 1972.

f) Launch Vehicles. Because of the variation in injection energy, there is a variation in the capability of launch vehicles. For most combinations of launch vehicles and spacecraft weights identified in previous sections, there is enough margin for the 1972 mission that any of the launch opportunities can be accommodated. The extra margin in opportunities with lower C_3 requirements could be devoted to a longer launch period or a shorter flight time. For one combination, a 564 pound, 3-axis stabilized spacecraft and the Atlas SLV3x/Centaur/TE-364-3 launch vehicle, the C_3 capability of 92.5 km^2/sec^2 is inadequate to provide a 20 day launch period in the years 1977, 78, and 79.

g) Spacecraft Design. There are no required design changes in the spacecraft concepts presented for 1972 Jupiter flyby missions to adapt them for use in other opportunities. However, as the use of a given launch vehicle-spacecraft combination leads to varying times of flight in different opportunities, the assessed probabilities of success may vary somewhat. Of course, the possibility exists that state-of-the-art improvements may be incorporated into the spacecraft design for launches in the latter part of the decade. Thus, reductions in weight might compensate for increased injection energy requirements, permitting equivalent mission performance with the same launch vehicle and basic spacecraft design.

4.2 FUNCTIONAL REQUIREMENTS

In this section the extension of the functional requirements imposed on the design of the spacecraft for the 1972 earth-Jupiter flyby mission is examined and extended to cover the period of one Jovian year, from the 1968 to 1969 opportunity to the 1980 to 1981 opportunity. It will be seen that a number of these functional requirements are not dependent on the year of the launch opportunity and are therefore unchanged.

4.2.1 Launch Vehicles

The characteristics of launch vehicle combinations considered to be available for missions in the period examined is considered to be unchanged from the description of Section 2.1 of Volume 2. It is recognized that some of the launch vehicle combinations indicated still require a substantial development phase; for example, the high energy kick stage, a component stage of two of the launch vehicle combinations, has not entered the development phase yet. Consequently the ability of

all of the launch vehicle combinations to meet the schedule requirements of the earliest missions in the 1970 to 1980 decade has not been established. However, for the purpose of this section, the launch vehicle characteristics are considered unvarying with launch opportunity.

4.2.2 Interplanetary Trajectories

As indicated above, there a number of properties of the interplanetary trajectories over the period studied which lead to variations in mission characteristics and in the functional requirements to be met by the spacecraft system design. A number of significant quantities have been abstracted from the characteristics of each opportunity of the period, and plotted as a function of the year of the launch opportunity in a manner which emphasizes the continuous but changing nature of these characteristics over the 12-year Jovian cycle. These plots, which for the most part pertain to minimum-C_3 Type I and Type II trajectories, are given in the following figures:

Figure 19, Launch Date (time of the year)

Figure 20, Declination of the Launch Asymptote (DLA)

Figure 21, Minimum Injection Energy (C_3) Requirements

Figure 22, Time of Flight

Figure 23, Asymptotic Approach Velocity at Jupiter

In these five figures some quantities are seen to undergo a variation in which the cycle is repeated once in the 12-year period. Other variations repeat twice as often. It is worth noting what these variations are, and relating them to the planetary geometrical characteristics to which they may be attributed. In Figure 19 it is seen that the launch date of minimum-energy earth-Jupiter trajectories occurs about one month later in each succeeding opportunity; this is expected, because the synodic period of Jupiter with respect to the earth is 13 months. It is also noticed that for two of these launch opportunities, the launch date coincides with the time when the earth crosses the line of nodes of Jupiter's orbital plane and the ecliptic plane. For these two opportunities, 1969 to 1970 and 1975, not only is the earth near the line of nodes when the spacecraft is launched but Jupiter is approximately at the

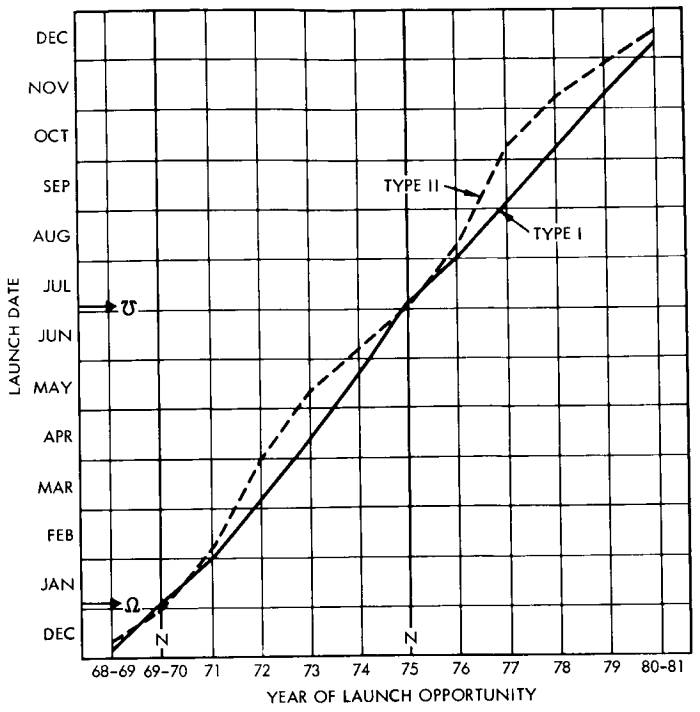

NOTES

Ω – EARTH CROSSES ASCENDING NODE OF JUPITER'S ORBIT PLANE

℧ – EARTH CROSSES DESCENDING NODE OF JUPITER'S ORBIT PLANE

N – OPPORTUNITIES IN WHICH NODE-TO-NODE TRAJECTORIES ARE POSSIBLE

Figure 19. Launch Date of Minimum-Energy Earth-Jupiter Trajectories Versus Launch Opportunity

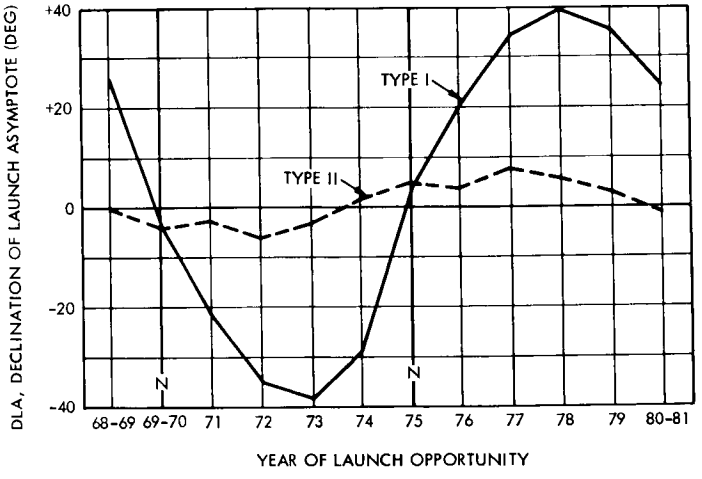

Figure 20. Declination of Launch Asymptote of Minimum-Energy Earth-Jupiter Trajectory Versus Launch Opportunity

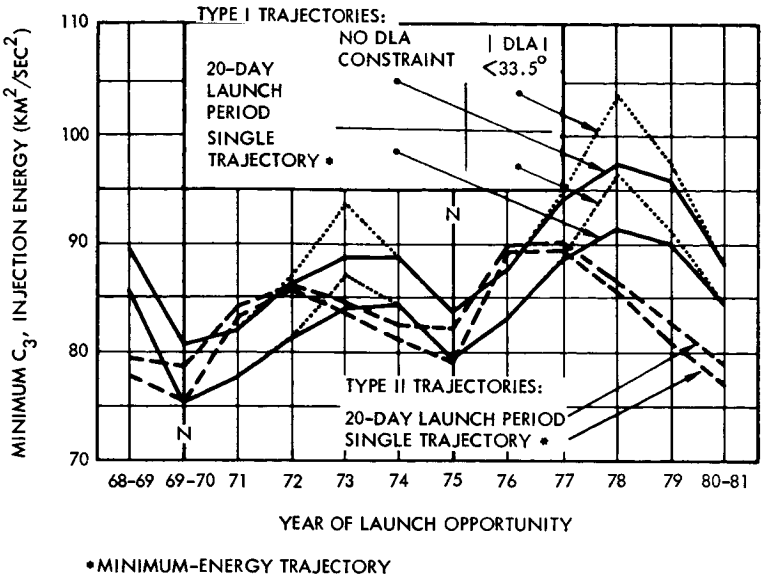

Figure 21. Minimum-Injection Energy Requirements Versus Launch Opportunity, Earth-Jupiter Trajectories

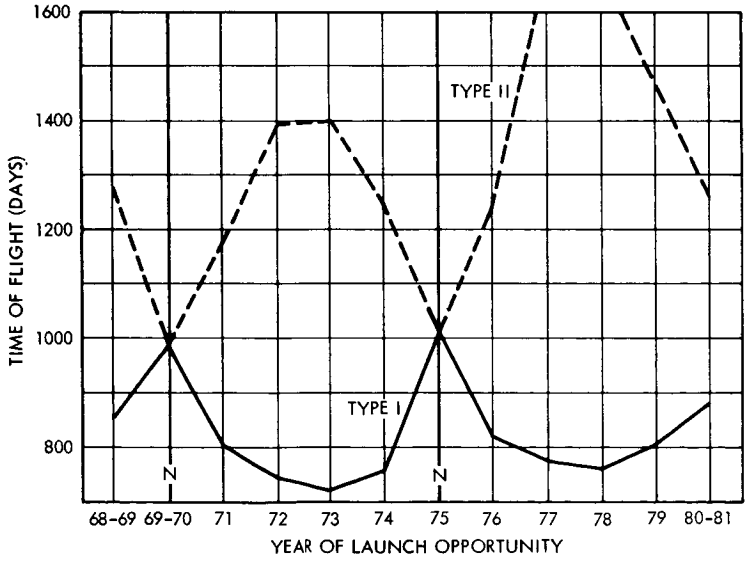

Figure 22. Time of Flight of Minimum-Energy Earth-Jupiter Trajectories Versus Launch Opportunity

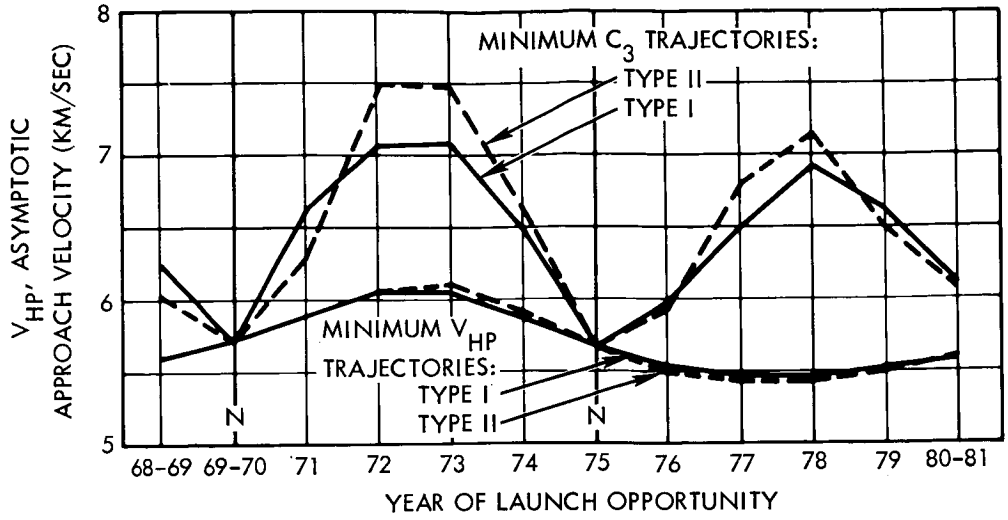

Figure 23. Asymptote Approach Velocity of Minimum-Energy Earth-Jupiter Trajectories Versus Launch Opportunity

opposite node at the time of arrival. Thus, twice in the 12-year Jovian cycle, Jupiter crosses the plane of the ecliptic, and interplanetary trajectories may approximate Hohmann transfers, lying in the plane of the ecliptic. At these times, minimum-energy Type I and II trajectories are very similar.

Between the node crossings by the planet Jupiter, the interplanetary trajectories are influenced by the out-of-ecliptic component of Jupiter's location. For arrival dates corresponding to the launch opportunities 1971 to 1974, Jupiter remains south of the plane of the ecliptic, and some of the prominent characteristics associated with Type I and Type II trajectories are indicated by the sketches of Figure 24 and Figure 25. For a Type I trajectory, in which the spacecraft traverses an angle about the sun of less than 180 degrees, Figure 24 shows that the heliocentric orbital plane of the spacecraft must be inclined so that the spacecraft is south of the plane of the ecliptic during the entire interplanetary phase. Since launches during this period take place in the months February to April, this southerly inclination with respect to the plane of the ecliptic increases the southerly declination which would characterize the launch asymptote of an in-ecliptic orbit.

For the same opportunities, Figure 25 indicates a reversal of these effects for Type II trajectories. The spacecraft orbit is inclined

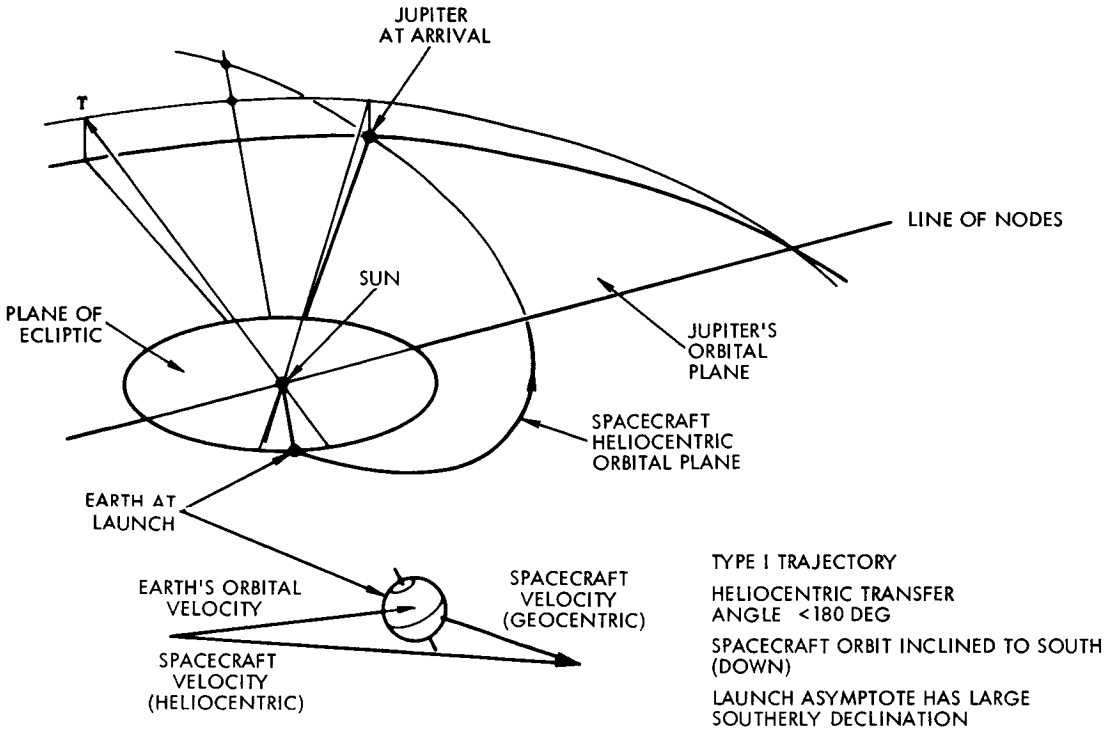

Figure 24. Typical Type I Trajectory, Earth-Jupiter, 1971-1974 Opportunities

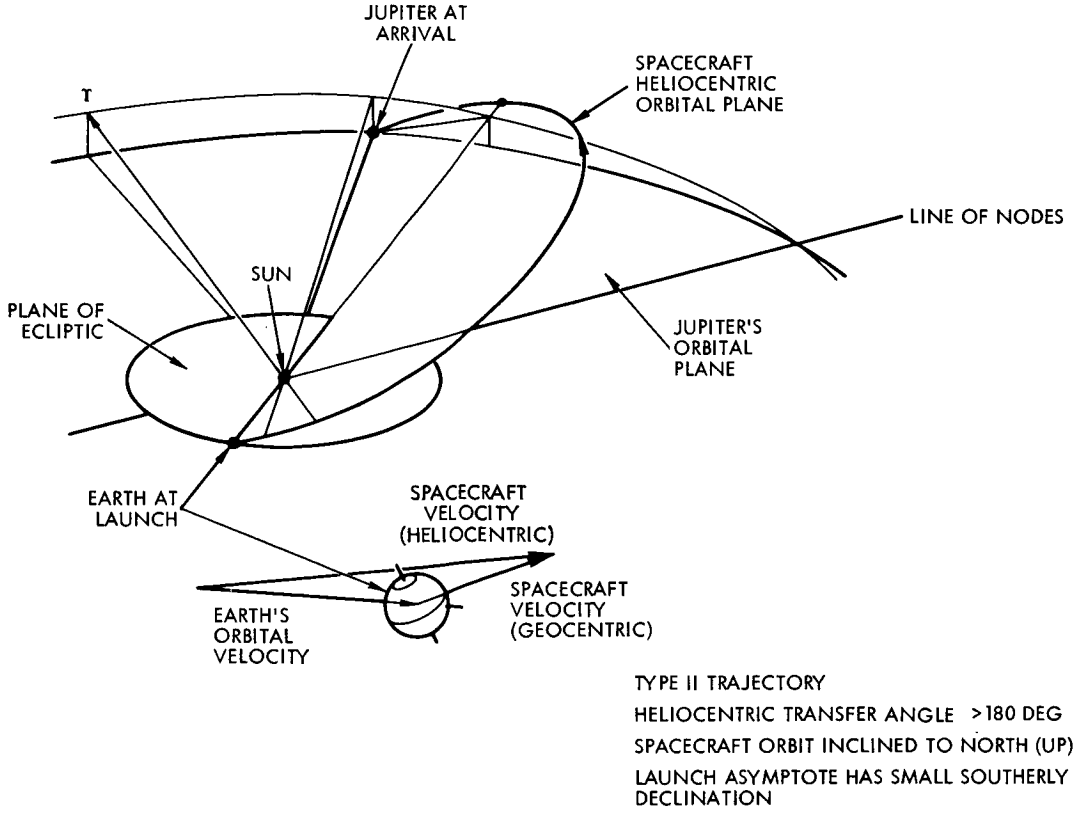

Figure 25. Typical Type II Trajectory, Earth-Jupiter, 1971-1974 Opportunities

so that the spacecraft is north of the plane of the ecliptic for all but the last portion of the interplanetary trajectory. This northerly inclination subtracts from the southerly declination of ecliptic-plane trajectories, resulting in launch asymptotes for Type II trajectories with typically small southerly declinations. As indicated by Figure 20, the trends of the launch asymptote declination are reversed for the launch years 1976 to 1980 to 1981, the portion of the Jovian cycle in which Jupiter is north of the plane of the ecliptic.

4.2.3 Encounter Geometry

The variation of the characteristics of encounter geometry over a cycle of successive launch opportunities is not great. Of course, the options for targeting, that is, selection of the impact parameter $\overline{B}$ to establish the direction and distance of the flyby passage from the planet, can be made independently of the interplanetary trajectory characteristics, and therefore do not depend on launch opportunity.

The principal effect to be considered is the variation in the direction of the spacecraft's approach to Jupiter, specifically the angles ZAP and ZAE. For the 1972 opportunity, it was seen that these angles are almost exclusively functions of arrival date at the planet. The same relationship holds for all other opportunities, but in comparing different opportunities, it is more appropriate to observe that these angles are functions of the time of flight. For variations in launch opportunity, ZAP is represented by slightly different functions of flight time. ZAE versus flight time similarly is almost independent at launch opportunity.

The variations in encounter geometry over a span of launch opportunities arise from two sources. Because of the variation in C_3 requirements, trajectories with different flight times are likely to be selected for different launch opportunities, even if the spacecraft and launch vehicle are the same. As the angles ZAP and ZAE vary with flight time, this leads to somewhat different approach asymptote orientations. The second effect is that the functions of ZAP and ZAE versus flight time change slightly with launch opportunity.

In terms of differentials, the increment in ZAP angle over a period of several launch years is

$$\Delta ZAP = \left(\frac{\partial ZAP}{\partial FT}\right)_{LY\ Const.} \Delta FT + \left(\frac{\partial ZAP}{\partial LY}\right)_{FT\ Const.} \Delta LY$$

where FT means flight time and LY launch year. ΔZAP will be small because ΔFT and $\left(\frac{\partial ZAP}{\partial LY}\right)_{FT\ Const.}$ are both small. ΔZAE is resolved into similar components.

The characteristics of the encounter geometry are not likely to impose any restrictions on the applicability of spacecraft to missions in different years. If enough margin exists in the launch vehicle performance to permit the selection of trajectories with significantly reduced flight times, the same margin can also be devoted to achieving a specific encounter geometry.

4.2.4 Interplanetary Environment

The requirements imposed by the interplanetary environment on the functional design of the spacecraft are essentially unchanged over the 12-year cycle of the Jovian year. The significant components of this environment include the micrometeoroids in solar orbits intermediate to the orbits of Mars and Jupiter, and the particles of the solar wind. It has been observed in the introduction of this section that alternations of the solar activity cycle, leading to maxima in 1969 to 1970 and in 1980 to 1981, have been accommodated by the 1972 spacecraft design of Volume 2. The micrometeoroid environment will not have any variations of significance between the different launch opportunities. Therefore the interplanetary environment does not lead to any spacecraft design influences as a function of launch opportunity. These requirements on the spacecraft design are initially unchanged in the sense that the estimates we have of the pertinent effects do not undergo a variation from one opportunity to the next. However, interim information, for example, observations from an earlier successful mission, could alter these requirements. But for the purpose of this section, as well as 4.2.5, 4.2.6, 4.2.7, and 4.2.11, each of these opportunities (1970 to 1980) is treated

as if it will be the first opportunity in which an earth-Jupiter mission is conducted.

4.2.5 The Environment of Jupiter

Any requirement affecting the functional design of the spacecraft arising from the estimated environment of Jupiter is unchanged in comparison with the statement of these requirements in Volume 2 for the 1972 mission.

The necessity to raise the Centaur's 25-minute limit on coast time in parking orbit to accommodate these missions with non-negative values of DLA (1975 to 1982) has been discussed in Volume 2, Section 2.2.

As the node-to-node interplanetary trajectories of the 1969 to 1970 and 1975 opportunities are very close to Hohmann transfers, the injection energy required for those opportunities is minimum. For other opportunities, injection energy requirements are increased, partly because the elliptic transfer orbits are not tangential to the earth's orbit, and partly because of the out-of-plane component required at injection. Figure 21 indicates these variations in the required injection energy (C_3). In that figure, curves are given for Type I and Type II trajectories showing the minimum C_3 requirement for both a single trajectory (i.e., the minimum energy trajectory) and a group of trajectories achievable over a continuous 20-day launch period. The 20-day launch period is defined as in Volume 2, Section 2.2 associated with a variable arrival date at Jupiter.

It is seen in Figure 20 that in the launch opportunities 1972, 1973 and 1977, 1978, 1979 the minimum energy Type I trajectories entail launch asymptotes with declination outside the range ±33.5 degrees. (This range of DLA constraints results from launch azimuth restrictions of 71 to 108 degrees.) Therefore, in Figure 21 additional curves show the penalty incurred in required C_3 for Type I trajectories during the affected years, if this constraint remains in effect. It is seen that a relaxation of the launch azimuth constraint would reduce injection energy requirements by as much as 6 km^2/sec^2, with this reduction concentrated during the opportunities where the C_3 requirements are greatest.

Other characteristics of the variation of injection energy with launch opportunity, evident in Figure 21 are the following.

- The Hohmann transfer energy in 1975, 79 km^2/sec^2 exceeds the minimum requirement in 1969 to 1970, 75 km^2/sec^2. This difference may be attributed entirely to the eccentricity of the earth's orbit about the sun; for the January launch of 1969 to 1970, the earth's position close to perihelion and its increased heliocentric velocity lead to the lower C_3 requirement. (Jupiter is about equidistant from the sun at the two node crossings, so its orbital eccentricity does not contribute to this effect.)

- C_3 requirements for Type I and Type II trajectories in the latter half of the 1970 to 1980 decade are greater than those for the first half. This effect is due to the eccentricity of Jupiter's orbit; Jupiter is at aphelion for arrival dates corresponding to the 1978 opportunity.

Figures 22 and 23 show the cyclic variation of the time of flight and asymptotic approach velocity of minimum energy earth-Jupiter trajectories. It is clear in Figure 22 that as trajectories deviate from Hohmann transfers to accommodate Jupiter's position out of the plane of the ecliptic, minimum-energy Type I trajectories have a reduced time of flight and Type II trajectories an increased time of flight. In either case, time of flight is higher during the second half of the decade, when Jupiter is near aphelion, than it is during the first half. The increases in asymptotic approach velocity for the minimum C_3 trajectories, shown in Figure 23, reflects these changes in flight time for the minimum energy trajectories.

By selecting trajectories with flight times about 1000 days, it is possible to reduce these asymptotic approach velocities, even in years when the ecliptic-plane, Hohmann transfers are unavailable. This effect, shown in Figure 23, is of significance principally for orbiter missions, considered in subsequent sections, in which low arrival velocities are important.

For three of the opportunities of the Jovian cycle examined, more detailed analysis of the available trajectories has been summarized in "pork chop" curves which display trajectory characteristics as

contours against launch date and arrival date coordinates. For the 1972 opportunity, these displays have been included in Volume 2. Similar displays for the 1974 and 1978 earth-Jupiter opportunities are given in this section in the following figures.

	1974	1978	Quantity Plotted as Contours
Figure	26	31	C_3, Injection Energy
Figure	27	32	DLA, Declination of Launch Asymptote
Figure	28	33	V_{HP}, Asymptotic Approach Velocity
Figure	29	34	ZAP Angle: At arrival, between V_∞ vector and Jupiter-sun vector
Figure	30	35	ZAL Angle: At launch, between V_∞ vector and sun-earth vector

For observing the significant trends as they apply to the complete range of launch opportunities, the information given in Figures 19 to 24 is adequate to cover the most salient features. Figures 26 through 35 permit more detailed trajectory selection analysis to be undertaken for the 1974 and 1978 opportunities, in a manner similar to the treatment of the 1972 opportunity in Volume 2. Figure 36, showing earth-Jupiter distance United States calendar time from 1973 to 1981, is an adjunct to these figures. From it, the communication distance at any arrival date can be determined.

Since some launch vehicle-spacecraft combinations provide enough margin to significantly reduce flight time, this possibility and its variation with launch opportunity are examined. Figure 37 gives, for each launch opportunity, injection energy United States time of flight of Type I trajectories. A point on that figure represents the minimum value of C_3 which can provide (for a 20-day launch period) trajectories with no greater than the indicated flight time. Figure 38 represents vertical cross plots of Figure 37, and shows C_3 requirements United States launch year for different flight times, again with

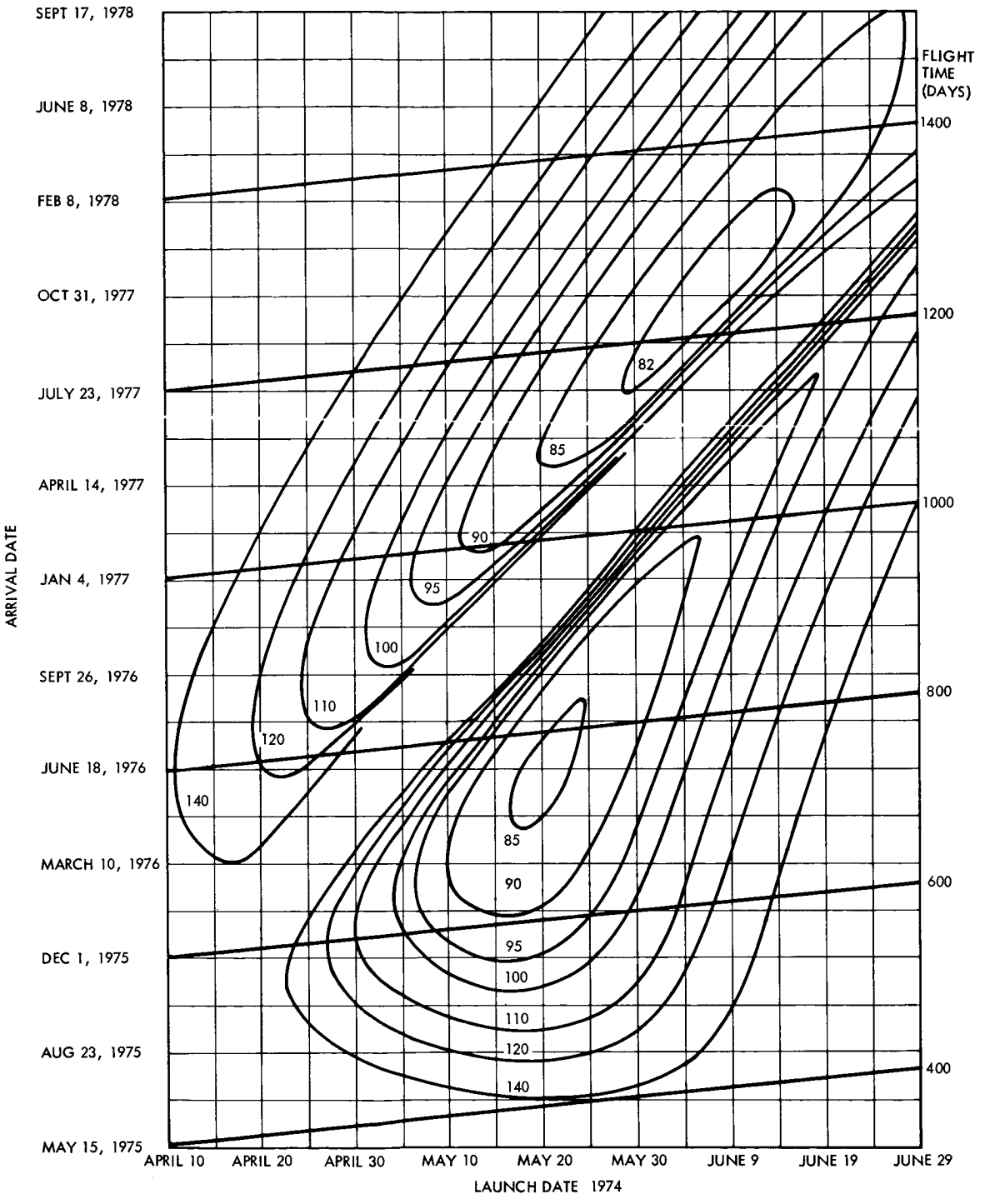

Figure 26. Earth-Jupiter 1974 Trajectories, C_3, Geocentric Launch Energy

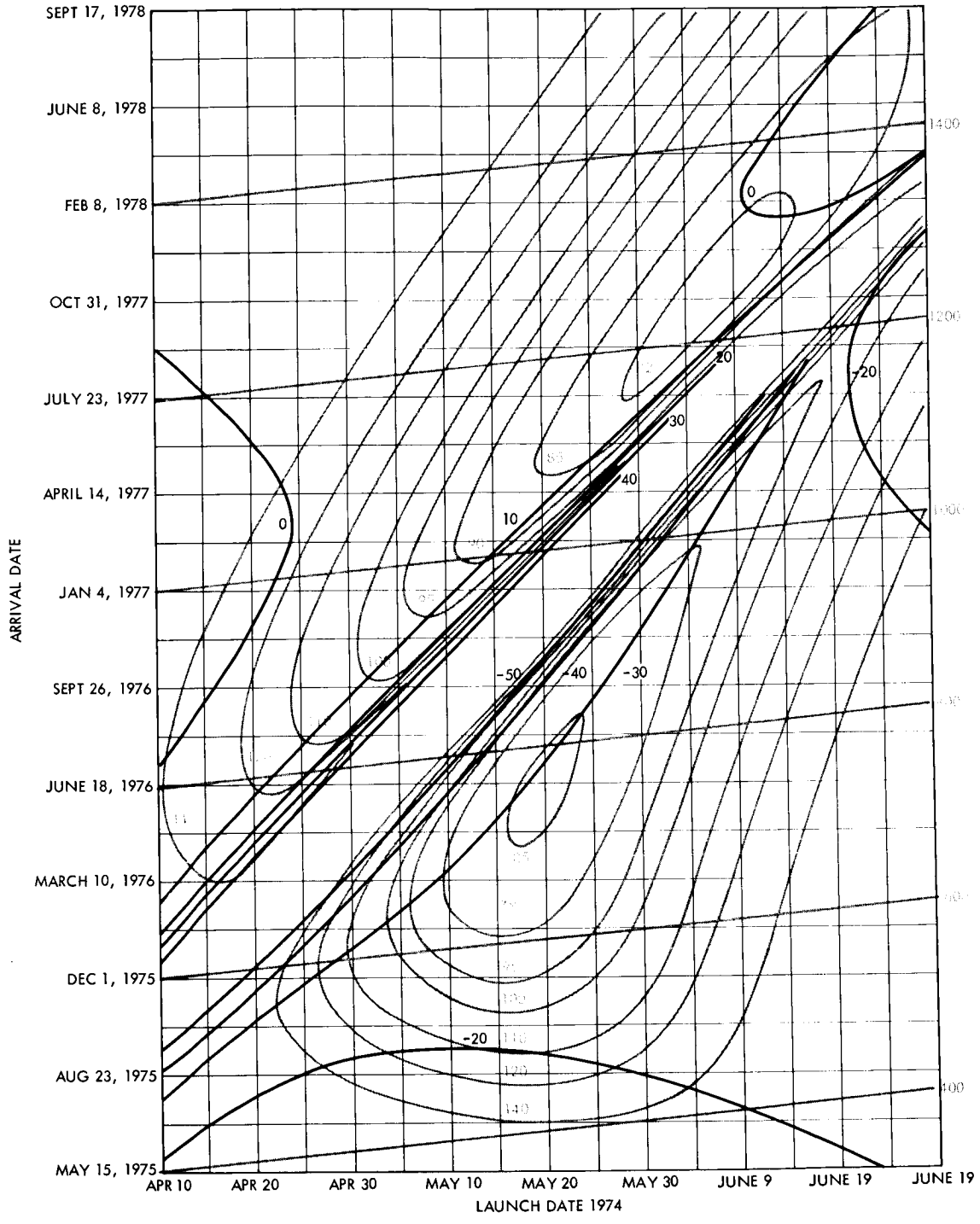

Figure 27. Earth-Jupiter 1974 Trajectories, DLA, Declination of Geocentric Departure Asymptote

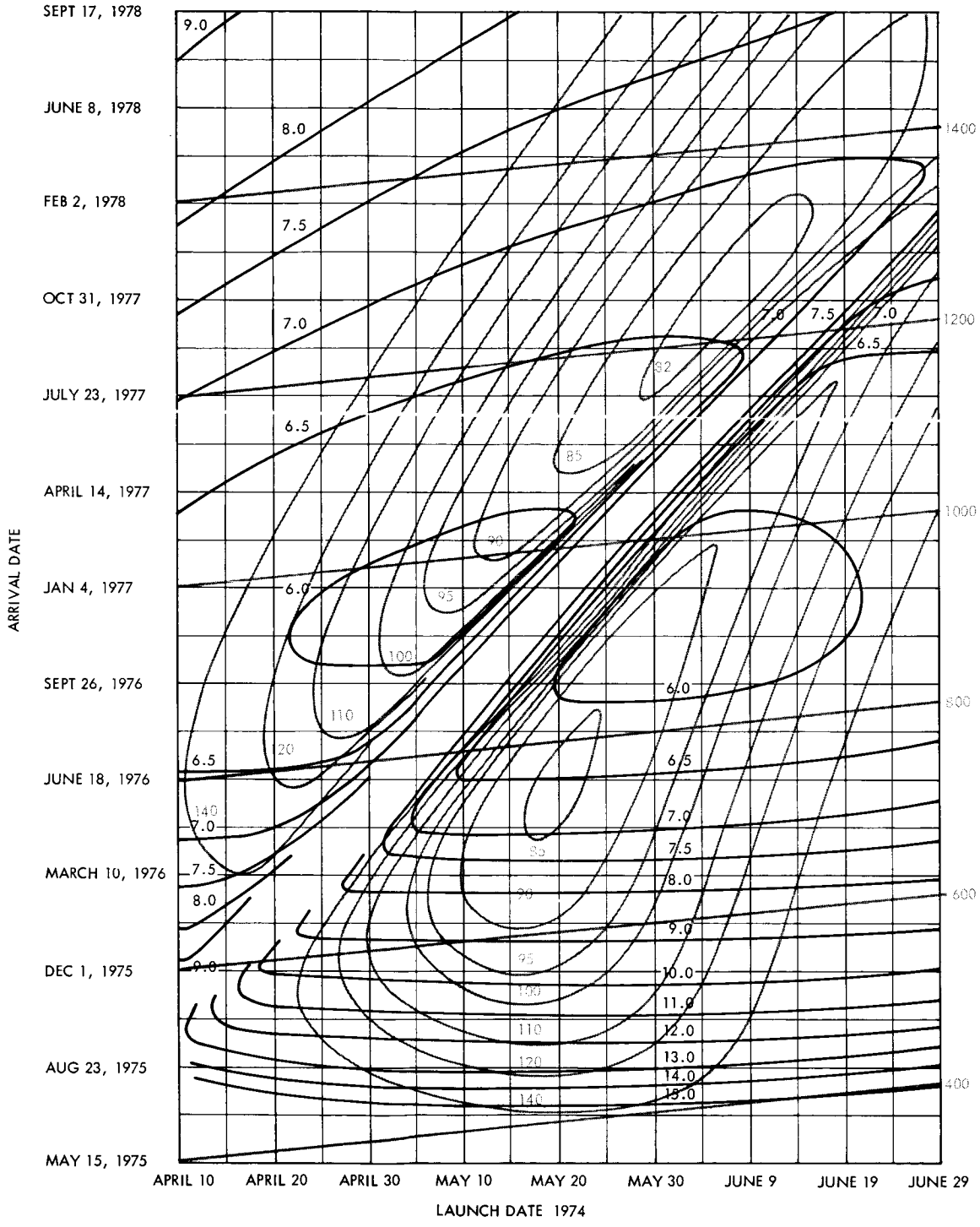

Figure 28. Earth-Jupiter 1974 Trajectories, V_{HP}, Planetocentric Asymptote Approach Velocity at Jupiter

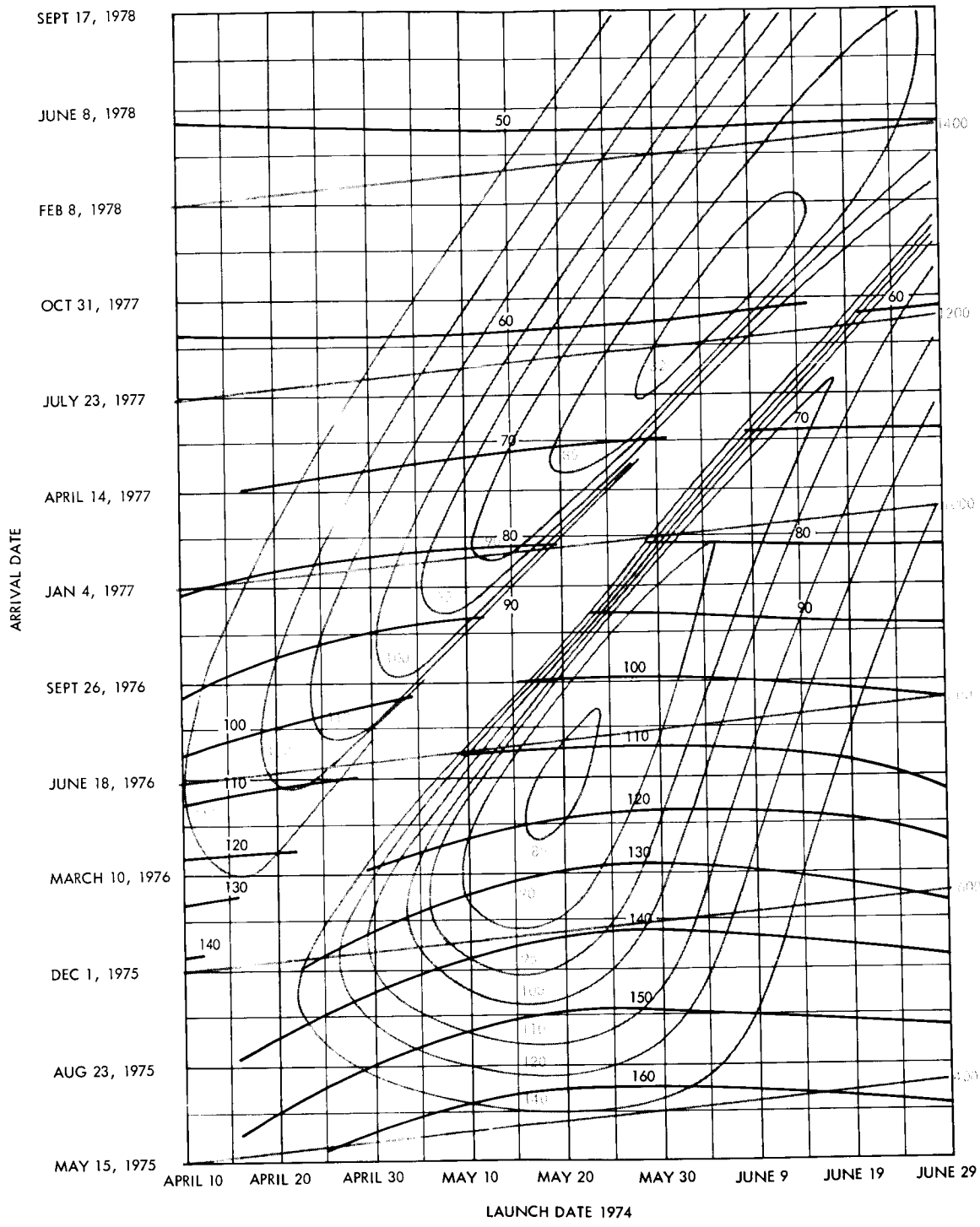

Figure 29. Earth-Jupiter 1974 Trajectories, ZAP, Angle Between Planetocentric Approach Asymptote and Jupiter-Jun Vector

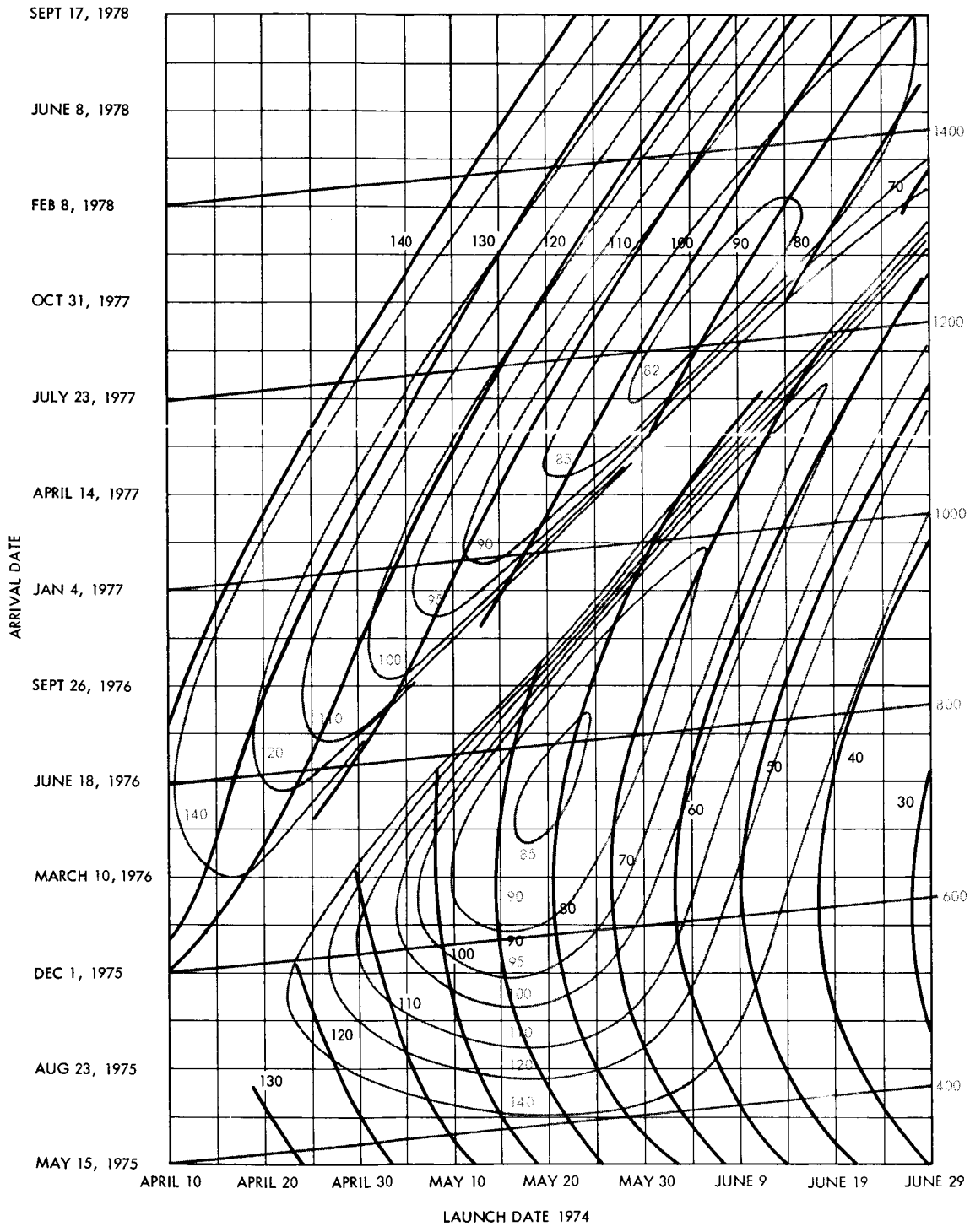

Figure 30. Earth-Jupiter 1974 Trajectories, ZAL, Angle Between Geocentric Departure Asymptote and the Sun-Earth Vector

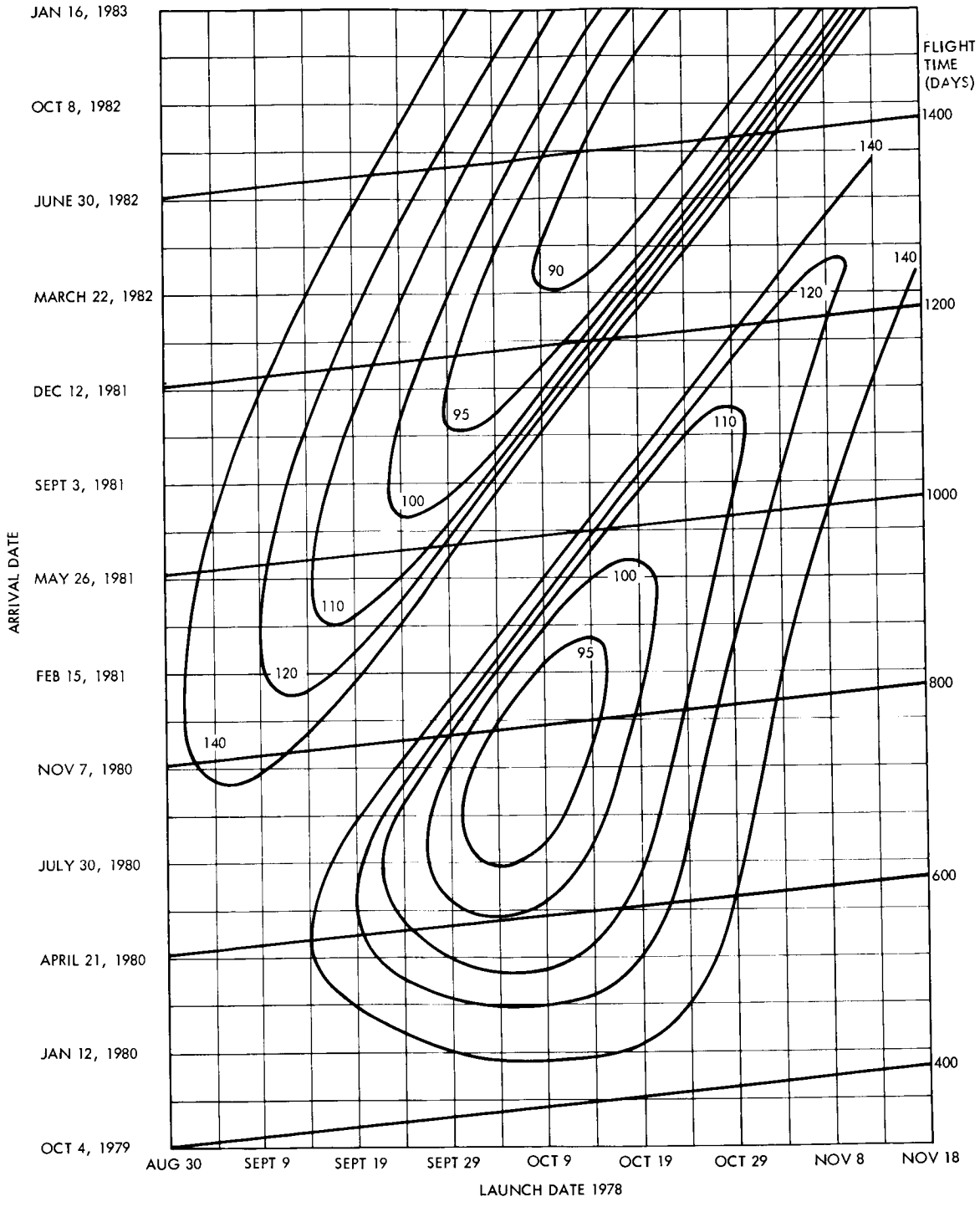

Figure 31. Earth-Jupiter 1978 Trajectories, C_3, Geocentric Launch Energy

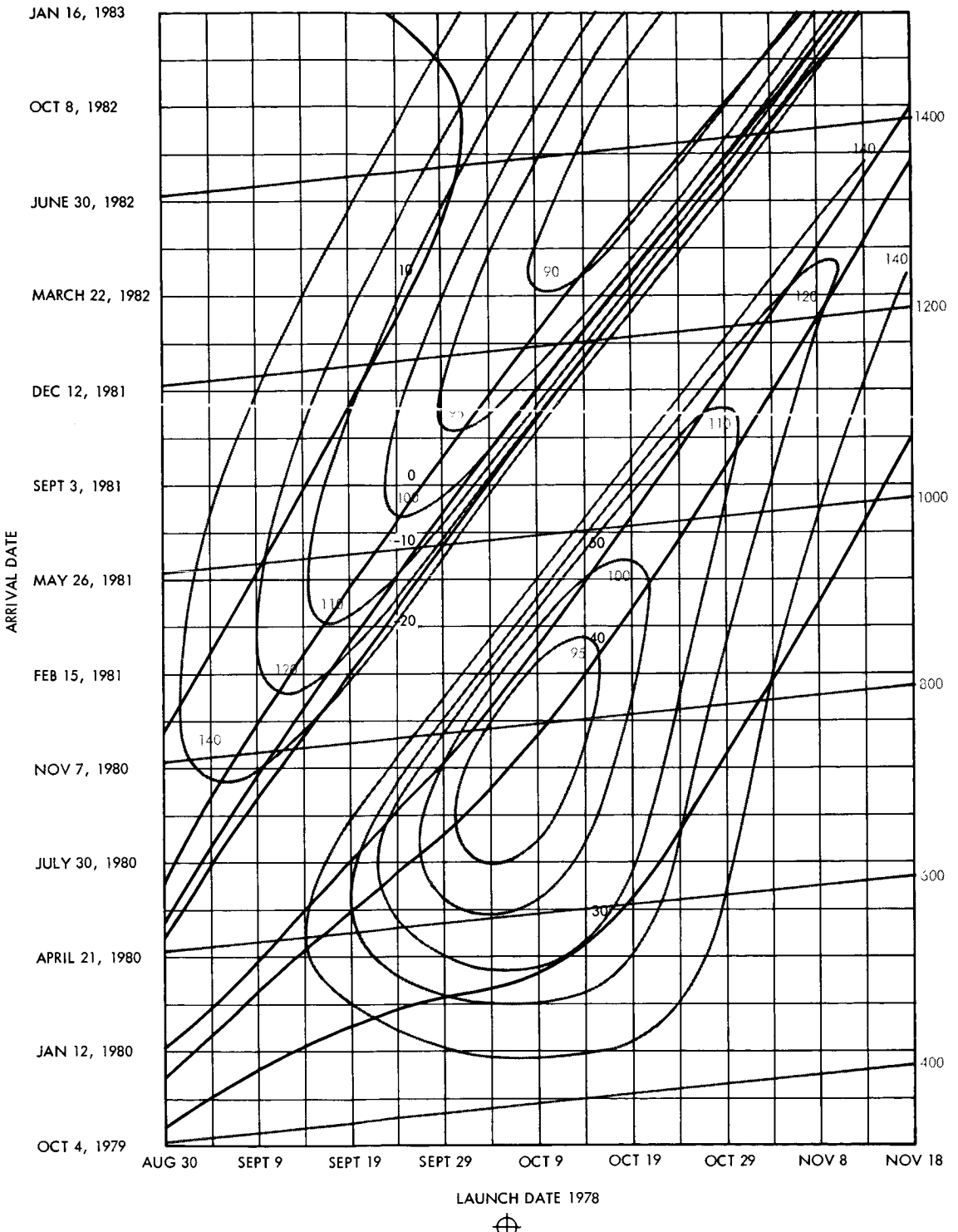

Figure 32. Earth-Jupiter 1978 Trajectories, DLA, Declination of Geocentric Departure Asymptote

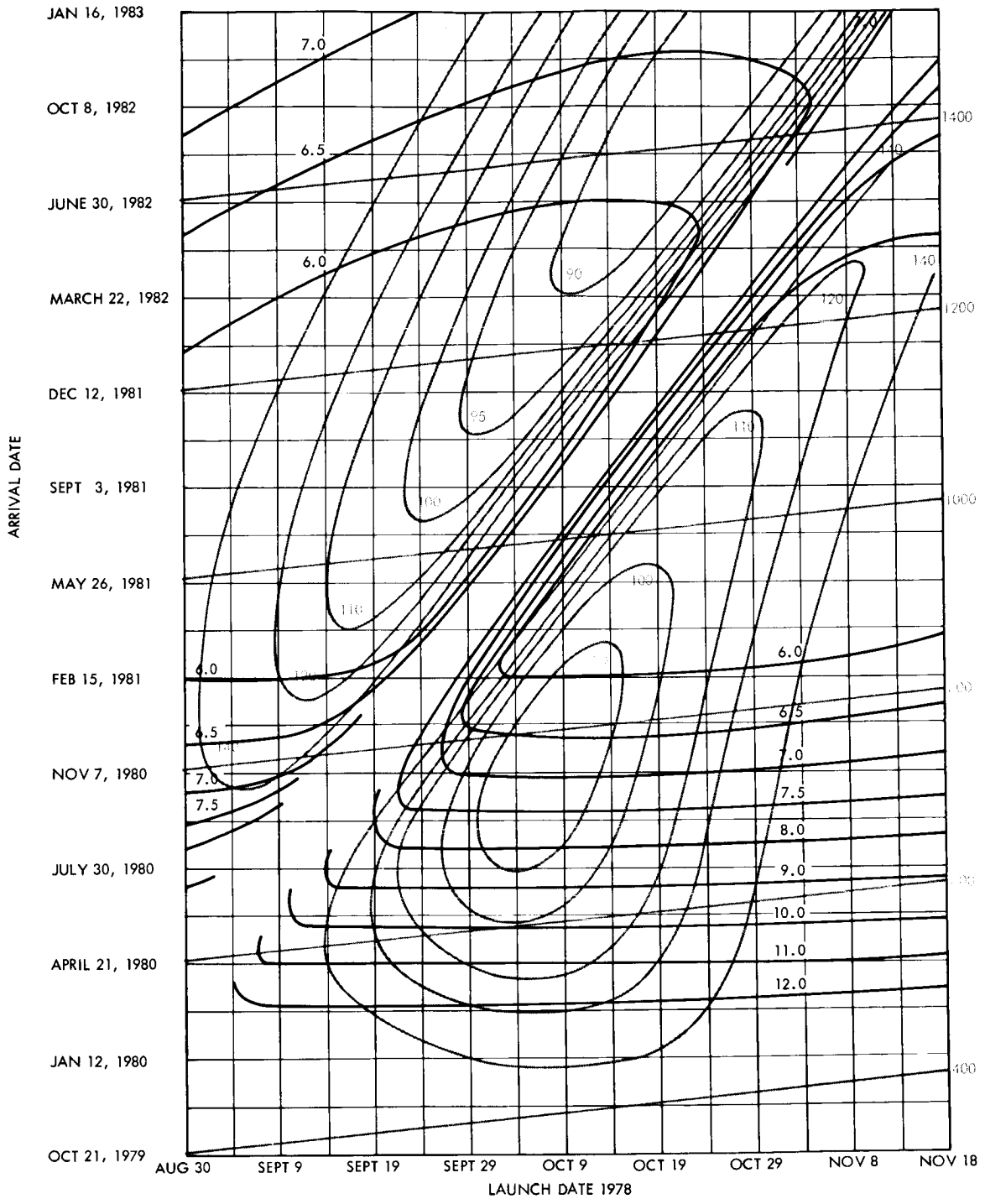

Figure 33. Earth-Jupiter 1978 Trajectories, V_{HP}, Planetocentric Asymptotic Approach Velocity at Jupiter

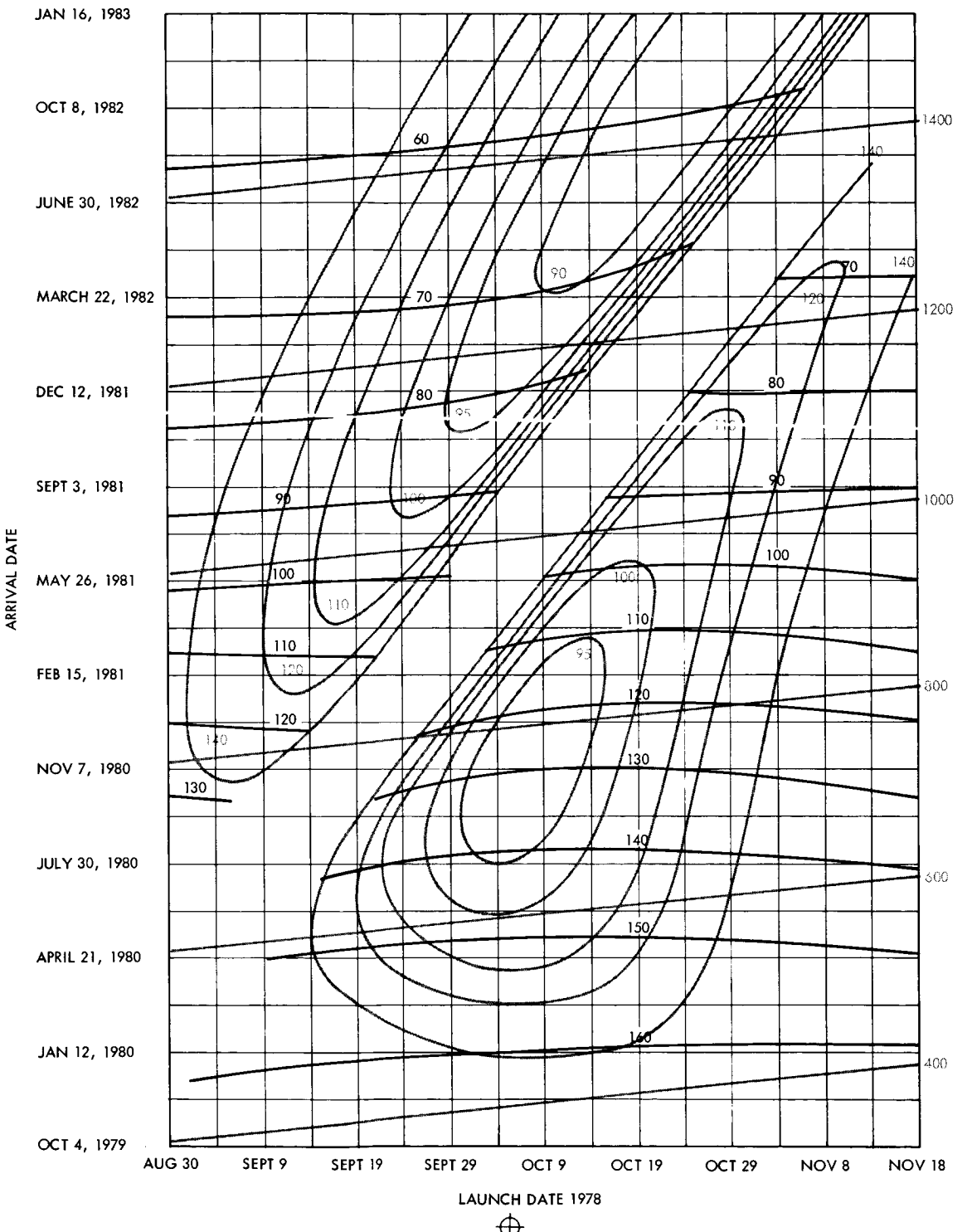

Figure 34. Earth-Jupiter 1978 Trajectories, ZAP, Angle Between Planetocentric Approach Asymptote and Jupiter

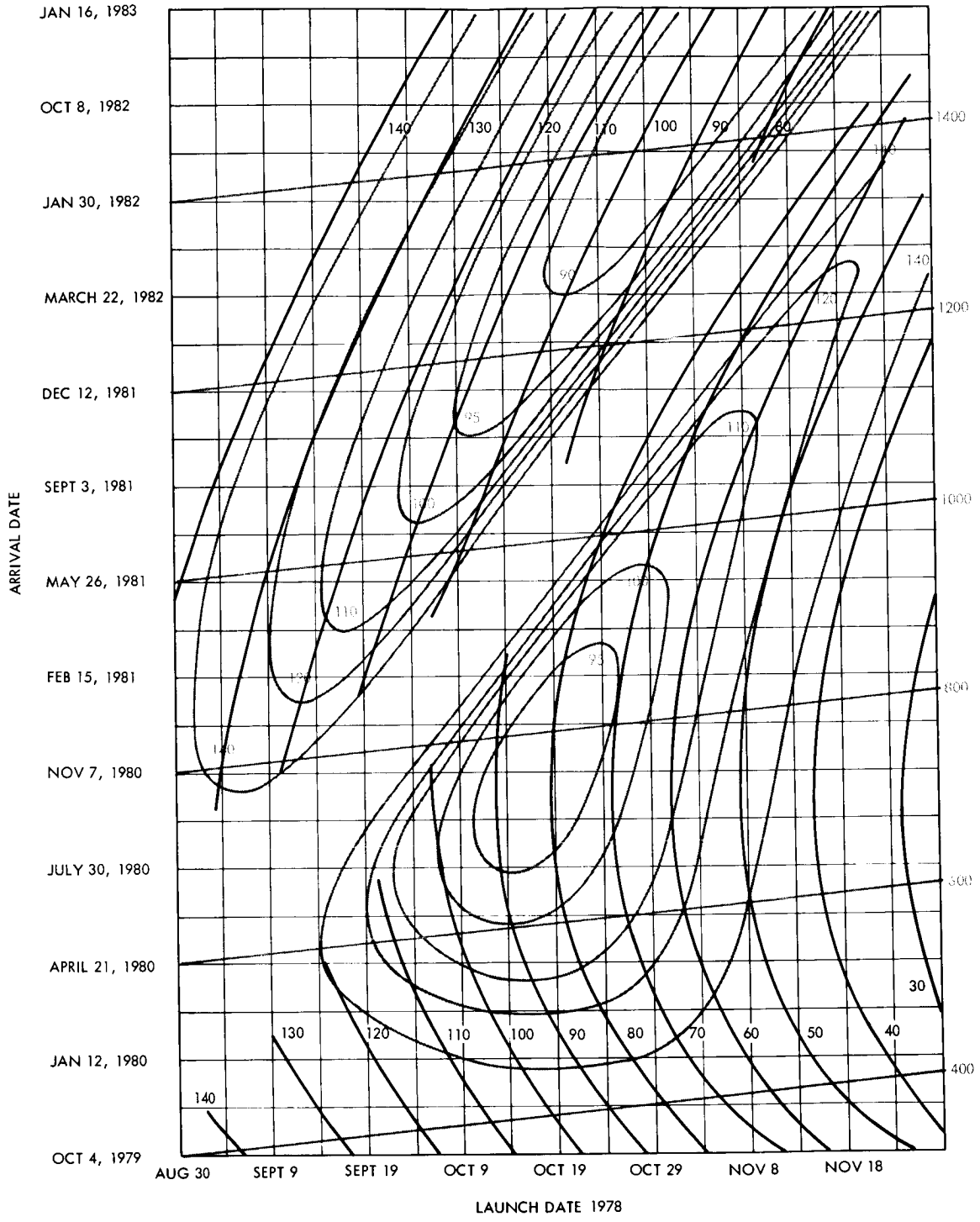

Figure 35. Earth-Jupiter 1978 Trajectories, ZAL, Angle Between Geocentric Departure Asymptote and the Sun-Earth Vector

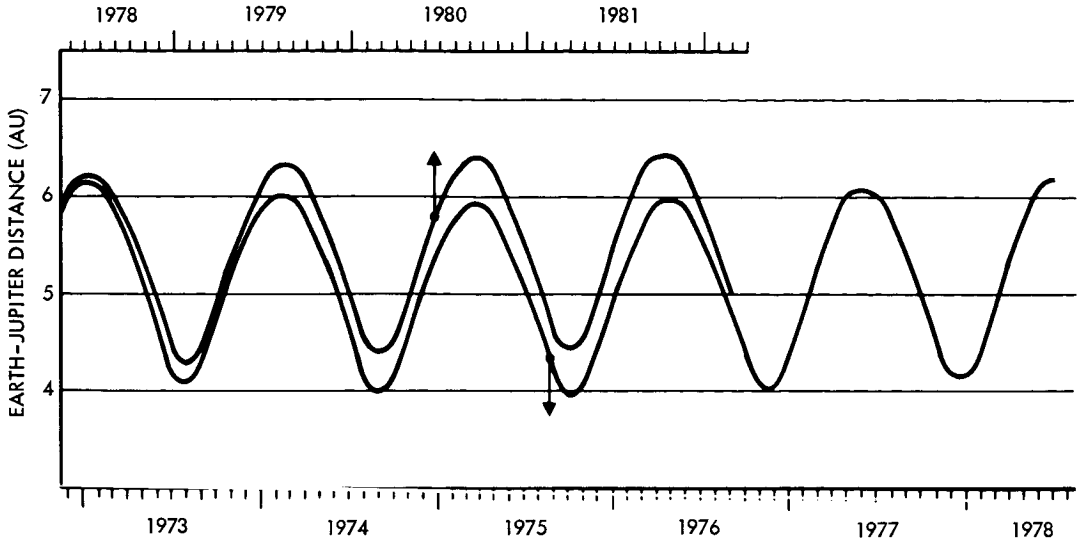

Figure 36. Earth-Jupiter Distance Versus Calendar Time

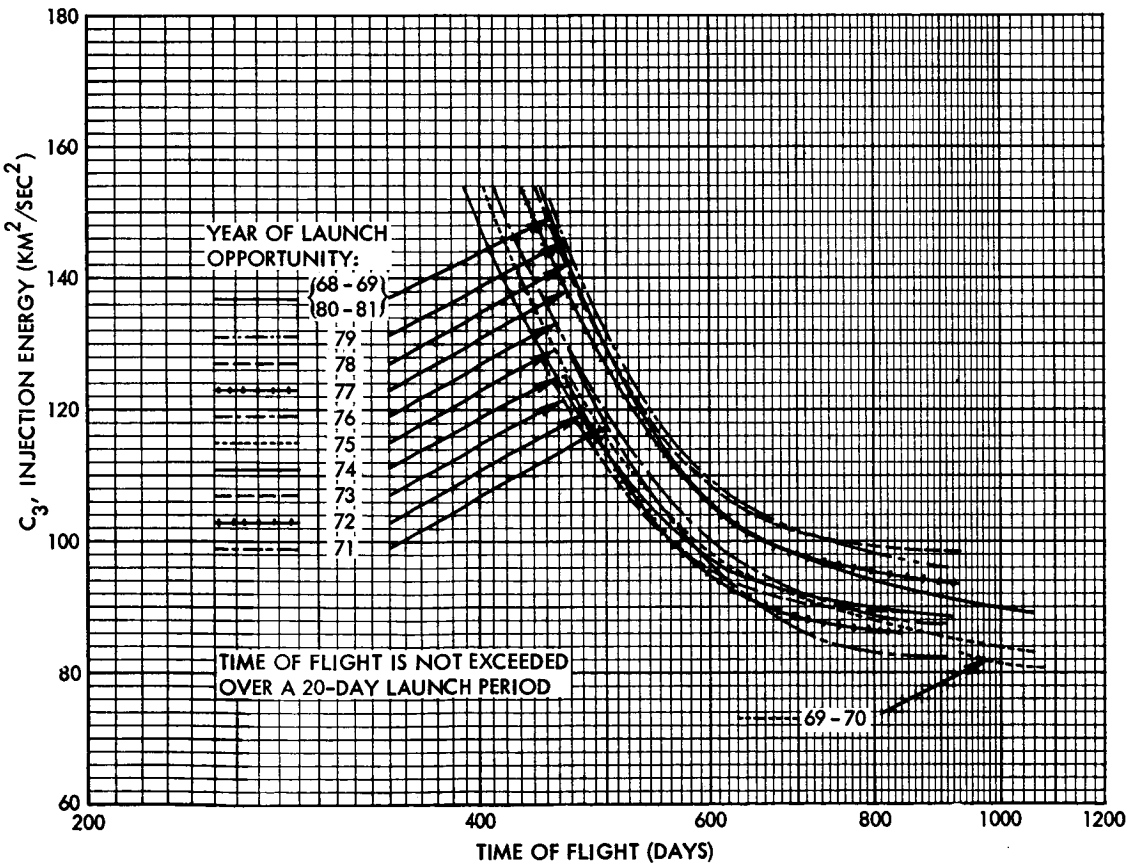

Figure 37. C_3 Requirements for Earth-Jupiter Type I Trajectories Versus Time of Flight

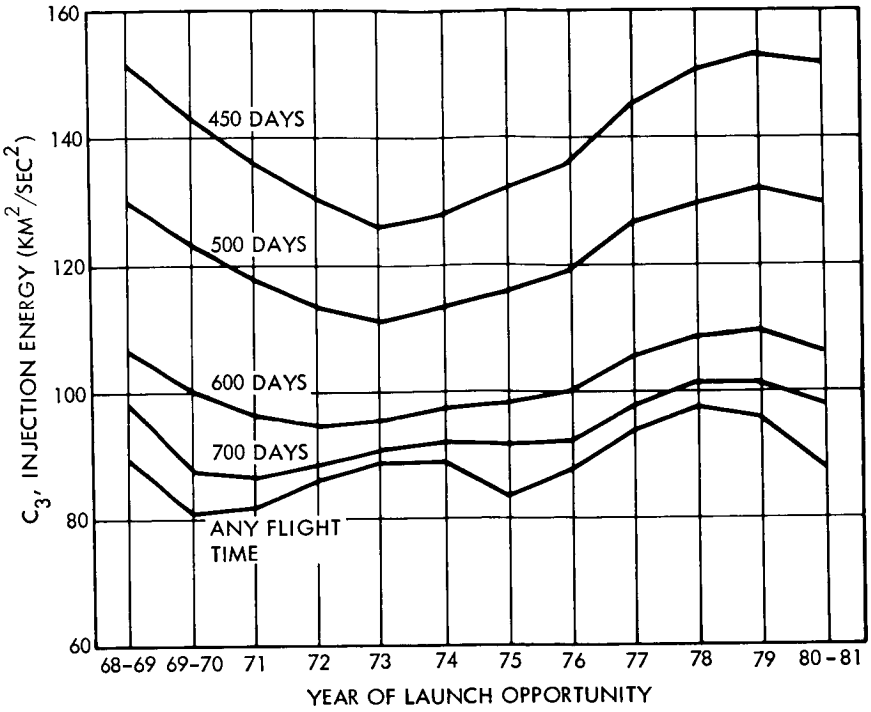

Figure 38. Injection Energy Requirements for Earth-Jupiter Type I Trajectories Versus Given Flight Time, 20-Day Launch Periods

a 20-day launch period. The lowest curve of Figure 38 is taken from Figure 21, and represents the minimum C_3 requirements over a 20-day launch period, with no restraint on flight time.

4.2.6 Requirements Imposed by the Science Payload

These requirements for the range of launch opportunities considered are similarly unchanged from 1972.

4.2.7 Trajectory Accuracy

Trajectory accuracy requirements are also unchanged from those stated for the 1972 mission.

4.2.8 Schedule Requirements

As noted in the introduction to this section, there are obvious schedule implications arising from the selection of different launch opportunities. The month and approximate day of an expected launch in any of the opportunities considered may be determined from Figure 19.

The schedule estimates in Volume 2 indicate that 1972 and later earth-Jupiter missions may be scheduled with adequate margin, allowing a normal time interval for all intermediate phases and events from the present until launch. A 1971 mission is feasible, but requires some compression of the normal schedule, for example by conducting some phases in parallel rather than in series. Missions earlier than 1971 cannot be practically scheduled.

4.2.9 Mission Duration

Although the extension of a 1972 concept to different launch opportunities may result in some variation in the time from launch to encounter at the planet Jupiter, it is not likely that these variations will be more than 100 days. Therefore the requirement that spacecraft design accommodate missions of the order of 700 to 800 days is not materially affected. Similarly, the duration of the period after encounter, in which the spacecraft may be devoted to secondary mission objectives associated with the exploration of interplanetary space beyond Jupiter, is not likely to change significantly with launch opportunity.

4.2.10 Probability of Success

The comments in Volume 2 (Section 2.7) on desired or target probabilities of success for a 1972 earth-Jupiter flyby mission are equally applicable to missions in other launch opportunities.

4.2.11 Growth Capability

The requirements for growth capability of the spacecraft to accommodate extended missions — orbiter and capsule entry missions as well as flyby missions to planets beyond Jupiter — is not changed with changes in the launch year.

4.3 SPACECRAFT COMPATIBILITY AND DESIGN MODIFICATIONS

It is evident from the preceding discussions of the functional requirements imposed on the spacecraft design that essentially all characteristics which vary with the launch opportunity affect the ability of the launch vehicle system and the launch and injection process to accommodate the variations in interplanetary trajectories, and that there are essentially no implications of a nature which call for a change in the physical design of the spacecraft system.

An operational consequence, associated with the process of launching the spacecraft, is the desirability of an increase in the launch azimuth range from the 71- to 108-degree range assumed for 1972, to accommodate the extreme launch azimuth declinations associated with Type I trajectories in the 1973 and 1978 opportunities.

A second effect which has been noted has implications with respect to launch vehicle configuration. This is the extension of the 25-minute upper limit in the parking orbit coast time of the Centaur launch vehicle stage. Although this limit is acceptable in 1972, launches from 1975 to 1982, when the launch asymptote has positive declinations, are essentially impossible without an increase in the maximum coast time.

There is also a substantial variation in the injection energy requirements for earth-Jupiter trajectories over a 12-year cycle. This effect has been examined in Section 4.2.2, and is illustrated in Figure 38. The suitability of specific launch vehicle-spacecraft combinations for missions in the 1970's is indicated by Figure 39 obtained by making horizontal cross plots from Figure 38. In Figure 39, the variable margin that a given launch vehicle-spacecraft combination has for different launch opportunities is assumed to be manifested in a variable time of flight, with a constant 20-day launch period. It is seen that for the spacecraft which have been identified in preceding sections of this report, and associated launch vehicles, the margin in 1972 is great enough that the feasibility of the mission extends over the entire decade. For one combination, however, the 564-pound, 3-axis stabilized spacecraft (50-pound science payload) and the Atlas SLV3x/Centaur/TE-364-3 launch vehicle, the C_3 capability of 92.5 km^2/sec^2 is inadequate to provide a 20-day launch period in the years 1977, 1978, and 1979, in which the C_3 requirements are greatest.

Although no design changes in the spacecraft concepts described in preceding sections are required to adapt 1972 Jupiter flyby missions to other opportunities, it is noted that the variations in time of flight which may result from launches in different years will lead to slight variations in the assessed probabilities of success. These possible variations are estimated to be of minor importance.

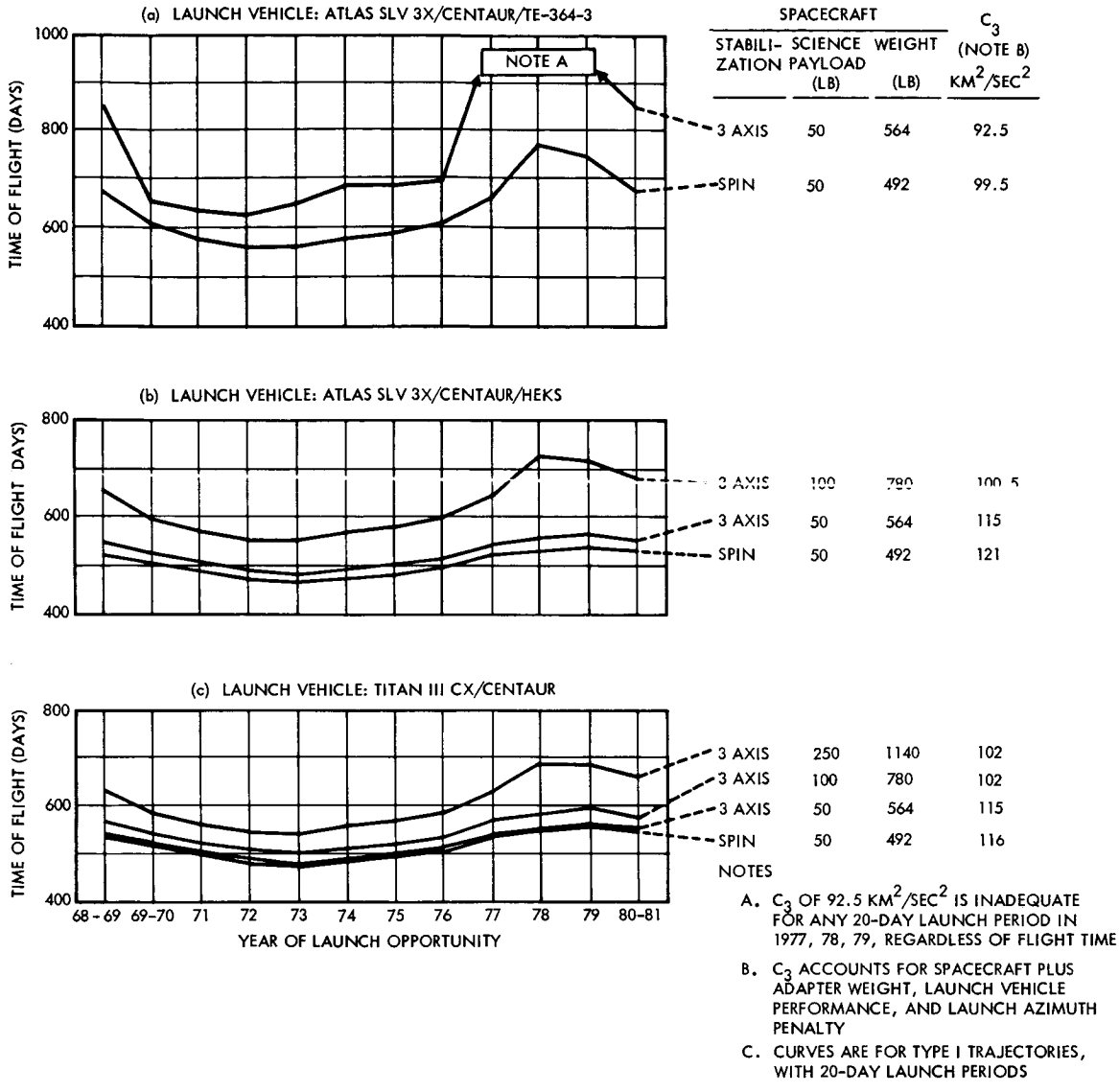

Figure 39. Flight Time Versus Launch Opportunity for Several Launch Vehicle-Spacecraft Combinations

The conclusion that spacecraft design changes are not necessary for the later missions does not preclude the possible desirability that one would want to effect a change to incorporate improvements in the state of the art which may come to light in intervening years. It is conceivable that such improvements may be exploited to reduce spacecraft weight so as to compensate for increased injection energy requirements, or to improve the spacecraft performance and the value of the mission. Areas in which such improvements are contemplated are given in descriptions of the various subsystems in Volume 2.

5. FLYBY MISSIONS TO PLANETS BEYOND JUPITER

5.1 INTRODUCTION AND CONCLUSIONS

The possibility of flyby missions to Saturn, Uranus, and Neptune with the spacecraft used for Jupiter flyby is examined in this section. Since we are concerned primarily with the growth potential of the configurations discussed, the emphasis in this section is upon the effects of the changed requirements upon the proposed configurations.

The principal conclusion of this section is that a Jupiter flyby spacecraft is basically compatible with missions to Saturn, Uranus, or Neptune. The required changes in spacecraft configuration are relatively minor, affecting primarily the reliability requirements, science, data rate, and for the spin-stabilized configurations its spin rate, reduced at encounter to allow longer TV exposure time. The Titan IIICx/Centaur/TE-364-3 is the minimum launch vehicle for direct flights to Saturn and beyond but at the same time this launch vehicle can carry the 50-pound science payload class of spacecraft to Neptune in 8.6 years, the 100-pound payload class in 10.1 years, and the 250-pound class to Uranus in 9 years. With Jupiter swingby (single opportunity) the Atlas SLV3x/Centaur/HEKS can put the 50-pound science class payload to Saturn in 3.1 years, Uranus in 5.8 years, and Neptune in 8.6 years. However, it appears extremely difficult to achieve adequate trajectory control for Jupiter swingbys.

The requirements for missions to planets beyond Jupiter are similar to those for missions to Jupiter except that the mission flight time will be increased, the distance from the earth and sun will be increased, and the guidance problem will be more difficult.

5.2 SCIENCE REQUIREMENTS

The science payload for a mission to any of the other planets will also be much like the Jupiter payload, consisting of the standard five interplanetary experiments:

- Galactic cosmic ray
- Solar plasma ray
- Magnetometer

- Micrometeoroid detector
- Radio propagation occultation

In addition, specific planetary experiments will be carried. The number and type depend on the payload capability for these missions. However, at least a trapped radiation counter, infrared radiometer, and a television experiment appear desirable.

5.3 DIRECT TRAJECTORIES

This section describes the trajectory requirements for direct transfers to the three outer planets. It also includes sample trajectories to Jupiter and Saturn.

Direct trajectories to the outer planets require more injection energy from the earth and have longer flight times than swingby trajectories past Jupiter. Injection energy requirements with respect to the earth and several different trajectory parameters have been computed for direct flights to Saturn during the 1974 and 1978 launch opportunities and for flights to Neptune during the 1978 opportunity.

Maps of the solar system are presented in Figures 40 and 41 which show the relative position of the planets for the 1970 to 1980 decade. In Figure 40, the orbit of the earth is expanded to twice the proportional size to better indicate the earth orbit central angle. Calendar day marks identify the time at various positions in orbit. Figure 41 shows the earth orbit in its proper proportion.

The trajectory parameters for the entire launch windows described above include the geocentric launch energy C_3, declination of the departure asymptote DLA, asymptotic approach velocity at the destination planet V_{HP}, angle between the approach velocity asymptote at the destination planet and the planet-sun line ZAP, and the angle between the geocentric departure asymptote and the sun-earth vector ZAL in Figures 42 through 55. These parameters are presented as contours on plots of launch day versus arrival day. The first figure in each set for a given launch window and destination planet shows the injection energy contours. The remaining figures show contours of the other parameters and include an underlay of the injection energy contours.

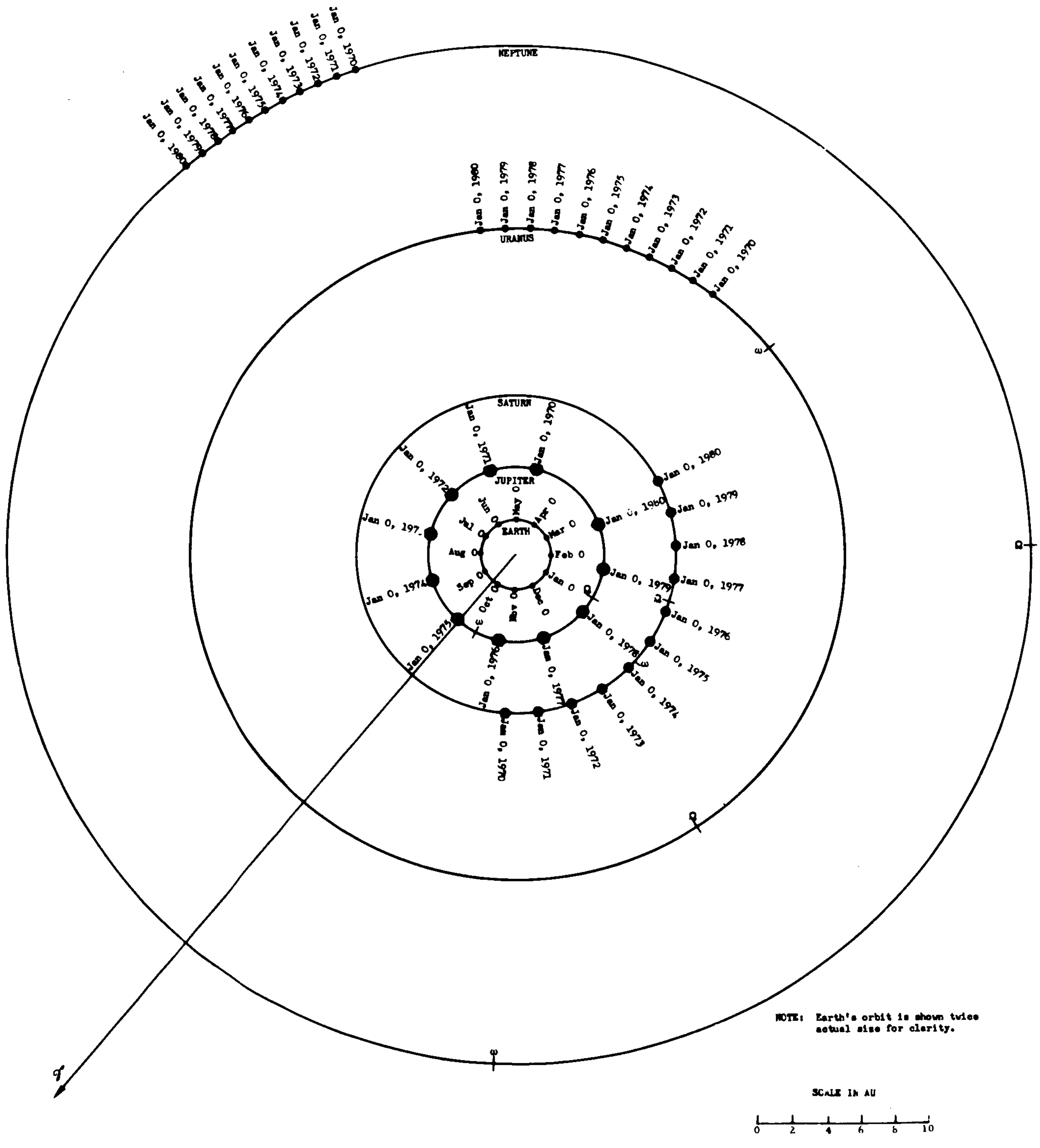

Figure 40. Partial Map of Solar System

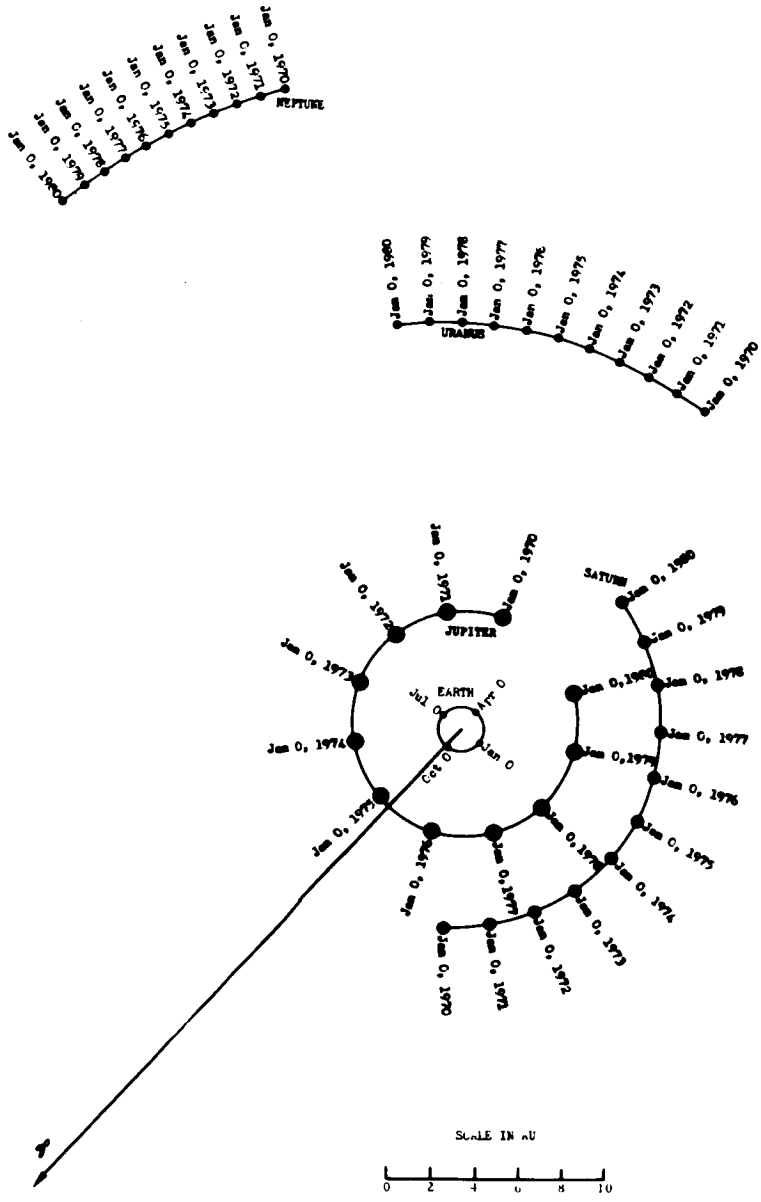

Figure 41. Partial Map of Solar System, 1970 to 1980

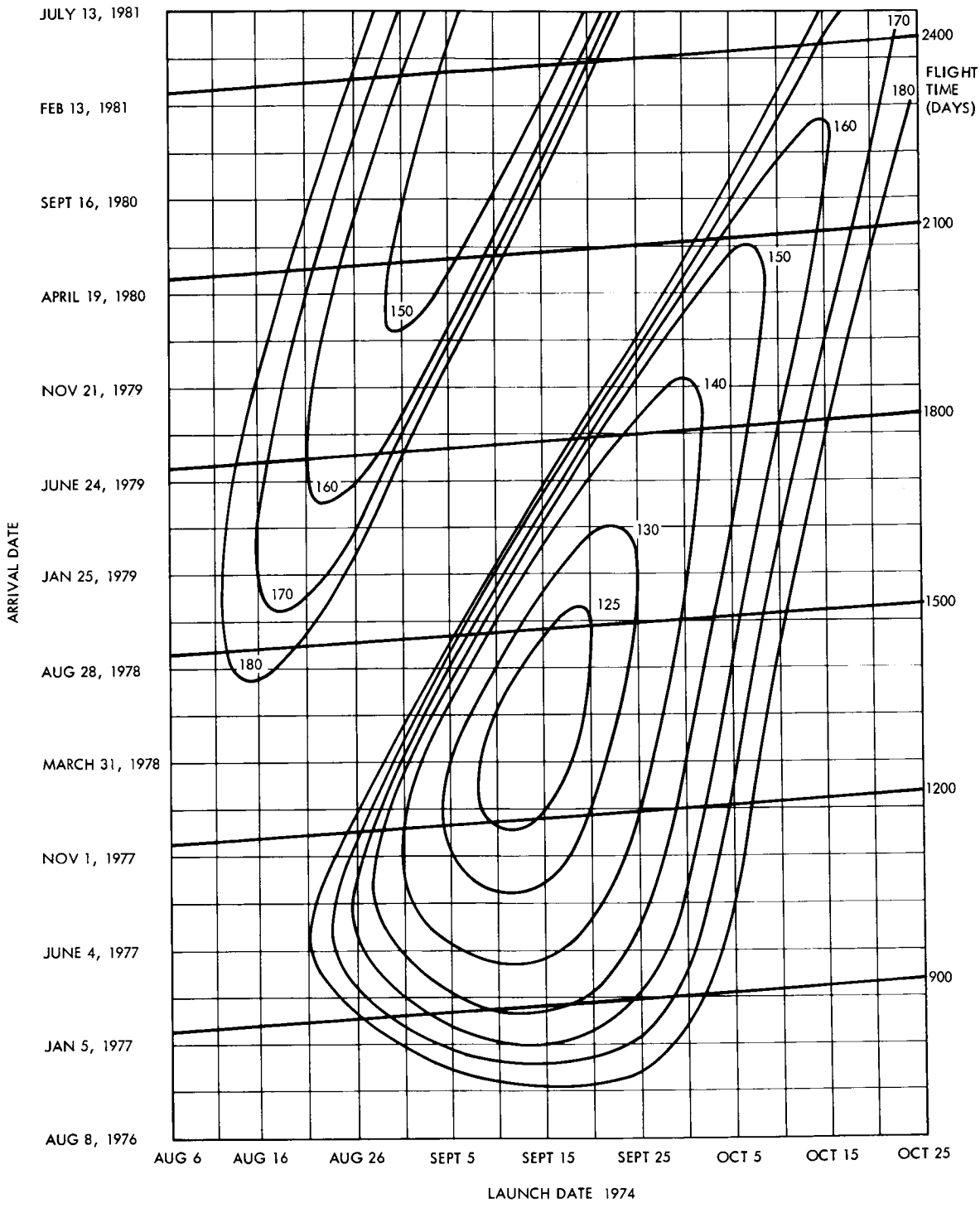

Figure 42. Earth-Saturn 1974 Trajectories, C_3, Geocentric Launch Energy

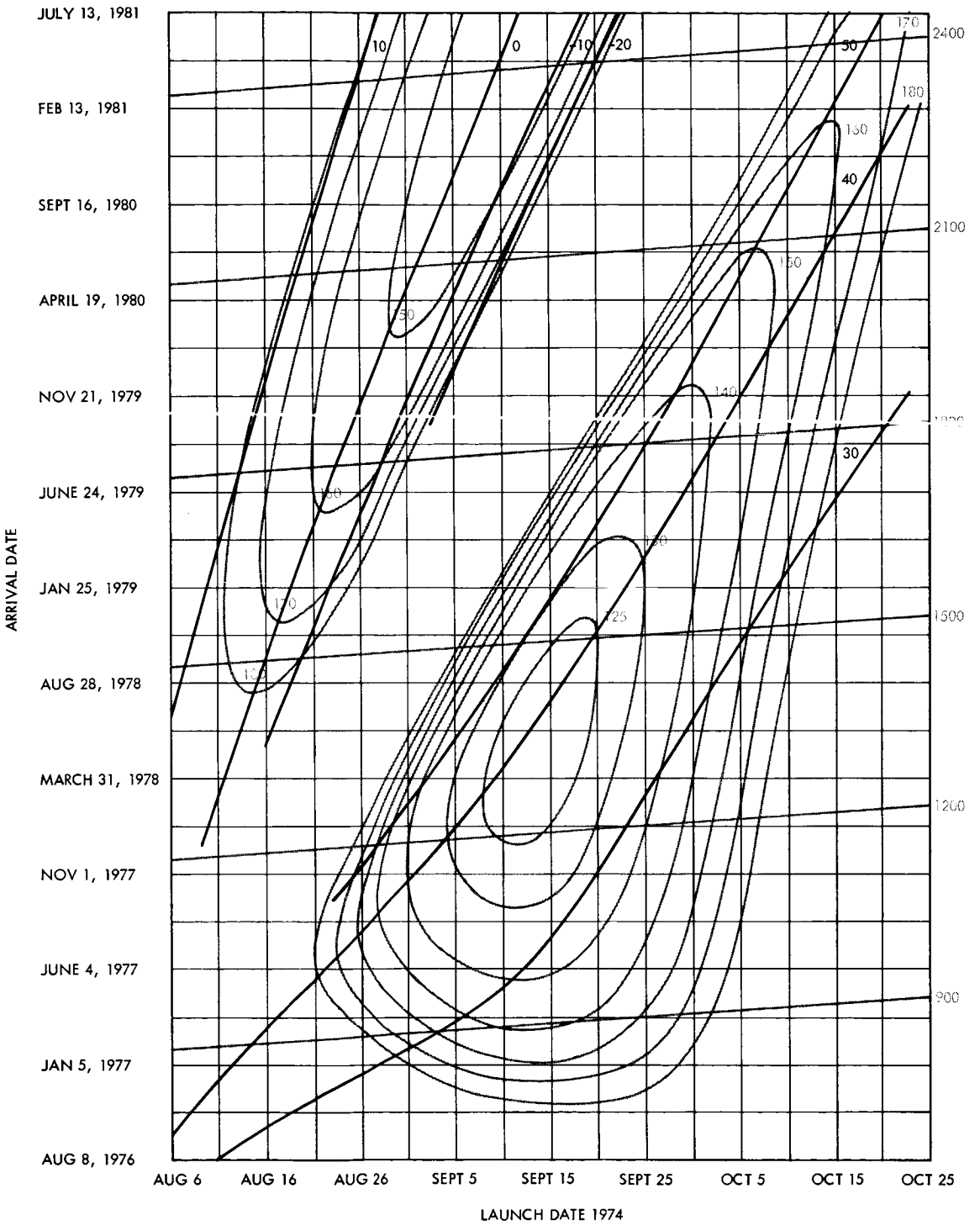

Figure 43. Earth-Saturn 1974 Trajectories, DLA, Declination of Geocentric Departure Asymptote

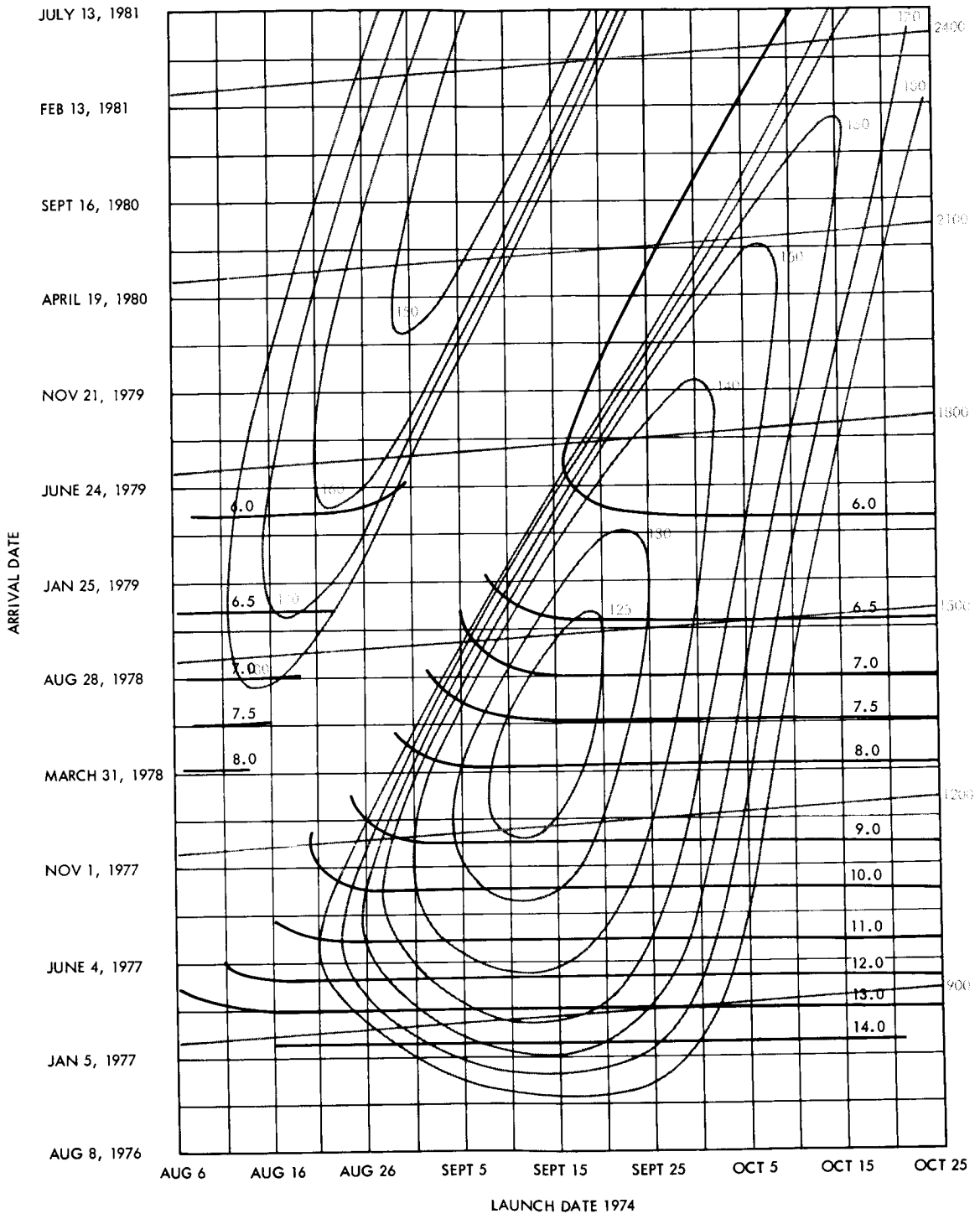

Figure 44. Earth-Saturn 1974 Trajectories, V_{HP}, Planetocentric Asymptote Approach Velocity at Saturn

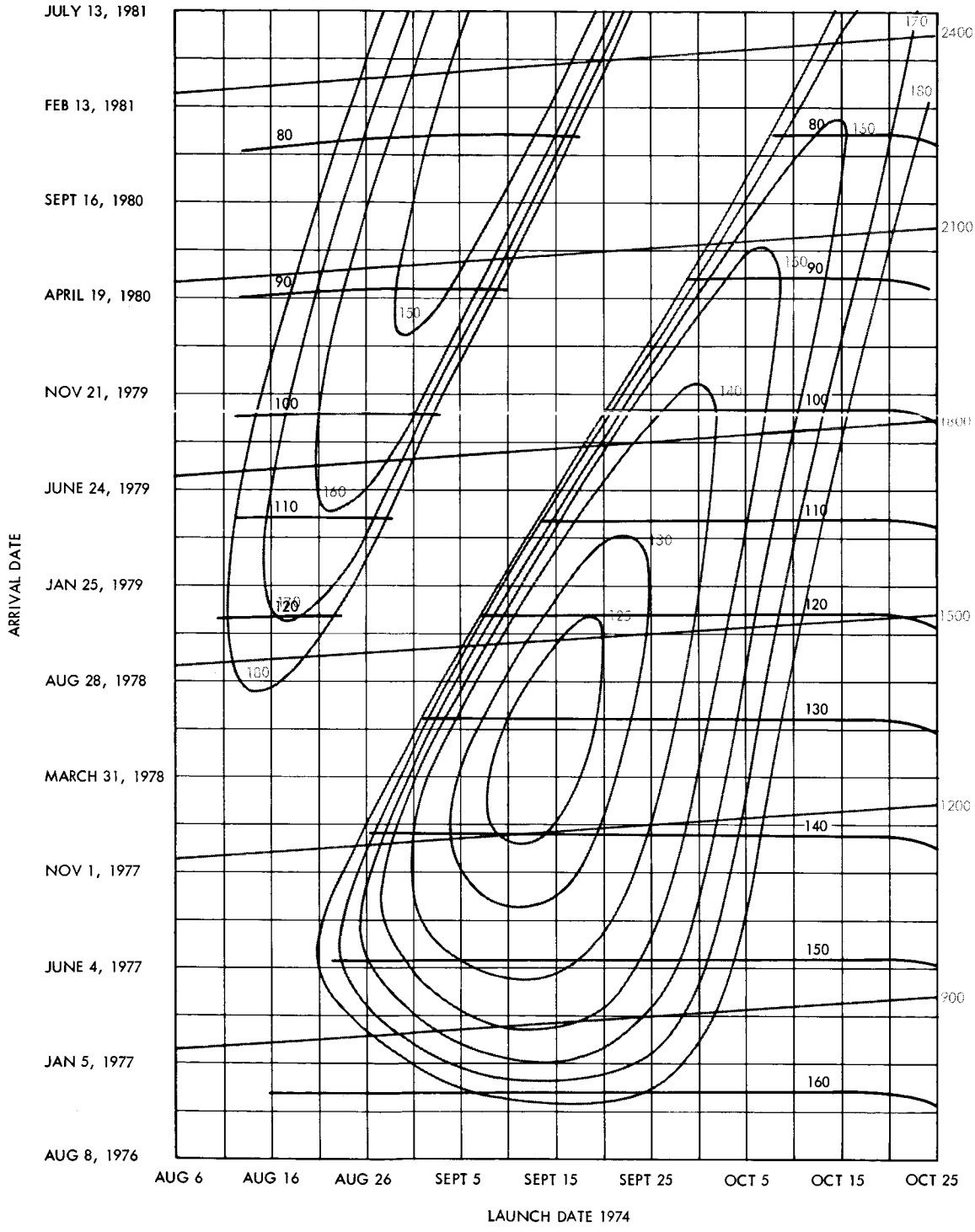

Figure 45. Earth-Saturn 1974 Trajectories, ZAP, Angle Between Planetocentric Approach Asymptote and Saturn-Sun Vector

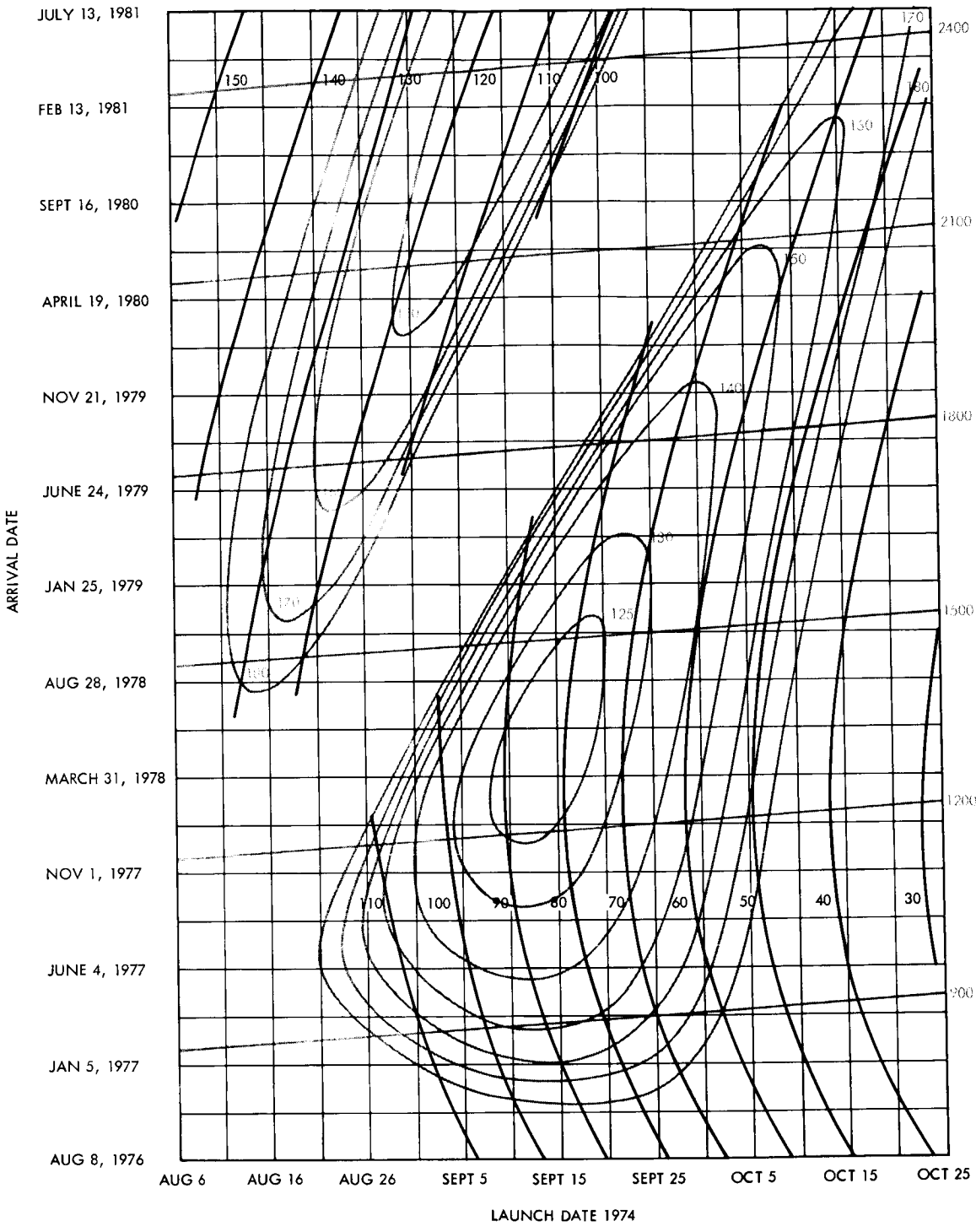

Figure 46. Earth-Saturn 1974 Trajectories, ZAL, Angle Between Geocentric Departure Asymptote and the Sun-Earth Vector

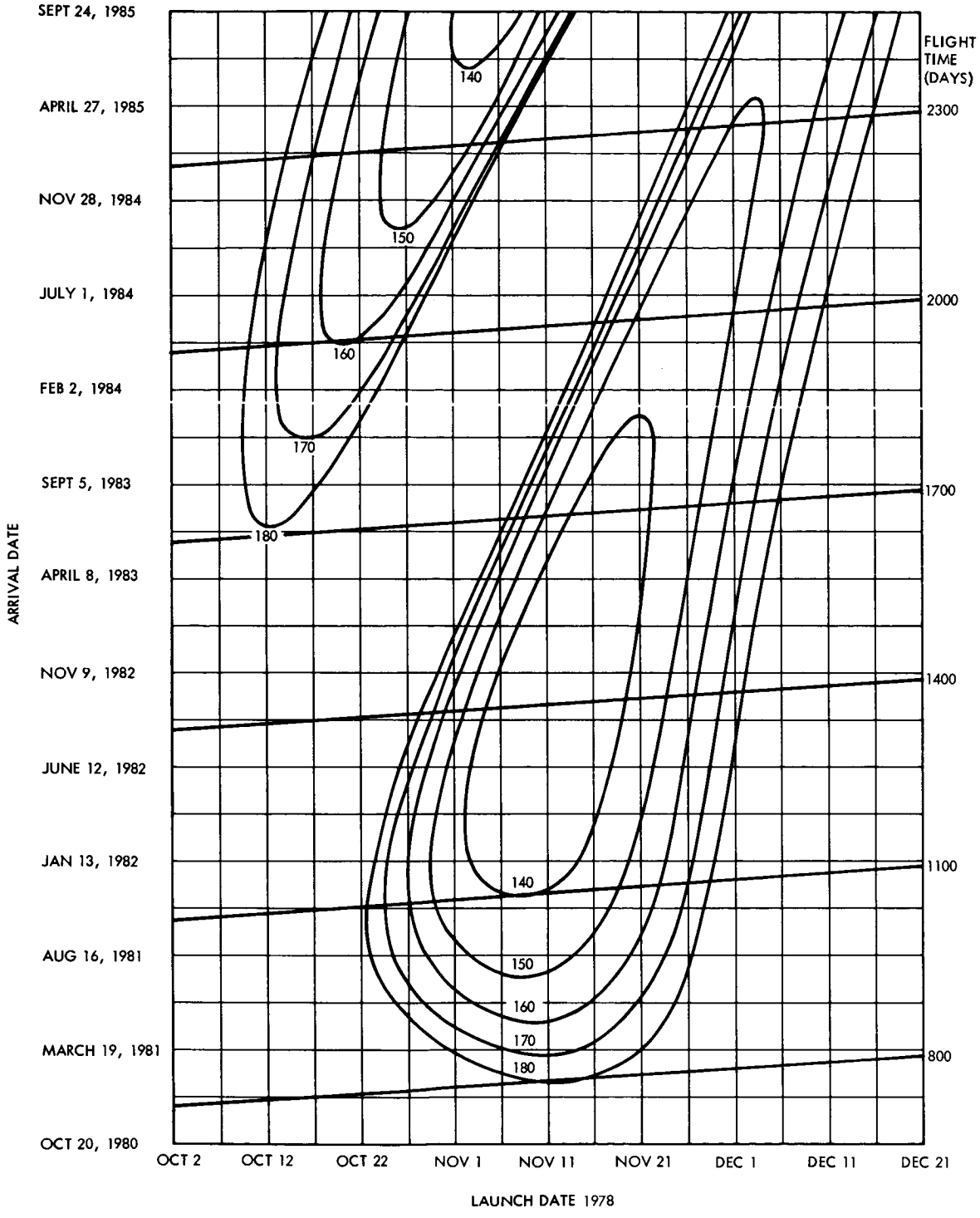

Figure 47. Earth-Saturn 1978 Trajectories, C_3, Geocentric Launch Energy

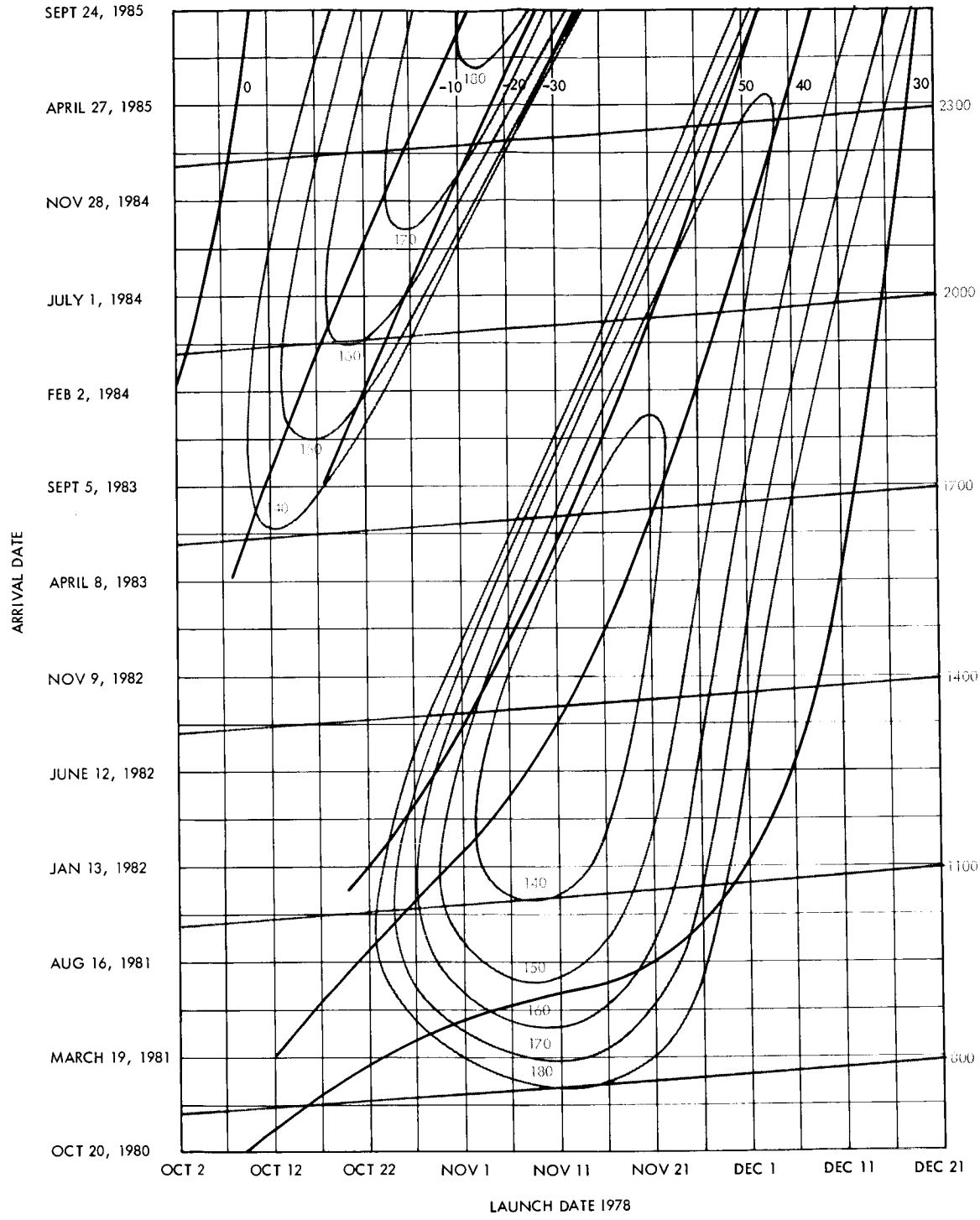

Figure 48. Earth-Saturn 1978 Trajectories, DLA, Geocentric Launch Energy

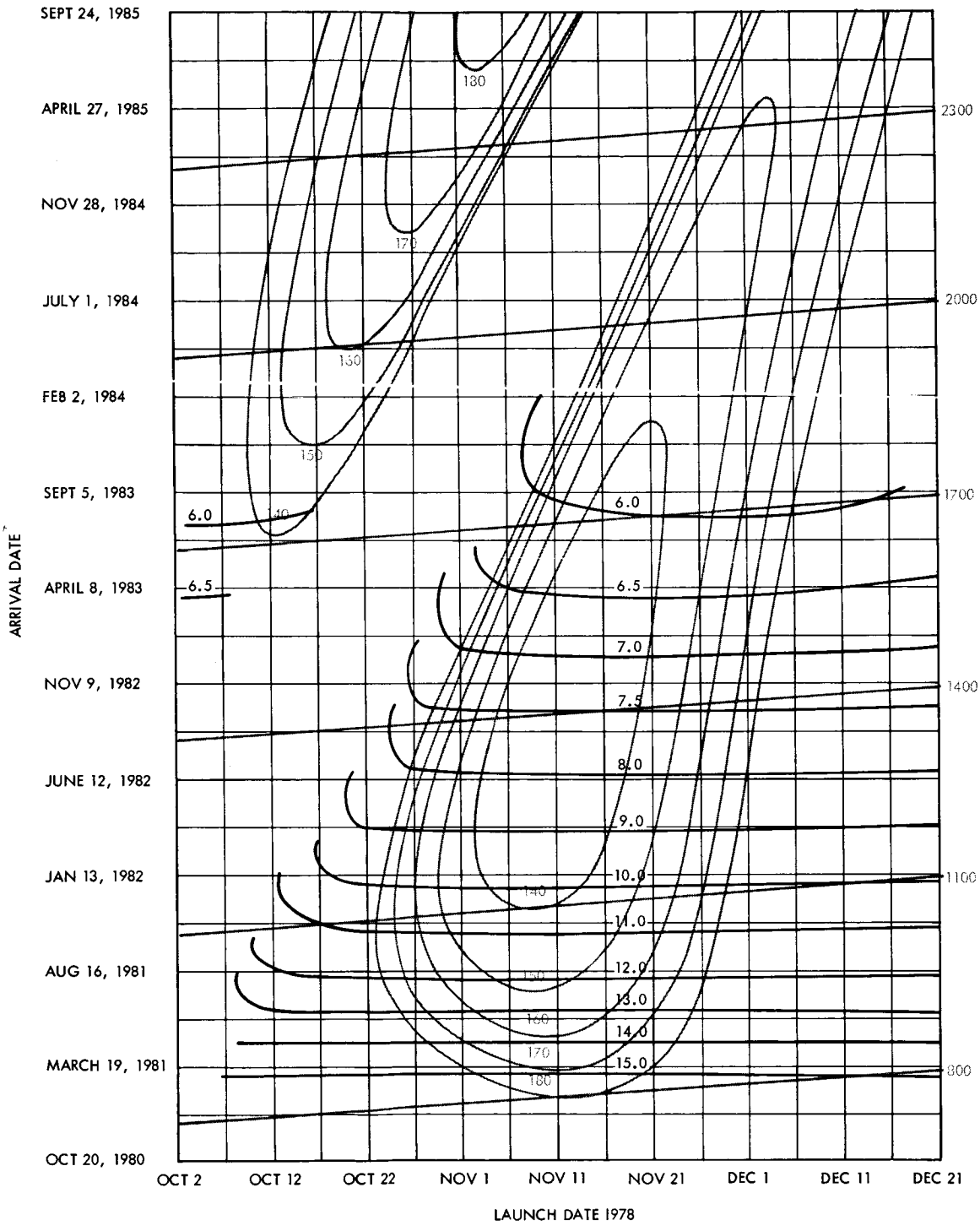

Figure 49. Earth-Saturn 1978 Trajectories, V_{HP}, Planetocentric Asymptote Approach Velocity at Saturn

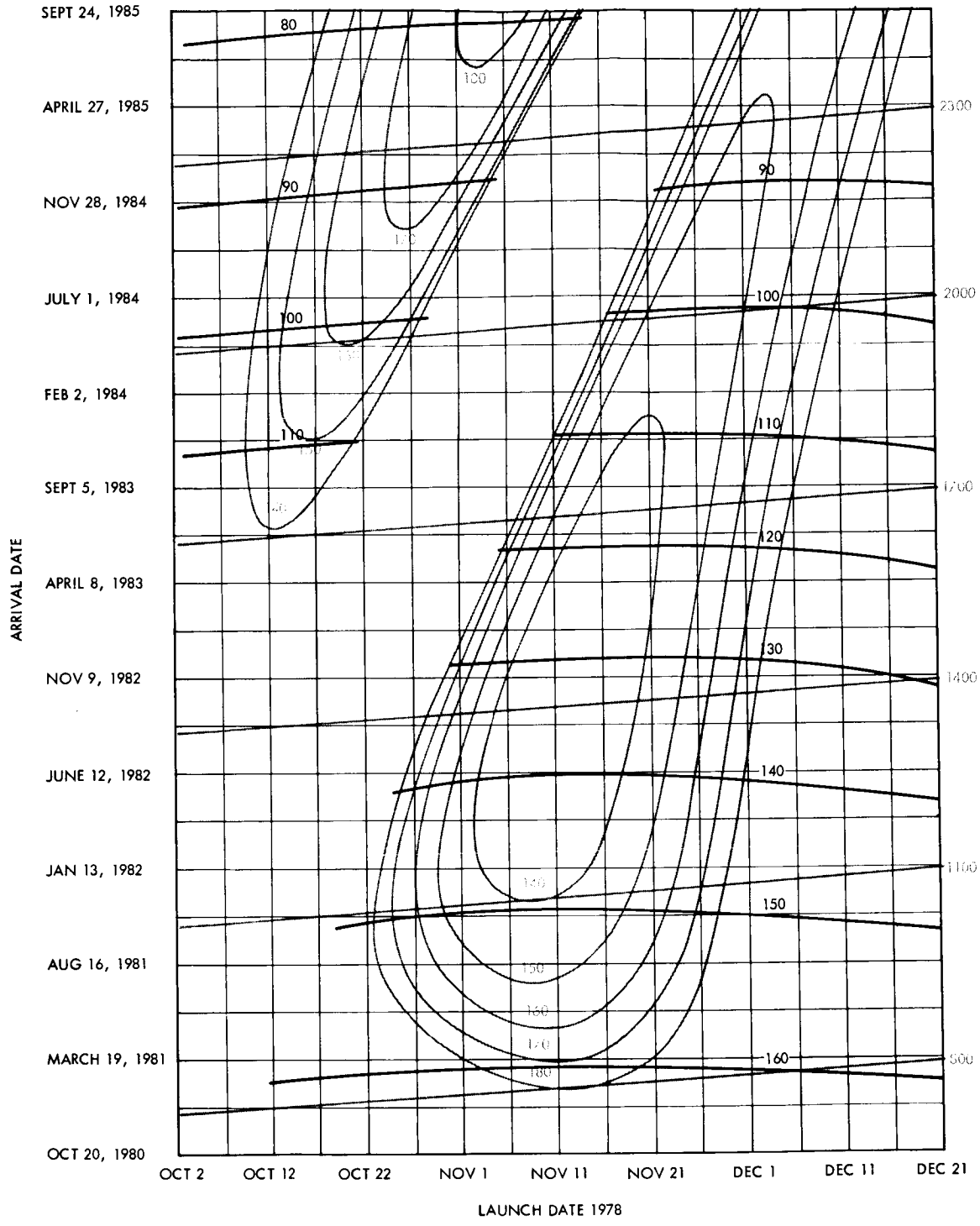

Figure 50. Earth-Saturn 1978 Trajectories, ZAP, Angle Between Planetocentric Approach Asymptote and Saturn-Sun Vector

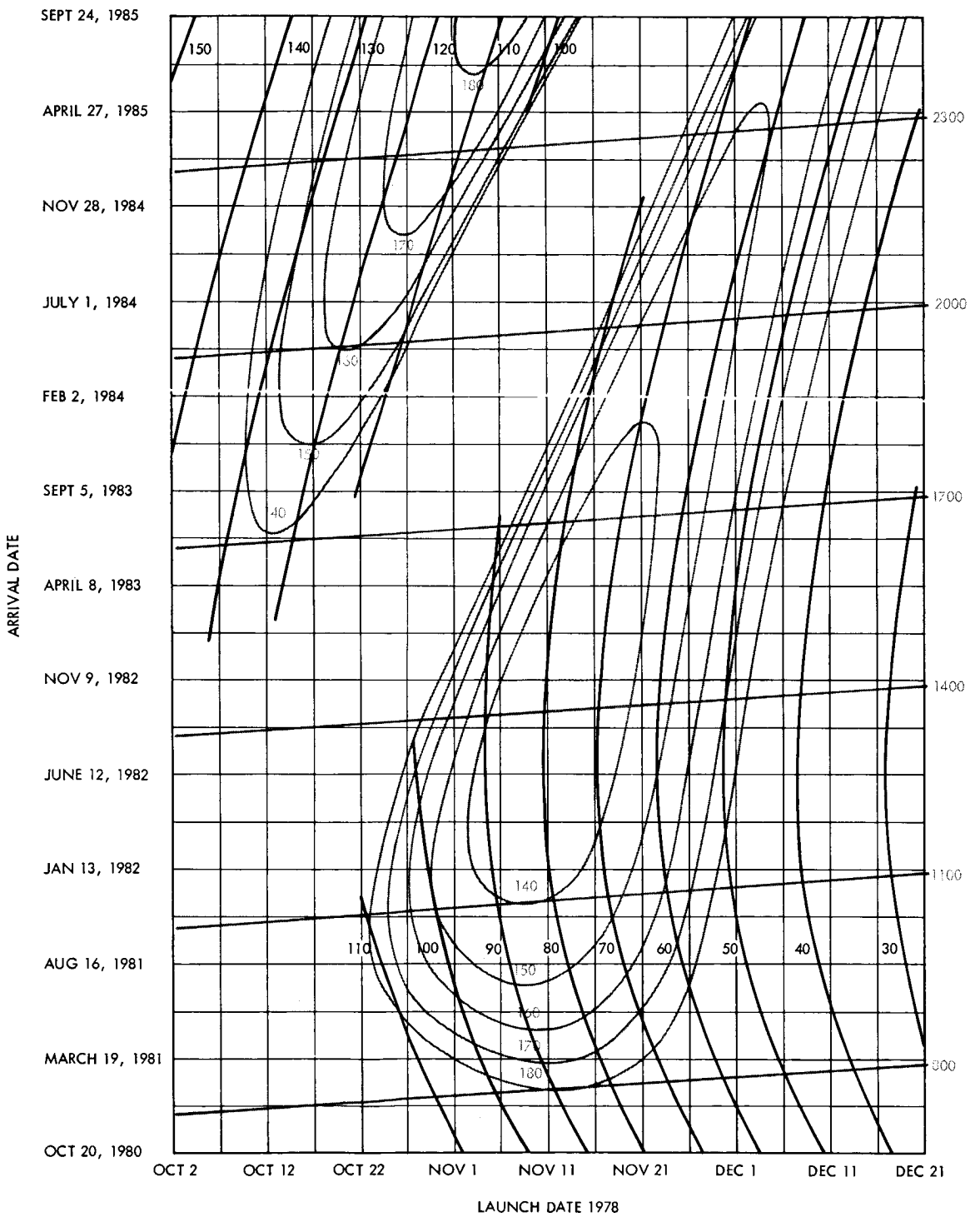

Figure 51. Earth-Saturn 1978 Trajectories, ZAL, Angle Between Geocentric Departure Asymptote and the Sun-Earth Vector

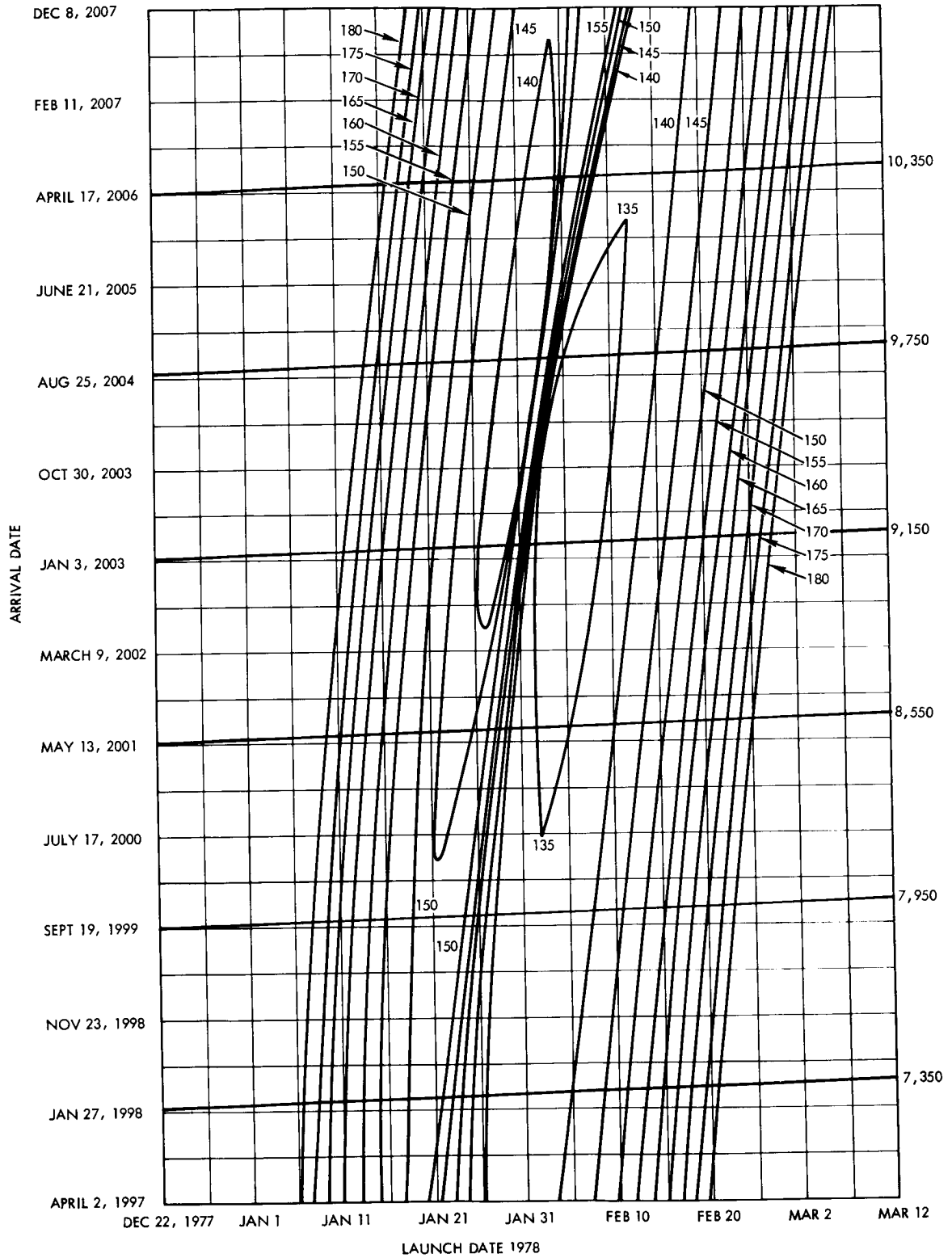

Figure 52. Earth-Neptune 1968 Trajectories, C_s, Geocentric Launch Energy

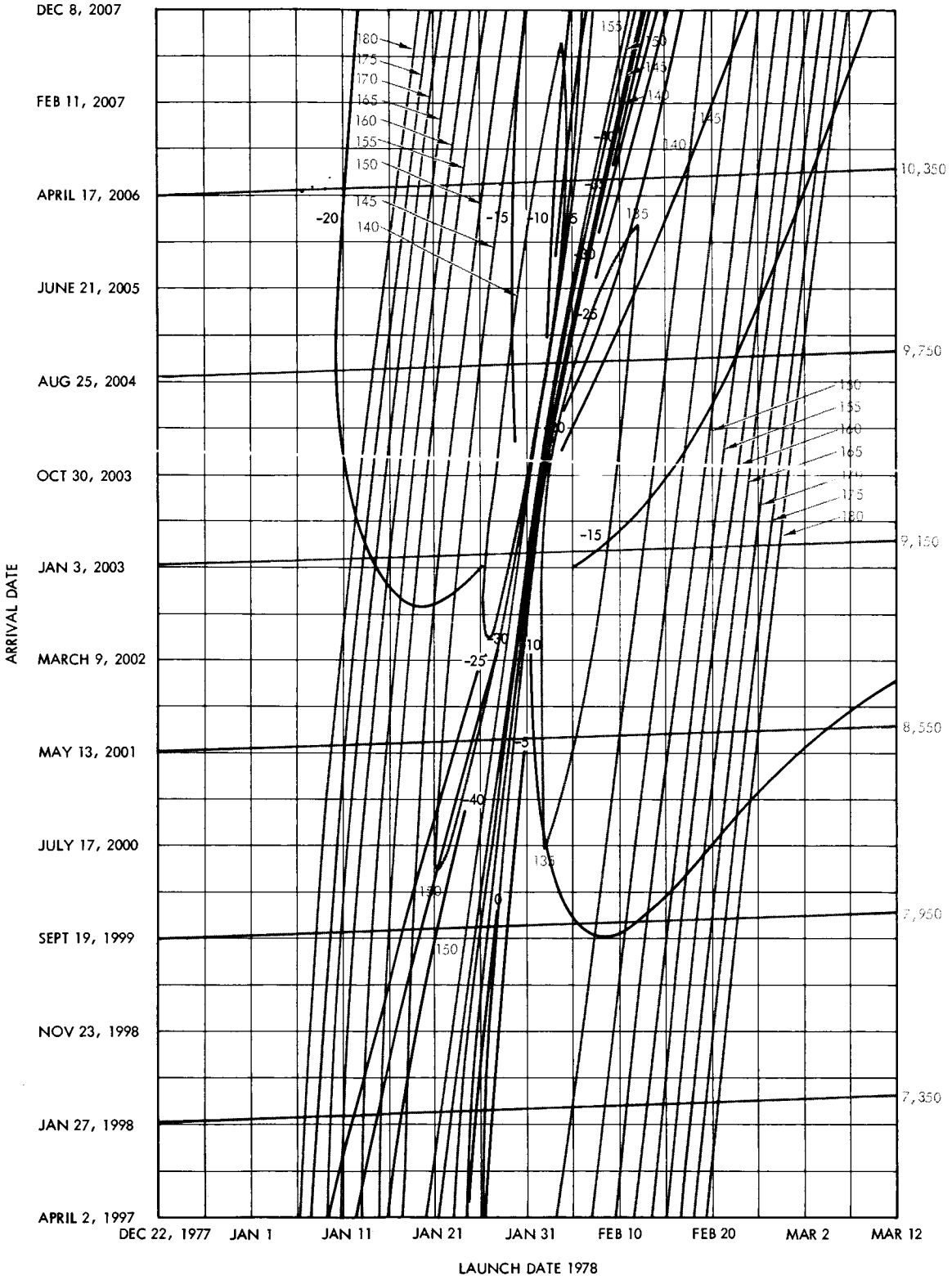

Figure 53. Earth-Neptune 1978 Trajectories, DLA, Declination of Geocentric Departure Asymptote

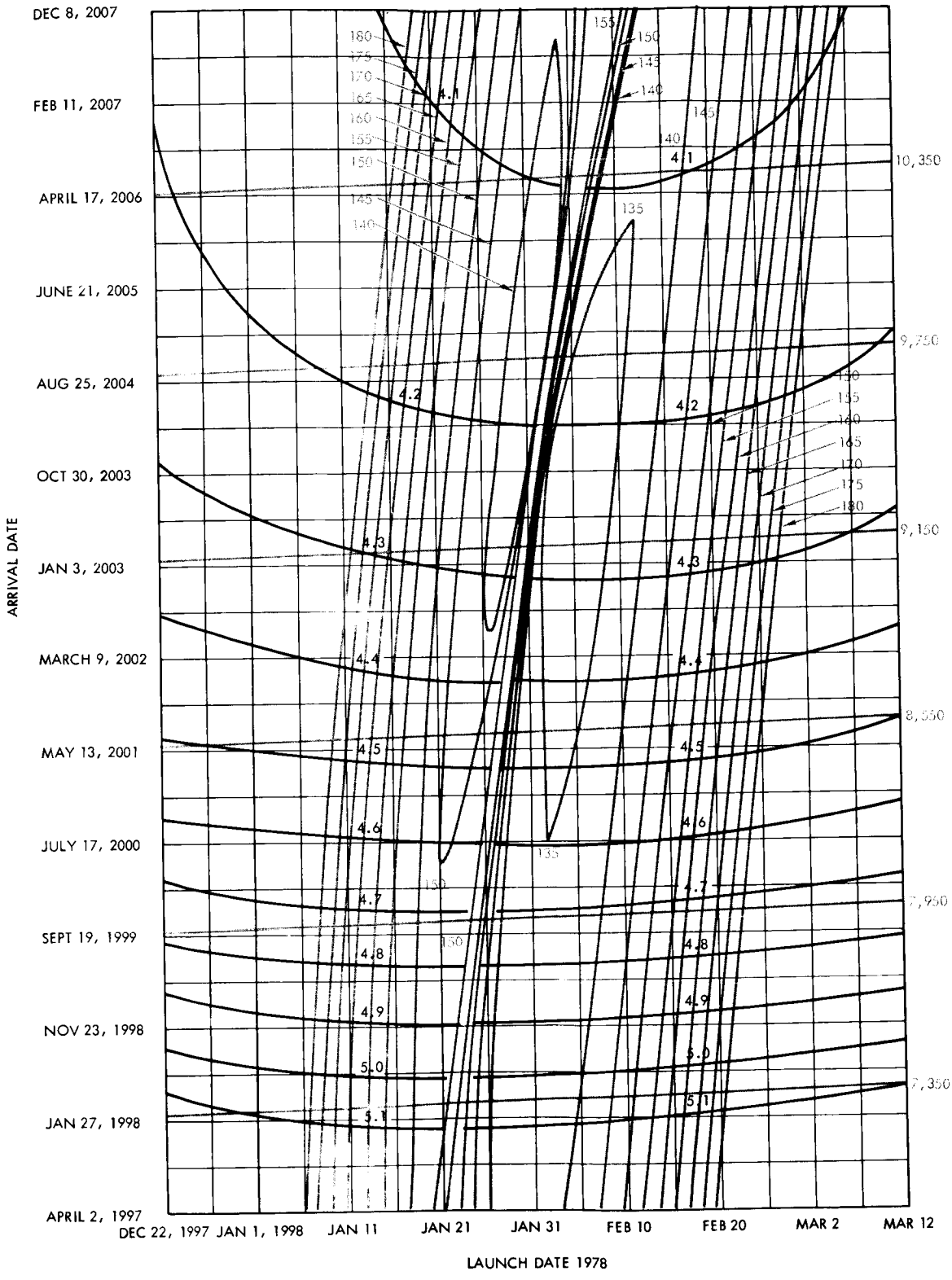

Figure 54. Earth-Neptune 1978 Trajectories, V_{HP}, Planetocentric Asymptote Approach Velocity at Neptune

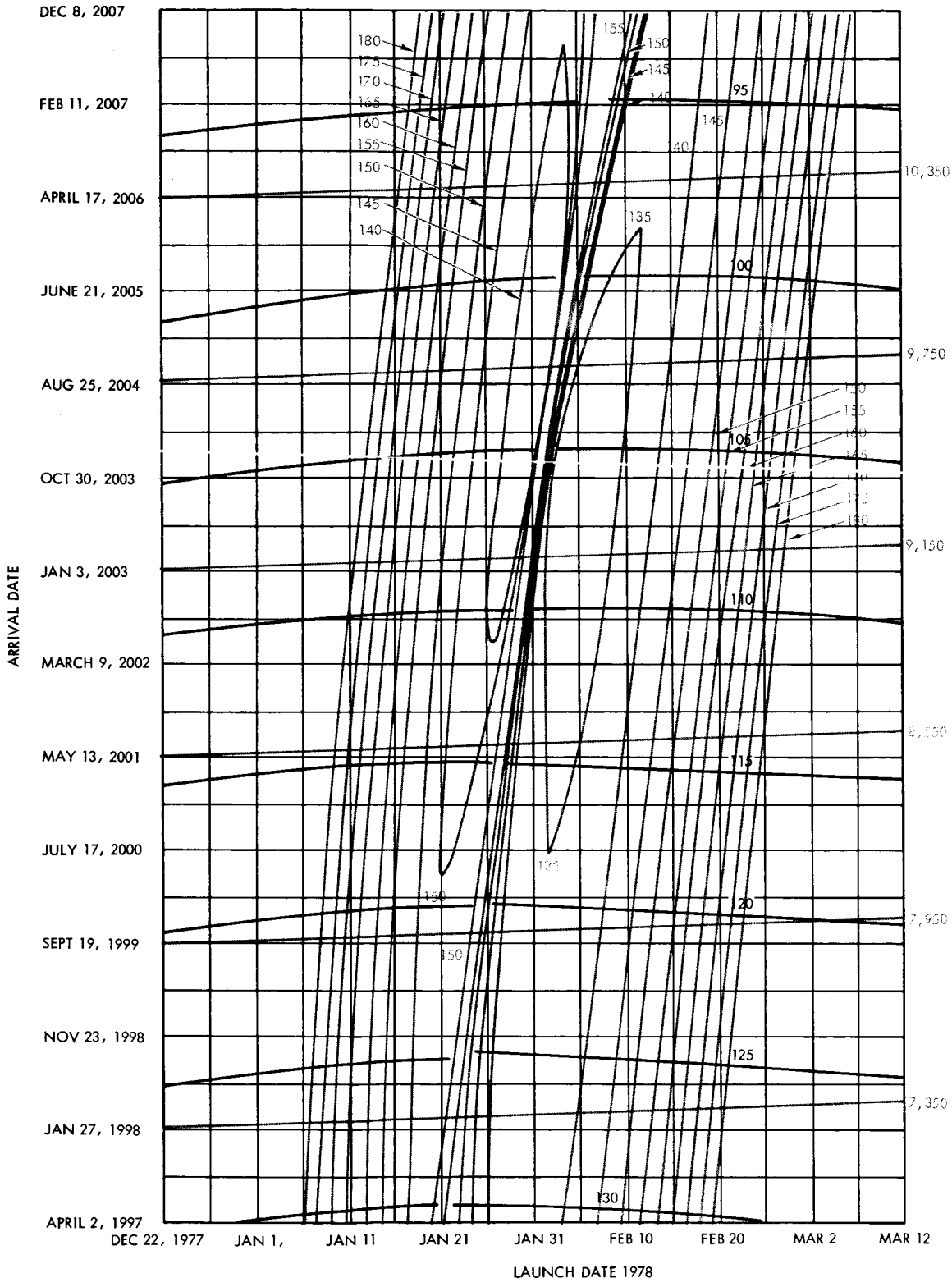

Figure 55. Earth-Neptune 1978 Trajectories, ZAP, Angle Between Planetocentric Approach Asymptote and Neptune-Sun Vector

The energy contours show that the minimum energy requirement for Saturn flights is less for the 1974 opportunity than for the 1978 opportunity. Approximately 122 and 132 km^2/sec^2 are the minimum energies for 1974 and 1978 launches, respectively. The least energy requirement which guarantees a 20-day launch window is 134 and 147 km^2/sec^2, respectively. For flight to Neptune in 1978, the approximate minimum energy is 135 km^2/sec^2.

Correlation of the minimum injection energy requirements with the year of launch opportunity indicates that in 1974 and 1978 Saturn trajectories are not near the node-to-node condition. A detailed discussion of the correlation between minimum energy requirements and the interplanetary trajectory characteristics is given in Section 4.2.2 for earth-Jupiter trajectories.

It is anticipated that the minimum energy requirement in 1982 would be greater and then would decrease for later launch windows. On the other hand, a 1978 flight to Neptune is nearly node-to-node and represents the least of the minimum energy conditions. Later launch windows require more energy.

Three representative direct transfer missions are analyzed in this section. The characteristics of these trajectories are given in Table 14. A solar system display of each of these trajectories is shown in Figures 56, 57, and 58. The heliocentric conics traversed and the times eclipsed from launch are indicated.

Figures 59 through 64 display the following:

- Sun-spacecraft-earth angle
- Spacecraft-earth-sun angle
- Earth-spacecraft-target planet angle
- Heliocentric longitude of projection of earth-spacecraft line on plane of ecliptic
- Spacecraft-earth distance
- Spacecraft-target planet distance

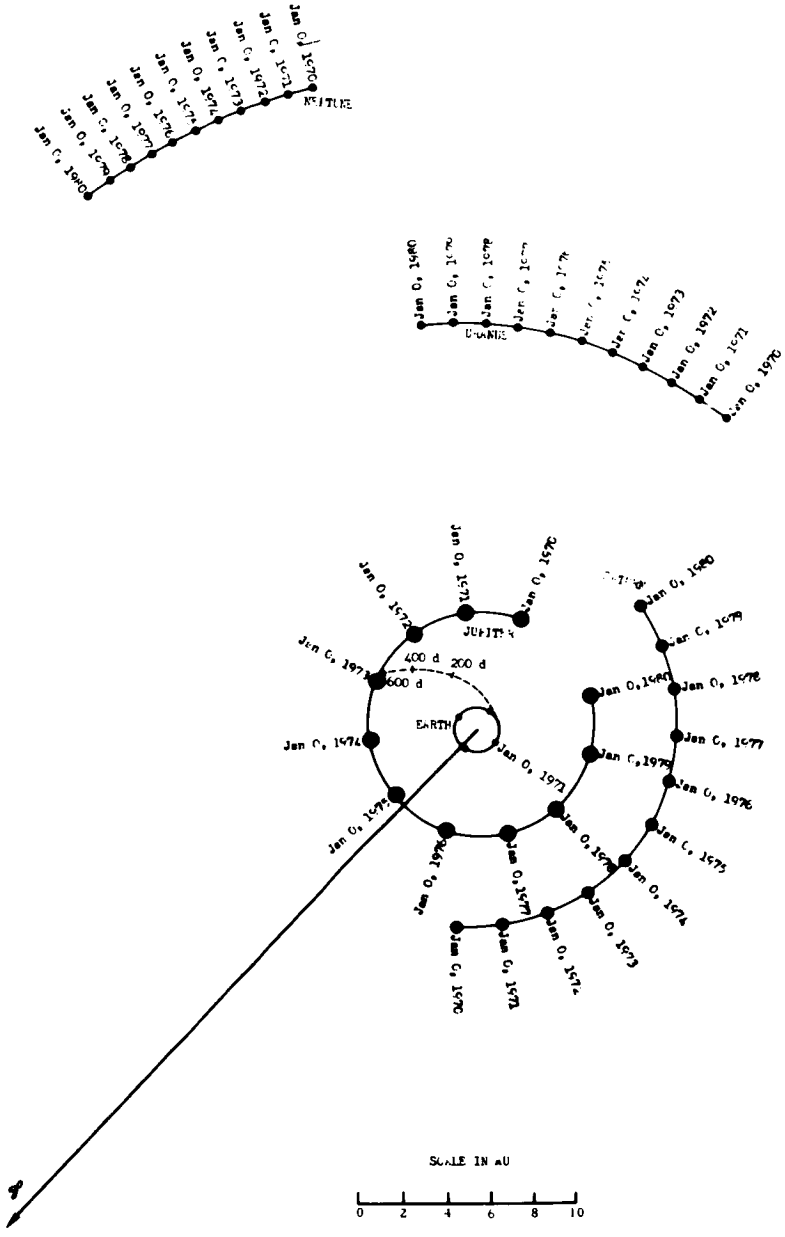

Figure 56. Display of Sample Trajectory A

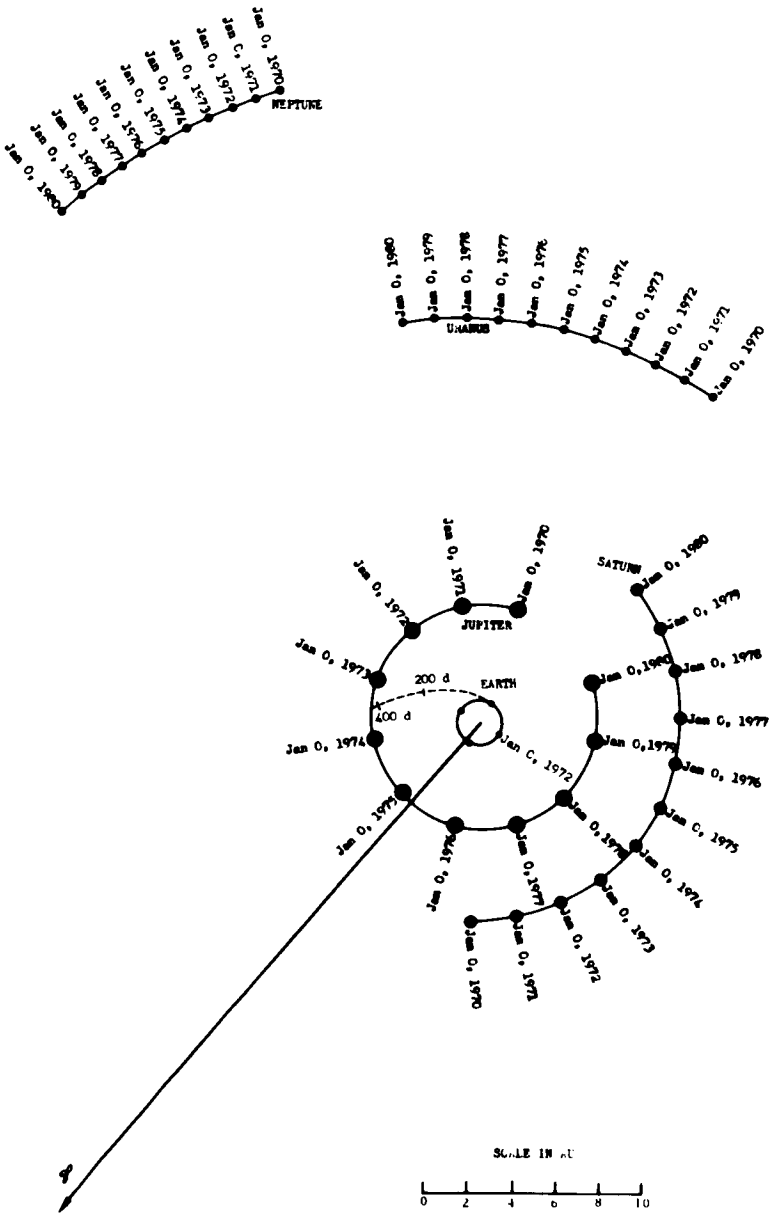

Figure 57. Display of Sample Trajectory B

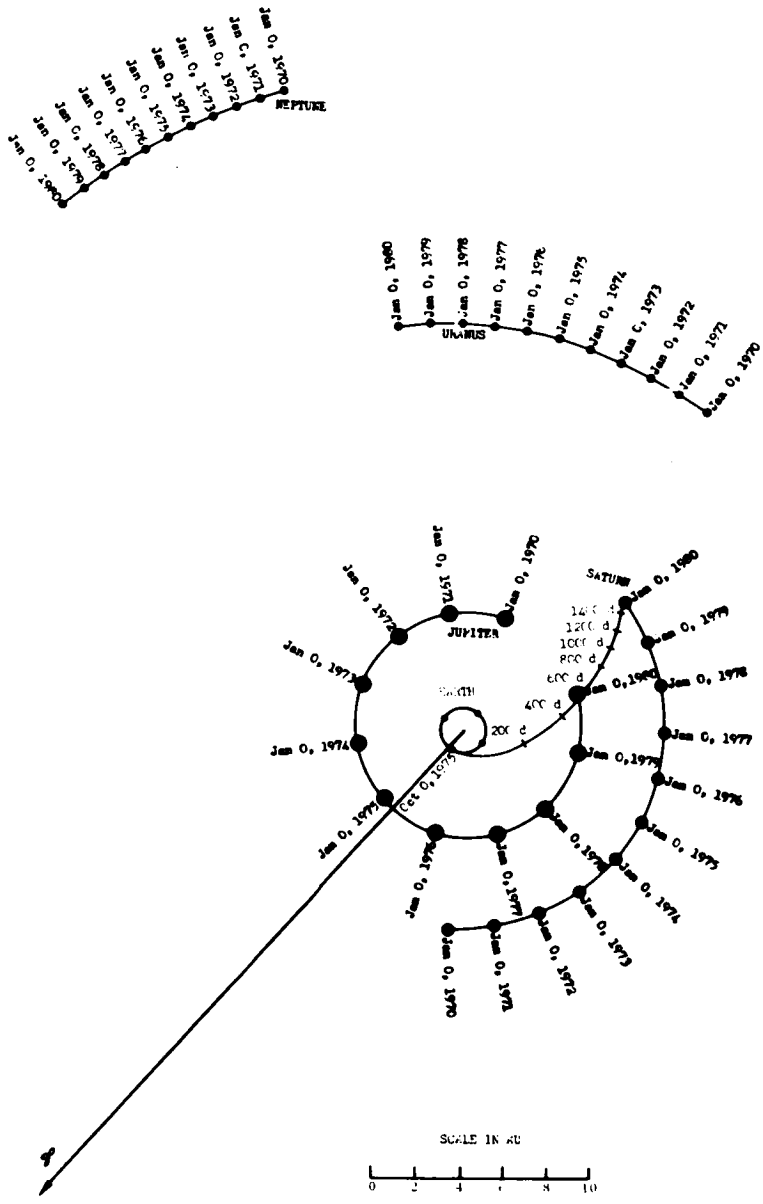

Figure 58. Display of Sample Trajectory C

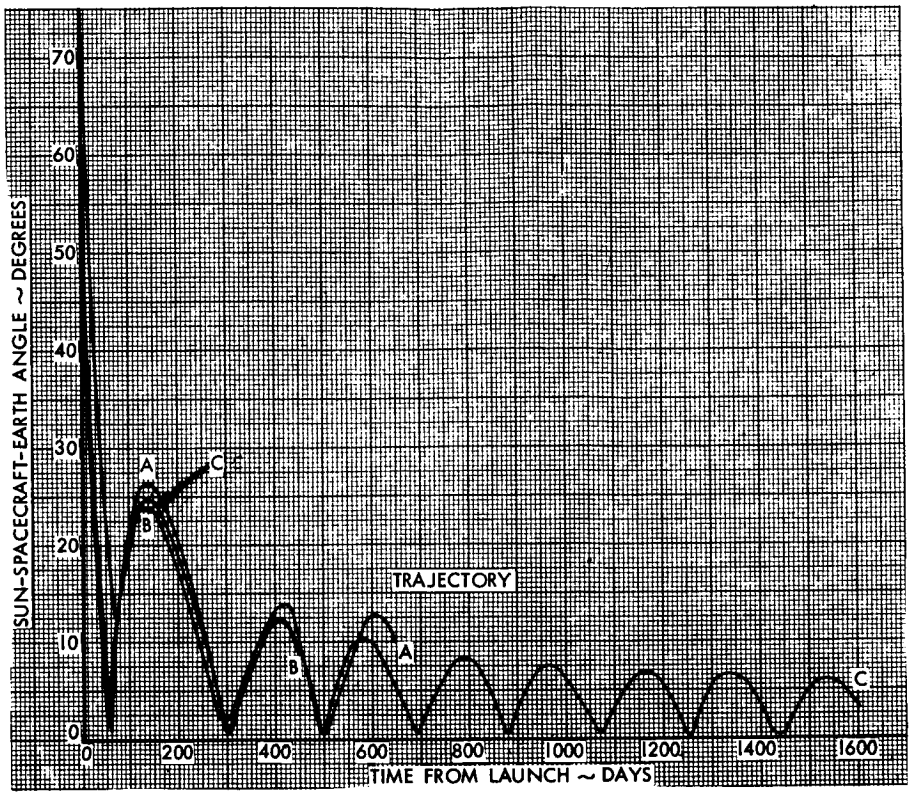

Figure 59. Sun-Spacecraft-Earth Angle for Three Trajectories

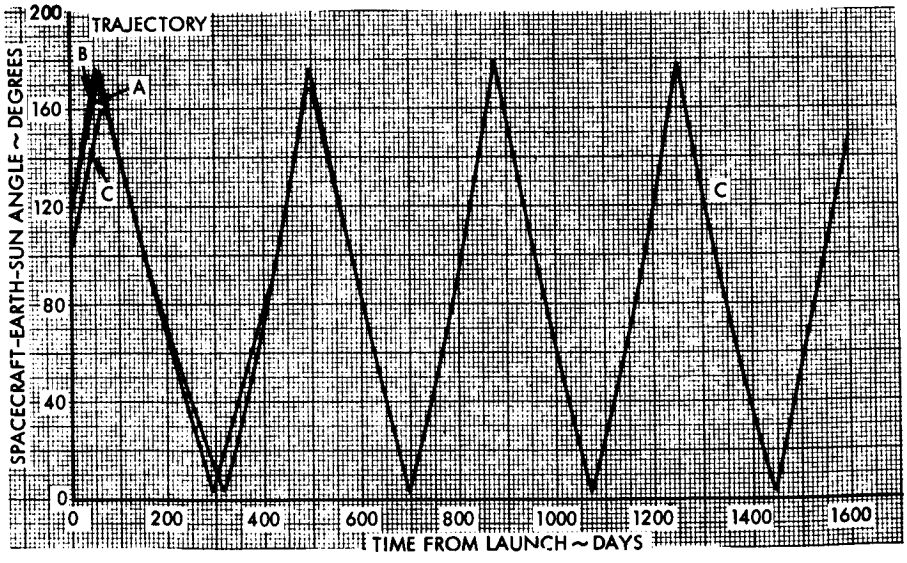

Figure 60. Spacecraft-Earth-Sun Angle for Three Trajectories

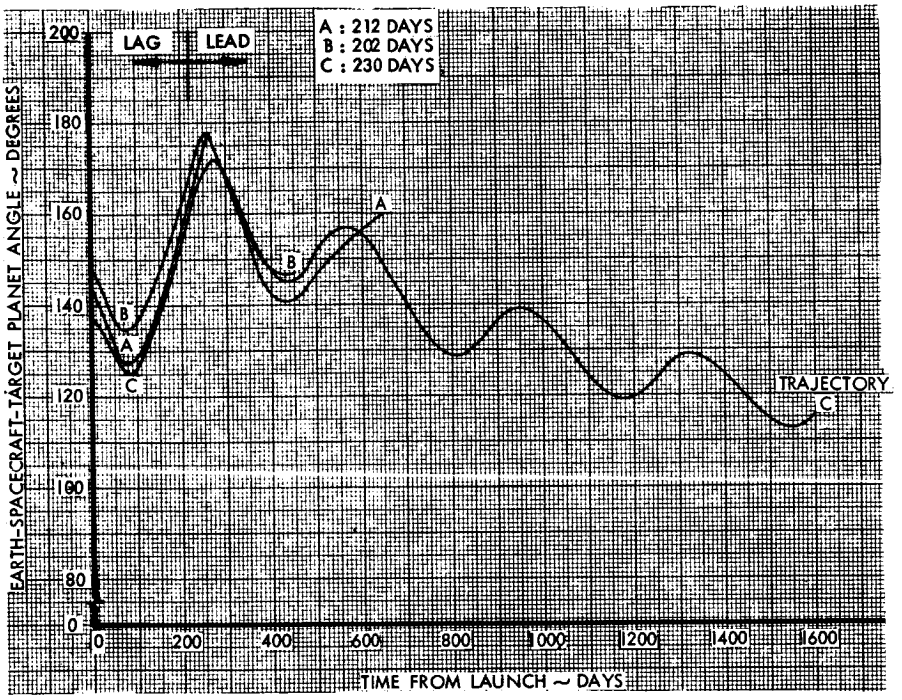

Figure 61. Sun-Spacecraft-Planet Angle for Three Trajectories

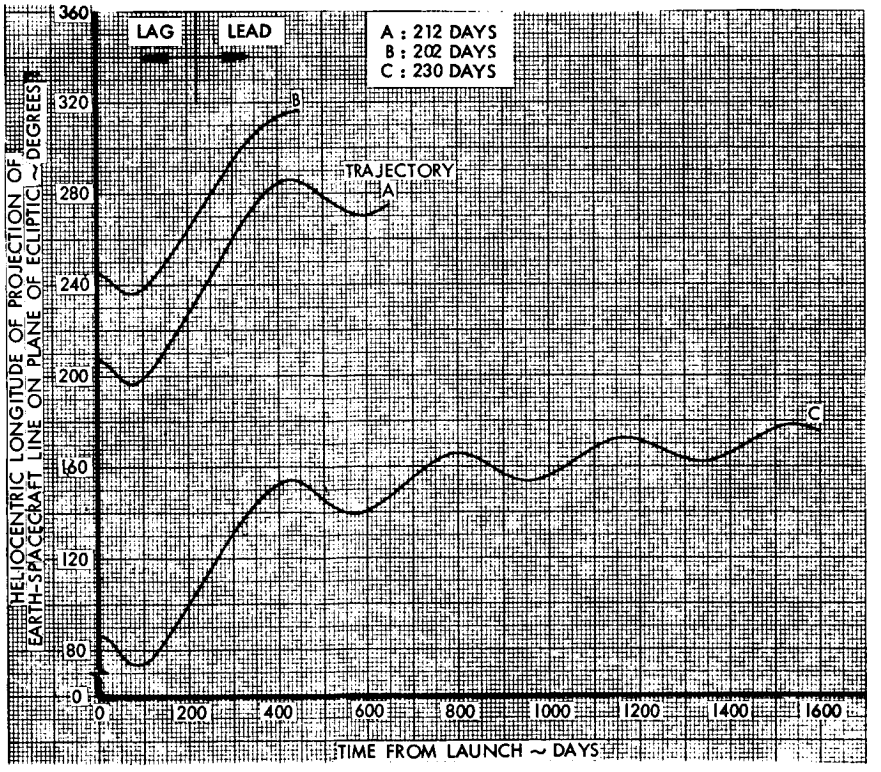

Figure 62. Heliocentric Longitude of Projection of Earth-Spacecraft Line on Plane of Ecliptic

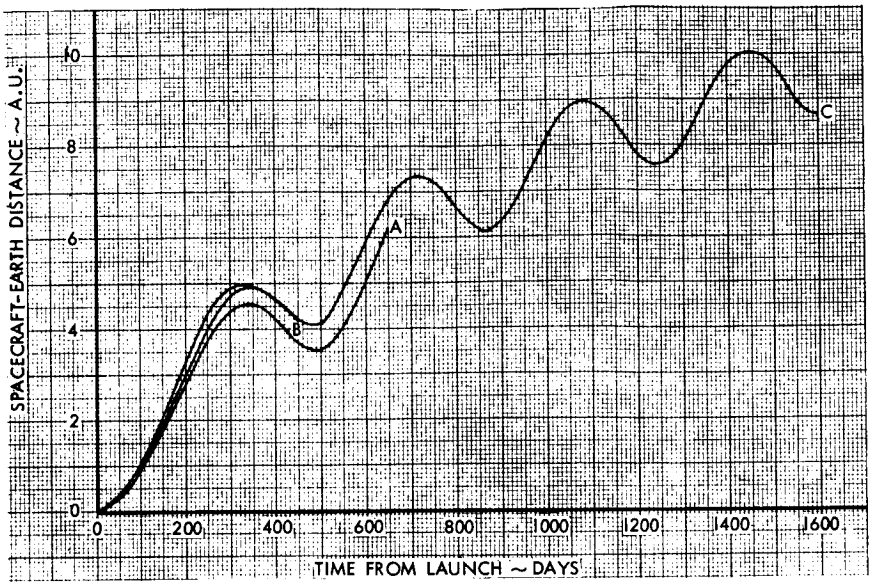

Figure 63. Spacecraft-Earth Distance for Three Trajectories

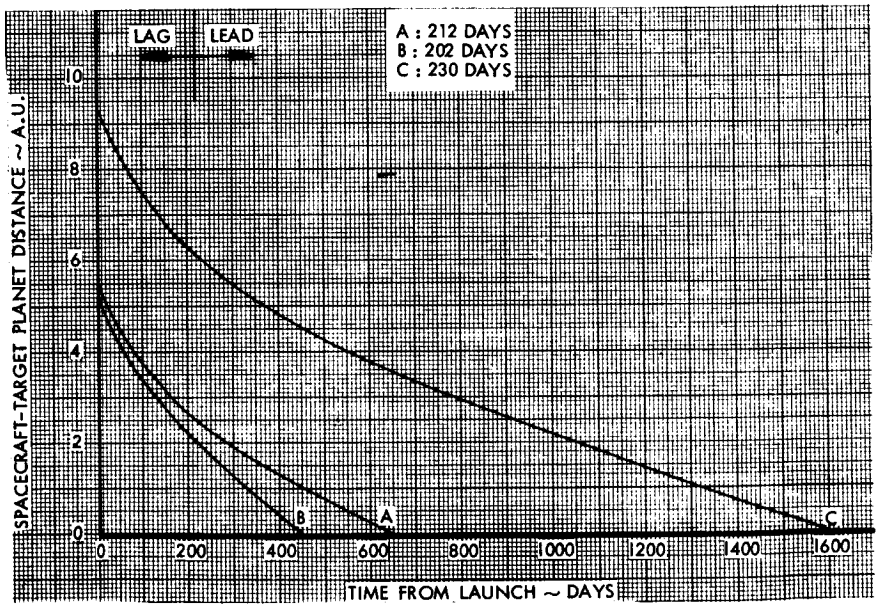

Figure 64. Distance from Target Planet for Three Trajectories

Table 14. Sample Trajectory Parameters

	A (Jupiter)	B (Jupiter)	C (Saturn)
Launch date	11 Feb 1971	24 Feb 1972	4 Oct 1975
Transfer time to target planet (days)	650	450	1600
Earth departure approach, V_∞ (EMOS)	0.3275	0.3971	0.3867
Target planet approach, V_∞ (EMOS)	0.2935	0.4850	0.2114
Heliocentric transfer angle (deg)	143.59	119.33	162.48
Heliocentric flight path angle (deg) ($\otimes_{dep}$, TP_{arr})	+6.38, +38.95	+8.70, +58.45	+2.92, +39.13

Where pertinent, these figures show the time of sun-spacecraft-target planet alignment. The lead-lag arrows indicate the position of the spacecraft with respect to the target planet, i.e., when the spacecraft is behind the target planet and approaching it and when the spacecraft is leading the target planet with the target planet approaching the spacecraft. The sun-spacecraft-target planet alignments, measured from time of launch for the sample trajectories, are: A 212 days, B 202 days, and C 230 days. The heliocentric angles oscillate with a cyclic character. This characteristic is attributed to the revolution of the earth around the sun; hence, the period of these oscillations coincides approximately with either one-half or one complete revolution of the earth. The heliocentric angles presented in Figures 59, 60, and 61 actually start at 0 degrees instead of at the higher values indicated on the graphs. However, the rise from 0 to the initial starting value on the graphs occurs so rapidly (0 to 3 days) that, for the time scale used, it is impossible to clearly indicate the initial variations.

The sun-spacecraft-earth angle has a high initial spike, and then oscillates with a continuously decreasing amplitude. The angles goes to approximately 0 every time an earth-sun-spacecraft or sun-earth-spacecraft alignment occurs. This angle remains small due to the relatively small size

of the earth's orbit and does not change very much at great distances from the earth. Therefore, this angle should not be used for the determination of spacecraft position if a high degree of accuracy is required.

The angle which offers the maximum time rate of change throughout the entire trip is the spacecraft-earth-sun angle. Utilization of this angle should yield the greatest degree of accuracy in spacecraft position. For earth-sun-spacecraft or sun-earth-spacecraft alignments, the spacecraft-earch-sun angle oscillates between approximately 0 and 180 degrees. Exact 0- and 180-degree angles are not attainable because the earth, sun, and spacecraft are not precisely colinear because of the relative inclinations of the orbit planes. For the purpose of discussion, let it be assumed that the earth, sun, and spacecraft may attain a colinear relationship. Figures 65 and 66 plot the projections of the heliocentric longitudes of the earth, spacecraft, and target planet on the ecliptic plane versus time from launch. By matching and overlaying the corresponding trajectory graph with the graphs of Figures 59, 60, and 61, and noting where the earth's heliocentric longitude lines cross the graph, one finds that the two alignments, earth-sun-spacecraft or sun-earth-spacecraft, occur at 0 or 180 degrees. As will be seen in the discussion of the spacecraft-earth distance graphs, 0 degrees corresponds to an earth-sun-spacecraft alignment and 180 degrees corresponds to sun-earth-spacecraft alignment.

The relative alignments of the sun, earth, and the spacecraft may present a problem in communications during some portions of the flight. For example, if the three bodies are in conjunction, i.e., colinear with the sun in the middle, direct communication between the earth and the spacecraft would be impossible. The amount of time spent in silence depends on the assumed sphere of interference of the sun and the distance of the spacecraft from the sun. A similar problem occurs when the earth and spacecraft are at opposition, i.e., the sun, earth, and spacecraft are colinear with the earth in the middle. In this case, the spacecraft might have problems in receiving information from earth.

The projections of the heliocentric longitude of the earth-spacecraft line on the plane of the ecliptic for the sample trajectories are shown in Figure 62. The cyclic nature of this graph reflects the periodic motion of the earth around the sun as previously mentioned.

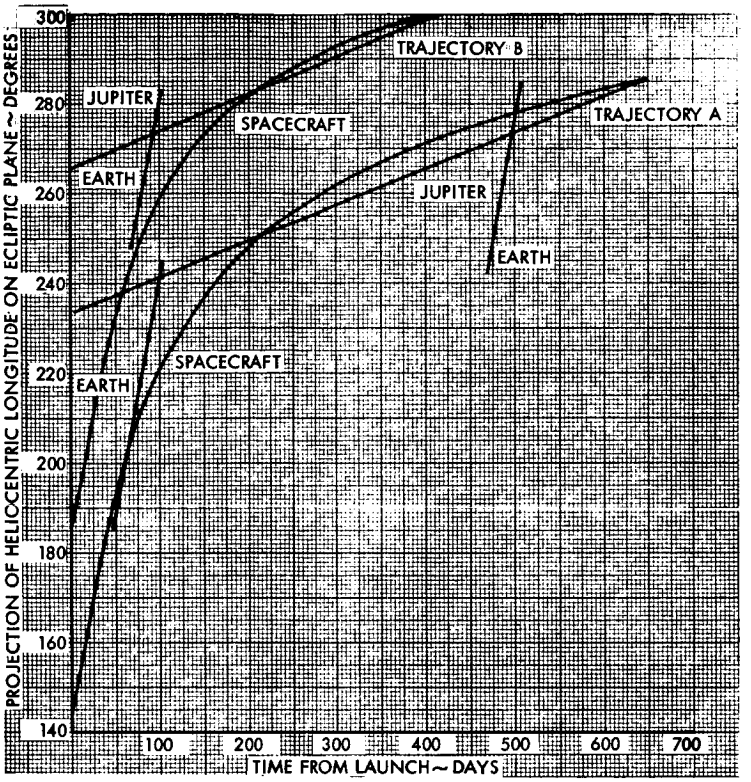

Figure 65. Projection of Heliocentric Longitude Earth, Spacecraft, and Planet on Ecliptic Plane for Trajectories A and B

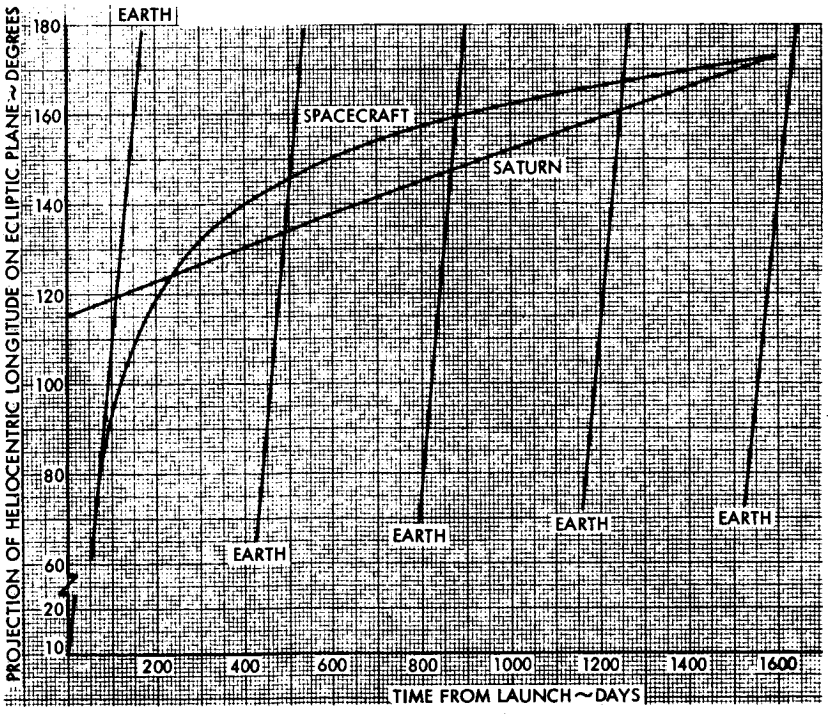

Figure 66. Projection of Heliocentric Longitude of Earth, Spacecraft, and Planet on Ecliptic Plane for Trajectory C

The spacecraft-earth distance relationship (Figure 63) is a sinusoidal curve. The cyclic nature of this curve corresponds approximately to the revolution of the earth around the sun, or one revolution of the earth for each cycle of the curve. At the peak of each cycle the distance is the greatest, corresponding to an earth-sun-spacecraft alignment, i.e., the spacecraft-earth-sun angle is 0 degrees. At the trough, where the distance reaches a minimum, the alignment is sun-earth-spacecraft, i.e., the spacecraft-earth-sun angle is close to 180 degrees. Again, by utilizing Figures 65 and 66 and overlaying the corresponding trajectory graph onto the spacecraft-earth distance graph and noting where the earth heliocentric longitude lines (nearly vertical) cross the distance graph, one can obtain the various earth, sun, spacecraft alignments for any period.

5.4 SWINGBY TRAJECTORIES

A comprehensive general description of swingby trajectories is presented by G. A. Flandro in "Utilization of Energy Derived from the Gravitational Field of Jupiter for Reducing Flight Time to the Outer Solar System," JPL Space Programs Summary No. 37-35, Volume 4, Pages 12-23, 31 August 1965.

Here, two swingby trajectories, one to Saturn and one to Neptune, are described. The general characteristics of these two are presented in Table 15.

Figures 67 and 68 present the solar system displays of these two trajectories. Figures 69 and 70 show the incremental velocity at Jupiter for these trajectories. Figures 71 through 76 present the heliocentric orientation angles and communication distances. Figures 77 through 80 show projections of the heliocentric longitudes of the earth-spacecraft and target planet on an ecliptical plane versus time from launch.

Figures 67 and 69 indicate that Trajectory D passes 93.12 planetary radii from Jupiter. At this distance the effect of Jupiter's gravitation, while appreciable, does not greatly alter the heliocentric energy. In short, Trajectory D is not a classic example of the benefits derived from the swingby technique, although the injection energy requirement at earth, 111.8 km^2/sec^2, is much lower than the minimum 1979 Type I earth-Saturn direct trajectory energy of over 130 km^2/sec^2. On the other hand,

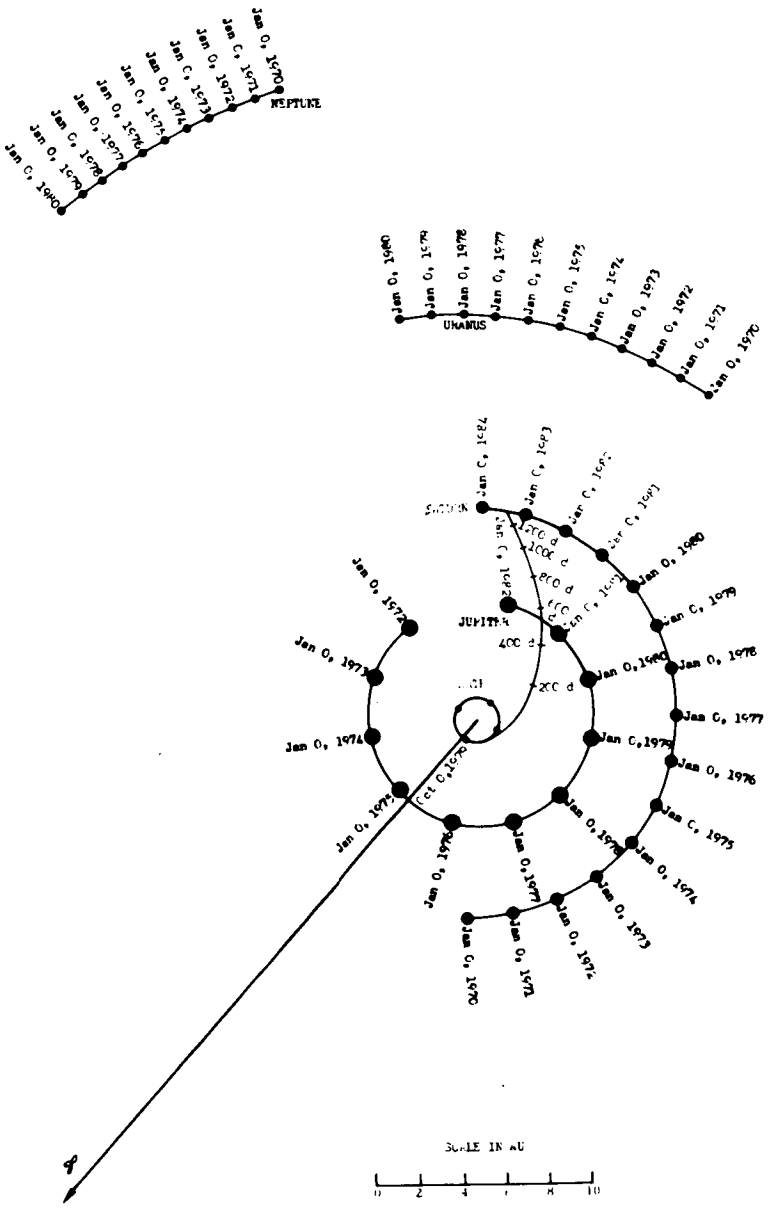

Figure 67. Display of Sample Trajectory D

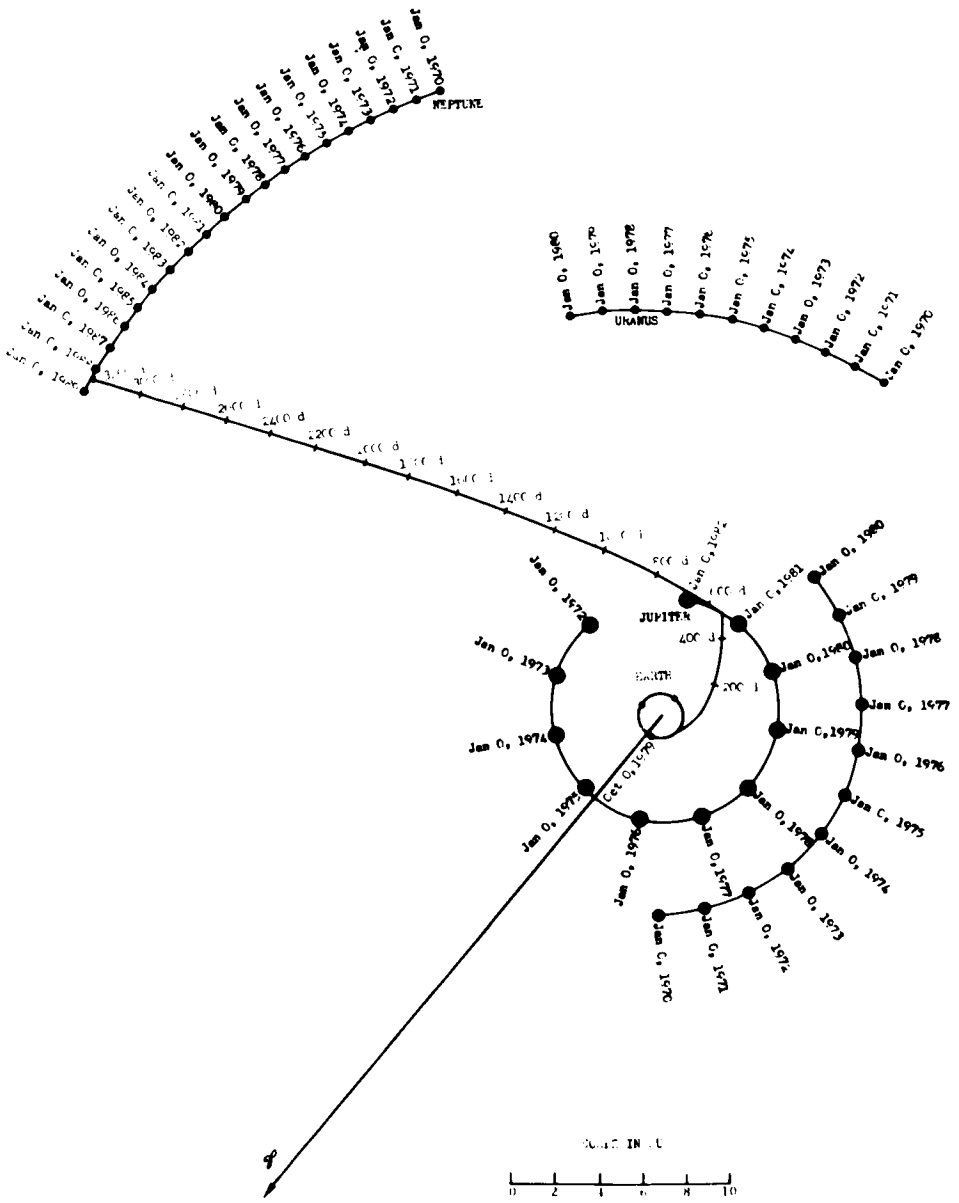

Figure 68. Display of Sample Trajectory E

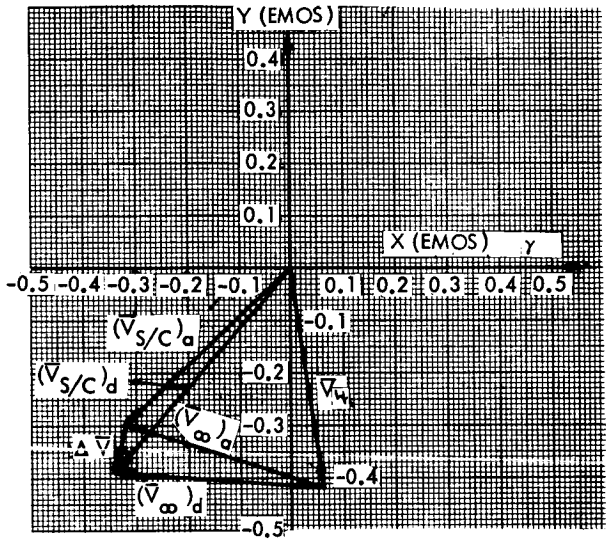

Figure 69. Incremental Velocity at Jupiter for Swingby Trajectory D (1 EMOS = 29.77 km/sec)

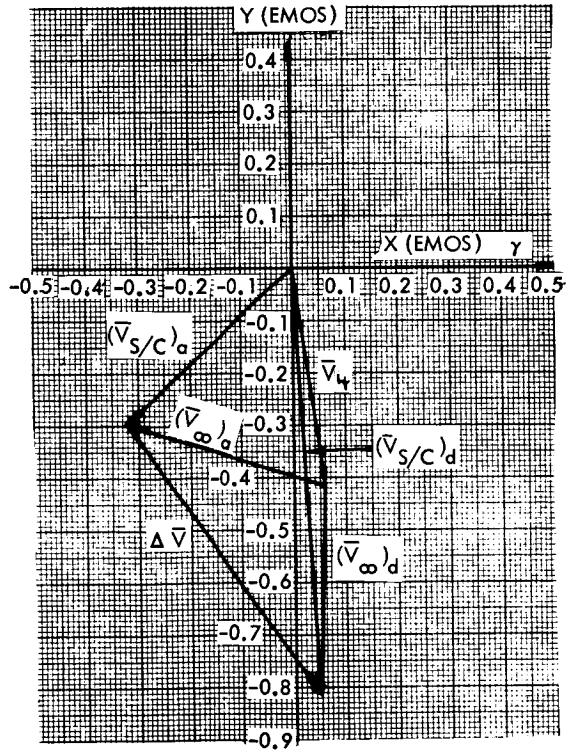

Figure 70. Incremental Velocity at Jupiter for Swingby Trajectory E

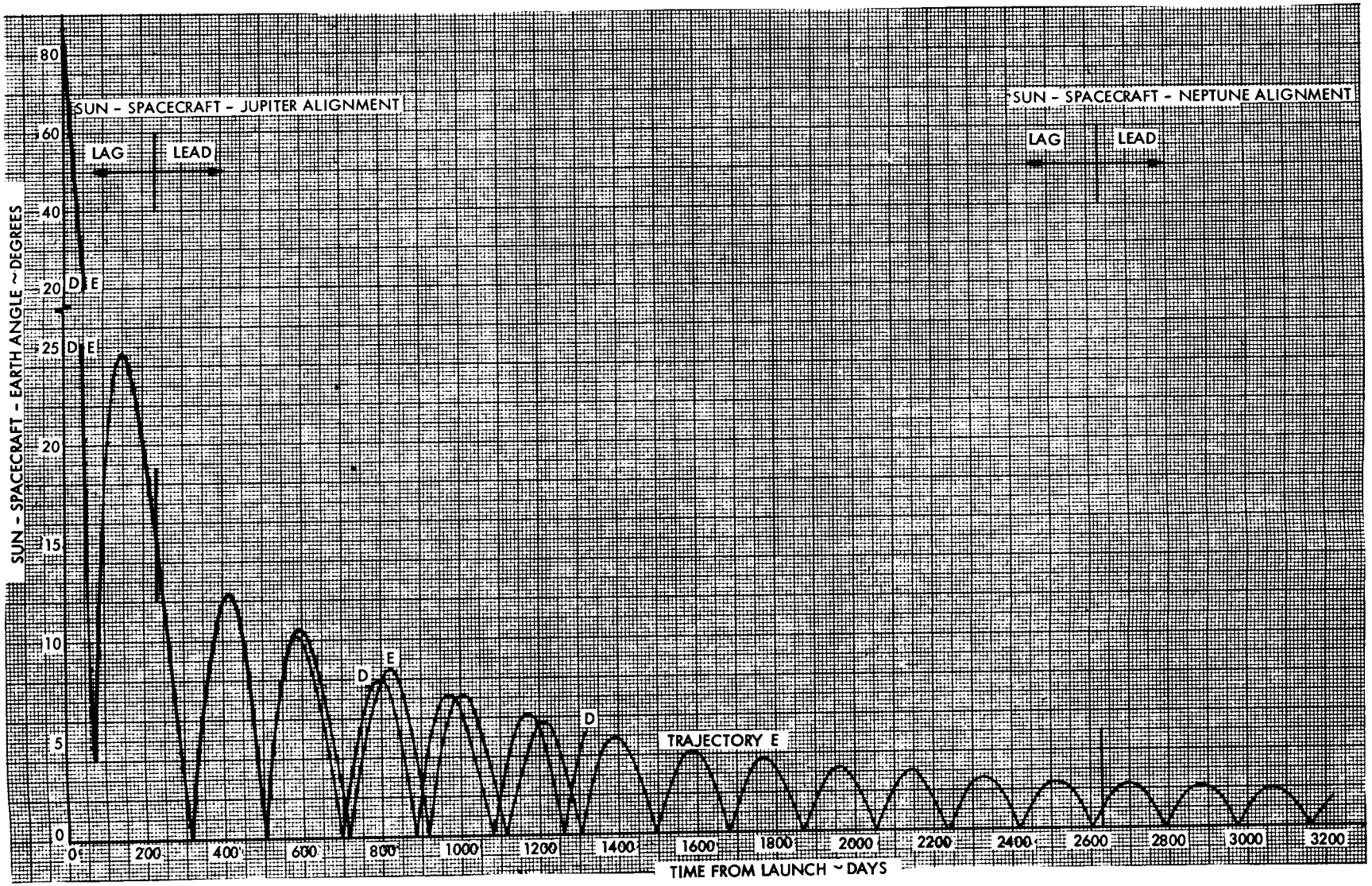

Figure 71. Sun-Spacecraft-Earth Angle for Trajectories D and E

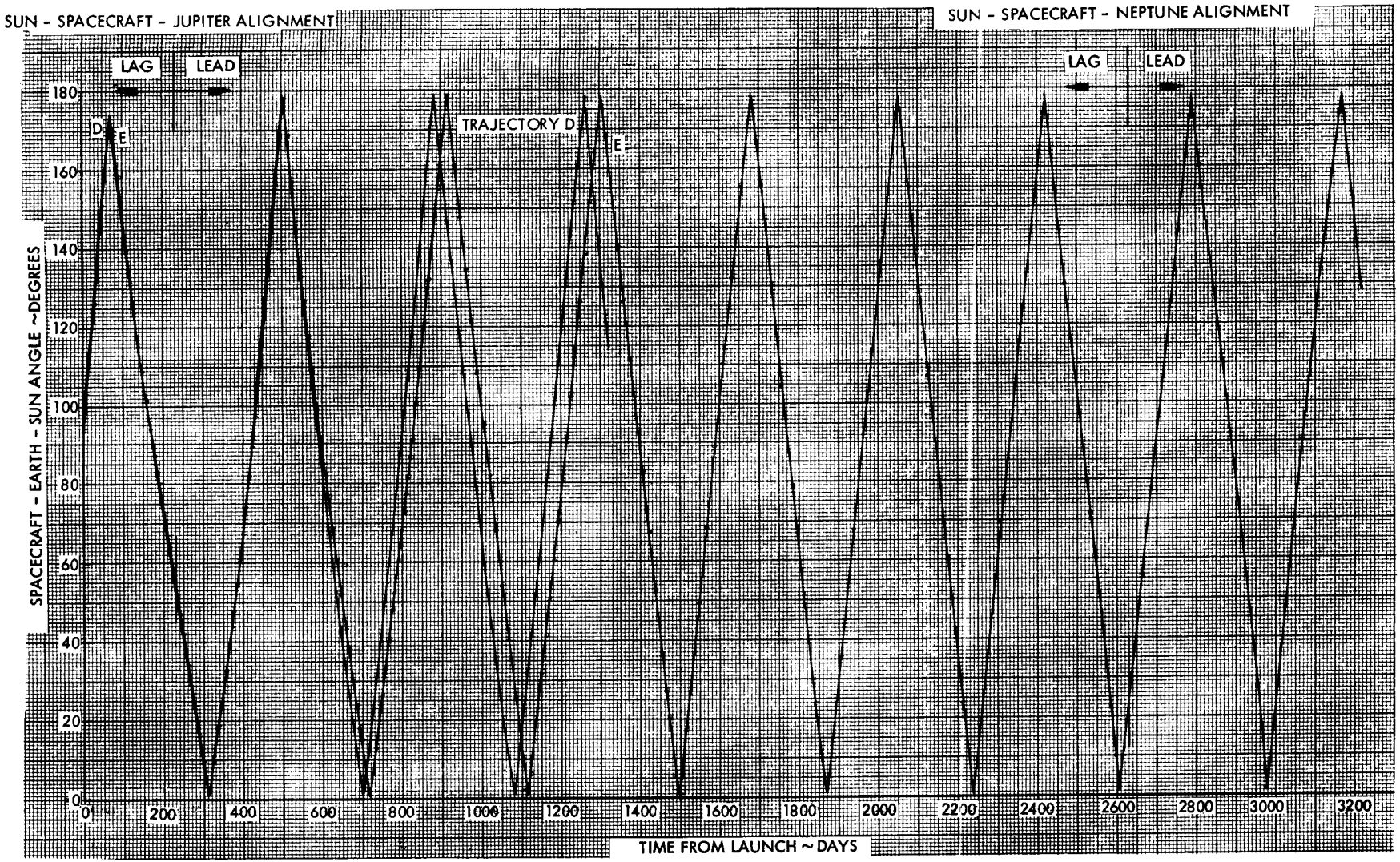

Figure 72. Spacecraft-Earth-Sun Angle for Trajectories D and E

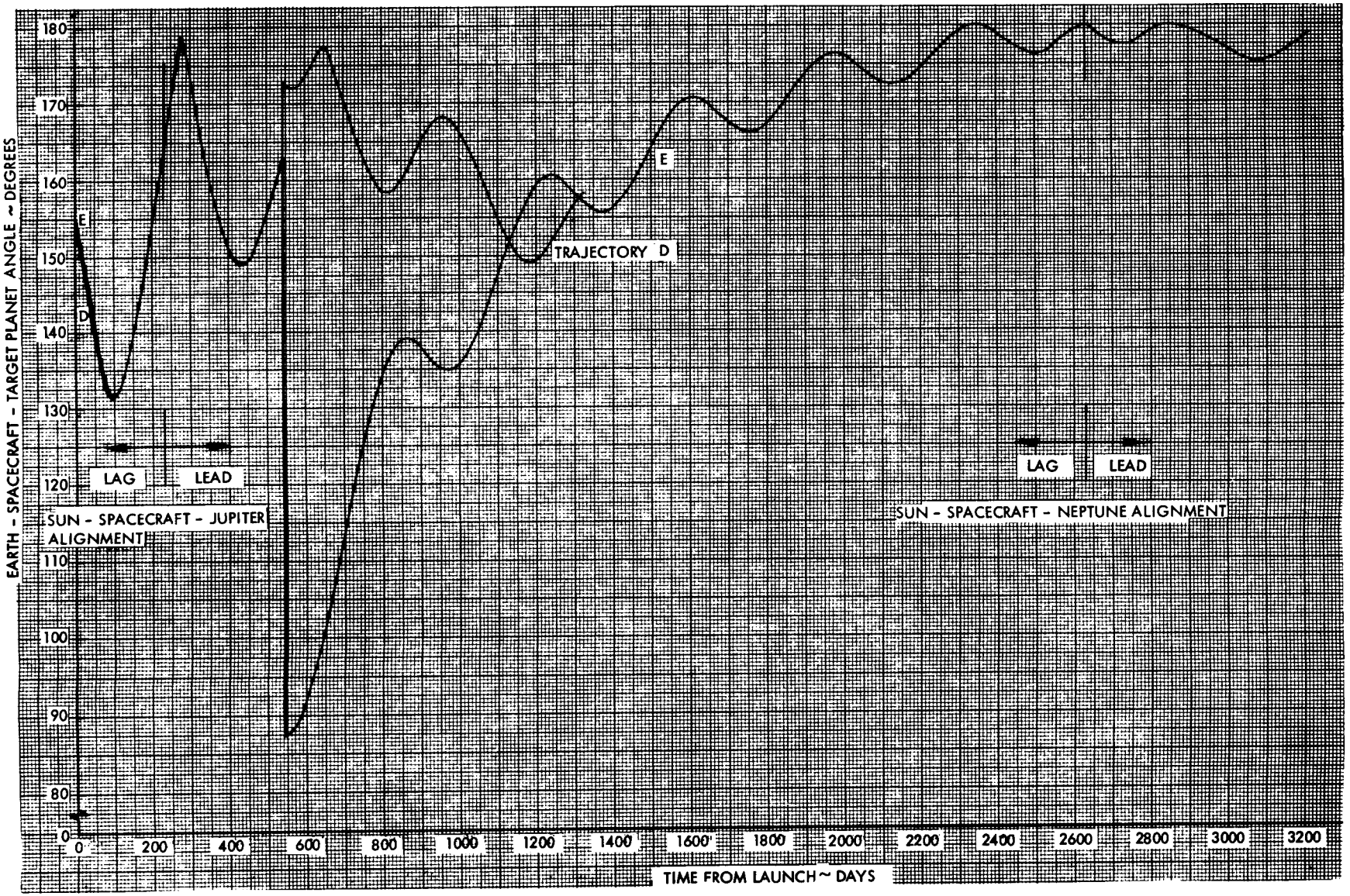

Figure 73. Earth-Spacecraft-Planet Angle for Trajectories D and E

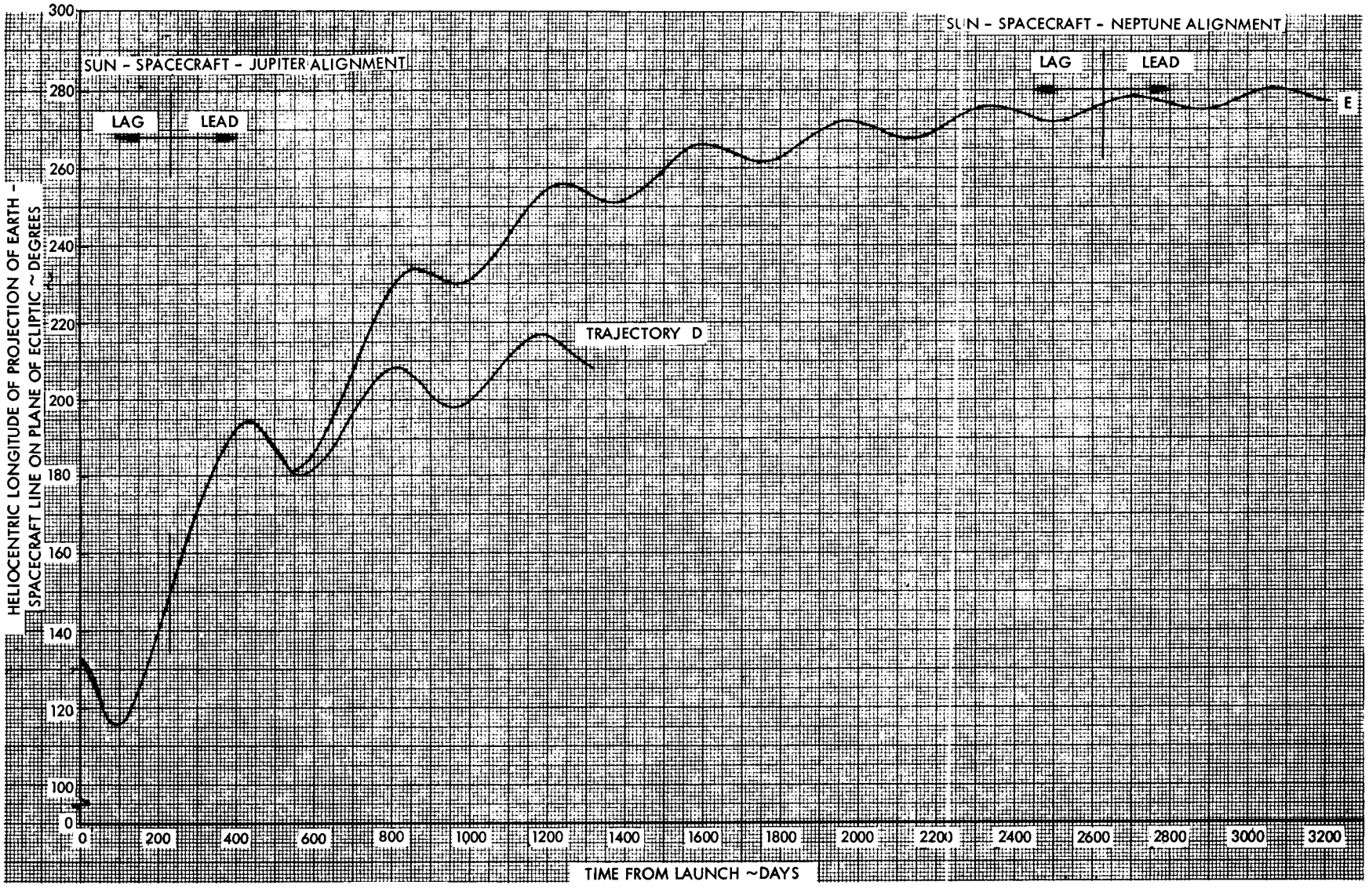

Figure 74. Heliocentric Longitude of Projection of Earth-Spacecraft Line on Plane of Ecliptic for Trajectories D and E

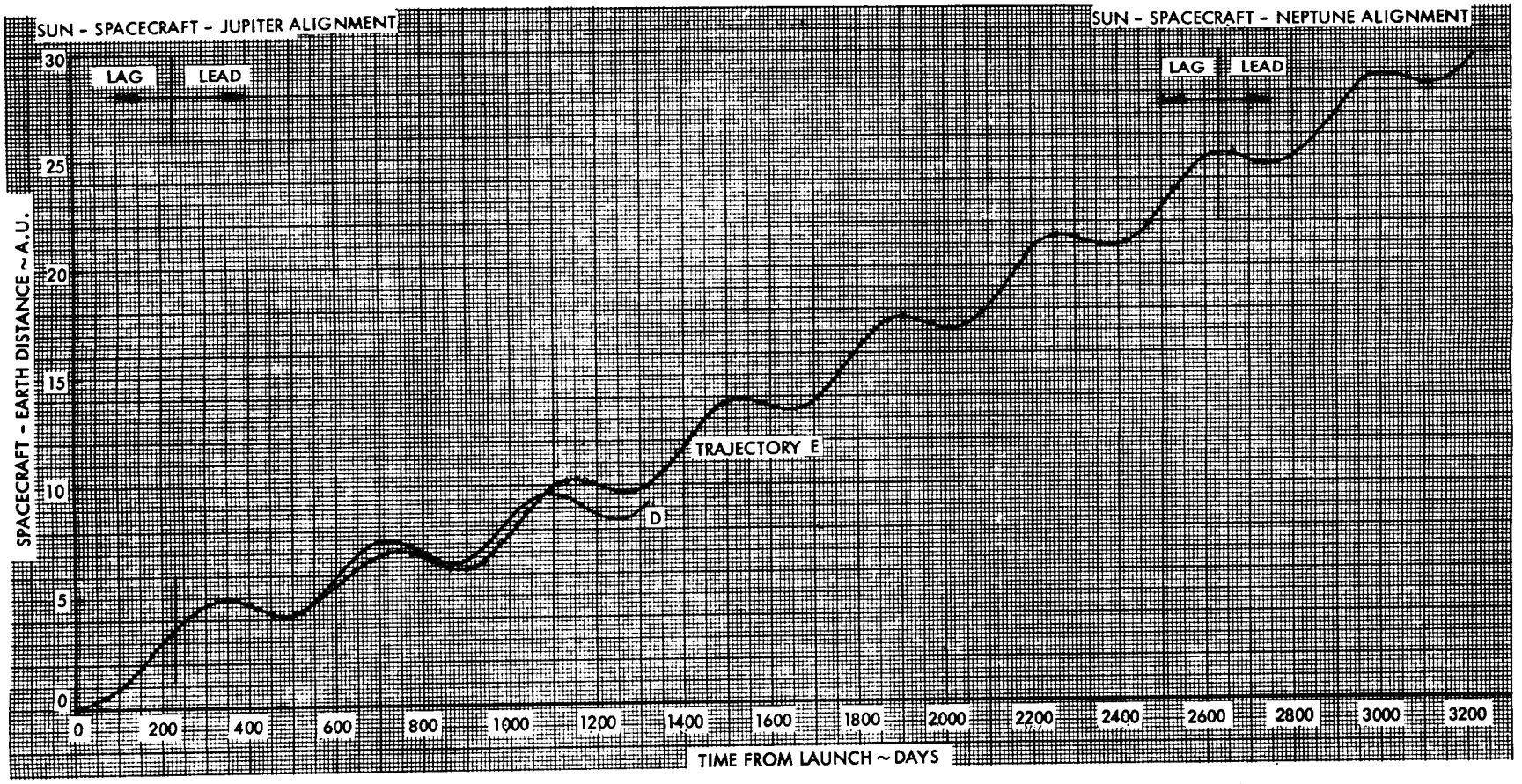

Figure 75. Distance of Spacecraft from Earth for Trajectories D and E

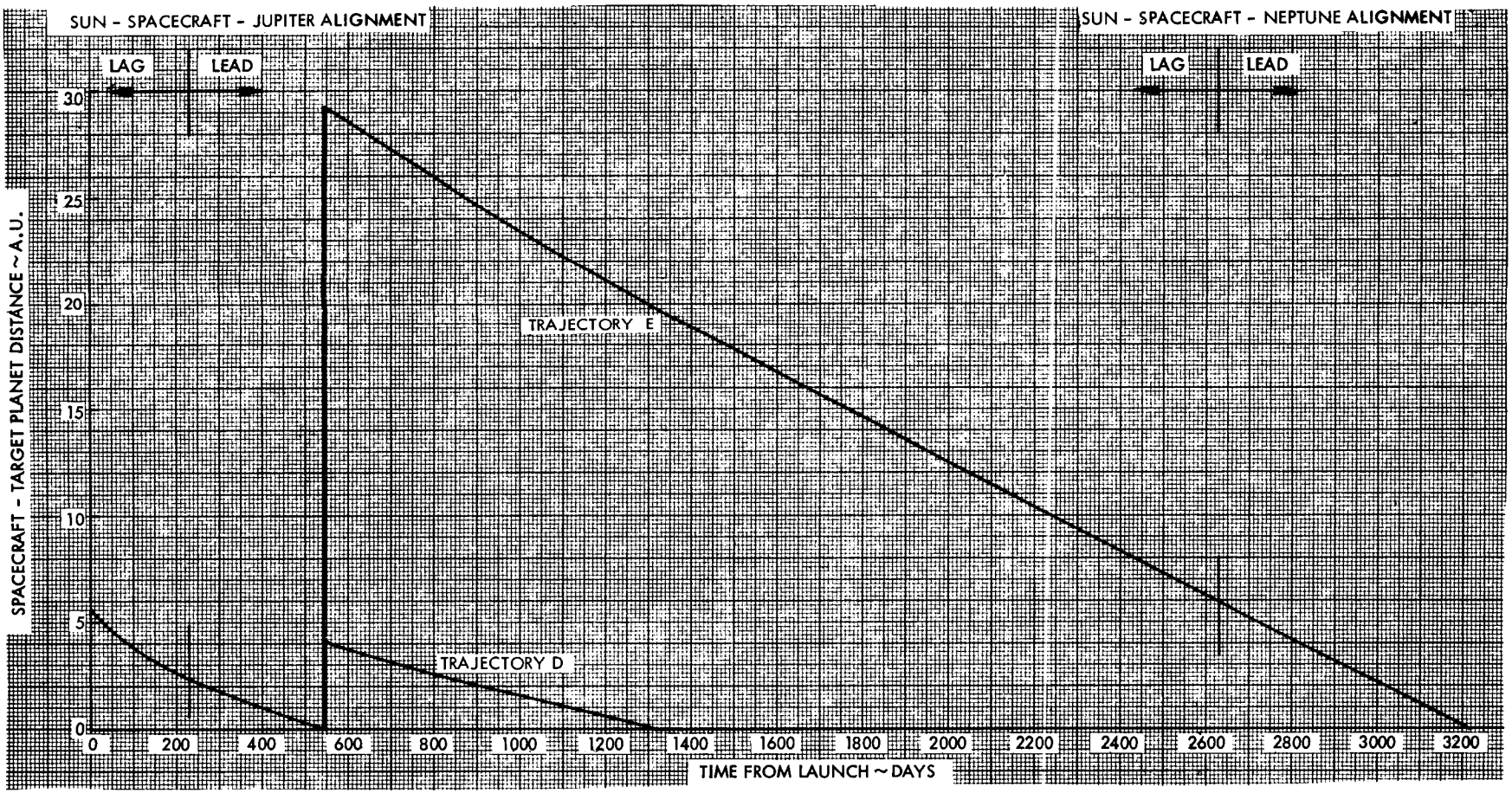

Figure 76. Distance of Spacecraft from Target Planet Trajectories D and E

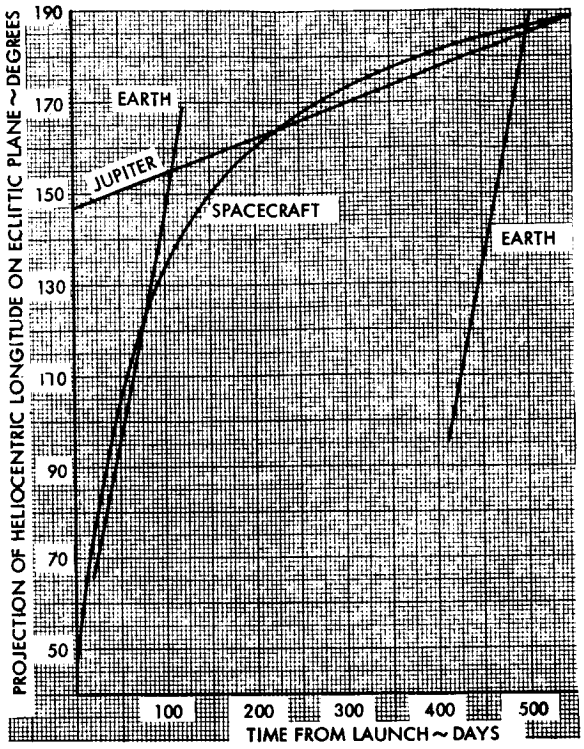

Figure 77. Projection of Heliocentric Longitude on Ecliptic Plane, Trajectory D, First Leg

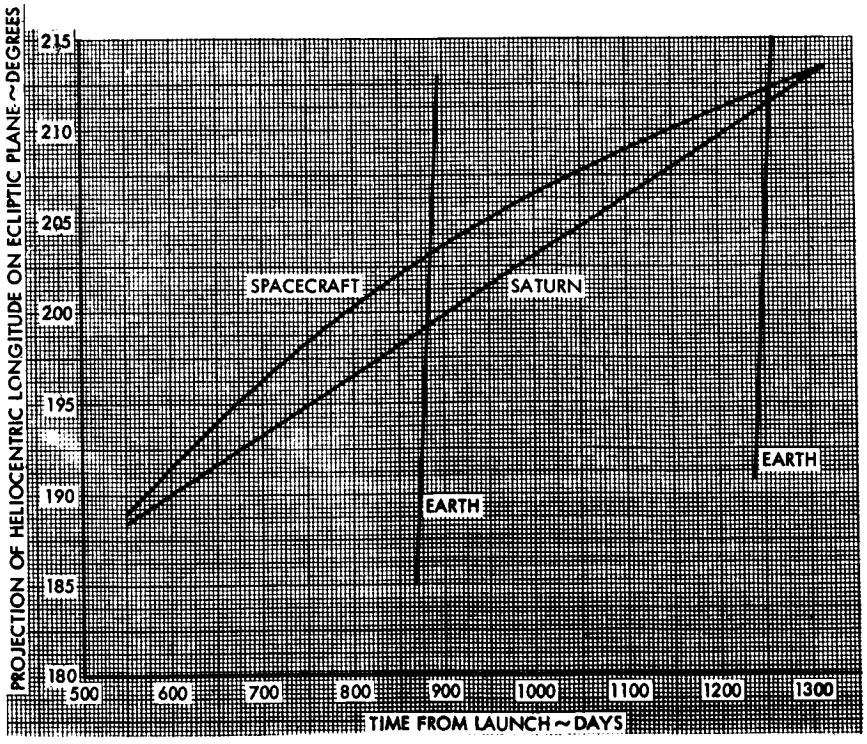

Figure 78. Projection of Heliocentric Longitude on Ecliptic Plane, Trajectory D, Second Leg

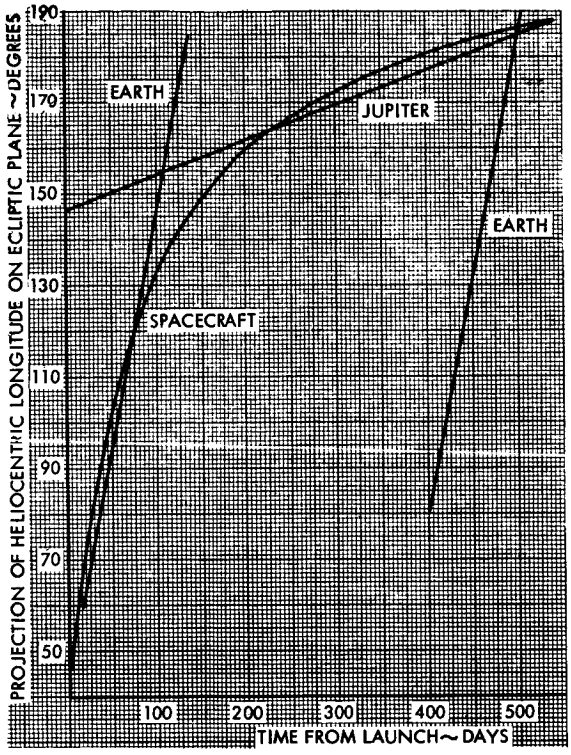

Figure 79. Projection of Heliocentric Longitude on Ecliptic Plane, Trajectory E, First Leg

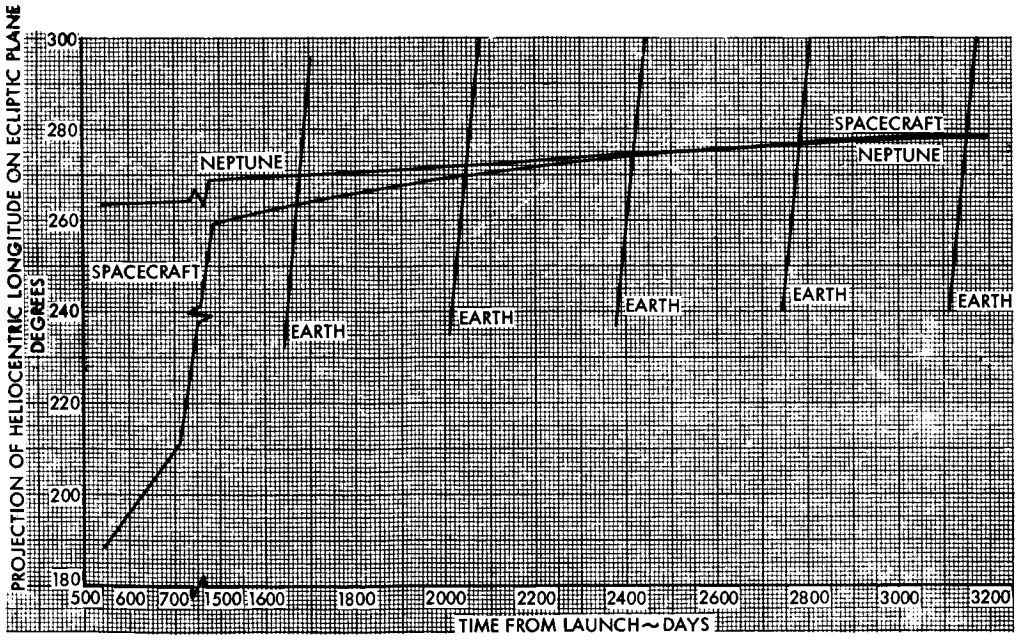

Figure 80. Projection of Heliocentric Longitude on Ecliptic Plane, Trajectory E, Second Leg

trajectory E, with the same earth injection energy, uses a close passage at Jupiter to obtain marked trajectory bending, and the subsequent trajectory is well over the heliocentric escape speed.

The earth-spacecraft-target planet angle graphs for Trajectories D and E (Figure 73) contain a step function. This is due to a change in "target planet" designation after Jupiter encounter. Saturn has been designated as the target planet for the second leg of Trajectory D, while Neptune is the target planet for the second leg of Trajectory E. In order to determine the precise geometry at Jupiter encounter, a transformation to planetocentric coordinates has been made.

Table 15. Sample Trajectory Characteristics

	D	E
Launch date	10 Nov 1979	8 Nov 1979
Transfer time to Jupiter (days)	542	544
Earth departure, V_∞ (EMOS)	0.3547	0.3533
Jupiter approach, V_∞ (EMOS)	0.4031	0.4025
Jupiter closest approach distance	93.12 Jupiter radii	2.18 Jupiter radii
Target planet approach, V_∞ (EMOS)	0.2818	0.5904
Total trip time (days)	1321.5	3215.7
Heliocentric transfer angle (deg)	140.9, 25.1	142.9, 90.8
Heliocentric flight path angle (deg) ($\otimes_{dep}$, γ_{arr}, γ_{dep}, TP_{arr})	+1.20, +56.10 +49.93, +55.08	+0.30, +56.03 +0.5, +75.97

Note: 1 EMOS = 29.77 km/sec

The step function in Figure 76 for Trajectories D and E is due to the change in "target planet" designation previously described. The spacecraft-target planet distance decreases sharply at first and then gradually falls off in a linear fashion. The transition occurs when the spacecraft overtakes

and passes the target planet, noted by the lead-lag line on the graphs. The spacecraft-target planet distance relationship for the Jupiter swingbys has also been analyzed in a Jupiter-centered coordinate system.

Encounter geometry is also important. To evaluate the spacecraft-trajectory during planetary encounter, it is necessary to refer to a planetocentric coordinate system. This transformation is applicable within the planet's sphere of influence. Within the sphere of influence the attraction of the sun can be ignored, with the result that the flight path can be represented by a planet-centered hyperbolic trajectory.* The Jupiter-centered hyperbolas for Trajectories D and E are shown drawn to scale in Figures 81 and 82, respectively. Time ticks are indicated on the trajectories along with the directions of $(\overline{V}_\infty)_a$ at arrival, $(\overline{V}_\infty)_d$ at departure, the earth and the sun.

The shadow cylinders of the earth and sun for Trajectory E are shown in Figure 82. In addition to periods of occultation by the earth and the sun separately, the spacecraft is occulted from both bodies simultaneously. The entrance and exit points of the simultaneous occultation are indicated by the breaks in the trajectory curve. The mutual occultation does not occur at the exact instant in which the spacecraft reaches the edge of the shadow cylinder, because the orbit planes of Jupiter, earth, sun, and the spacecraft are not exactly coplanar. Knowledge of the positions and times of entrance and exit are of significant scientific value in performing photographic and occultation experiments as well as in determining periods of communication blackout. The true anomaly and time at the entrance and exit points are 47.55 degrees, 0.071 day, and 67.06 degrees, 0.117 day, respectively, measured from periapsis. From the sun and earth directions indicated on Figure 80, it is seen that no occultation exists for Trajectory D.

Figures 83 and 84 display a time history of spacecraft-Jupiter distance during Jupiter encounter for Trajectories D and E. Time is measured from periapsis, the zero point on the graph, with negative times corresponding to periapsis approach and positive times to departure.

---

*The sphere of influence of Jupiter is taken to be 674.48 Jupiter radii.

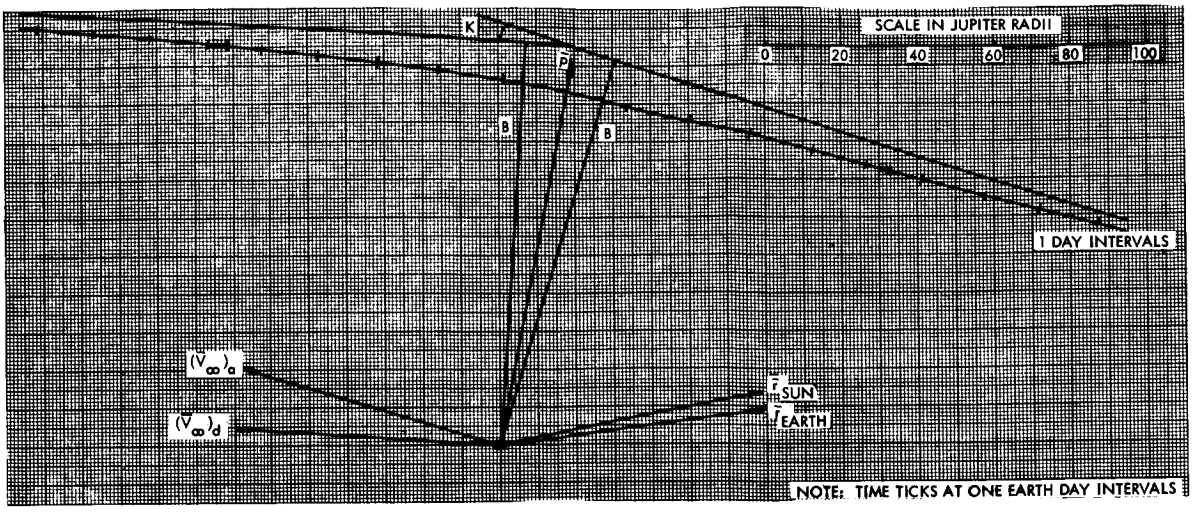

Figure 81. Jupiter Encounter Geometry, Trajectory D

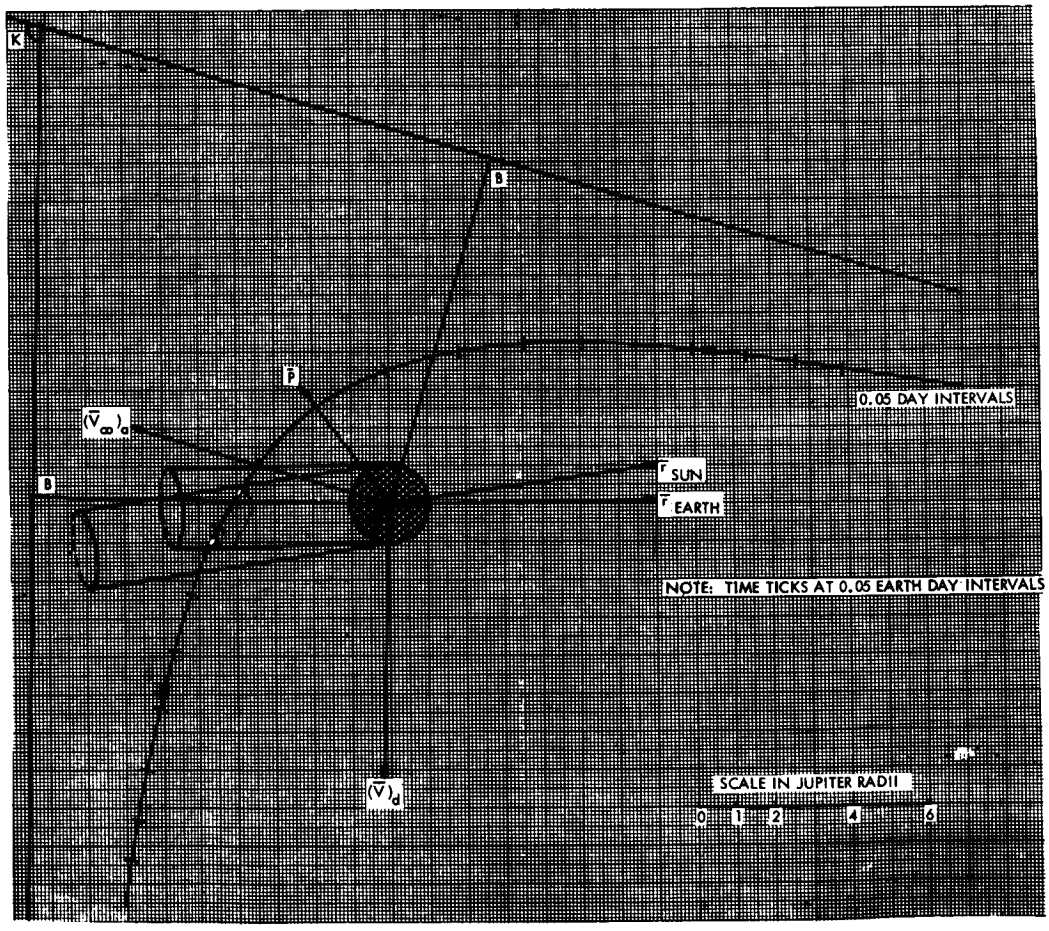

Figure 82. Jupiter Encounter Geometry, Trajectory E

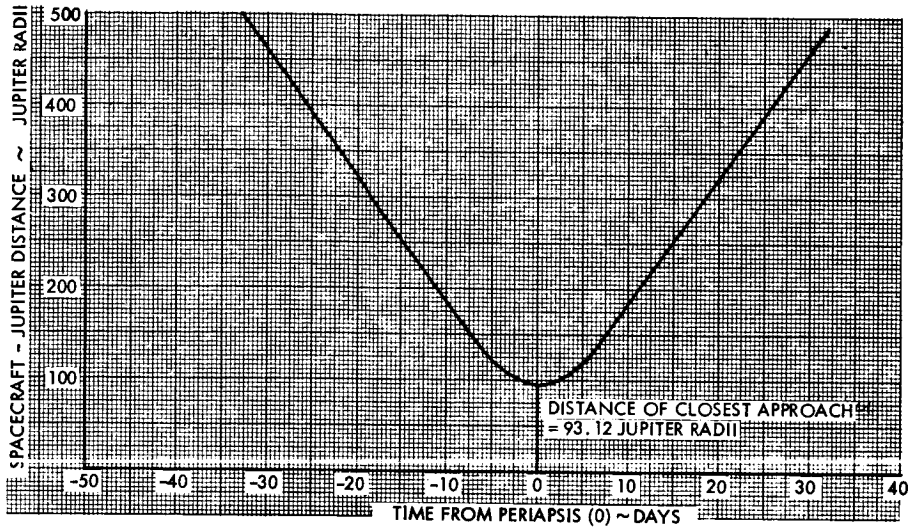

Figure 83. Distance of Spacecraft from Jupiter, Trajectory D

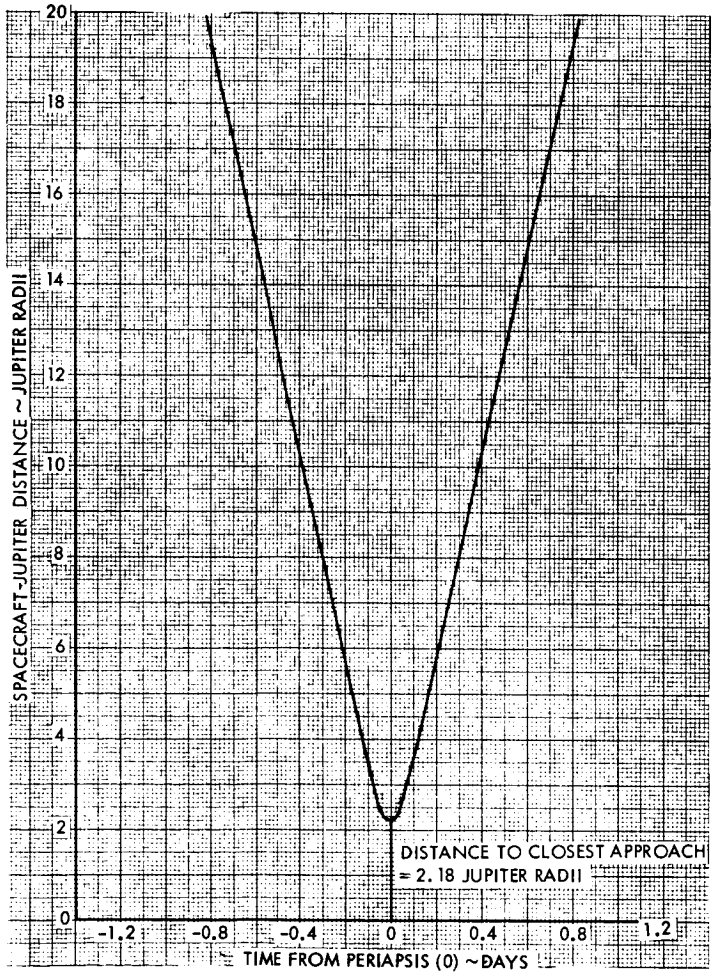

Figure 84. Distance of Spacecraft from Jupiter, Trajectory E

In the discussion of the heliocentric orientation angles it was noted that the earth-spacecraft-target planet angle for Trajectories D and E contains a step function resulting from the change in "target planet" designation from Jupiter to Saturn or Neptune, i.e., the angle is computed first as earth-spacecraft-Jupiter, and then as earth-spacecraft-Saturn or earth-spacecraft-Neptune. In order to determine the behavior of this angle in the vicinity of Jupiter, a transformation from heliocentric to planetocentric coordinates has been made. Figures 85 and 86 indicate, in planetocentric coordinates, the actual behavior of the angle during the planetary encounter for Trajectories D and E. These two graphs are not blowups of the step functions in the heliocentric graphs, because a transformation of coordinate systems has been made. Figure 85 shows that the earth-spacecraft-Jupiter angle drops sharply from approximately 170 to about 20 degrees and then gradually approaches zero degrees as the spacecraft recedes from Jupiter. However, for Trajectory E Figure 86 shows that the angle reaches 180 degrees and then very rapidly — in approximately 1.4 days — goes to 0 degrees. The 180- and 0-degree angles correspond to earth-spacecraft-Jupiter and earth-Jupiter-spacecraft alignments, respectively. The earth-Jupiter-spacecraft alignment does not occur at periapsis but 0.08 day after periapsis passage, as shown in the hyperbolic trajectory graph of Figure 82. Note, however, that neither of these graphs of the earth-spacecraft-Jupiter angle (Figures 85 and 86) indicates a discontinuous function.

5.5 POWERED SWINGBY TRAJECTORIES

This section discusses the use of a propulsive maneuver in the vicinity of Jupiter as a means to further reduce the transfer times to Saturn and Neptune.

To make valid comparison of powered and unpowered swingbys, the assumption has been made that the same payload weight will be delivered to the target planet (Saturn or Neptune) by both the powered and unpowered swingbys. As a result, the gross weight of the payload in earth orbit for the powered swingby has been adjusted to be 20 percent greater than that for the unpowered swingby to allow for the added fuel required to perform the propulsive maneuver at Jupiter. Pertinent launch data for the powered and unpowered swingbys are as follows:

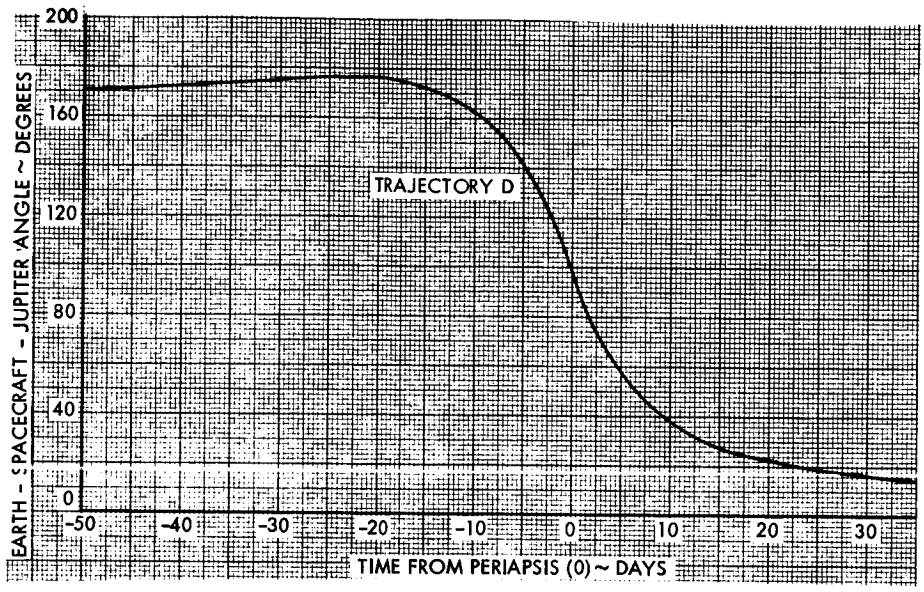

Figure 85. Earth-Spacecraft-Jupiter Angle for Trajectory D

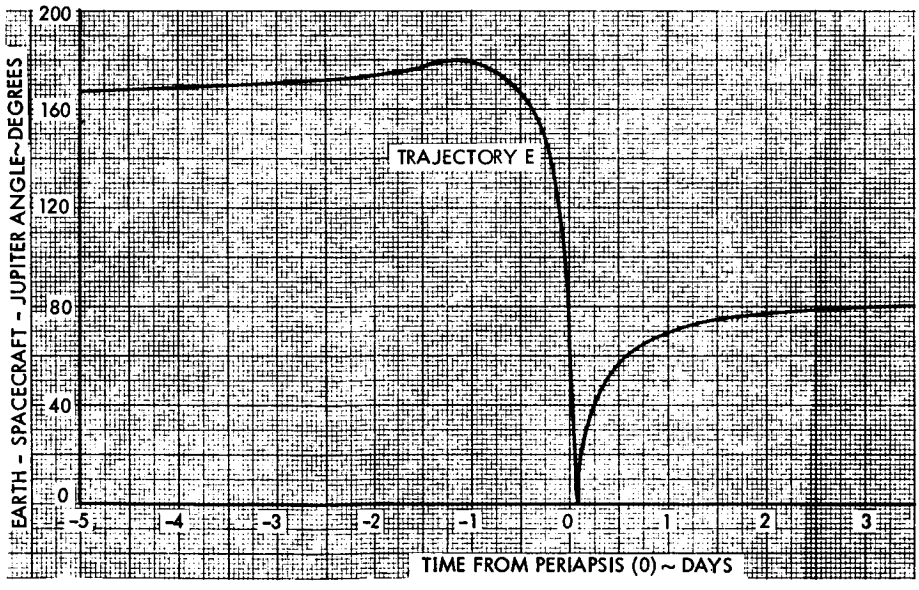

Figure 86. Earth-Spacecraft-Jupiter Angle for Trajectory E

Mission Designation	C_3 at Launch (km^2/sec^2)	Gross Payload Weight at Injection (lb)
Unpowered swingby earth-Jupiter-Saturn (trajectory D)	111.5	625
Powered swingby earth-Jupiter-Saturn	103.5	750
Unpowered swingby earth-Jupiter-Neptune (Trajectory E)	110.6	640
Powered swingby earth-Jupiter-Neptune	103.0	768

The launch energies and payload weights were determined from the Atlas SLV3X/Centaur/HEKS launch vehicle performance data given in Section 2.1 of Volume 2. For example, the launch energy for unpowered swingby trajectory D is 111.5 km^2/sec^2. The injected payload weight is 625 pounds. A 20 percent increase in weight has been added to allow for the powered maneuver at Jupiter, resulting in a payload weight for the powered swingby of 750 pounds. This weight corresponds to an available launch energy of 103.5 km^2/sec^2. Weights and launch energies for the unpowered and powered earth-Jupiter-Neptune swingbys were obtained in an analogous manner.

Unpowered swingby trajectories D and E were determined by specifying the dates of earth launch and Jupiter encounter and interpolating for the target planet arrival date which satisfies the constraint that the magnitudes of the hyperbolic excess velocity vectors ($\overline{V}_\infty$) at Jupiter arrival and departure be equal. A Jupiter encounter date of 5 May 1981 was specified for trajectories D and E.

The analysis of powered swingbys was initiated by fixing this Jupiter encounter date and selecting the appropriate earth launch dates so as to satisfy the C_3 constraints noted previously. In this manner, both the first leg (earth-Jupiter) trip time and the $\overline{V}_\infty$ vector at Jupiter arrival have been fixed. The $\overline{V}_\infty$ vector at Jupiter departure is fixed as soon as a target planet arrival date (second leg trip time) has been selected. In general these $\overline{V}_\infty$ vectors will not match and a powered

maneuver must be made at Jupiter encounter in order to transfer from the incoming Jupiter-centered hyperbolic to the outgoing hyperbola. Figure 87 illustrates the powered swingby nomenclature for several classes of transfers.

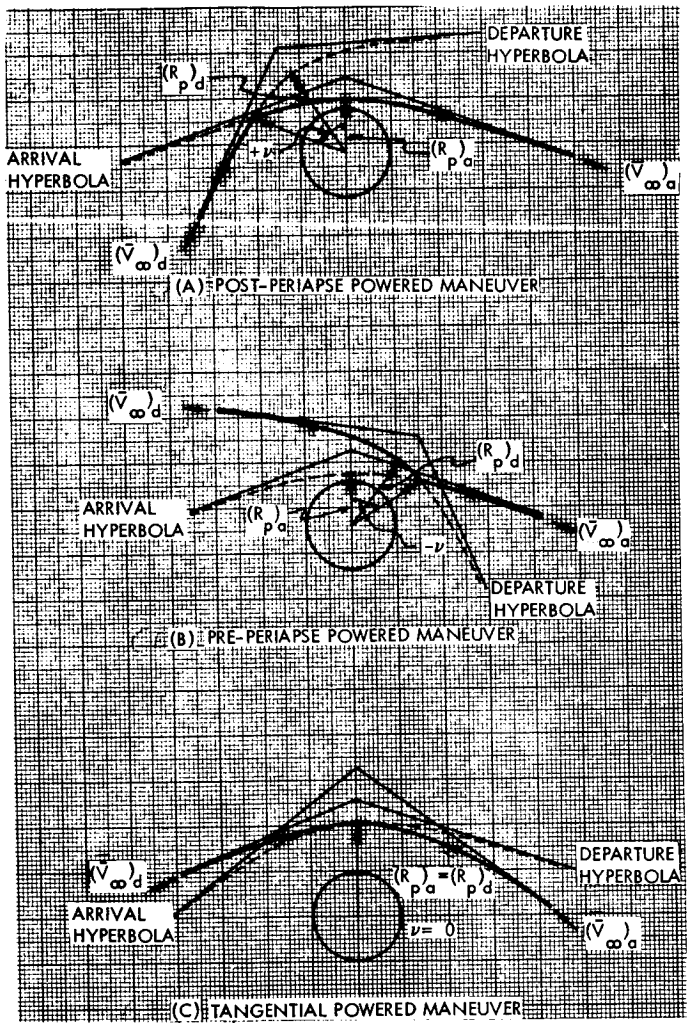

Figure 87. Powered Swingby Nomenclature

Powered swingby data were generated for several reduced trip times and various Jupiter approach periapse radii $(R_p)_a$. The position (true anomaly) on the incoming hyperbola at which the powered maneuver was performed has been successively incremented and the ΔV required to transfer to the outgoing hyperbola has been evaluated. A typical variation of V with true anomaly (point of transfer) for several trip times

and a constant approach periapse radius is given in Figures 88 and 89. Negative true anomalies correspond to positions prior to periapsis passage and positive true anomalies correspond to positions after periapsis passage. Ninety Jupiter radii and 2 Jupiter radii were chosen as examples for the approach periapse radii in Figures 88 and 90, respectively, because they coincide with the R_p's of unpowered swingby trajectories D and E.

Figure 88 shows that ΔV for the earth-Jupiter-Saturn powered swingbys is relatively independent of the position (ν) on the incoming hyperbola at which the maneuver is made. Figure 90, however, indicates a very strong variation of ΔV with true anomaly for the earth-Jupiter-Neptune powered swingbys. These results are not entirely unexpected, since one would anticipate a difference in behavior between those trajectories which pass close to Jupiter (Figure 88) and those which do not (Figure 90). The effect of a more subtle parameter, the ratio of $(\overline{V}_\infty)_a$ to $(\overline{V}_\infty)_d$, also has some bearing upon the variation of ΔV with true anomaly. This effect has not been investigated.

It must be remembered that Figures 88 and 90 show variations in ΔV for only one representative $(R_p)_a$. A new choice of $(R_p)_a$ will result in a new graph of ΔV. The minimum ΔV for various values of $(R_p)_a$ have been cross-plotted in Figures 89 and 91 as a function of total trip time. The curve labeled "T" in these figures represents a tangential propulsive maneuver, i.e., one in which the R_p's of the arrival and departure hyperbolas are the same and the maneuver is performed at periapsis (see Figure 87).

Figure 89 indicates that a high ΔV is required for even a small reduction in earth-Jupiter-Saturn total trip time. For example, a minimum ΔV of 3.52 km/sec is required to reduce the unpowered swingby trajectory D trip time by 100 days — a savings of only 7.6 percent. On the other hand, Figure 91 shows that when this same amount of ΔV is applied at Jupiter for the earth-Jupiter-Neptune mission, a significant reduction in total trip time can be realized. The unpowered swingby trajectory E trip time is reduced by 970 days, a savings of 30.2 percent.

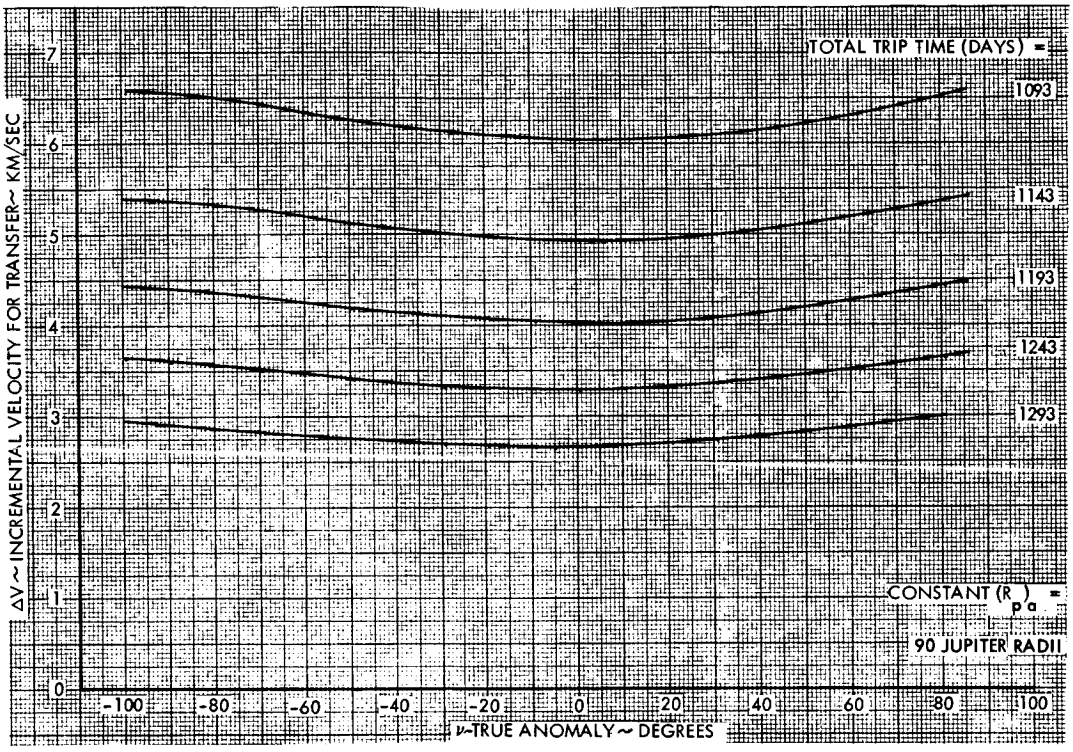

Figure 88. Earth-Jupiter-Saturn Powered Swingbys, Incremental Velocity Versus True Anomaly

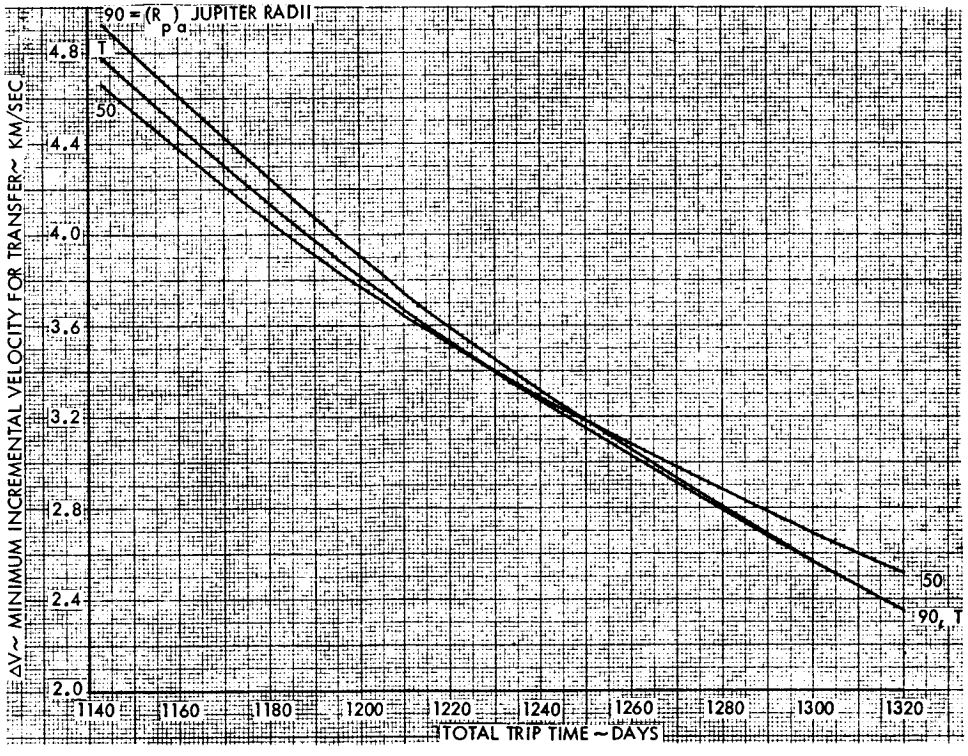

Figure 89. Earth-Jupiter-Saturn Powered Swingbys, Minimum ΔV for Transfer

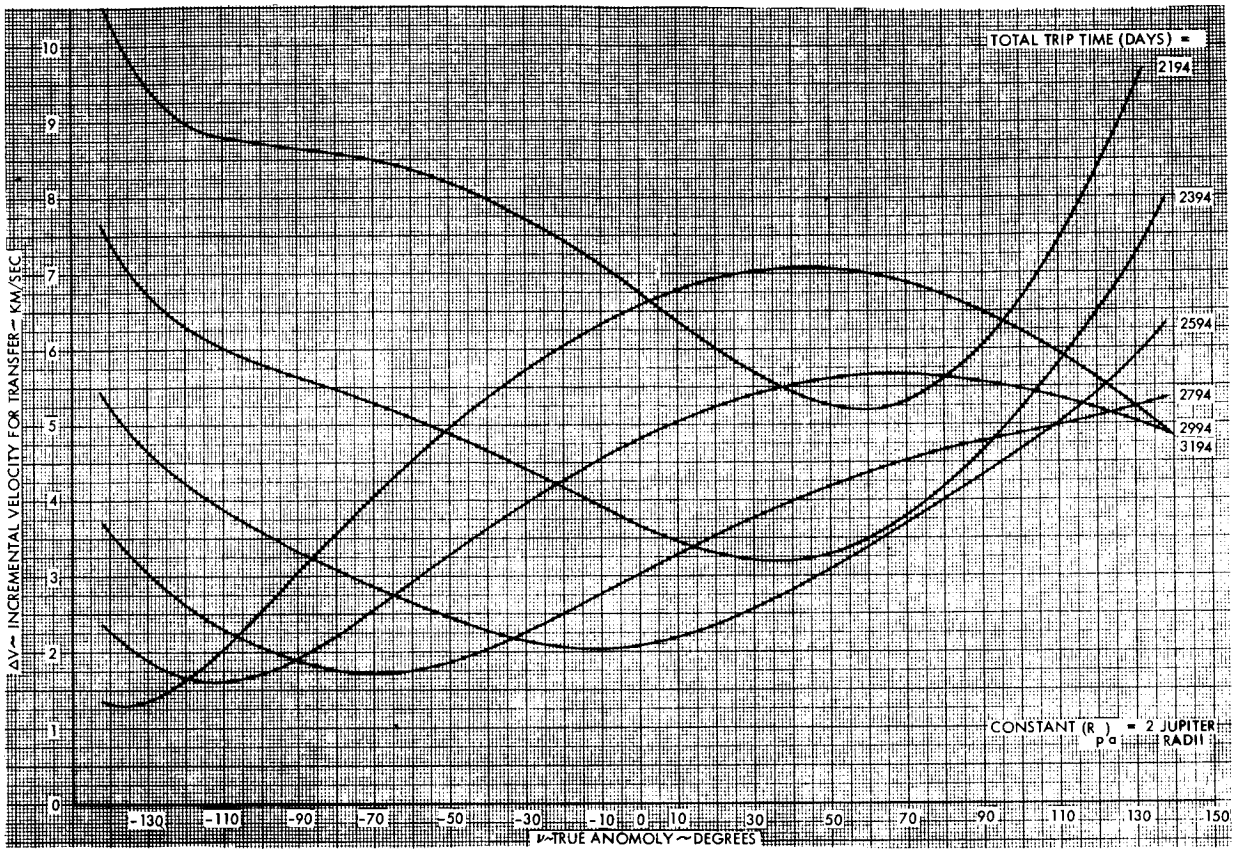

Figure 90. Earth-Jupiter-Neptune Powered Swingbys

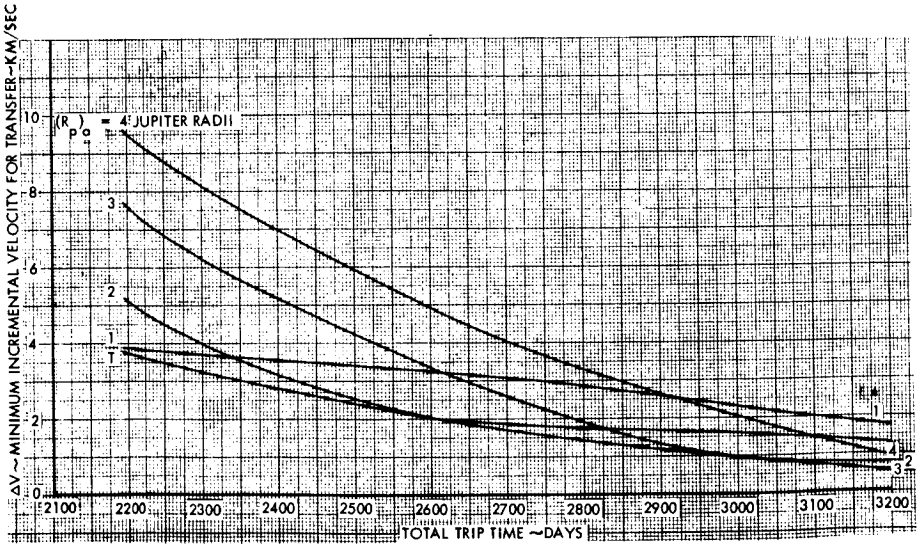

Figure 91. Earth-Jupiter-Neptune Powered Swingbys, Minimum ΔV for Transfer

The following conclusions can be drawn from Figures 88 through 91, and other comparisons:

- ΔV does not vary significantly with true anomaly at great distances from Jupiter.
- The tangential propulsive maneuver is nearly the optimum powered maneuver.
- A ΔV applied during the earth-Jupiter-Neptune swingby mission offers a considerable savings in total trip time.
- However, the advantage of applying it during the Jupiter swingby in comparison with accepting a higher injection energy from earth (using the same launch vehicle, but a spacecraft lightened by removal of swingby propellant), has not been established by the limited investigation made.
- The powered swingby may compare favorably with an unpowered swingby for low-energy, long duration missions, while unfavorably for high-energy, shorter duration missions to the most distant planets.

5.6 GUIDANCE REQUIREMENTS

The trajectory must be guided with sufficient accuracy to enable meaningful scientific experimentation near the target planet. For a number of experiments, this requires that the distance of closest approach be controlled to an accuracy of approximately one planetary radius. It was concluded in Volume 2 that this accuracy is desirable for a Jupiter encounter mission. For other scientific experiments which are related to planet surface features, such as albedo determination, it is reasonable to plan control of closest approach so that a proportionally better measurement is made similar to what can be expected at Jupiter. This means that a 100,000 kilometer miss at Jupiter, which is 5 AU away, corresponds to a 600,000 kilometer miss at Neptune, which is 30 AU away.

Other scientific experiments may provide meaningful data at further distances from an outer planet. More precise determination of the astronomical unit might be made from the gravitational attraction of the outer planet (Volume 2, Section 7.4). The space environment this far from the sun probably is more free of interplanetary matter, and the effects of uncertainties in solar force acting on the spacecraft are small. This may reduce the error in processing orbit data.

5.6.1 Trajectory Determination

A critical factor in determining flight regions where guidance can be performed concerns the quality of the trajectory determination. Earth-based tracking using the Deep Space Instrumentation Facility can determine the trajectory accurately near the earth because tracking angle information can be collected and because of the variation of the relative spacecraft velocity with respect to the tracking stations (velocity parallax), caused by the rotation of the earth. Trajectories which are far from the earth do not exhibit these characteristics. The primary factor which determines the quality of the trajectory determination in these regions is the dynamic nature of the trajectory. For example, passage into the gravitational field of another planet changes the spacecraft velocity, providing new information because the gravitational field and the location of the planet are accurately known.

The accuracy of the spacecraft orbit determination prior to a midcourse correction 10 days after launch causes the uncertainity in the Jupiter impact parameter to be approximately 5000 kilometers. (See Volume 2, Section 7.4.) Similar accuracy following the midcourse correction would probably require 100 days of tracking. If a midcourse correction were performed 100 days after launch, tracking for the remaining flight time to Jupiter might never give similar accuracy.

Orbit determination following Jupiter swingby will probably be the least accurate for any portion of the trajectory. Tracking data provides information about the trajectory in the ecliptic plane but provides little information about the component of the trajectory out of the ecliptic. Thus, the uncertainty of the trajectory estimate may be greater than the a priori estimate or greater than the actual trajectory error. In this instance, orbit determination information would be useless to support a midcourse correction.

Alternate orbit determination methods might provide increased accuracy. These include data taken by spacecraft sensors. There are many different types of instruments which can be carried by a spacecraft. Measurements by these instruments give information which can be classified into the following categories:

- Angle information involving a near body. For example, the earth-probe-Jupiter center angle might be measured, or Jupiter might be photographed against the background of stars.
- Altitude information from a near body. The aspect angle of Jupiter might be determined from which an estimate of the altitude can be computed.
- Rate information from a near body.
- Event time information. These measurements include occultation times of particular objects being sensed, and terminator detection.

Inclusion of spacecraft sensors for the specific purpose of orbit determination, of course, constitutes a change in the spacecraft concept.

5.6.2 Accuracy Requirements

Additional guidance is required for the missions to the outer planets which involve both swingby past Jupiter and direct flight. Midcourse guidance between earth and Jupiter provides control of the distance of closest approach for Jupiter swingby. Because of the control uncertainty, however, the actual distance of closest approach can only be statistically predicted prior to launch from the earth. This uncertainty requires that an additional number of midcourse corrections be planned prior to Jupiter encounter or that the trajectory beyond Jupiter be actively guided in order to guarantee subsequent encounter with another planet. Additional guidance is also required for direct flight to the outer planets.

A single midcourse correction 10 days past launch can control the impact parameter error at Jupiter to within about 25,000 kilometers for the spin-stabilized spacecraft and to within about 12,000 kilometers for the 3-axis controlled version. (See Volume 2, Section 4.2.) This represents a reduction of the initial impact parameters error cuased from the launch vehicle injection errors of 100 and 50 meters/sec for the spin and 3-axis versions, respectively. Another midcourse correction performed at 100 days, where the orbit determination accuracy might be comparable to that of the first correction, would remove most of the remaining errors. Orbit determination errors will likely account for the major portion of the remaining error, which would amount to approximately 5000 kilometers. This represents a reduction of the impact parameter error following the first correction of about a factor of 2 to 5. Errors from other corrections

performed later in flight would also probably be dominated by orbit determination uncertainties.

An error in the impact parameter of 5000 kilometers would mean that the direction of the outgoing asymptote would be in error and encounter with a second planet might not be successful. This aspect is discussed later in this section.

The additional velocity increment which would be required for multiple midcourse corrections is slight, on the order of 10 meters per second.

As an alternative or in addition to multiple midcourse corrections between the earth and Jupiter, midcourse corrections can be performed following Jupiter swingby. To estimate the midcourse correction velocity requirements following Jupiter encounter, it will be assumed that Keplerian two-body conic formulas near Jupiter describe the trajectory of the spacecraft. The errors in the impact parameter $\overline{b}$ of the incoming hyperbolic asymptote cause the direction of the outgoing asymptote to be incorrect. Let ϵ denote the angle separating the two asymptotes illustrated in Figure 92. The partial derivative of ϵ with respect to a change in the magnitude of the impact parameter b is

$$\frac{\partial \epsilon}{\partial b} = \frac{2}{ae^2}$$

where a is the semimajor axis and e is the eccentricity of the hyperbolic orbit. The inclination change Δi of the orbit with respect to a plane described by the nominal orbit is equal to the angular error of $\overline{b}$ projected to the impact plane. This geometry is illustrated in Figure 92. The deflection $\Delta\phi$ of the asymptote caused from the inclination change Δi is a function of the angle turned about the planet ϵ

$$\Delta\phi = \Delta i \sin \epsilon$$

Figure 93 shows how the direction of the outgoing asymptote is deflected because of an error in b which causes ϵ to vary and because of the error $\Delta\phi$.

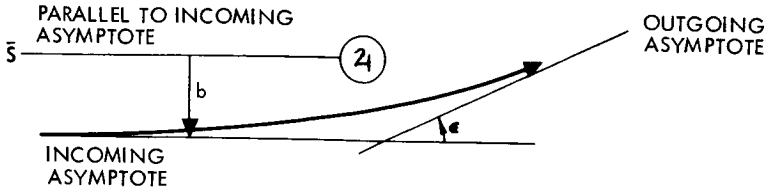

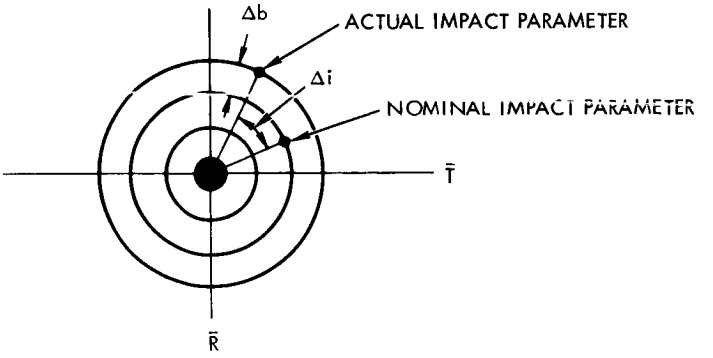

Figure 92. Impact Error Components

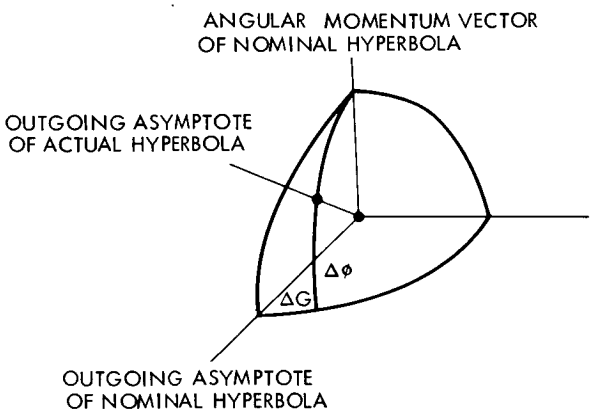

Figure 93. Outgoing Asymptote Deflection

The distance of closest approach to Jupiter probably will not be less than one planet radius for either simple flyby missions or swingby missions to other planets. The closest approach for these computations therefore, is assumed equal to one radius and the hyperbolic excess velocity V_∞ is selected equal to 7 km/sec. The 99 percent probability

miss dispersion at Jupiter caused from control errors of a single midcourse correction on the earth-Jupiter trajectory is assumed to be a circular region in B·T, B·R space of 25,000 kilometers radius. Using these numbers, it is found that

$$\Delta\epsilon = 1.01 \text{ deg } (99\%)$$

$$\Delta\phi = 0.924 \text{ deg } (99\%)$$

Beyond Jupiter, midcourse correction velocity requirements are computed by assuming that the correction velocity removes the pointing errors $\Delta\epsilon$ and $\Delta\phi$ along the asymptote where the spacecraft velocity is equal to V_∞. This will give a worst case estimate because critical plane type corrections typically require minimum correction ΔV midway along the trajectory.

$$\Delta V_1 \cong (V_\infty)\,\Delta\epsilon$$

$$\Delta V_2 \cong (V_\infty)\,\Delta i$$

$$\Delta V \cong \sqrt{\Delta V_1^2 + \Delta V_2^2} = V_\infty \sqrt{\Delta\epsilon^2 + \Delta i^2}$$

and the total correction velocity ΔV is $\Delta V = 167$ m/sec (approximately 99 percent velocity loading).

The 99 percent probability miss dispersion at Jupiter caused from control errors of multiple earth-Jupiter midcourse corrections is assumed to be a circular region in B·T, B·R space of 5000 kilometers radius. The estimate is discussed earlier in this section. Using this number and the same assumptions identified above, it is found that

$$\Delta\epsilon = 0.202 \text{ deg } (99\%)$$

$$\Delta\phi = 0.185 \text{ deg } (99\%)$$

which gives a total correction velocity requirement v equal to $\Delta V = 33$ m/sec (approximately 99 percent velocity loading).

To guarantee that the impact parameter at Neptune have less than 600,000 kilometers error the outgoing asymptote from Jupiter must be controlled to within approximately 0.0001 degree. For direct flight to

Neptune, the outgoing asymptote from the earth must be controlled to within approximately the same value. Because of the orbit determination problem following Jupiter swingby, trajectories can be controlled more accurately on direct flights.

5.7 FLIGHT TIMES

The long flight times to the outer planets are one of the dominant characteristics of Advanced Planetary Probe missions. In any attempt to analyze and reduce these flight times one realizes that they are intimately bound with the injection energy requirements of the mission. Figure 94 gives the relation between launch energy and transit time for direct and swingby missions to the various planets as follows, with data sources indicated:

- Earth-Jupiter (direct trajectories). Type I and Type II. (Type I curves are given in more detail in Section 4.)*
- Earth-Saturn (direct trajectories). Type I.**
- Earth-Uranus (direct trajectories).
- Earth-Neptune (direct trajectories).
- Earth-Saturn (Jupiter swingby trajectories). Launch opportunity: 1978.***
- Earth-Uranus (Jupiter swingby trajectories). Launch opportunity: 1979.***
- Earth-Neptune (Jupiter swingby trajectories). Launch opportunity: 1979.***

---

*V. C. Clarke, et al., "Design Parameters for Ballistic Interplanetary Trajectories, Part II, One-Way Transfers to Mercury and Jupiter," JPL TR 32-77.

**"Interplanetary Trajectory Analysis for Missions from Earth to Mercury, Jupiter, and Saturn," NASA TMX 53046.

***G. A. Flandro, "Fast Reconnaissance Missions to the Outer Solar System Utilizing Energy Derived from the Gravitational Field of Jupiter," JPL Report.

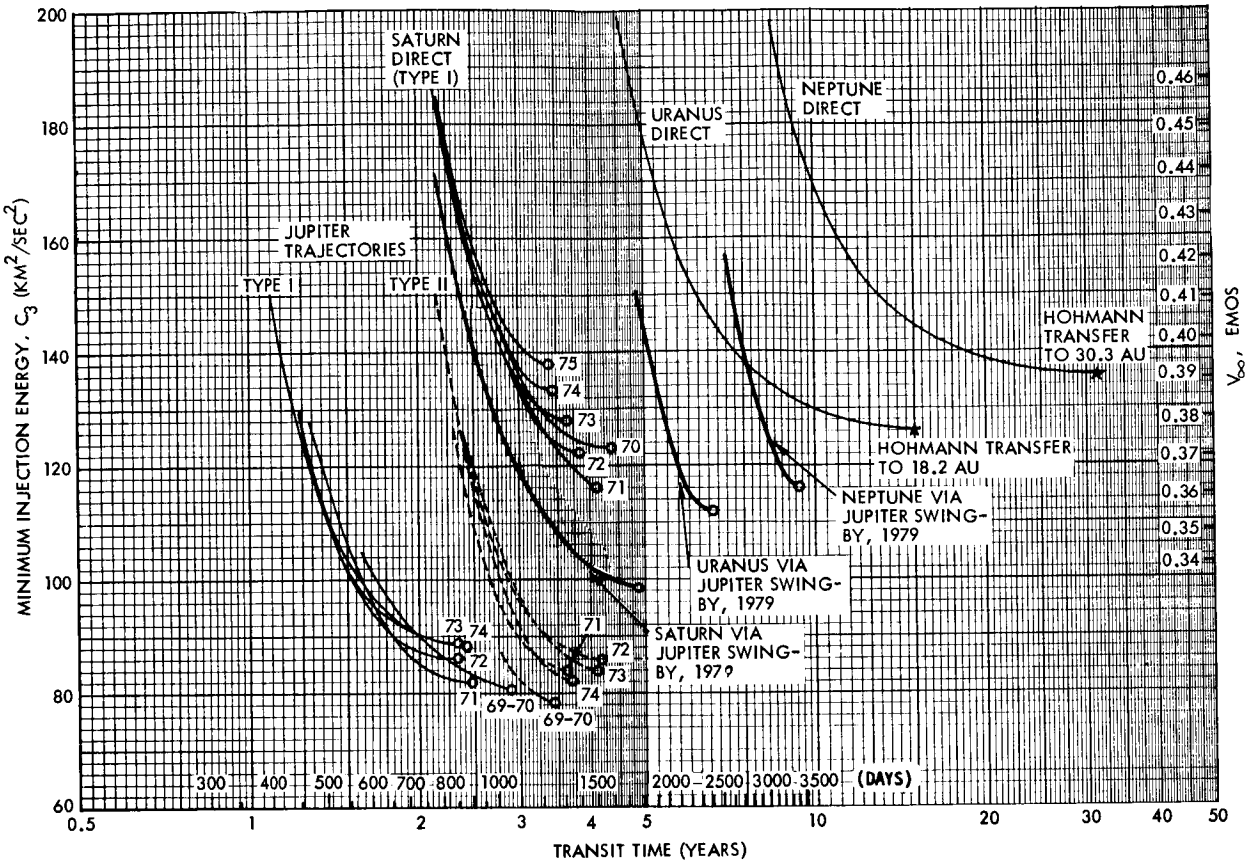

Figure 94. Injection Energy Versus Transit Time

For all except direct trajectories from the earth to Uranus and Neptune, the curves give minimum injection energy requirements over a 20-day launch opportunity. For the direct earth-Uranus and earth-Neptune trajectories, in the absence of more precise data, the curves were based on these assumptions:

- The earth's orbit is circular, with a radius of 1 AU.
- The target planet is at a constant distance from the sun. This distance, 18.2 AU for Uranus and 30.3 AU for Neptune, approximates the actual distance from the sun to these planets during the 1980's.
- The orbits of the earth and the target planets are coplanar.

As a result of these assumptions, the curves show no distinction between the different (annual) launch opportunities and show no division into Type I and Type II categories. (However, the results for Neptune are confirmed

by the detailed analytical curves given earlier in this section for the characteristics of the 1978 opportunity.) Also, no provision for a finite launch-opportunity duration was made. (Redrawing the curves to accommodate the penalty imposed by the requirement of a 20-day launch opportunity would increase C_3 by 3.5 km^2/sec^2.) The limiting case of these curves, reflecting the minimum-energy trajectories, corresponds to the Hohmann transfers.

The interpretation of the minimum energy requirement over a 20-day launch opportunity is illustrated by a point on one of the curves. For example, the 1975 curve for direct trajectories to Saturn passes through the point 3.1 years, 140 km^2/sec^2. For the 1975 opportunity, the minimum injection energy which need not be exceeded to produce trajectories to Saturn with transit times no greater than 3.1 years for 20 consevutive launch days is 140 km^2/sec^2. Or, conversely, given an injection energy of 140 km^2/sec^2, the smallest transit time which need not be exceeded for 20 consecutive launch days is 3.1 years.

Figure 94 indicates the expected progressive increases in transit time and required injection energy for target planets more distant from the sun. In addition, the family of curves for any one target planet shows the tradeoff between C_3 and transit time. Thus increasing C_3 (for a Jupiter mission) from 90 to 130 km^2/sec^2 reduces transit time from 2 to about 1.25 years.

For missions to the planets beyond Jupiter, the advantages of swingby trajectories over direct trajectories are seen in Figure 94. For Saturn missions, the reduction in transit time for a given launch energy is not extreme. At best, the swingby trajectories reduce transit time from 4 to 3 years. However, the swingby technique reduces the minimum energy requirement below 100 km^2/sec^2. For direct trajectories the corresponding minima are 116 to 140 km^2/sec^2, depending on the launch year. Thus, the swingby technique probably has more value in reducing C_3 requirements than in reducing transit time for Saturn missions.

For missions to Uranus and Neptune, however, although launch energy requirements are reduced appreciably by the swingby technique, the striking advantage appears to lie in the substantial reduction in transit times for values of C_3 in the range of 130 to 150 km^2/sec^2.

Of course, it is recognized that the swingby trajectories are related to the long (12 to 20 years) synodic periods between Jupiter and the outer planets, and are not available annually, as the direct trajectories are. Flandro (op. cit.) points out that 1978, 1979, and adjacent years appear to provide the best opportunities for the swingby missions considered here.

5.8 INTERPRETATION OF REQUIREMENTS

5.8.1 Direct Flight Missions

Table 16 summarizes typical flight times for various spacecraft weights based on the Titan IIICx/Centaur/TE-364-3 which is the least expensive launch vehicle with the capability of direct flight missions beyond Jupiter.

Table 16. Typical Flight Time (Years)

Science Payload (lb)	Nominal Spacecraft Weight (lb)	Saturn	Uranus	Neptune
50	500	2.0 (2.1)*	4.6 (4.8)*	8.6 (9.0)*
100	800	2.3	5.5	10.1
250	1200	3.0	7.6	22.0

* 3-axis stabilized spacecraft at 580 pounds.

If we go to the Saturn IB/Centaur/HEKS, flight times for the 100-pound science payload spacecraft are about as short as those for the 50-pound science payload on the Titan booster.

Nominal reliabilities for two-year lifetimes were calculated earlier to be 0.79 and 0.70 for the spinner and 3-axis stabilized spacecraft, respectively, for the Jupiter mission. Table 17 gives the corresponding spacecraft reliabilities for missions to Saturn, Uranus, and Neptune. These estimates do not include tape recorders or the science payload.

As is to be expected, the relative simplicity of the spinner combined with the shorter transit time for a 500-pound spacecraft has increasing effect as more distant target planets are considered. Its superiority over the 3-axis stabilized, 50-pound payload spacecraft becomes clearer and

Table 17. Typical Spacecraft Reliability Through Encounter Plus 0.1 Year

Science Payload (lb)	Nominal Spacecraft Weight (lb)	Stabilization	Saturn	Uranus	Neptune
50	500	Spin	0.781	0.575	0.359
50	580	3-axis	0.675	0.417	0.197
100	800	3-axis	0.652	0.368	0.162
250	1250	3-axis	0.575	0.253	0.0195

would be even further exaggerated if the gyros were included as an in-line element during possible occultation.

Thus, the effects of the long flight time to planets beyond Jupiter and particularly to Uranus and Neptune present a strong bias towards the basic spinner described in Volume 2. This is not to imply that reliability upgrading is not desirable for Uranus and Neptune missions even for this spacecraft.

Increased solar distance primarily affects sun sensor sensitivity requirements, temperatures of unheated external objects such as the antenna dish, and guidance accuracy. Taking the dish temperature at 1 AU as 200°F, or 660°R, the temperatures of the dish at the outer planets are:

Jupiter	289°R
Saturn	214°R
Uranus	150°R
Neptune	120°R

Thus, most of the temperature drop has already occurred at Jupiter. What is surprising is that solar heating still keeps the temperatures as high as shown. Heater power requirements for external equipment are essentially unchanged from Jupiter as are the effects of heat leaks of solar energy into the spacecraft equipment compartment. These are already small by design

even at 1 AU and negligible at Jupiter in comparison to dissipated power; going beyond Jupiter does not influence thermal control design.

The increased solar distance has a significant effect on guidance accuracy requirements, since miss distance propagates in a manner roughly proportional to this distance. At Jupiter, with one midcourse correction, the semimajor axis of miss distance in the impact plane (unfocused) was 25,000 and 12,500 kilometers for spin and 3-axis stabilized spacecraft, respectively. A second midcourse correction should reduce this miss by about a factor of five. Presuming that miss distances of the order of 20,000 kilometers are acceptable at the outer planets, it is clear that a second midcourse correction will be necessary, at least for Uranus and Neptune. It might even be desirable to have provisions for a third earth-line correction late in the mission to account for ephemeris uncertainties and the uncertainties in solar light pressure effects.

Increased solar distance also heavily influences illumination, resulting in increased TV exposure time requirements. For the spinners, this means that the spin rate must be reduced during encounter, probably not a difficult requirement since disturbance torques diminish rapidly with solar distance; however, it does mean designing the precession and tracking circuitry to handle more than one spin rate.

Increased communication distance has a pronounced effect on data rate capability. Table 18 gives the bit rate capabilities of the three spacecraft classes at the various outer planets.

Table 18. Transmission Rate Capabilities (Bits/Second)

Science Payload	Jupiter	Saturn	Uranus	Neptune
50	700	240	65	30
100	1400	480	130	60
250	2800	960	260	120

Clearly, the larger spacecraft are favored either for a larger data return or for lower DSIF utilization for a given data return. On the other hand, it is not clear that, far from the sun, cruise science needs the data rate appropriate to the more active inner region. In fact, it is possible that the frequency spectrum of plasma disturbances, etc. falls off at about the same rate as the communications capability.

Considering the encounter phase, it is clear that none of the spacecraft has a real time data capability as high as it desirable, requiring greater reliance to be placed on data storage. However, data storage represents one of the less reliable elements of the system. This combination again favors the larger, higher real-time data rate systems, particularly since current storage time limitations on the TV tube itself, for real-time readouts, may be exceeded. On the other hand, a lower data return from Neptune, for example, possibly has as much scientific value as a higher rate from Jupiter, since the existing information on that environment is substantially less.

Cost effectiveness is discussed in Section 8, placing these factors in a broader framework, including orbiter missions. In that framework, it appears desirable to use the light weight spinner for precursor missions to all the planets, followed by a heavier, more sophisticated orbiter. In this context, the lower absolute cost and higher reliability of the spinner appears more important than improved TV resolution for the precursor missions. The heavier payloads which emphasize encounter science are better handled by the 3-axis stabilized spacecraft but clearly do not take full advantage of their encounter measurement capability until upgraded to the orbiter class.

5.8.2 Jupiter Swingby Missions

Jupiter swingby missions to the outer planets are double attractive; they provide a significant shortening in flight time or C_3 requirement, and they provide additional Jupiter data during the course of a mission to another planet. For example, swingby upgrades the Atlas SLV3x/Centaur/HEKS to the capability of missions to any planet beyond Jupiter for the 50-pound payload spacecraft, and the Titan IIICx/Centaur/TE-364-3 is upgraded to 100-pound science class orbiter or 250-pound science class

swingby missions to any planet beyond Jupiter. There is even the theoretical possibility of a "grand tour" mission, a single mission which flies by Jupiter, Saturn, Uranus, and Neptune.

But there are significant disadvantages which include a single opportunity for each mission in the period of interest with recurrent opportunities varying from 20 years for Saturn to 12 years for Neptune. All the opportunities in 1970 to 1980 cluster around 1979. If this were the only disadvantage, it still might be cost effective to attempt these swingby missions. There are, however, some crucial guidance accuracy and reliability implications.

As shown in Section 5.2, the encounter with Jupiter must be controlled with much greater accuracy if subsequent midcourse corrections are to be kept to a reasonable magnitude. This means at least two midcourse corrections early, typically at 10 to 50 days, and possibly an earth line maneuver prior to encounter. After encounter, one or more midcourse corrections are required, and at least one of these will involve an out-of-ecliptic component. This is a severe requirement, since even uplink communications may be lost at these ranges if the spacecraft is reoriented. Further, it is not yet clear if DSIF tracking alone can provide adequate information for the out-of-ecliptic component since the geometry is so nearly coplanar, particularly for Uranus and Neptune. Neptune is 0.9 degree out of the ecliptic at arrival; therefore, there is an apparent change in range rate due to the earth's velocity being modified by the cosine of 0.9 degree. With range rate measurements of an absolute accuracy of 10^{-3} m/sec and without considering any other sources of error, the out-of-ecliptic error could be determined to within about 10,000 kilometers, which is more than satisfactory. Since there is probably much more than 10^{-3} m/sec uncertainty in the velocity of the earth, the measurements would have to consider this velocity also as an unknown. Measurements taken over several years should help clarify these and other uncertainties, but it is doubtful if anything like the 10,000 kilometers accuracy can be achieved. Further study is necessary to clarify achievable accuracy. On the other hand, a miss uncertainty of an order of magnitude larger than 5 Neptune radii in the impact plane (unfocused) could still lead to significant encounter data.

Thus the swingby mission provides reduced flight time or the possibility of using a cheaper launch vehicle, demands the ability to make a post-Jupiter flyby midcourse correction with an out-of-ecliptic component, and significantly degrades the accuracy of approach to the outer planet as compared to direct flight missions.

5.9 SPACECRAFT SYSTEM CONCEPT

5.9.1 Direct Flight Missions

Any of the Jupiter flyby spacecraft discussed earlier in Volumes 2 or here are suitable, with minor changes, for direct flights to the planets beyond Jupiter. However, to be specific in this section, and because of the cost effectiveness factors given in Section 8, it will be assumed that the 50-pound science class spinner discussed in Volume 2 is used.

The overall configuration will be the same, with a 16-foot antenna and 10-watt transmitter with bit rates as shown in Table 18. The launch vehicle will be changed to the Titan IIICx/Centaur/TE-364-3 with flight times as indicated in Table 16. A modest increase in midcourse propellant loading might be used to allow for the higher probability of a late earth-line midcourse correction. Power should be increased slightly because of degradation associated with the longer lifetime, but the thermal control system should remain unchanged and external heater power requirements should change only in that a slightly higher duty cycle would be demanded.

Reliability will be a major problem. Table 17 gave reliabilities for the spacecraft of 0.781, 0.575, and 0.359 for missions to Saturn, Uranus, and Neptune, respectively. Thus, particularly for the Uranus and Neptune missions, it will be desirable to upgrade overall reliability.

Typical upgrading might involve:

- Use of a greater number of smaller tape recorders or development of a basically more reliable data storage technique.
- Additional redundancy in the command decoding and distribution, digital telemetry, communication, attitude control, and science subsystems. Note that after development and flight of the spacecraft for the Jupiter mission, precise definition of appropriate techniques for reliability improvement should be possible.

Since solar illumination is reduced at encounter as well as disturbance torques, it is desirable to reduce the spin rate to keep TV image smear from increasing directly proportionally to the longer exposure times required. Appropriate spin rates, without increasing optical aperture or reducing resolution, would be

Jupiter	Saturn	Uranus	Neptune
5 rpm	1.5 rpm	0.37 rpm	0.15 rpm

The conical scan system is basically suitable for any spin rate; however, the electronic counter system would need to be modified to accommodate two speeds, one for the early part of flight and another for late flight and encounter. Changes by modulo 2 could be readily accommodated in the counting circuits used to fire the gas jets in relation to the zero crossing of the conical scan system. Then 5/4 = 1.25 rpm would be suitable for Saturn, 5/16 = 0.3125 rpm for Uranus, and 5/32 = 0.15625 would be suitable for Neptune. Although the gas jet impulse/revolution should be proportional to the spin speed, it is probably undesirable to reduce the gas jet on-time, for example, to 1/32 of its current value. Thus, an additional low pressure regulator may be required. Despin to the low speeds should be slow enough to be controlled from the ground; it might be desirable to use cold gas pulses for this fine operation.

The data rates must be selected for optimum utilization on these long missions. The design of the data handling unit given in Volume 2 is appropriately flexible. Bit rates as high as 1400 down to 8 bits/sec can be readily selected without modification to the digital telemetry unit. The bit rates possible are somewhat better than those on Mariner 4, which means that during the encounter television pictures stored on the tape recorder could be transmitted after flyby within a reasonable period of time. In fact " real time" pictures would be possible at Saturn about once every four hours, while at Neptune about one picture a day is possible.

Another aspect is the long communications turn-around time as related to acquisition. For example, the turn-around transmission time for Neptune is eight hours. Thus a large fraction of the single station acquisition time is absorbed in the simple problem of RF acquisition. Handover from one station to another solves the technical problem of long term tracking, but this is not an economic solution.

Angular acquisition should be automatic once the ranges for the medium- and low-gain antennas are exceeded, i.e., automatic angular acquisition should commence as soon as a DSIF signal is received at the spacecraft. Even with this mode, the timing of acquisition becomes critical since the DSIF acquisition time for tracking involves more than the round-trip time and, for Neptune, this becomes equivalent to a day's observation from a given ground station. As a result, handover from one station to another is critical if tracking and data are to be efficiently received.

Generally, then, a spacecraft suitable for flyby missions to Jupiter is, with minor upgrading, suitable for missions to the outer planets. This is equally true for spacecraft of heavier science payload class except for the reliability effect of slower flight times for higher weight spacecraft.

5.9.2. Swingby Missions

For Jupiter swingby missions to the outer planets, it is clear that midcourse maneuvers after the swingby will be required, assuming that DSIF tracking proves adequate to define the required corrections. While there is a small possibility that an earth-line correction may be satisfactory, in most cases the correction will have to be in the direction generally out of the ecliptic. Since communications with the spacecraft will be impossible without a large antenna pointing toward earth, a reorientation maneuver will be somewhat risky. However, if the system is proven, such an orientation without earth communication may be acceptable. If it is not acceptable, a midcourse maneuver would be difficult. With a 3-axis control system, two engines mounted perpendicular to the spacecraft earth-line axis and two engines along the earth line could provide such a correction capability, but even this would be far from optimum.

With a spinner which also does not lose communication, an engine would need to be mounted through the c.g. and perpendicular to the spin axis. This engine would be pulsed using a directional timing sensor such as a Canopus sensor to pulse the jet at the correct time for out-of-ecliptic velocity corrections. Such a system is not only complex but would require a complex sequence of firings, probably requiring ground command.

This midcourse correction requirement means that all of the proposed configurations for outer planet missions will require significant modification for a Jupiter swingby mission. In addition, just as on the direct missions, increased reliability is required and a multiple spin rate capability. With these requirements satisfied, and if the restricted launch opportunities are satisfactory, a significant savings in booster cost can be realized. Even with a smaller booster, it would be feasible to increase the science payload substantially.

6. JUPITER ORBITER MISSIONS

This section describes how the spacecraft concepts described earlier might be adapted to a Jupiter orbiter mission. The basic spacecraft configuration is the same concept described earlier with the three general requirements of 1) RTG power supply, 2) large body-mounted antenna, and 3) earth pointing. The critical difference between this spacecraft and the other configurations is the addition of propellants and an engine for deboost into orbit at the planet.

The basic conclusions of this portion of the study are that a spacecraft whose gross weight at injection is 2500 pounds can place a 250-pound science payload in orbit about Jupiter and perform an excellent orbiting mission. The Saturn IB/Centaur/HEKS provides over 1500 pounds of margin for this mission.

The larger science payload matches the increased capability of an orbiter to gather planetary data. Basically an orbiter is a second generation mission and should have much more capability than the precursor flyby spacecraft. Section 8 discusses this cost effectiveness tradeoff in more detail.

6.1 FUNCTIONAL REQUIREMENTS

The functional requirements during the launch and transfer phases for the Jupiter orbiter mission are identical to those for the flyby missions. However, during planetary encounter the deboost requirement changes system characteristics enough to require a new spacecraft design.

Figure 95 shows the launch vehicle capability on which are plotted the estimated weight requirements for three orbiter missions: a 1000-pound spacecraft with a 50-pound science payload, a 1600-pound spacecraft with a 100-pound science payload, and a 2500-pound spacecraft with a 250-pound science payload. These preliminary weight allocations are reached by studying typical approach velocities to Jupiter as well as to the other outer planets and then determining what orbits could be achieved with the typical ΔV's.

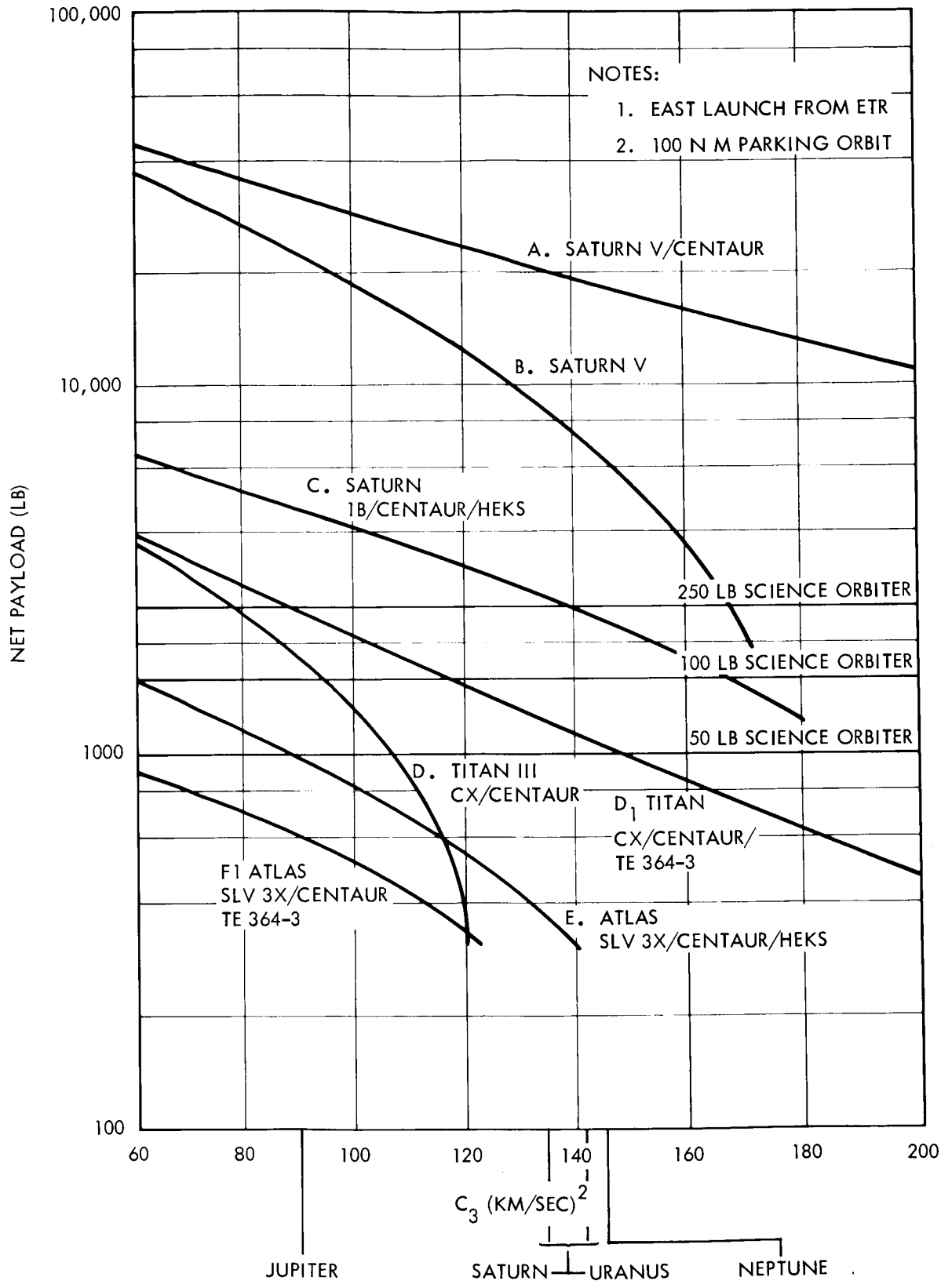

Figure 95. Launch Vehicle Performance Capability

6.1.1 Orbit Sizes and Velocity Increment

Figure 96 shows the orbits that can be achieved around these planets with a ΔV of 1.4 km/sec, and Figure 97 shows the same for a ΔV of 2 km/sec. As shown, the assumed approach velocities (V_{∞}) with respect to the target are relatively low, which in general indicates long flight

NOTES:

1. IMPULSIVE, OPTIMUM ORBIT INSERTION
2. APPROACH V∞ CORRESPONDS TO REASONABLY LOW VALUE ACHIEVABLE EACH OPPORTUNITY
3. ΔV = 1.4 KM/SEC

PLANET	V∞ (KM/SEC)	ESCAPE VELOCITY (KM/SEC)
JUPITER	6.0	60.1
SATURN	6.0	36.4
URANUS	5.5	22.1
NEPTUNE	4.9	25.1

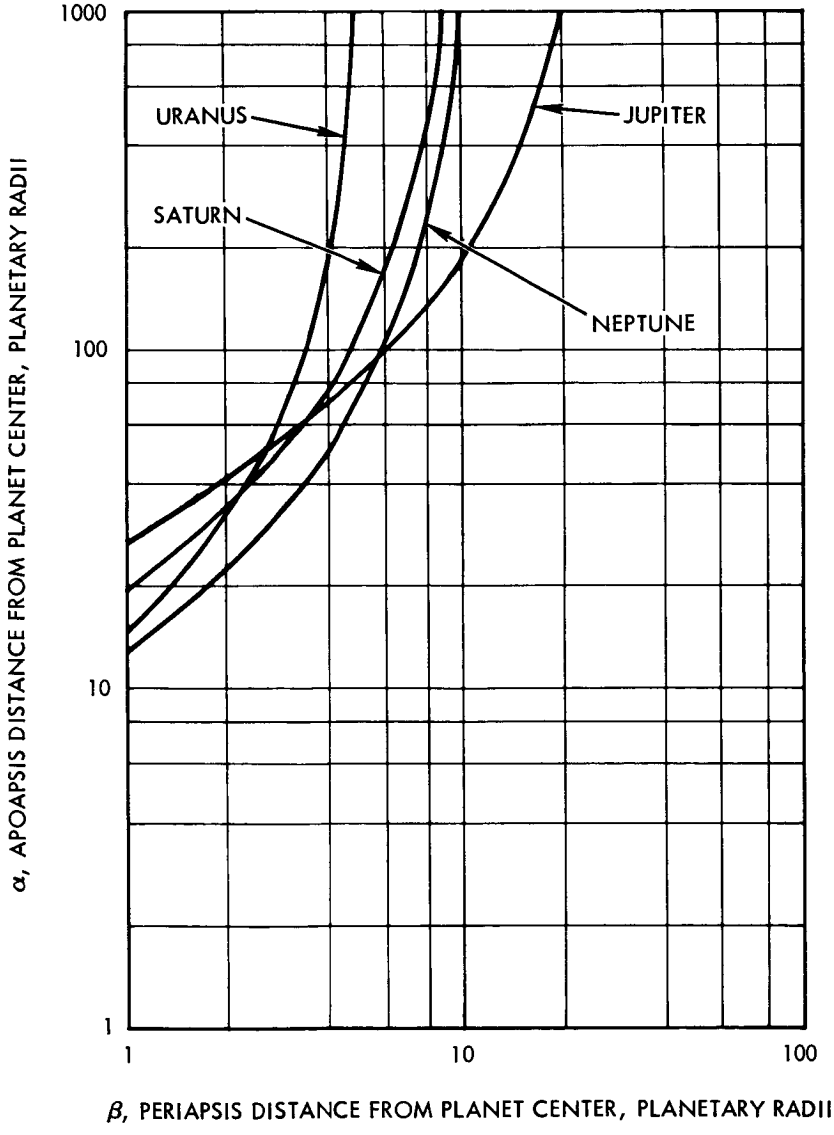

Figure 96. Planetary Orbits Attainable, ΔV = 1.4 km/sec

NOTES:

1. IMPULSIVE, OPTIMUM ORBIT INSERTION
2. APPROACH V∞ CORRESPONDS TO REASONABLY LOW VALUE ACHIEVABLE EACH OPPORTUNITY
3. ΔV = 2.0 KM/SEC

PLANET	V∞ (KM/SEC)	ESCAPE VELOCITY (KM/SEC)
JUPITER	6.0	60.1
SATURN	6.0	36.4
URANUS	5.5	22.1
NEPTUNE	4.9	25.1

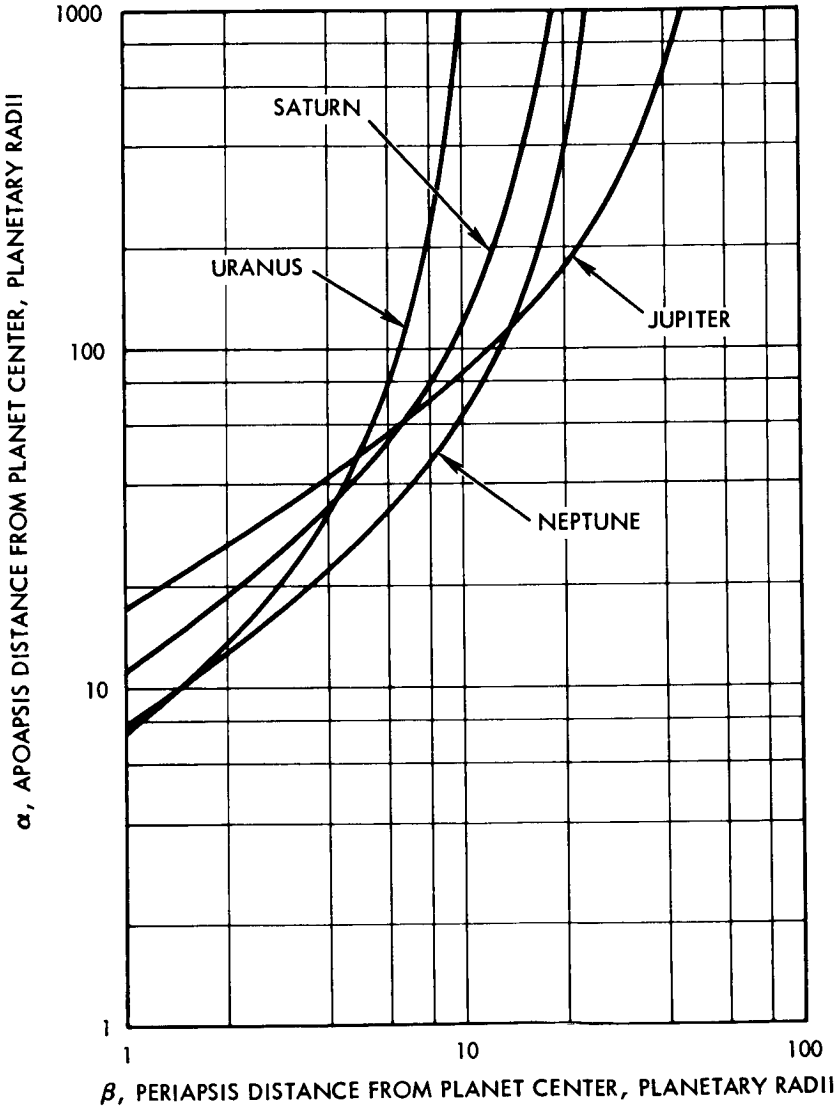

Figure 97. Planetary Orbits Attainable, ΔV = 2.0 km/sec

times. The V_∞'s used in these figures and the corresponding flight times are as follows, with Hohmann transfer values for comparison:

Target Planet	Values Used		Hohmann Transfer	
	V_∞ (km/sec)	Flight Time (years)	Min. V_∞ (km/sec)	Flight Time (years)
Jupiter	6.0	2.4	5.6	2.6
Saturn	6.0	4.7	5.4	5.6
Uranus	5.5	10	4.5	15
Neptune	4.9	20	4.1	31

Further savings in flight times can be made, but only by accommodating increases in V_∞, which raise ΔV requirements. (For Uranus and Neptune V_∞ is essentially the same function of flight time whether direct or Jupiter swingby trajectories are used.) For example, shorter flight times to Jupiter have the following consequences:

Flight Time (years)	V_∞ (km/sec)	ΔV Required to Enter a 2 x 42 Orbit (km/sec)	Orbits Attainable (in planet radii)	
			With ΔV = 1.4 km/sec	With ΔV = 2.0 km/sec
2.6	5.6	1.36	2 x 41	2 x 26
2.4	6.0	1.40	2 x 42	2 x 27
1.9	8	1.76	2 x 67	2 x 35
1.6	10	2.20	2 x 200	2 x 53

With a deboost ΔV of 1.4 km/sec at 2 planetary radii from Jupiter's center the apoapsis is about 42 radii, while at Neptune with the same conditions the orbit is 2 x 22 radii. Although Neptune is much smaller than Jupiter, the V_∞ is also smaller. With a ΔV of 2 km/sec, a possible orbit about Jupiter would be 2 x 27 radii and at Neptune 2 x 13 planetary radii.*

*Orbit dimensions are given in planetary radii from the center of the planet. Thus a 2 x 42 radii orbit has altitudes of 1 radius at periapsis and 41 radii at apoapsis.

These relations between ΔV requirements and orbits attainable are idealized, based on optimum, impulsive orbit insertion. In actuality the optimum orbit insertion process is degraded by these effects:

- Inaccuracies in control of the interplanetary trajectory results in a planetary approach hyperbola whose periapsis distance from the planet differs from the desired orbital periapsis distance.
- Tracking inaccuracies cause errors in the estimated time of periapsis of the approach trajectory, leading to timing errors in orbit insertion execution.
- The finite burn time at a reasonable thrust level causes gravity losses (as part of the impulse is delivered farther from the planet than the periapsis distance) and guidance law losses (simplified guidance, such as fixed inertial thrust direction, will be adopted).
- If the most simplified guidance—retaining the earth-pointing cruise attitude—is used, this orientation may deviate from the optimum fixed inertial direction.
- Orbit insertion execution errors result in a direction and magnitude of the ΔV vector which differ from the intended values.
- A nonoptimum orbit transfer may be programmed intentionally, to achieve a specific final orbit inclination or major axis orientation.

The proper orbit is basically selected by the type of science to be carried out, but there is obviously a tradeoff between the amount of propellant carried and the weight of the science. It is fortunate that in general a highly elliptical orbit offers the most science potential since it allows a good sample of the radiation belt and magnetic fields about the planet and also permits high resolution pictures at closest approach and broad coverage pictures at apoapsis. The other planetary observing experiments also gain equally by the variation in orbit altitude.

Another factor to be considered is the period of the orbit since this has considerable effect upon coverage lifetime. An orbit about Jupiter of 1.5 x 35 planetary radii has a period of 9.5 (earth) days, an orbit of 2 x 50 is 16 days and an orbit of 2 x 100 is 44 days. It would seem in general that the orbit period should be short enough that both periapsis and apoapsis are reached rather frequently. A period greater

than a month would seem to be excessively long but one of about 15 days appears to be reasonable. Since an orbit about Jupiter of a 15-day period can be achieved with a ΔV of 1.4 km/sec, this more modest propellant requirement was assumed. Using propellants with an I_{sp} of about 290 seconds means the total propellant weight (including midcourse) is on the order of 1000 pounds. Using the prior analyses of the 250-pound science payload spacecraft, the gross weight of such an orbiter would be about 2500 pounds. Again using the same scaling rules the gross weight of a 100-pound science orbiter would be 1600 pounds, and a 50-pound science orbiter would be 1000 pounds.

6.1.2 Orbit Perturbations

Nodal regression and apsidal advance are the dominant orbit perturbations of the planetary orbiters considered here. The perturbations are given as functions of orbit dimensions and inclination angle i as follows* (in degrees per revolution):

$$\text{Nodal regression} = \frac{d\Omega}{dt} = 360 \frac{JR^2}{a^2\left(1 - e^2\right)^2} \cos i$$

$$\text{Apsidal advance} = \frac{d\omega}{dt} = 360 \frac{JR^2}{a^2\left(1 - e^2\right)^2} \left(2 - \frac{5}{2} \sin^2 i\right)$$

where

$J = 0.02206$ for Jupiter

For three typical Jupiter orbits these perturbations were calculated:

Orbit Dimensions (Jupiter radii)	Orbit Period (Earth days)	Maximum Nodal Regression (deg/month)	Maximum Apsidal Advance (deg/month)
1.5 x 35	9.5	3.26	6.50
2 x 50	16	1.08	2.16
2 x 100	44	0.38	0.76

*Leon Blitzer, "The Orbit of a Satellite in the Gravitational Field of the Earth," 3 September 1965, STL Document 8655-6020-RU000.

The maximum values listed above apply to the equatorial orbit. The nodal regression decreases 15 percent as orbital inclination increases to 30 degrees, while the apsidal advance decreases by 30 percent. For orbit inclinations of interest the apsidal advance is nearly twice as large as the nodal regression. Since the angle ω is measured from the node and the nodal position Ω is measured from a fixed point on the celestial sphere, it is seen that in inertial coordinates the line of apsides advances at the same rate as the line of nodes regresses.

Interest in the orbit perturbations is concerned primarily with whether the relative geometry with respect to the sunlit part of the planet is significantly altered over the course of a year or longer while the orbiter mission is performed. Thus in the interest of daytime observation at closest approach it would be undesirable if the periapsis position would shift beyond the terminator too soon as a result of the rotation of the apsidal line. The numerical results show that even the largest value, i.e., 3.3 deg/month of apsidal rotation relative to the celestial sphere, obtained for the case of the closest orbit of practical concern, is quite small. It exceeds by approximately 1 deg/month the rotation of the sun line, which for Jupiter is approximately 2.5 deg/month, in the same direction as the apsidal rotation. Thus the orbital perturbation for all practical purposes does not affect the performance of experiments including daytime observation and occultation measurements.

Orbits achievable around Saturn with the available orbit insertion propellant weight have similar or possibly somewhat smaller dimensions in terms of planetary radii than the achievable Jupiter orbits, as seen in Figures 96 and 97. Typically, an orbit of 2 x 35 radii can be achieved with a ΔV of 1.4 km/sec. However, to stay clear of the immediate vicinity of the Saturn rings a minimum periapsis distance of 2.5 radii is required; a typical orbit achievable with ΔV = 1.4 km/sec would therefore be 2.5 x 42 radii with an orbit period of 17.9 (earth) days.

Since the dominant gravitational harmonic constants of Saturn (J = 0.02501) and of Jupiter (J = 0.02206) are of similar magnitude we obtain essentially the same rates of rotation for the nodal line and apsidal line per revolution of the orbiter. However, the orbit periods

for Saturn having the same relative dimensions α and β as Jupiter orbits are approximately 30 percent longer. The resulting apsidal motions relative to the celestial sphere are of the order of 2.5 deg/month. However, the sun line rotates only at the rate of about 1 deg/month relative to Saturn. Consequently, the maximum apsidal rotation exceeds that of the sun line by 1 to 2 degrees per month.

If the periapsis is initially established near the terminator, by using the simple cruise attitude orbit insertion technique, the perturbations have the effect of gradually shifting the periapsis over the dark side of the planet at the small rate of 1 to 2 degrees per month. An orbiter revolving in the plane of Saturn's motion around the sun, i.e., approximately in the ecliptic plane, would have an orbit inclination of 26.7 degrees relative to the planet's equator. This orbit inclination decreases the apsidal rotation, as discussed previously, such that the relative motion exceeding the rotation of the sun line is further reduced and becomes insignificant. Actually, a large orbit inclination relative to the planetary equator is desirable in the case of Saturn to permit observation of the rings from a favorable perspective.

6.1.3 Launch Vehicles

Figure 95 shows that missions to all four planets can be carried out with the Saturn IB/Centaur/HEKS booster. That booster can deliver a 250-pound science orbiter to Jupiter or Saturn, and a slightly smaller payload to Neptune or Uranus. On the other hand, a Titan IIICx/Centaur/TE-364 can carry out missions to all of these planets with a 100-pound science orbiter to Jupiter but only a 50-pound science orbiter to the farther planets. If the HEKS third stage were used it would increase the boost capability. Still the 250-pound science orbiter could be launched only to Jupiter.

In general for the orbiter missions as large a science payload as possible is desirable since the duration of the planetary encounter is essentially indefinite and each opportunity should be used to its fullest. For this reason we have assumed the 250-pound science payload for the Jupiter orbiter mission, which means that the boost vehicle must be the Saturn IB/Centaur/HEKS or possibly the Titan IIICx/Centaur/HEKS.

For Uranus and Neptune with the Saturn IB boost, the science payload would have to be reduced or the orbit eccentricity would have to be increased to reduce propellant requirements.

With a 2500-pound spacecraft carrying about 1100 pounds of propulsion system and propellants, 1400 pounds remain for the spacecraft system and science. To get a high data rate compatible with the type of science data to be gathered from an orbiter, and to keep the RTG fuel requirements within modest limits, a relatively low power transmitter should be used in conjunction with as large an antenna as possible. Thus a considerable amount of weight must be allocated to the spacecraft and its equipment. It appears then that a science payload of approximately 250 pounds would be appropriate and should consist of the following equipment:

Instrument	Weight (lb)	Bit Rate (bits/sec)
Magnetometer	20	24
Radio propagation and occultation experiment	15	72
Trapped radiation counter	10	24
Auroral detector	15	30
Microwave radiometer	20	30
Topside sounder	20	Variable
Infrared radiometer	10	28
Visual spectrometer	10	64
VLF detector	10	12
Visual solar occultation	15	64
Low energy proton monitor	5	16

giving a total of 150 pounds exclusive of the television system. With about 100 pounds to allocate to the television system a large set of optics should be used, perhaps a zoom lens and either television tubes operating at individual frequencies or a set of movable filters. Such a television system on a 3-axis controlled spacecraft could take a large

number of pictures of Jupiter at varying resolution down to perhaps a meter. The complement of instruments which comprise this spacecraft payload could perform a genuine mapping of the environment and the visible surface of Jupiter over all regions and evaluate short and long term time-varying effects, including diurnal variations.

6.2 INTERPRETATION OF REQUIREMENTS

The three basic ground rules of the study, that is 1) use of RTG's, 2) large antenna, and 3) earth pointing, are completely compatible with an orbiter mission. However, such a mission appears to require 3-axis control while in orbit since the exposure times required for the type of television system proposed are not compatible with the spinner, spin creating too much smear. On the other hand, it is conceptually feasible to make the transfer to Jupiter in a spin-stabilized mode, thereby gaining some reliability through simplicity, and assuming the 3-axis mode of control after orbit insertion. However, the 3-axis system for the entire mission appears preferable at this time.

6.2.1 Earth-Line Orbit Insertion

Whether the spacecraft spins or is 3-axis stabilized, it is desirable to make the orbit insertion maneuver while in the earth-line cruise attitude, because of the greater operational simplicity compared to a maneuver with commanded turns to an off-cruise orientation and because of the continuous high-gain antenna communications link to earth for operation monitoring and failure analysis.

However, to incorporate earth-line orbit insertion into the mission imposes certain constraints. It is necessary to locate the deboost engine on the axis pointing away from the earth; this raises minor design conflicts with the equipment compartment. Also, it is seen that orbits must have low inclinations to the equator of Jupiter; to enter a highly inclined orbit requires a substantial component of the deboost ΔV to be perpendicular to the ecliptic plane.

A third constraint affects the choice of interplanetary trajectories. To satisfy the requirement that the orientation of the thrust line for orbit insertion is approximately parallel to the earth line, the angles ZAE (from $\overline{S}$ vector to earth line) and γ (from $\overline{S}$ vector to optimum thrust

line) must be nearly supplementary, as shown in Figure 98. Since ZAE is essentially a function of arrival date and γ is a function of β (dimensionless radius at periapsis) and V_{HP} in turn a function of arrival date.

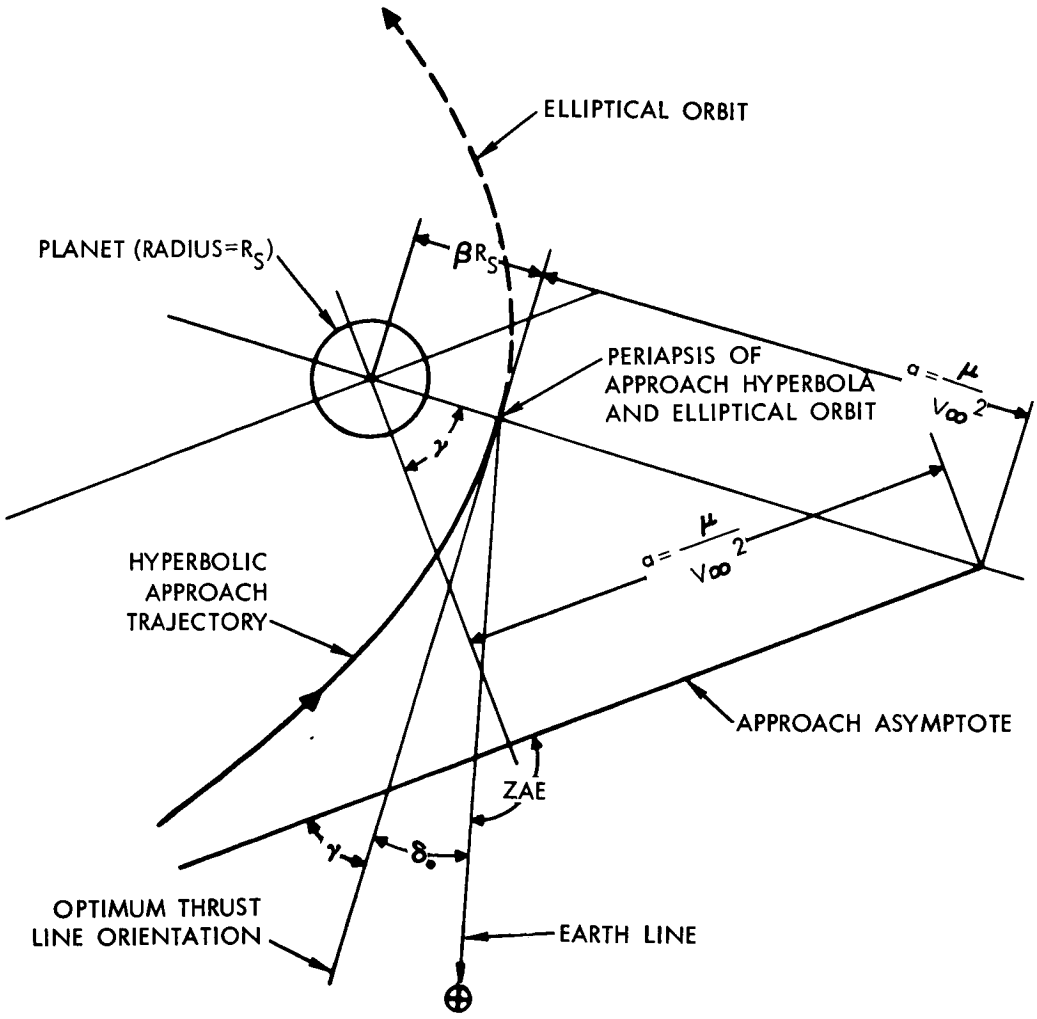

Figure 98. Geometry of Earth-Line Orbit Insertion

This constraint, therefore, is essentially a constraint on arrival date. From the figure, γ, the angle through which the approach trajectory is deflected from asymptote to periapsis, is obtained by

$$\csc \gamma = 1 + \frac{\beta R_s}{a} = 1 + 2\beta\left(\frac{V_{HP}}{V_{es}}\right)^2$$

where

βR_s = periapsis distance from the planet center

R_s = radius of the planet

a = semimajor axis of approach hyperbola = μ/V_{HP}^2

μ = gravitational constant of the planet

V_{HP} = asymptotic approach velocity

V_{es} = escape velocity at the planet surface

Assuming that the common plane of the hyperbolic approach and the elliptical orbit is parallel to the earth line, then the deviation of the optimum thrust line (tangential to the trajectory at periapsis) from the earth line is given by

$$\delta_o = (180^o - ZAE) - \gamma$$

For the 1972 earth-Jupiter opportunity 180^o - ZAE and γ are plotted against arrival date in Figure 99, and the arrival dates for which the

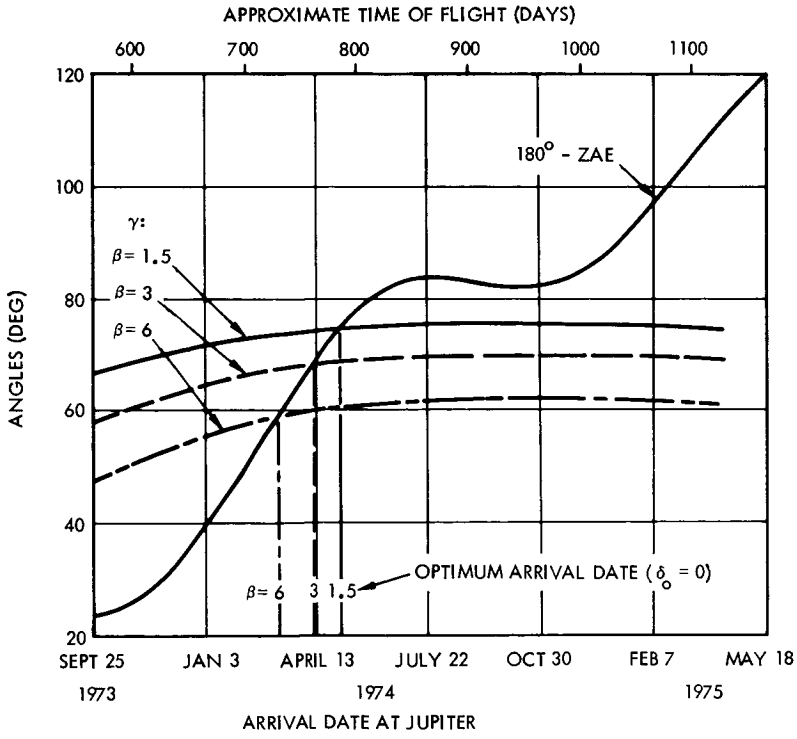

Figure 99. Determination of Optimum Arrival Date for Earth-Line Insertion

deviation $\delta_o = 0$ are:

β, Dimensionless Radius at Periapsis	Optimum Arrival Date ($\delta_o = 0$)	Approximate Flight Time (days)
1.5	May 6, 1974	788
3	April 11, 1974	763
6	March 9, 1974	730

However, because the degradation of orbit insertion maneuver efficiency is proportional to $(1 - \cos \delta_o) \approx \frac{1}{2} \delta_o^2$, a reasonably large band of arrival dates can be tolerated:

Degradation of maneuver efficiency, %	2.5	5
Maximum $\lvert \delta_o \rvert$ (deg)	12.8	18.2

β	Range of flight times (days)	
1.5	737 to 1012	718 to 1049
3	715 to 831 and 915 to 975	692 to 1025
6	679 to 782	654 to 810

The extension to very long flight times for $\beta = 1.5$ and 3 is due to the leveling of the ZAE angle for these flight times, as seen in Figure 99.

Of course, the utilization of these appropriate bands of arrival dates for the earth-line orbit insertion maneuver is subject to the other constraints on interplanetary trajectory selection discussed in Volume 2, Section 2.2. In particular, to delineate a 20-day launch period which accommodates orbit-insertion requirements of flight times over about 715 days, it is necessary to relax the launch asymptote declination constraint, $|DLA| < 33.5$ deg, to $|DLA| < 40$ deg, or to raise the injection C_3 requirement from the flyby value of 87 km^2/sec^2 to 96 km^2/sec^2, or to combine lesser changes in each limit.

We suggest that the appropriate conceptual design for the orbiter spacecraft be capable of conforming to the above constraints in order to make use of the earth-line orbit insertion maneuver, and have growth capability (by addition of star scanners for closed loop pointing away from the earth line, and appropriate maneuver commands and logic) to perform the more general arbitrary-pointing orbit insertion maneuver. In addition to permitting the attainment of highly inclined orbits, this growth capability is consonant with the guidance requirements of swingby trajectories to planets beyond Jupiter, discussed in the preceding section of this volume.

6.2.2 Orbit Insertion Guidance

An elementary analysis of some of the factors affecting the efficiency and accuracy of the orbit insertion maneuver is presented to indicate that the orbits about Jupiter which can be attained are reasonably close to the ones identified at the beginning of this section.

6.2.2.1 Interplanetary Trajectory Accuracy

We have seen in Volume 2 that the earth-Jupiter interplanetary trajectory can be controlled with a single midcourse correction maneuver to about these values (99 percent) in the R-T plane: semimajor axis, 25,000 km; semiminor axis, 15,000 km. The arrival time is controlled to 3.6 hours, 1σ. Although the R-T inaccuracies could be tolerated by the orbit insertion process, they need not be, because tracking after midcourse correction will reduce the uncertainties substantially, and the orbit insertion programming can be based on the estimated trajectory rather than the intended trajectory. The arrival time error, as of the midcourse correction, cannot be tolerated, but it too is reduced greatly by subsequent tracking. Two-way doppler tracking by DSIF, assuming range rate discrimination to 0.01 meter/sec, can determine the spacecraft's distance from Jupiter to 600 km 3 weeks before encounter. This alone permits the time of periapsis to be predicted so that commanded events near periapsis on a close trajectory (1.5 radii from the planet center) occur within 2.5 degrees (Jovian central angle) of the desired point. The tangent to the trajectory will deviate less than 1.25 degrees from its direction at the desired point, which introduces a negligible error in orbital characteristics.

For a nominal orbit size of 1.5 x 35 Jovian radii, entered at periapsis from an approach with V_∞ = 6.5 km/sec, the impact parameter B = 810,000 kilometers. An error in $\overline{B}$ causes the orbit plane to be rotated (about the $\overline{S}$ vector) 1.77 degrees from the nominal orientation, but produces no change in the orbit size. An error of 25,000 km in the magnitude of $\overline{B}$, if the nominal ΔV is exerted at periapsis, results in a change in apoapsis distance, as follows

$$\delta a = \left(\frac{\partial a}{\partial \beta}\right)\left(R_s \frac{\partial \beta}{\partial B}\right)\left(\frac{\delta B}{R_s}\right)$$

$$= (15)(0.259)\left(\frac{25,000 \text{ km}}{71,400 \text{ km}}\right)$$

$$= 1.36$$

The first parenthetical term is obtained from the slope of the curve of Figure 96, and the second represents Jupiter's gravitational focusing. Thus, if the approach is directed 25,000 kilometers too far from the planet, the nominal orbit insertion ΔV produces an orbit of 1.509 x 36.36 rather than 1.5 x 35 radii. Of course, with sufficient propellant margin and a variable impulse maneuver, the miss could be compensated to achieve a 1.509 x 35 orbit. It is evident that these targeting errors are not severe, and can be compensated to achieve the desired orbit closely.

6.2.2.2 Orbit Insertion Accuracy and Efficiency

The change in apoapsis distance due to variation in the longitudinal component of ΔV is given approximately by

$$\delta a = \frac{2a^2}{\frac{1}{\beta^2}}\left(\frac{\Delta V}{V_{es}}\right)\left[\frac{\delta(\Delta V)}{\Delta V}\right]$$

where

a, β = dimensionless radii of apoapsis, periapsis

V_{es} = escape velocity at the surface

and $\delta(\Delta V)$, the variation in velocity increment, may arise from execution errors or equivalent losses due to pointing errors, earth-line insertion constraint, gravity losses, or guidance law losses. For a 1.5 x 35 orbit, a variation in ΔV which is 2.5 percent of the nominal ΔV leads to $\delta a = 1.2$, or a resulting orbit of 1.5 x 36.2 planetary radii.

A simplified estimate of the effects of a finite burn (nonimpulsive ΔV) and an assumed constant inertial thrust direction for the guidance law lead to equivalent ΔV losses as follows (again for a 1.5 x 35 orbit):

Burn Angle (relative to periapsis) (deg)	Burn Duration (sec)	Equivalent ΔV loss, $\frac{\delta \Delta V}{\Delta V}$ (%)
± 20	1,600	1
± 32	2,600	2.5

This suggests a minimum thrust level for orbit insertion. To limit the degradation of orbit insertion efficiency due to burn time losses to 1 percent, the 1000 pounds of propellant should be consumed in 1600 seconds, giving a minimum thrust of

$$T = I_{sp} \cdot \frac{\text{propellant weight}}{\text{burn time}} = 290 \cdot \frac{1000}{1600} = 180 \text{ lb}$$

We may also examine the effect of pointing errors or deviations on equivalent ΔV losses and on the elements of the resulting orbit. For a nominal orbit of 1.5 x 35 radii from the planet center, consider pointing errors of $\theta = 0$, 10, and 20 degrees (Table 19). Regardless of the direction of the pointing error, an equivalent loss of ΔV is given by $(1 - \cos \theta)$, or approximately $\theta^2/2$, with a consequent increase in a, dimensionless apoapsis, as discussed above. If the pointing error is directed in the nominal orbit plane, the result, in addition to the increase in a, is a rotation of the line of apsides. On the other hand, if the pointing error is directed out of the nominal plane, the result is that the final orbit plane is inclined to the nominal orbit plane. These effects are estimated in Table 19. It is seen that substantial pointing errors may be tolerated without severely affecting the attained orbit.

Table 19. Effects of Orbit Insertion Pointing Errors

	Pointing Error, θ (deg)		
	0	10	20
Equivalent loss in velocity increment, $\frac{\delta(\Delta V)}{\Delta V}$, %	0	1.55	6.1
Resulting apoapsis distance, a	35	35.75	37.9
If pointing error is in the orbit plane, then the line of apsides is rotated by $\delta\omega$:	0	0.6	1.15
If pointing error is out of the orbit plane, then the orbit plane is inclined to the approach orbit plane by i:	0	0.3	0.6

6.3 SPACECRAFT CONCEPT

Figure 100 is an inboard profile of a 250-pound science class orbiter spacecraft. This can be thought of as a second generation spacecraft and as such an effort has been made to achieve greatly improved planetary data return over the precursor type spacecraft, commensurate with the increased cost of the Saturn IB/Centaur/HEKS launch vehicle. This is reflected in the use of a maximum diameter antenna, increased transmitter power, the inclusion of a large two-degree-of-freedom planetary scan platform and expanded data handling capability.

Within the fairing constraints for the SIB/Centaur/HEKS, an antenna of about 32 feet in diameter can be used. Since such a deployable parabola has already been constructed in the Sunflower solar collector program, this size was selected, providing 6 db more gain than the 16-foot antenna. Since it is assumed that the orbiter mission will be in the late 1970's, RTG fuel cost should be reduced although still high. For this reason a 40-watt transmitter was used, increasing transmitted power by a factor of four over the 50-pound science configuration. The net gain is 12 db resulting in a communication bit rate of slightly over 11,000 bits/sec at 6 AU from the earth.

The spacecraft is launched from a SIB/Centaur/HEKS in a standard "A" fairing. The interstage is a semimonocoque structural cylinder

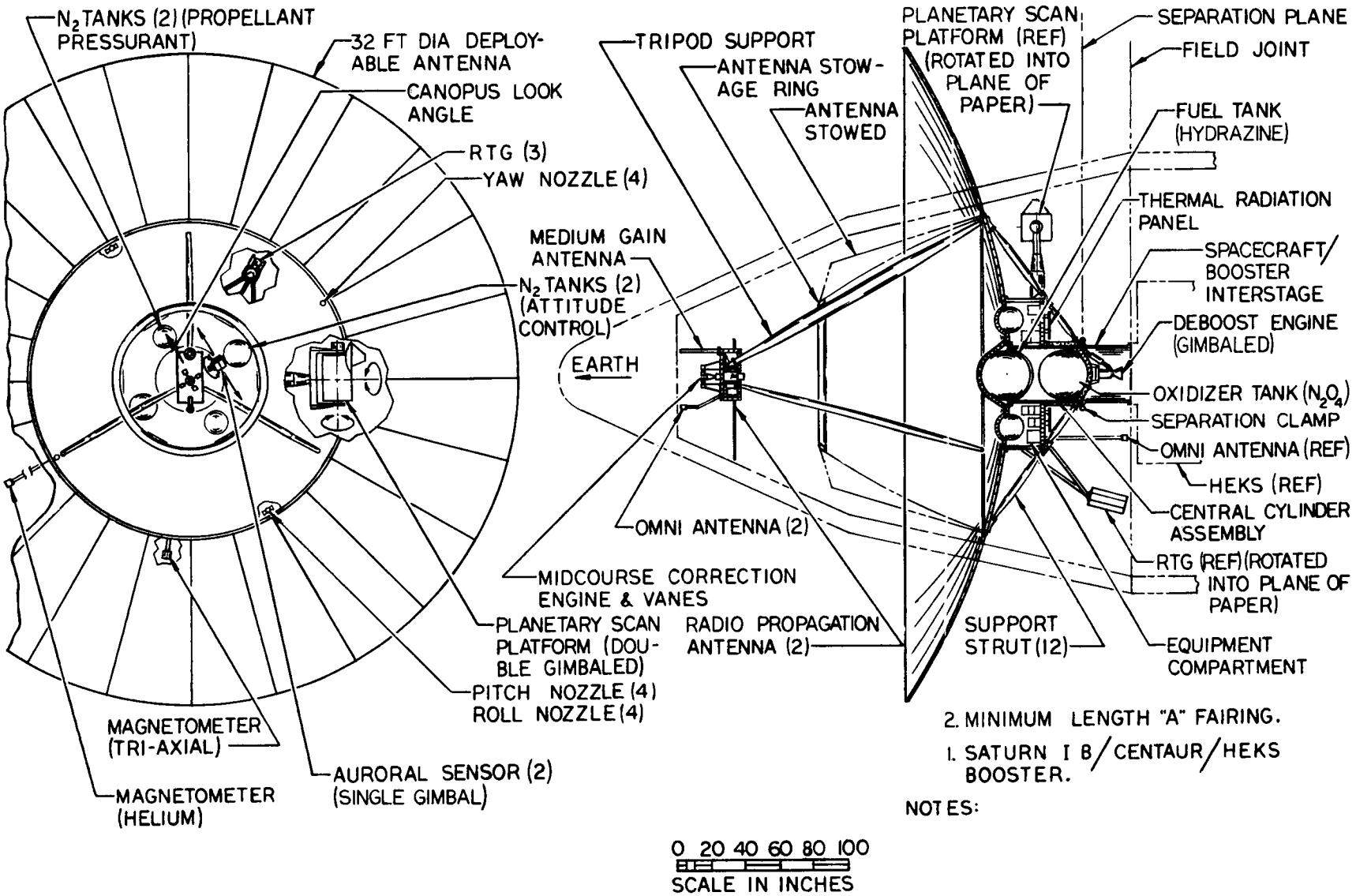

Figure 100. Jupiter Orbiter, 250-Pound Payload, 3-Axis Stabilized

31 inches in diameter and 28 inches long. The ring at the aft end of the cylinder is bolted to the high energy kick stage of the launch vehicle. This is the spacecraft booster field joint. The spacecraft is attached to the interstage with a V-band clamp assembly, which is for the spacecraft-launch vehicle separation. The interstage has a magnesium skin with aluminum rings and stringers. It provides a structural path with uniformly distributed loads. The gimbaled 250-pound thrust engine for the bipropellant deboost stage is mounted in the interstage area with the oxidizer tank attached just over the engine. Heaters are provided for the engine and the gimbal actuators. The central cylinder assembly housing the propellant tanks is 31 inches in diameter with a magnesium skin and aluminum rings and longerons. It is semimonocoque construction from the aft end to the equipment mounting platform. It is truss structure from the platform to the forward end providing uniform support to the propellant tanks.

This arrangement provides a good micrometeoroid protection for the tanks, good load distribution, and good thermal coupling between the propellant tanks and the main equipment compartment. The open ends of the cylinder are covered with 2-inch thick foamed aluminum sandwich panels which provide for micrometeoroid protection of the propellant tanks.

The main equipment compartment surrounding the cylinder is a toroid with a hexagonal outside structure. It is 18 inches high and provides four times the equipment mounting area as that provided by the spacecraft designed for the 50-pound science payload. A large two-degree-of-freedom planetary scan platform is mounted to the compartment, permitting an excellent field of view for observing the planet. The three fixed RTG's are mounted as on the other 3-axis controlled spacecraft. Four nitrogen tanks are symmetrically located about the roll axis. Two are for the propellant pressurant and two for the attitude control system. The high-gain antenna is the same general configuration as that proposed for the other configuration. The petal hinge ring is 188 inches, the maximum fixed diameter within the "A" fairing. The petal stow ring is 88 inches in diameter. The attitude control nozzles are all mounted to the petal hinge ring. The antenna feed assembly is

unchanged from prior configurations containing the medium-gain antenna, omni-antenna, and the 25-pound thrust monopropellant midcourse engine.

Table 20 gives the weight estimate for the entire spacecraft. The structure has been increased in weight to account for the larger vehicle, and micrometeoroid protection has been increased to 100 pounds because of the increased diameter. A planetary scan platform of 18 pounds empty weight has also been added.

The thermal control subsystem is increased in weight to account for the additional thermal switches required and increased area insulation. The three RTG's and power supply were sized to provide 340 watts of raw power. Communications 127 watts, electrical integration 9 watts; data handling 10 watts; attitude control 25 watts; heaters 22 watts, science 56 watts. Because of the increased power requirements 10 shunt elements were used for excess heat dissipation. The power control unit has been increased in size to provide additional power conversion.

Electrical integration equipment has been resized for the increased diameter and added functions. The data handling subsystem has been increased, allowing for three tape recorders with a total bit storage of 1.8×10^8 bits. Additional commands and sequencing for deboost have increased the size of the integrated decoder and sequencer. The communication subsystem has been increased in weight to allow for the 32-foot diameter antenna and for the use of a 40-watt TWT. The attitude control subsystem has been resized to allow for increased mass of the system and a larger margin of safety has been added in the event that a number of reacqusition sequences are necessary while in orbit. Two types of engines are used, a 25-pound hydrazine monopropellant for midcourse with jet vanes for thrust vector control and a 250-pound pressurized bipropellant using hydrazine and nitrogen tetroxide. The hydrazine tank is common to both engines. A study was made comparing solid propellants and bipropellants and the weight of blowdown versus regulated bipropellant systems.

If blowdown bipropellant systems are employed instead of regulated configurations, a good deal of the reliability loss can be averted but a weight penalty will result as shown in Figure 101, curve C. The weight penalty increases with increasing propulsion system weight as is evident from the diverging curves.

Table 20. Weight Estimate: 3-Axis Stabilized Spacecraft with 250-Pound Science Payload, Jupiter Orbiter Mission

Item		Weight (lb)
Structure and Thermal Control		289.4
Structure		123.2
Planetary scan platform		18.0
Thermal control		45.2
Meteoroid protection		100.0
Radiation protection		3.0
Power Supply		198.3
RTG Installation		180.4
RTG units (3)	166.0	
Boom assemblies (3)	14.4	
Power control unit (1)		10.4
Shunt elements (10)		7.5
Integration		105.5
Command distribution (1)		8.5
Umbilical (1)		3.0
Pyrotechnic control box (1)		7.0
Cabling and connectors		87.0
Data Handling		50.9
Data handling unit (1)		15.0
Tape recorder (3)		23.9
Integrated decoder and sequencer (1)		12.0
Communications		263.6
Receiver (2)		6.6
Modulator/exciter (2)		3.0
TWT (2)		2.0
Circulator switch (6)		1.8
Diplexer (2)		2.0
Antenna selector (1)		0.5
Receiver selector (1)		0.5
Power amplifier monitor and selector (1)		1.0
Directional coupler (1)		0.5
Omni-antenna installation (2)		1.5
Helical antenna installation (1)		2.8
High-gain antenna installation (1)		241.4
Attitude Control		121.9
Orientation system		121.9
Gyro reference assembly (1)	10.0	
Accelerometer (1)	1.0	
Guidance and control electronics (1)	6.0	
Canopus tracker (1)	6.0	
Coarse sun sensor (1)	0.2	
Fine sun sensor (1)	1.9	
Gimbal for fine sun sensor (1)	2.0	
Sun sensor electronics (2)	0.3	
TVC (2)	3.5	
Regulator/relief valve (2)	2.6	
Solenoid valves (12)	6.0	
Fill valves (2)	0.6	
High-pressure transducer (2)	0.4	
Low-pressure transducer (2)	0.6	
Nozzles (12)	1.2	
Lines and fittings	4.0	
Nitrogen	31.5	
Nitrogen tank and residual (2)	44.1	
Propulsion		1,122.6
N_2 Pressurization system		66.5
Valves and plumbing	7.9	
Nitrogen	24.4	
Nitrogen tank (1)	34.2	
Propellant system		1,056.1
Thrusters (2), valves and plumbing	18.6	
N_2O_4 tank and residuals (1)	23.4	
Hydrazine tank and residuals (1)	21.1	
Usable propellant	993.0	
Scientific Payload		250.0
Contingency		115.9
Spacecraft Weight		2,518.1

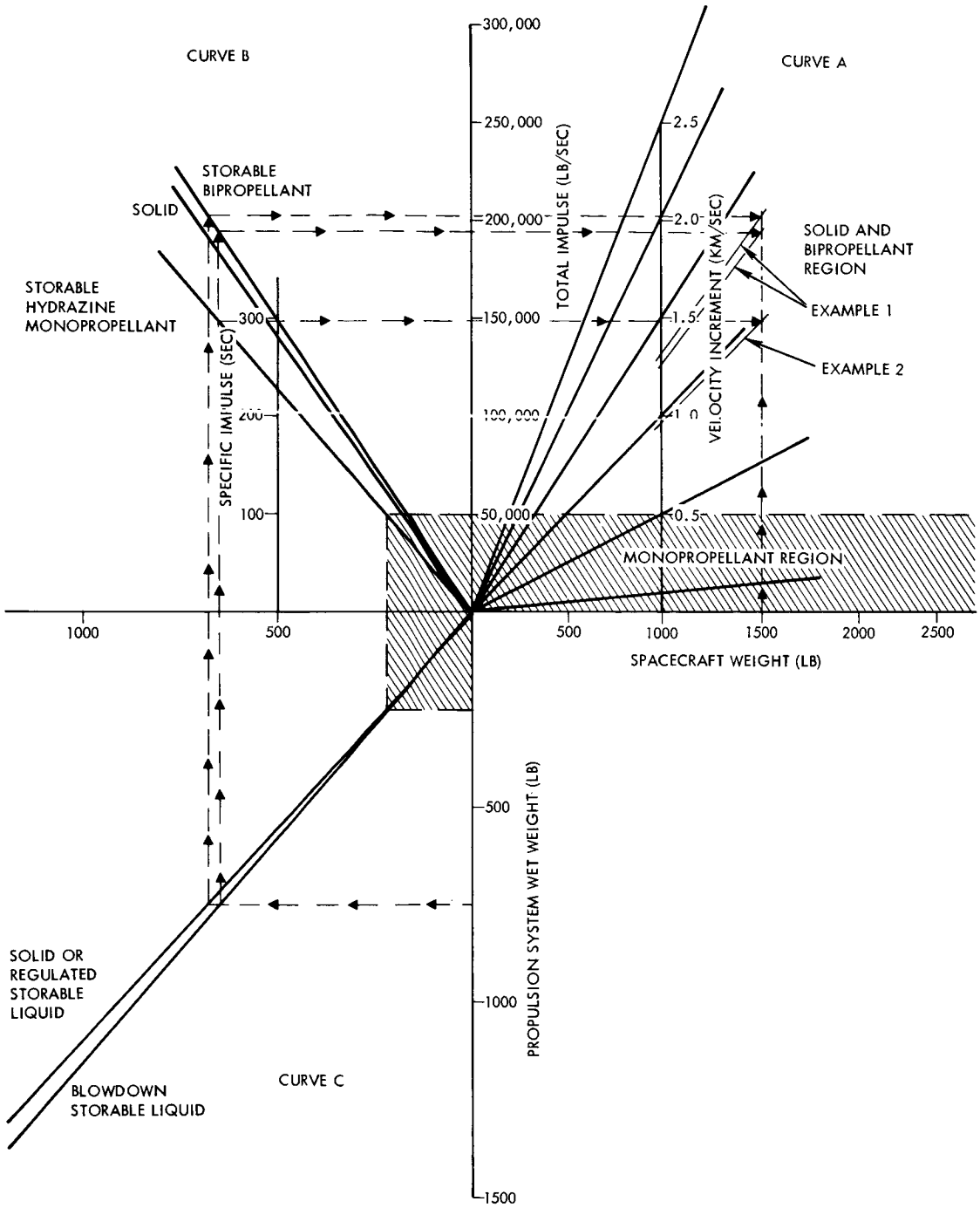

Figure 101. Propulsion System Weight Versus Spacecraft Gross Weight

Figure 101 indicates that all flyby spacecraft considered with a 0.1 km/sec velocity increment fall in the monopropellant region. On the other hand, orbiters which require from 1.3 to 2 km/sec velocity increment appear to fall in the solid or bipropellant region from an overall weight standpoint.

For a typical orbiter spacecraft, the propulsion system is one-half the weight of the total spacecraft. Figure 101 indicates the velocity increment attainable as shown in Example 1, where the intersection of a 1500-pound spacecraft and a 750-pound regulated bipropellant and blowdown propulsion system results in a 1.3 and 1.27 km/sec velocity increment. A 750-pound blowdown monopropellant system would provide only a 0.98 km/sec increment, as shown by Example 2. The orbiter mission to Jupiter, in this case, could be accomplished with a bipropellant system but not with the monopropellant configuration. A bipropellant system would clearly be indicated.

Curve C was generated using curves A and B to determine needed propellant quantities and Figures 102 through 108 to determine feed system and engine weights. The curve is based on liquid systems with one thruster with a 1000-second burn time. The system has a capability for two starts employing explosive valves to control propellant flow. The curve can be adjusted for any number of starts or for additional thrusters along with their additional manifolding by using Figures 105 and 106.

Centroidal moments of inertia (Table 21) were obtained for the more important points in the flight trajectory. The HEKS/spacecraft field joint is the reference station from which the longitudinal center-of-gravities are measured.

6.4 RELIABILITY AND COST

For orbiter missions, the reliability problem is not substantially greater than that for the flyby missions, although there are differences. The first difference, discussed earlier, is the requirement for a reliable deboost system after a 2-year flight time. Propellant storage and thrust vector control requirements must be designed not only for the lifetime

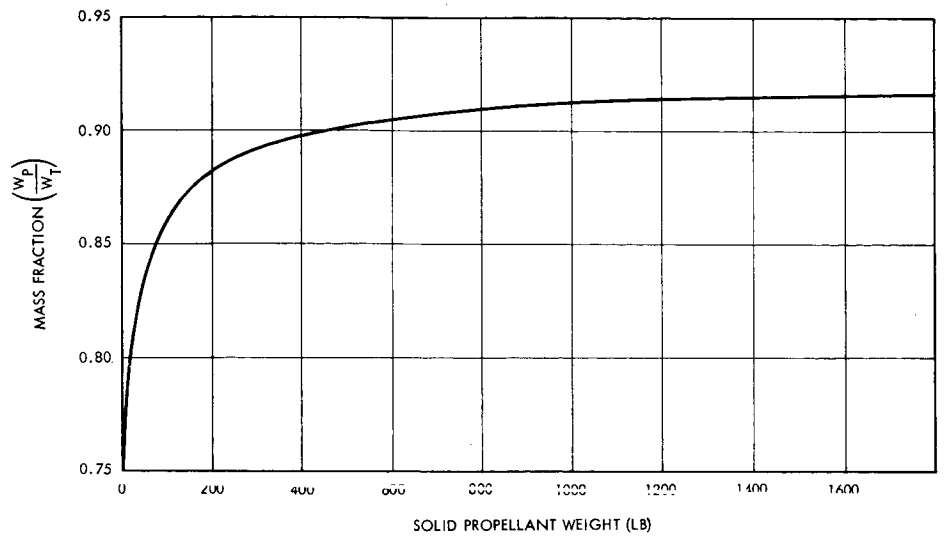

Figure 102. Solid Propulsion Mass Fraction

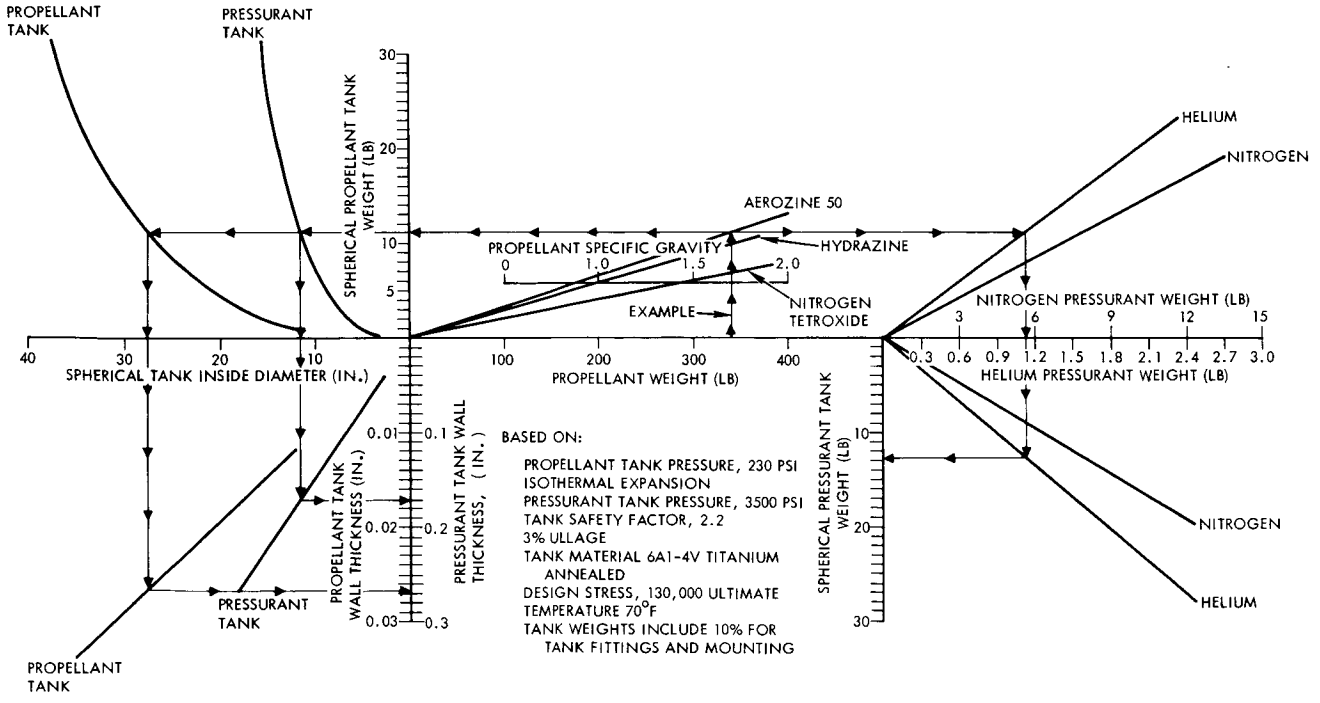

Figure 103. Propellant Tank Weight and Diameter; Pressurant Weight, Tank Diameter and Weight Versus Propellant Weight (0 to 500 Pounds) for Regulated System

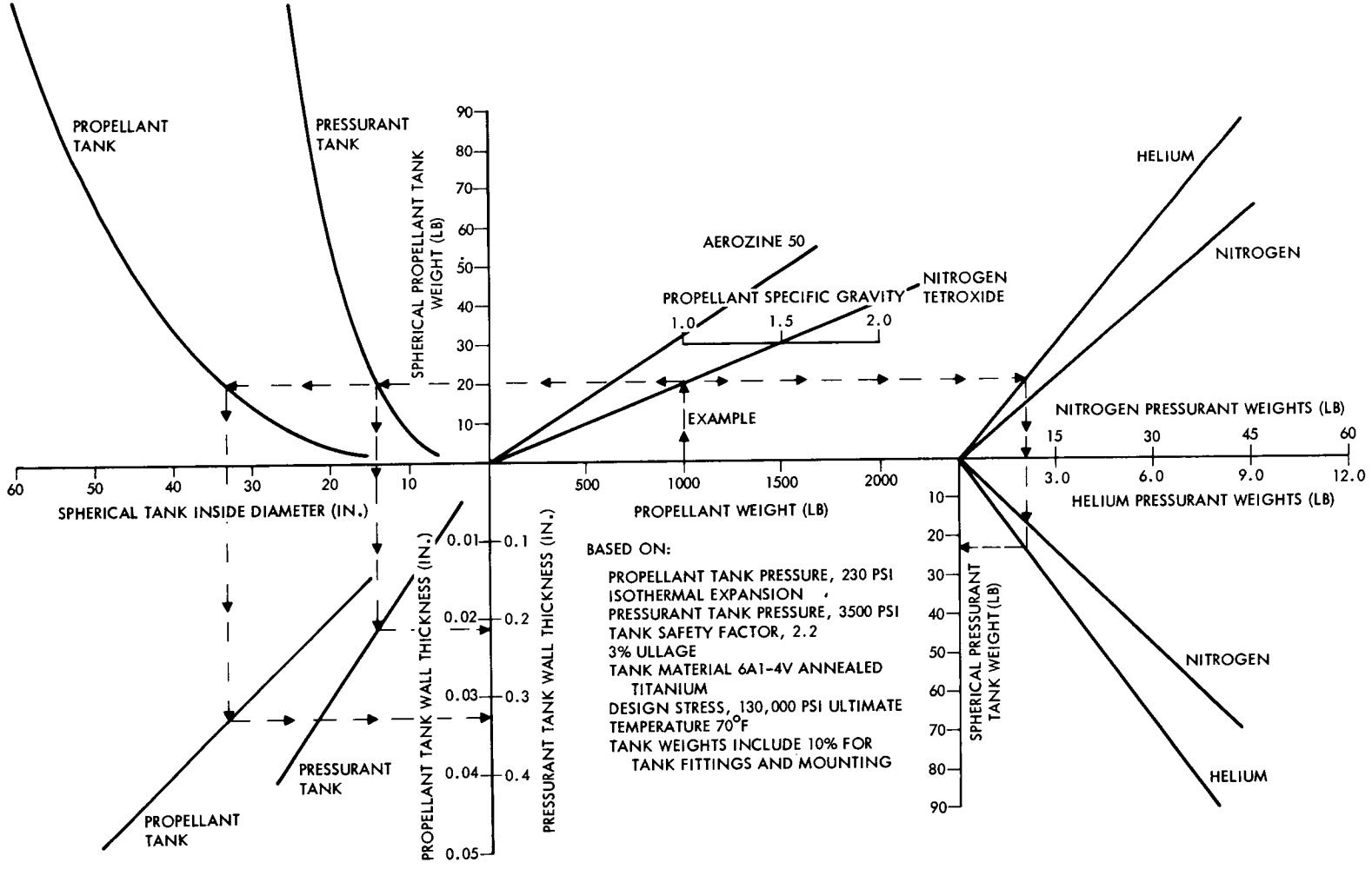

Figure 104. APP Propellant Tank Weight and Diameter; Pressurant Weight, Tank Diameter and Weight Versus Propellant Weight (0 to 2500 Pounds) for Regulated System

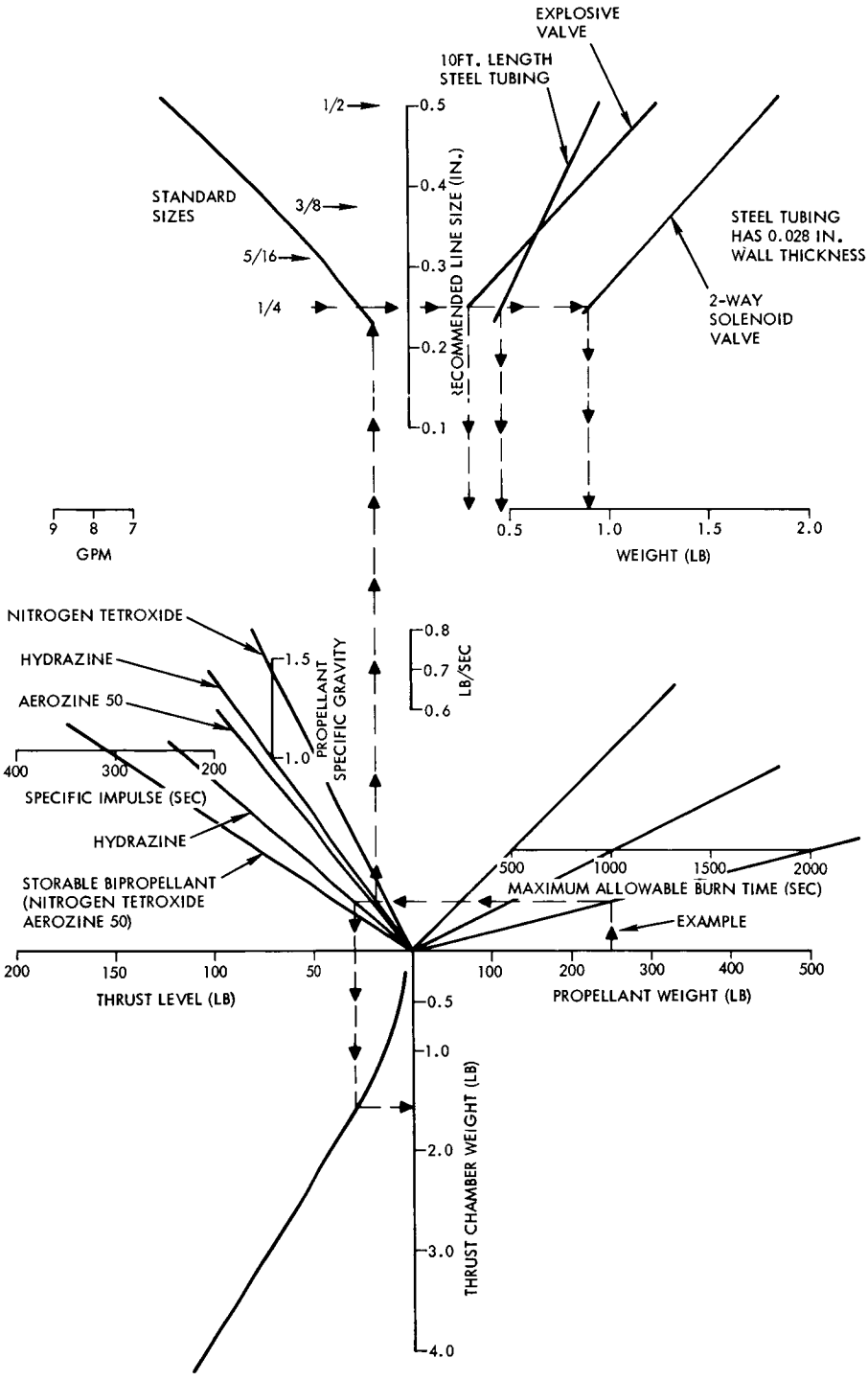

Figure 105. Engine Hardware and Propellant Manifolding Sizes and Weights Versus Propellant Weight (0 to 500 Pounds)

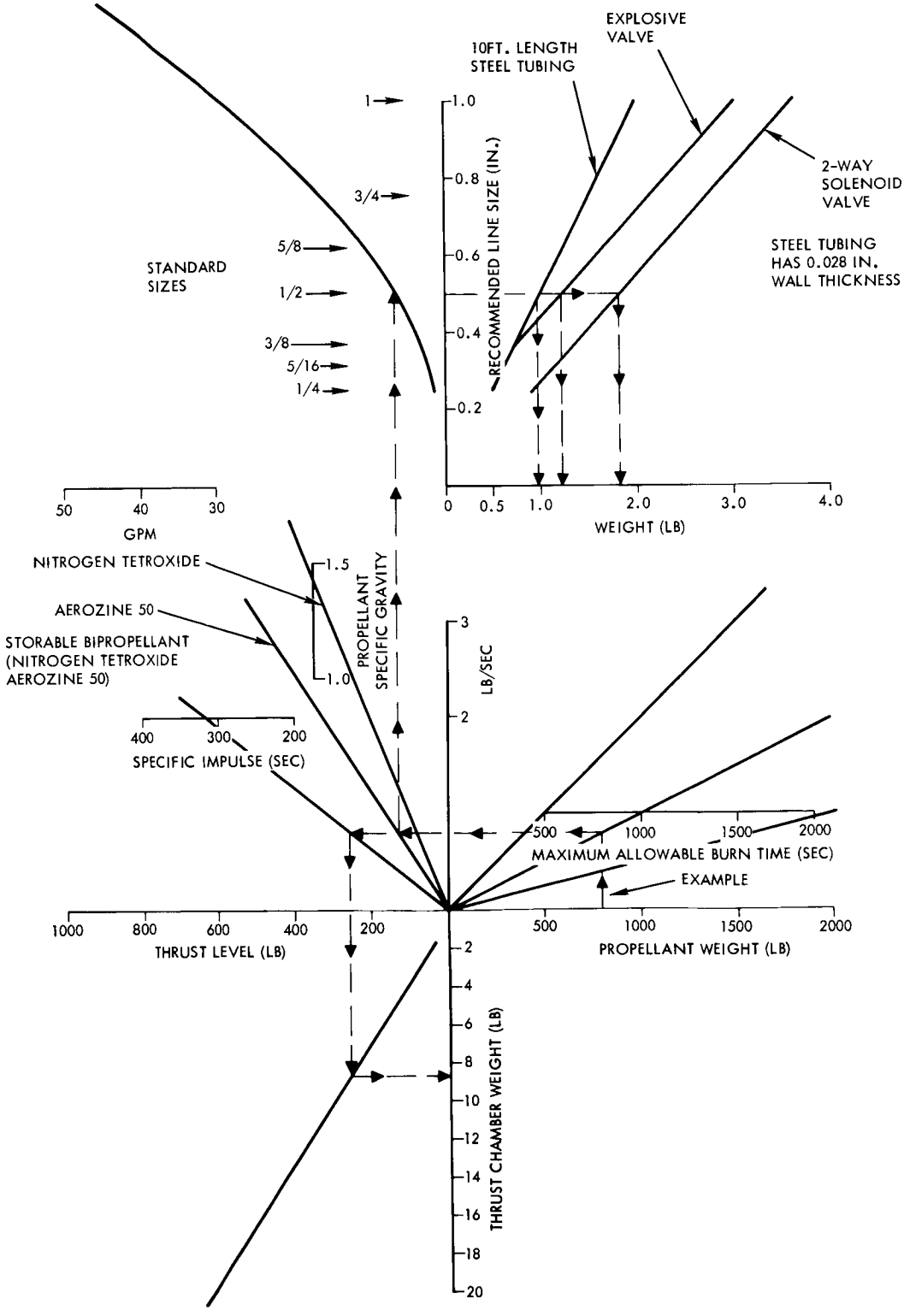

Figure 106. Engine Hardware and Propellant Manifolding Sizes and Weights Versus Propellant Weight (0 to 2000 Pounds)

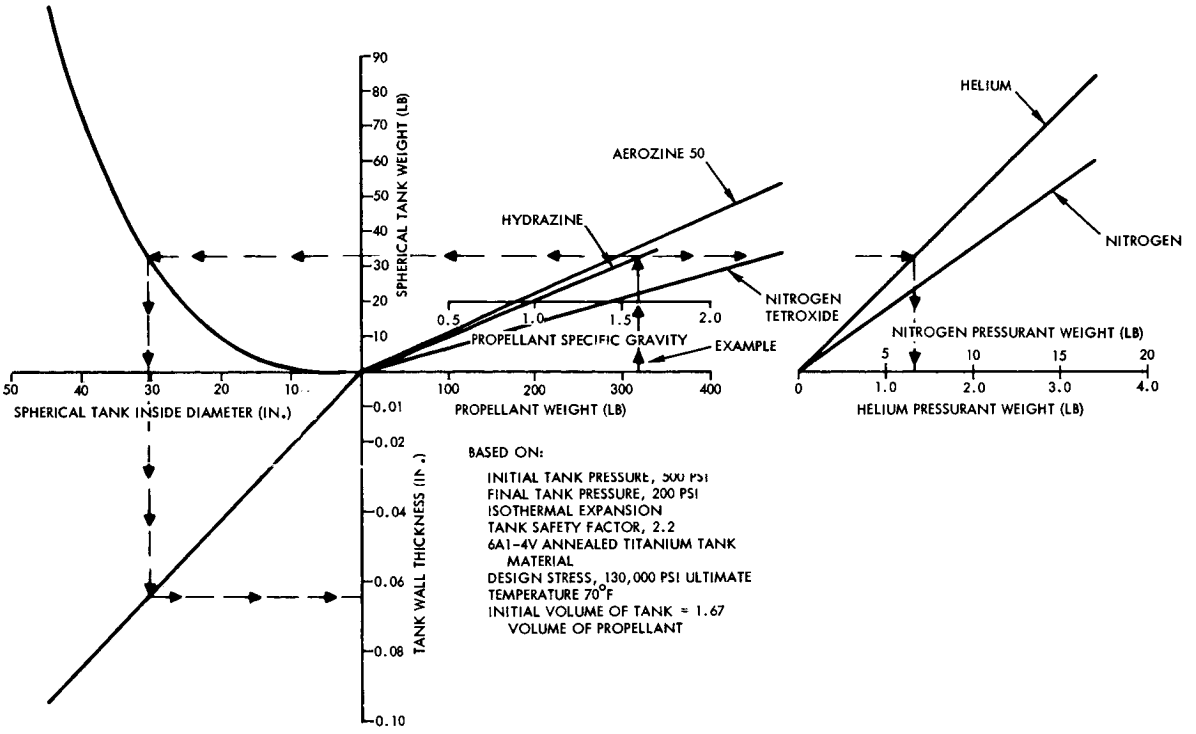

Figure 107. Tank Weight, Tank Diameter, Pressurant Weight Versus Propellant Weight (0 to 500 Pounds) for Blowdown System

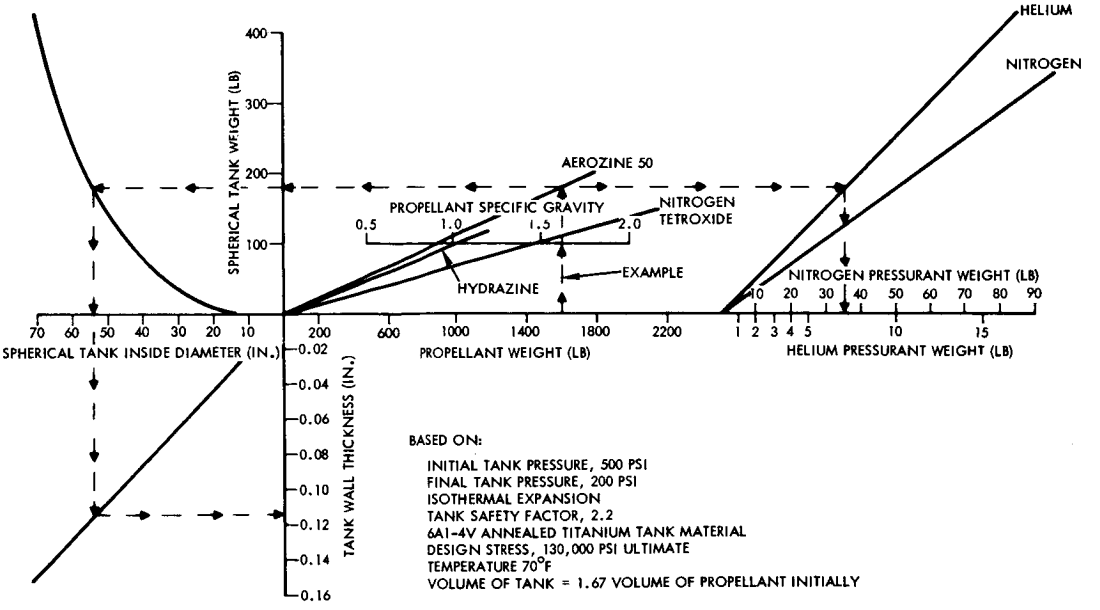

Figure 108. Tank Weight, Tank Diameter, Pressurant Weight Versus Propellant Weight (0 to 2500 Pounds) for Blowdown System

Table 21. Spacecraft Moments of Inertia and Center-of-Gravity

Condition	Weight (lb)	$\bar{Z}$ (in.)	Moments of Inertia (slug-ft^2)		
			I_x	I_y	I_z
Spacecraft prior to deployment of antenna	2518.1	65.5	1245.2	1275.5	740.2
Spacecraft after deployment of antenna	2518.1	64.1	1433.7	1463.9	1371.4
Spacecraft in cruise mode	2518.1	64.1	1450.7	1469.6	1394.1
Spacecraft in orbit	1525.1	71.7	1343.8	1355.8	1387.1

but for the specific environment. Consideration must be given to the micrometeoroid environment and long term thermal effects. In addition, the gyro assembly required as a reference for thrust vector control must also be carefully evaluated and redundant gyros are desirable.

The costs of the orbiter program discussed will be about three times greater than those for the 50-pound science payload 3-axis controlled spacecraft. The gross weight has increased from 500 to 2500 pounds, but eliminating propellants from consideration the comparison is 575 to 1400 pounds. The estimated cost of the total spacecraft development including two flight units is about $100 million, which includes $6.5 million for the development of the deboost propulsion system. The recurring cost of a spacecraft, however, are estimated to be about $13 million.

There is one major problem area, the unknowns concerning the radiation belts about Jupiter. If the belts present a great hazard to standard spacecraft components, then a program must be begun to develop radiation insensitivity components, or an orbit which does not pass through the belts must be selected. If the levels are very severe and an orbit of, say, 10 x 200 planetary radii were all that was feasible (for an assumed ΔV of 1.4 km/sec), then the orbit period of about four months might compromise the environmental mapping portion of the mission. It would also reduce the TV resolution. Of course, even

for orbits penetrating to 1.5 radii from the planet center, the percentage of time spent in the regions of possible intense radiation is small. For a 15-day orbital period, the spacecraft is within 10 radii only 20 hours per orbit, or 5.5 percent of the time, so that exposure time does not accumulate very rapidly.

7. CAPSULE ENTRY MISSIONS

This section presents preliminary mission concepts and discusses feasibility and problem areas involved in measuring atmospheric characteristics either with a probe which enters the atmosphere or with an orbiter with a very low periapsis. The discussion is confined to second generation spacecraft since this mission is clearly not a precursor mission.

The basic conclusions of the study are that the entry problems, including heating, structural loads, communication, and payload, are so great as to essentially eliminate a light-weight, aerodynamic-braking probe from consideration at this time. However, the possibility of using an orbiter with a very low periapsis, perhaps 0.01 Jupiter radii from the surface, is not only feasible but extremely attractive.

7.1 FUNCTIONAL REQUIREMENTS

The principal spacecraft requirements imposed by the atmospheric probe mission are derived from the science payload, the mission profile, and the operational constraints of the entry capsule. These requirements are discussed in terms of general characteristics of the entry mission without reference to a specific capsule design concept. In addition, the discussion includes requirements arising from the alternate mission concept of lowering the spacecraft periapsis altitude by small incremental impulses at apoapsis, thus permitting gradual orbit decay and observation of upper atmosphere phenomena without the use of a capsule probe.

7.1.1 Scientific Requirements

The scientific objectives of an atmospheric probe mission include:

- Probing the Jupiter atmosphere for composition, density distribution, etc.; typical experiments for such a mission include mass spectrometers, accelerometers, temperature sensors.

- Observing phenomena of the planetary environment at the boundary between the atmosphere and the magnetosphere; typical experiments may include a mass spectrometer to determine H/He ratio and the abundance of other molecules, and ion density measurements using a top side sounder or other techniques.

- Penetrating and probing the matnetosphere to a greater depth than is possible with a spacecraft having a periapsis fixed by injection altitude, i.e., at approximately 0.5 Jupiter radii (see Section 6).

7.1.2 Capsule Requirements

At the present stage of knowledge of the Jovian atmosphere, the design of an atmospheric probe and the definition of a simple, lightweight, practical scientific payload raises many unresolved problems. The most formidable is presented by the extreme entry velocities encountered, which are approximately equal to Jupiter's escape velocity, i.e., 60 km/sec. A capsule entering the atmosphere at this velocity would be subjected to heat and structural loads which would cause it to disintegrate before it emerged from communications blackout. By appropriate aerodynamic shaping of the entry body using a sharply pointed nose of approximately 10 degrees cone angle, the communications blackout problem can possibly be alleviated. However, with the low data rates available in the relay communication link, the time for transmission of acquired atmospheric data may not be adequate before the capsule disintegrates.

In designing the relay communication link the following difficult problem areas will have to be resolved. A large doppler shift will occur soon after entry, the magnitude of which is rather uncertain in view of the uncertain density distribution in the atmosphere. To avoid communication loss due to the doppler shift, the relay link receiver of the parent spacecraft must have a very large bandwidth. In the presence of uniformly high RF noise environment at Jupiter ranging from frequencies of 175 through 3000 MHz, the relay link receiver must operate with a low signal-to-noise ratio, which results from a) the wideband receiver channel, b) the low-gain omnidirectional transmitting antenna on the capsule, and c) the wide angle receiving antenna on the orbiter. To improve the SNR, it would be necessary to raise the capsule transmitter power. However, a low level, typically 25-watt transmitter is dictated by the small battery power available in a small entry capsule of the weight class considered here, ranging from 40 to 60 pounds.

On the basis of the present limited knowledge of the Jovian atmosphere, a practical payload complement for a small entry capsule in

this weight class is difficult to formulate. A mass spectrometer experiment would probably be ruled out for weight reasons. The state of development of shock layer spectroscopy does not make such an experiment very promising. The major difficulty is to distinguish between atmospheric constituents and ablation products of the entry body. Observation of wake phenomena from the entry capsule is also technically very difficult. A more feasible experiment would involve deceleration measurements, either by means of a rugged onboard instrument or by tracking the doppler shift from the parent spacecraft. The above experiments would presuppose an ability to circumvent communication blackout problem and a solution to the difficult technical problems posed by the communication link.

The major problem inherent in the extreme entry velocities is the insertion of the entry probe into the narrow corridor required to survive sufficiently long for performing the measurement and transmitting the data via relay link. Computations of the corridor have not been made to establish whether in fact there is a corridor of a finite dimension which would permit adequate survival time. But the extreme guidance accuracy imposed by the capsule mission rules out the ejection of the capsule from a point on the approach trajectory prior to planetary encounter because the miss parameter of the parent spacecraft is not sufficiently well known. The only feasible alternative for achieving a grazing entry is a capsule separation after insertion of the parent spacecraft into Jupiter orbit and after establishing orbit characteristics with sufficient accuracy by earth tracking.

However, the relative geometry between capsule and spacecraft is less favorable from the communication standpoint when the capsule is separated after orbit insertion than in the case of direct capsule descent from the planetary approach trajectory. With the capsule descending from orbit, much larger communication ranges and line-of-sight angle variations will be encountered. In view of the large eccentricity of the orbit of the parent spacecraft, it would appear desirable to perform the capsule separation and retro maneuver at the orbiter's apoapsis, in the interest of maximum propellant economy. However, this selection will result in large terminal communication ranges. For

example, for a spacecraft orbit dimension of 2 x 50 Jupiter radii the communication range at capsule entry would be on the order of 5×10^5 kilometers. Tradeoff between propellant weight requirements and relay link requirements shows that a more acceptable terminal communication range can be achieved if the separation point is placed closer to spacecraft periapsis.

Determination of altitudes at which the probe performs atmospheric measurements will be difficult since a clearly defined planetary surface is not available for reference and direct altitude measurement cannot be made. To resolve this problem it will probably be necessary first to determine the probe position relative to the parent spacecraft and subsequently to determine the position relative to the planet from the spacecraft ephemeris.

In view of the difficulties outlined above it appears that the only entry experiment which can be performed without enormous difficulties and with a reasonable probability of success is one in which the probe enters the sensible atmosphere of grazing angle and skips out after a relatively brief interval. A number of repeated grazing entries and skip-outs will occur before final entry and destruction. Relay communication may be lost during the entry period but can be re-established after skip-out. Guidance requirements would be less extreme than for a single entry probe since, instead of a narrow entry corridor, a greater regime of altitudes can be defined in which survival and skip-out is possible. Trajectories above the critical entry altitude and angle will experience various depths of entry. In this approach only a brief and shallow atmospheric entry is achieved and it remains questionable what types of experiments can be conducted to determine atmospheric constituents and densities.

7.1.3 Suborbiting Probe Requirements

A promising alternative to the entry capsule concept is to use a suborbiting probe which does not enter the planetary atmosphere during the period of its useful life. Such a probe can perform measurements of great scientific interest in the transition zone from the magnetosphere to the upper atmosphere. Relay communication problems are lessened

because the large doppler shift inherent in atmospheric entry will not be encountered. However, the orbit periods of the parent spacecraft and the capsule probe are slightly different and therefore a phasing problem will occur which introduces large variations of communication range and line-of-sight angles with periodic occultation by the planet. Times of favorable relative spacecraft positions can be determined by ground computation based on the known orbit characteristics of both vehicles. Thus, periods of capsule relay communication can be resumed on ground command.

In general, the probing of the magnetosphere at altitudes to which the parent spacecraft cannot descend will offer an important extension of the scientific objectives of the mission. Feasibility and design requirements for this experiment should be analyzed in greater depth. The sub-orbiter experiment can provide information on Jupiter's radiation belts without exposing the parent spacecraft and its more sensitive payload instruments to the high radiation environment.

7.1.4 Alternate Low Periapsis Mission

A different concept which would permit probing at low altitudes without using an ejected capsule involves the use of orbit change maneuvers by the orbiter at or near the apoapsis. This concept can be further developed if precursor measurements indicate that the trapped radiation environment is acceptable.

With the large eccentricities envisioned for the spacecraft orbit the ΔV required for changing the periapsis altitude will not be excessive for orbit parameters selected with this objective in mind. For an apoapsis altitude of 50 Jupiter radii the amount of ΔV required to change the periapsis altitude from 0.5 Jupiter radii to 0.3 radii will be 120 m/sec. If the apoapsis altitude is 100 radii this maneuver would require 60 m/sec. A propellant weight of approximately 2 percent of the orbiter's gross weight would be required for the latter maneuver.

Although the extended mission profile serves to enhance the range of measurements that can be performed by closer approach to the planet, the added complexity of the extra maneuver must be considered in addition to the weight penalty of carrying extra fuel. In order to achieve

orbit trim as discussed, a reorientation of the spacecraft is required except in the favorable case where an impulse applied in cruise attitude is satisfactory to achieve the desired maneuver. Such a maneuver is compatible with orbits that have their apsidal axes perpendicular to the earth line as discussed earlier (Section 6).

7.2 SPACECRAFT DESIGN IMPLICATIONS

Because of the difficulties inherent in the capsule mission a specific design concept for a low or high W/C_DA probe has not been developed. While spacecraft design interfaces remain undefined, it is clear that the basic spacecraft concept is quite compatible with the entry probe mission. The spacecraft can satisfy the guidance and control requirements for this mission and provide the necessary communication link to earth. However, in the process of formulating a specific capsule descent mode it is important to consider its implications on the spacecraft design and on functional interfaces.

Selection of a favorable capsule descent trajectory can greatly simplify the design requirements of the spacecraft relay link, e.g., by permitting the use of a fixed relay antenna array. The guidance requirements are also determined by the capsule trajectory. For a capsule descent mission to be performed during planetary flyby, the guidance requirements would probably impose excessive demands on spacecraft trajectory accuracy and on the accuracy and timing of the separation maneuver, while capsule descent from an orbiter does not impose such stringent requirements. In the latter case the capsule ejection maneuver can be made compatible with the earth-pointing cruise attitude of the spacecraft by appropriate timing relative to periapsis passage.

Because of the small capsule weight the choice of the stowage position and relative orientation of the capsule ejection angle remains quite flexible. For example, as an alternative to ejecting the capsule axially which would interfere with the axial location of the spacecraft's orbit injection engine, a lateral ejection angle would be preferable. This direction is compatible with a desired capsule retromaneuver tangential to the spacecraft orbital velocity if the separation time is chosen in a region of central angles 90 to 120 degrees before periapsis passage.

This choice of separation time is desirable in the interest of simplifying the relay communication requirements.

The alternate mission objective discussed in Section 7.1.4 which does not involve an entry capsule on board the spacecraft imposes no design constraints other than the addition of orbit trim maneuver propellant. A number of firings of the retro engine at separate apoapsis passages would be required to approach the intended low periapsis altitude gradually, and to permit adequate time for orbit determination by earth tracking. From the observation of orbit decay and from the known ΔV increments imparted at periapsis the drag acting on the spacecraft in the upper atmosphere can be deduced. The required propellant weight should be properly considered as weight carried for science experiments since the approach to low periapsis and the (limited) atmospheric measurements attainable would be mission objectives in this case. Clearly, this final mission objective should only be attempted after all other objectives of the orbit missions have been achieved and the spacecraft is approaching the end of its operational usefulness.

8. COST EFFECTIVENESS

This section discusses the cost effectiveness of all missions, spacecraft, and booster configurations. It is based upon the analyses given in Volume 2, Section 12, and Section 2.10 in this volume. Hence only the implications upon cost effectiveness of the other configurations are discussed in detail here.

There are four major elements for judging the cost effectiveness of scientific space missions: 1) science considerations, 2) cost, 3) reliability, and 4) mission growth potential. Science considerations involve the effectiveness of the spacecraft system in attaining the scientific mission objectives measured by the quality and quantity of science data returned to earth. Costs accrue primarily from four sources: 1) experiments, 2) boosters, 3) spacecraft, and 4) ground station time and data reduction. Reliability is affected by the spacecraft system design, environmental characteristics in space, and flight time and thus by the booster. Mission growth potential involves the combination of all these criteria and includes, in particular, a measure of the compatibility of launch vehicles, spacecraft design concepts, and science payloads of the early missions with those of subsequent missions. Mission growth extends the mission objectives either to more distant planets or to more complex mission profiles in advancing from flyby to orbiter and capsule entry missions.

In addition to these criteria the planetary exploration program must be considered from an overall schedule planning standpoint. Flexibility of system concepts and adaptability to changes resulting from the discovery of unexpected and perhaps critical environmental phenomena in space will be important factors in mission planning, program evolution, and hence in the achievement of desired cost-effectiveness goals.

8.1 SCIENCE CONSIDERATIONS

The acquisition of scientific data in interplanetary space and during planetary encounter is the primary mission objective. Along with these data certain engineering data will be acquired and transmitted to earth;

both types of data are needed in the definition of follow-on mission requirements and system design criteria. Great cost savings will be realized if the scientific knowledge gained by the earlier missions is integrated effectively into the subsequent missions. The system design concept must provide the required adaptability.

As discussed in Section 12 of Volume 2, four basic payloads for a Jupiter mission have been developed, 12, 50, 100, and 250 pounds. Although these payloads are oriented toward Jupiter missions, they are also generally suitable for missions to Saturn, Uranus, and Neptune.

The spacecraft designed to incorporate these payloads have different design characteristics. A primary difference is in data transmission rate. At 6 AU the 12-pound payload can transmit 35 bits/sec, the 50-pound payload 700 bits/sec, the 100-pound payload 1400 bits/sec, and the 250-pound 2800 bits/sec. The interplanetary science data rate requirement of about 110 bits/sec is met by all spacecraft except the smallest. At encounter the data rate requirements increase substantially, especially as the payload weight increases. The estimated total amount of data gathered at a Jupiter flyby are 5×10^8 bits for the 50-pound payload; 10^{10} for 100 pound; 2×10^{11} for 250 pound. By far the largest portion of this information is television data which, in the case of the Jupiter mission, can be transmitted back in "real time" using data stored on the television tube itself.

For missions to the outer planets the required tube storage time would exceed two hours, and hence tape storage would be required. Since the missions to the distant planets take up to eight or nine years, the reliability of a tape recorder will be a critical factor. Moreover, extensive tape storage is not desirable since, if a tape storage of 1.2×10^8 bits as proposed in Volume 2 were used for a Neptune mission, it would take about 50 days of continuous operation to transmit that data back from the 50-pound science payload and more than 12 days with the 250-pound science payload, considering the reduced data rate of 28 and 115 bits/sec, respectively. Continuous transmission for such time intervals might be an unacceptable burden on the ground stations. To reconcile the scientific payload characteristics and the spacecraft system

characteristics, a relatively low data sampling rate should be a requirement for missions to the distant planets. The information contained in one or a few television frames of Uranus or Neptune may have great scientific value. The value of additional information to be gained from a larger number of frames is expected to decrease markedly, i.e., out of proportion with the cost and complexity it would impose on the system.

In the comparison of spin-stabilized spacecraft with 3-axis stabilized spacecraft (Volume 2, Section 12), the principal merit of the 3-axis system is increased television resolution which, although desirable, may not be justifiable for missions to the distant planets. A system which pays a large penalty in cost and reliability for high TV resolution on such a mission should be avoided. One conclusion that might be drawn from this reasoning is that for very long missions only experiments with modest data rate requirements but maximum scientific value should be carried. This category would include all of the interplanetary experiments and such basic planetary observations as simple television, radiometers, trapped radiation counters, and radio occultation experiments, all of which are compatible with the simple spinner design concept; 3-axis control would have no advantage. The reliability of scientific experiments themselves should be considered in this context. Where extremely long flight times are involved, those experiments which function only at encounter are intrinsically at a disadvantage regardless of their scientific merit since the equipment must survive many years of transit before being placed in operation.

Another way of regarding this problem is in terms of our present knowledge of the phenomena to be observed. Most of the experiments to be performed in interplanetary space can be calibrated to reasonably well predicted measurement levels. Phenomena of the planetary environment are much less well known. Hence selection of instrument sensitivity is more problematic. More primitive instruments capable of establishing intensity limits may therefore be adequate. The value of obtaining a large number of television pictures even of Jupiter is not firmly established on the basis of our present knowledge of distinct

features in the upper atmosphere, but such a series may provide meteorological data and data on the dynamics of atmospheric change which are needed to understand related phenomena.

8.2 COST

The major elements of cost in system development and mission performance are payload, boosters, spacecraft, ground station operation, and data reduction. The cost of experiments has previously been estimated to be about $1 million per experiment on the 50-pound payload spacecraft. Although this estimate is somewhat arbitrary, it is clear that with larger, more sophisticated payloads, the cost of the more sophisticated experiments will be higher. We assumed here that the additional experiments will cost on the order of $2 million apiece. The 50-pound complement includes 10 experiments; three more are included in the 100-pound payload, and four more on the 250-pound payload. The cost of experiments is thus estimated as about $10 million, $16 million, and $24 million, respectively.

The cost of the boosters and spacecraft previously discussed in Volume 2 are

Cost of Boosters:	$ Millions
Atlas/Centaur/TE-364-3	9.5
Atlas/Centaur/HEKS	14.5
Titan IIIC/Centaur	19.9
Titan IIIC/Centaur/TE-364-3	20.4
Saturn IB/Centaur/HEKS	43.0
Saturn V	125.0
Saturn V/Centaur	130.0
Estimated Recurring Cost of Spacecraft	
50-lb payload, spin-stabilized	4.5
50-lb payload, 3-axis stabilized	5.0
100-lb payload, 3-axis stabilized	6.5
250-lb payload, 3-axis stabilized	8.5

The cost of the spacecraft accounts for ground station time and data reduction. As previously discussed $10,000 per day has been assumed for missions to Jupiter. For longer missions such as those to Neptune the cost of ground operations must be estimated on a different basis since ground stations are not being used continually and incoming data rates are relatively low over much of the mission. Nevertheless, a total of $10 to $30 million can accrue depending on the operational burden, data evaluation procedures adopted, and the like. It is clear that the costs for the processing and evaluation of the science data must be considered from a different standpoint. Obviously, an increase in the amount of valuable, nonredundant data received increases the cost-effectiveness of the mission. The effectiveness decreases as the data transmission demands more extensive ground support, particularly if the data is redundant.

8.3 RELIABILITY

Reliability and probability of mission success are the most critical factors in determining cost effectiveness. The goal of achieving high reliability must be the primary concern in every phase of system design and development, but with greatest emphasis placed on the initial design concept and its inherent reliability characteristics. Reliability of the spin-stabilized, 500-pound spacecraft was analyzed in Section 9, Volume 2; the reliability of other configurations is discussed in this volume. For the 750-day Jupiter missions the reliability of most of these system configurations was determined to be in the neighborhood of 0.7 or higher; none have reliabilities of less than 0.5.

Missions to the distant planets requiring up to nine years in transit introduce reliability problems of a new order of magnitude compared to any previous space probe missions. The need for launching several probes in order to achieve at least one successful mission leads to a direct multiplication of the recurrent cost elements.

Two approaches for achieving high reliability are either the choice of a minimum-complexity configuration at comparatively lower cost and, possibly, with a sacrifice in payload composition and performance, or the use of maximum sophistication and redundancy in a more complex

and costly system implementation. As the numerical examples given in Section 12 of Volume 2 have shown, the latter approach leads to a less cost-effective system for two reasons: the total cost of each launch is high, considering primarily the recurrent spacecraft system and launch vehicle cost; the total (nonrecurrent) development cost will be so much higher than in the simplified approach that the share of this cost per mission would remain large unless many launches are made. But the intent of the more complex design approach was the reduction of required launches. These generalized considerations would have to be applied to each specific design concept to determine the desired cost versus reliability compromise.

A unique problem in missions requiring many years is the possible occurrence of failure just prior to encounter. The mission may be rated at least as a partial success, depending on the value and quantity of interplanetary data acquired and transmitted to earth. However, to achieve a higher probability of obtaining planetary data, a sequence of missions must be launched without first waiting for the success of the initial ones. An advantage in cost effectiveness can be realized in the case of successful completion of several of these missions by the following strategy:

- Design complementary payload packages for the different spacecraft in order to obtain nonredundant data of equal priority from each successful mission
- Use different trajectories, different launch opportunities, different arrival times to obtain coverage of wider interplanetary regions and phased coverage to interplanetary and planetary phenomena
- Use alternate midcourse maneuver sequences and operational modes wherever possible. This approach minimizes the probability of occurrence of similar critical failure modes in the different spacecraft and permits acquisition of additional engineering data on system performance which may be used advantageously in later missions.

8.4 MISSION GROWTH POTENTIAL

The discussion of cost effectiveness must take into consideration the growth potential of selected booster-spacecraft combinations in the framework of the overall planetary exploration program. In this section

a number of favorable atlernatives will be selected on the basis of launch vehicle performance and minimum requirements for flyby and orbiter missions to Jupiter and the outer planets, with the different objectives of percursor and follow-on missions in mind.

8.4.1 Launch Vehicle Performance

Figure 109 shows payload weight capabilities of boosters of the Atlas SLV3X/Centaur class, the Titan 3CX/Centaur class, Saturn IB/Centaur/HEKS, and Saturn V with and without augmentation by a Centaur stage. Using the injection energy C_3 as abscissa, the diagram shows spacecraft weights launched by these boosters (left scale) and typical flight times for direct flights to Jupiter and the outer planets and for flights via Jupiter swingby (right scale). Actually, the mission requirements represented by the curves of flight times versus injection energy vary between launch opportunities. The curves shown in Figure 109 are excerpts from a more detailed chart presented in Section 4.2. As an example we consider a flight to Saturn via Jupiter swingby with injection energy $C_3 = 101\ km^2/sec^2$ illustrated in Figure 109 by a dashed line. This is the lowest value of C_3 for the 1979 launch opportunity and yields a flight time of 4.3 years. The Atlas SLV3X/Centaur/HEKS can inject an 800-pound spacecraft on this trajectory, while the same launch vehicle without the HEKS but augmented by TE-364 can handle only 500 pounds. The Titan 3CX/Centaur would be capable of injecting 1300 pounds on this mission.

For convenience the spacecraft weights versus flight times obtained from Figure 109 are replotted in Figures 110 and 111 to present the performance of the Atlas SLV3X/Centaur/TE-364 and Atlas SLV3X/Centaur/HEKS, the Titan 3CX/Centaur/TE-364, and the Saturn IB/Centaur/HEKS boosters. Figure 110 shows direct flights. Figure 111 shows swingby missions via Jupiter. In these diagrams four curves of injected payload (spacecraft) weight are shown for each planet corresponding to the payload capabilities of each launch vehicle.

The launch vehicle performance curves shown in these figures can be used directly to assess science payload weight capabilities by assigning estimates of spacecraft gross weight to payload weights of

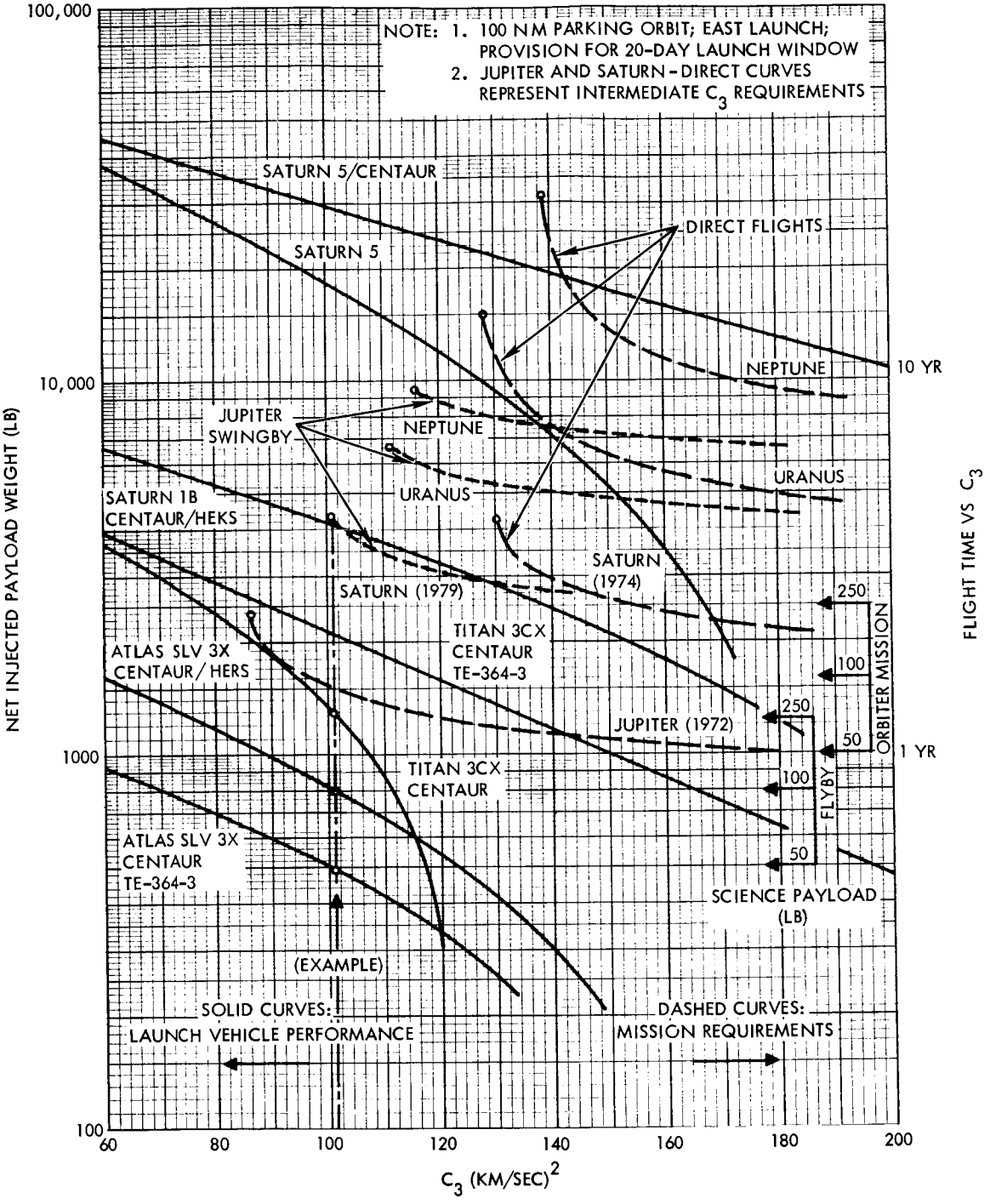

Figure 109. Launch Vehicle Performance and Mission Requirements

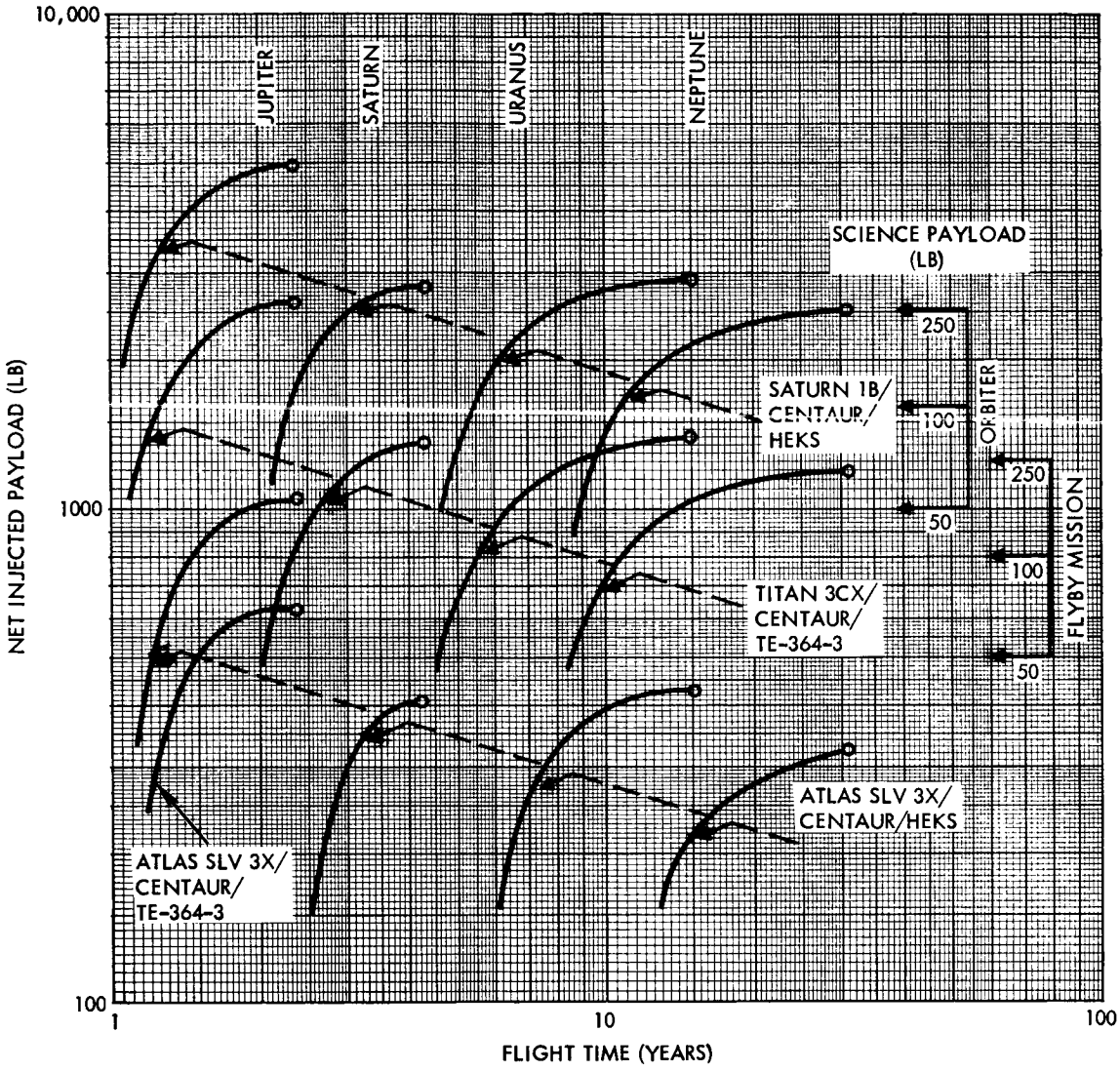

Figure 110. Spacecraft and Science Payload Weight Capability of Four Launch Vehicles (Direct Missions)

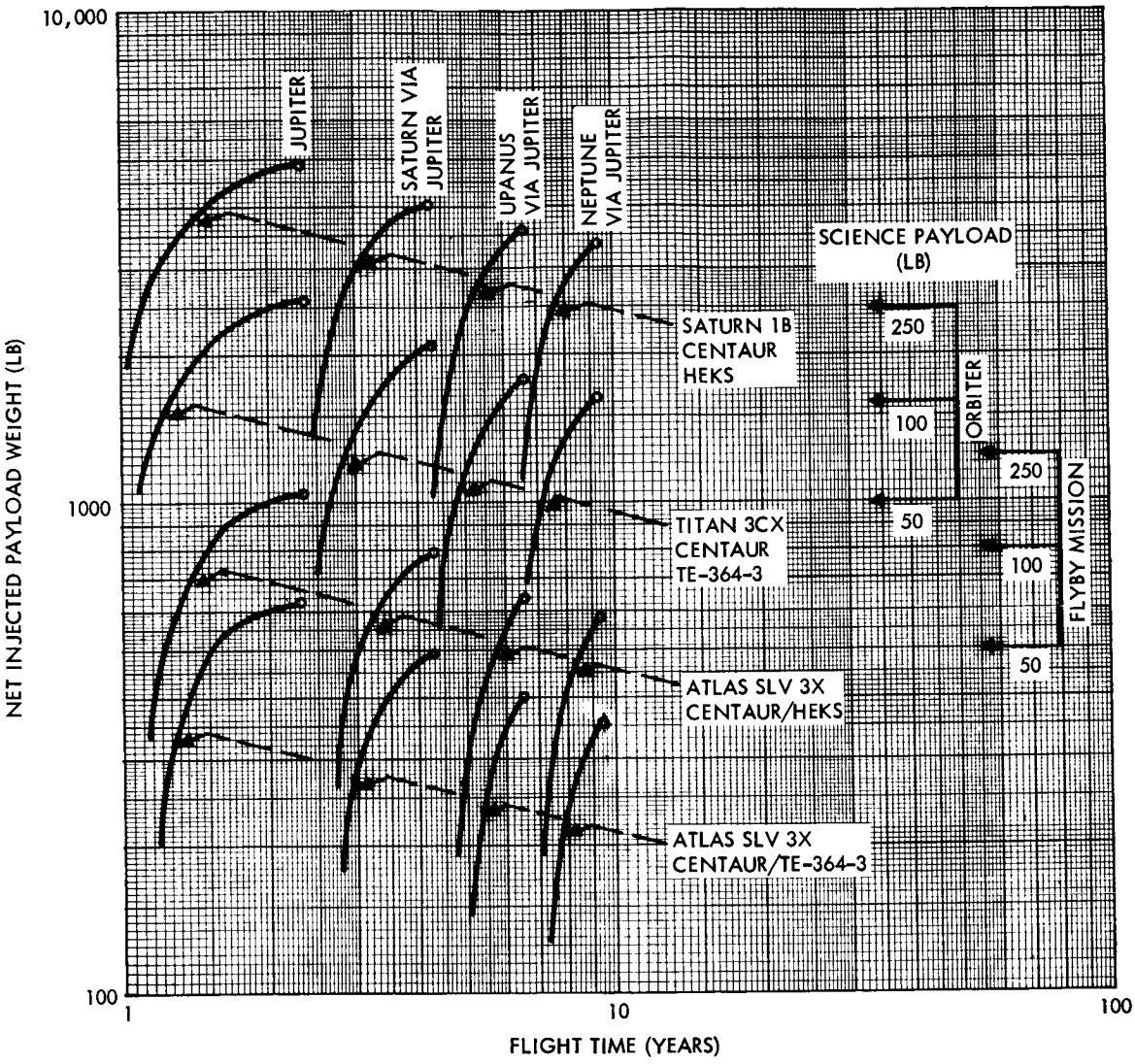

Figure 111. Spacecraft and Science Payload Weight Capability of Four Launch Vehicles (Jupiter Swingby)

50, 100, and 250 pounds. These estimates are indicated in the charts by groups of arrows for flyby and for orbiter missions. The estimated spacecraft gross weights and payload weights, in pounds, are tabulated below:

Payload Weight	Spacecraft Weight	
	Flyby	Orbiter
50	500	1000
100	800	1600
250	1250	2500

In Figure 110 it is shown that the Atlas SLV3X/Centaur/TE-364 can achieve a Jupiter flyby for a 50-pound payload but no direct missions to the outer planets. The same launch vehicle can also achieve a 50-pound Saturn flyby via Jupiter, as seen in Figure 111, but with no weight margin. The higher performance Atlas SLV3X/Centaur/HEKS can achieve Jupiter flyby of a 100-pound payload spacecraft with weight to spare and flyby missions to all outer planets* for 50-pound payload spacecraft aided by Jupiter swingby.

For the higher performance Titan 3X/Centaur/TE-364-3 we observe in Figures 110 and 111 that flyby missions for payload weights of 250 pounds and orbiter missions for 100-pound payloads can be achieved to all planets if Jupiter swingby is employed. Direct flyby missions of 250-pound payload can be made to the outer planets including Neptune. However, the missions to Uranus and Neptune having little or no margin in the direct flight mode would required excessive flight times and should be performed via Jupiter swingby. Orbiter missions can be achieved to all planets for 50- and 100-pound payloads.

The Saturn IB/Centaur/HEKS has sufficient performance for orbiter missions with 250-pound payload to all planets, but Uranus and Neptune could best be reached via Jupiter swingby to avoid excessive flight times, Figure 111 shows that a large weight margin is available in all these orbiter missions if the Jupiter swingby technique is employed.

*Missions to Pluto are not included in this discussion

The performance curves do not show the feasibility limitations of orbit injections at the destination planet, which must acutally be considered for all orbiter missions of interest. The above gross spacecraft weight estimates allow for an injection velocity increment $\Delta V = 1.4$ km/sec, which permits orbit injection only for relatively low arrival velocities, i.e., for relatively long flight times to the destination planet (see Section 6). A more detailed analysis of the spectrum of achievable orbiter missions and flight times for each launch vehicle is therefore required.

8.4.2 Mission Classes

From the foregoing discussion we arrive at possible groupings of missions which can be achieved by individual launch vehicles or by launch vehicles which can be augmented by higher performance upper stages during the evolution of the planetary exploration program.

One useful approach is to subdivide the missions into low payload percursor missions and high payload orbiter missions. As previously discussed, a precursor mission carrying 50 pounds of payload on a planetary flyby offers a good compromise between planetary and interplanetary science measurements. For precursor missions no increase in interplanetary measurements seems necessary. An increase of planetary measurements would be sensible only if the spacecraft could make effective use of this payload by an extended mission time in the vicinity of the planet, i.e., only if the mission were an orbiter mission. This leads to the conclusion that the smallest payload which adequately serves the purpose of interplanetary and planetary measurements should be selected for first generation flights. Such a payload would be of the order of 50 pounds. This payload is compatible with the spin-stabilized concept which yields the lowest spacecraft weight and the simplest design implementation. The mission can be performed by the low-cost Atlas/Centaur class boosters.

On the other end of the scale are spacecraft designs which have a much larger payload, emphasizing planetary observation and requiring 3-axis stabilization for most effective uses of sophisticated planet-oriented observation instruments. Such spacecraft must possess a large data storage capability, automatic command and sequencing, multiple back-up modes, and redundancy. These objectives establish a trend

toward the 100- to 250-pound payload class to be used in orbiter missions which requires high performance launch vehicles such as Sturn IB/Centaur/HEKS.

On the basis of these arguments a two-pronged plan for the evolution of the planetary exploration program can be formulated. This plan would use the least expensive boosters for early planetary flyby missions, carrying the 500-pound spinner with payloads of the order of 50 pounds. The Atlas SLV3X/Centaur/TE-364 can be used for the earliest Jupiter flyby mission and for Saturn flyby via Jupiter. An upgraded Atlas/Centaur augmented by a HEKS upper stage can achieve flyby missions to the more distant planets. The high payload capability of Saturn IB/Centaur/HEKS will be employed only as the program enters the second stage, at which time the engineering and scientific data from the precursor missions have been sufficiently evaluated to justify the development of highly sophisticated, heavy 3-axis stabilized orbiters with up to 250 pounds of payload.

A second approach can be formulated which recognizes the performance growth potential of a single family of launch vehicles such as Titan 3CX/Centaur. This has the attraction of basing the planetary program on the concept of a more gradual evolution of mission performance requirements starting with a much higher margin of initial payload capabilities. Using the unaugmented Titan 3CX/Centaur for the initial series of flyby missions, the program can accomplish Jupiter flyby missions of spacecraft weighing in excess of 1000 pounds or with greatly reduced flight times, e.g., 500 days for spacecraft weights of 500 pounds. As the Titan 3CX/Centaur performance is augmented by addition of the TE-364, 250-pound flyby missions of all outer planets by the Jupiter swingby route can be accomplished as well as orbiter missions with up to 100 pounds of payload.

Comparing the two approaches to the planning of the planetary exploration program the first alternative has the attraction of not employing more booster capability initially than would be justified by a reasonable planetary flyby payload in a precursor mission. This approach offers greater cost effectiveness, at least in the initial stages. The second approach tailored to a different program evolution concept and final payload requirements may be justified by cost effectiveness in the later portion of the program. Much will depend on the return of science data from the earliest planetary probes.

8.4.3 Program Flexibility

The two program approaches formulated in the preceding section reflect differently on the schedule of the overall planetary exploration program, especially from the standpoint of schedule flexibility and schedule inplications of critically important information received from successful precursor missions. A case in point would be the detection by the first flyby mission of an extreme radiation environment around Jupiter. As a result of such a finding subsequent orbiter missions require a spacecraft design in which sensitive components and payload elements are adequately protected to survive extended and repeated exposure to the radiation belts. Otherwise, the orbiter mission may require a high periapsis altitude in excess of the maximum altitude of the radiation belts. The second alternative would impose severe weight penalties in terms of the higher velocity increment required for orbit injection at Jupiter. In either case, the orbiter design and its payload weight capabilities must undergo a substantial revision with attendant increase in the development cycle, if the radiation data are greatly in excess of anticipated upper bounds.

This example illustrates that a gradual evolution of spacecraft design from a minimum payload flyby configuration to a more sophisticated orbiter configuration runs the risk of severe schedule setbacks depending upon scientific and engineering data received from the earliest flyby mission.

The two-stage development program which anticipates a major step forward in design sophistication and payload performance in the transition from flyby to orbiter missions can more readily absorb critical environment discoveries. In the first place, the step to orbiter configurations must be delayed in this program plan to make best use of data returned from the early precursor missions. Secondly, the anticipated greater weight margin provided by the higher performance launch vehicle (Saturn IB/Centaur) postulated for implementation of the second generation missions would provide greater flexibility and immunity to weight penalties.

Schedule differences between the two program approaches are illustrated in Figure 112. This diagram shows a succession of launch

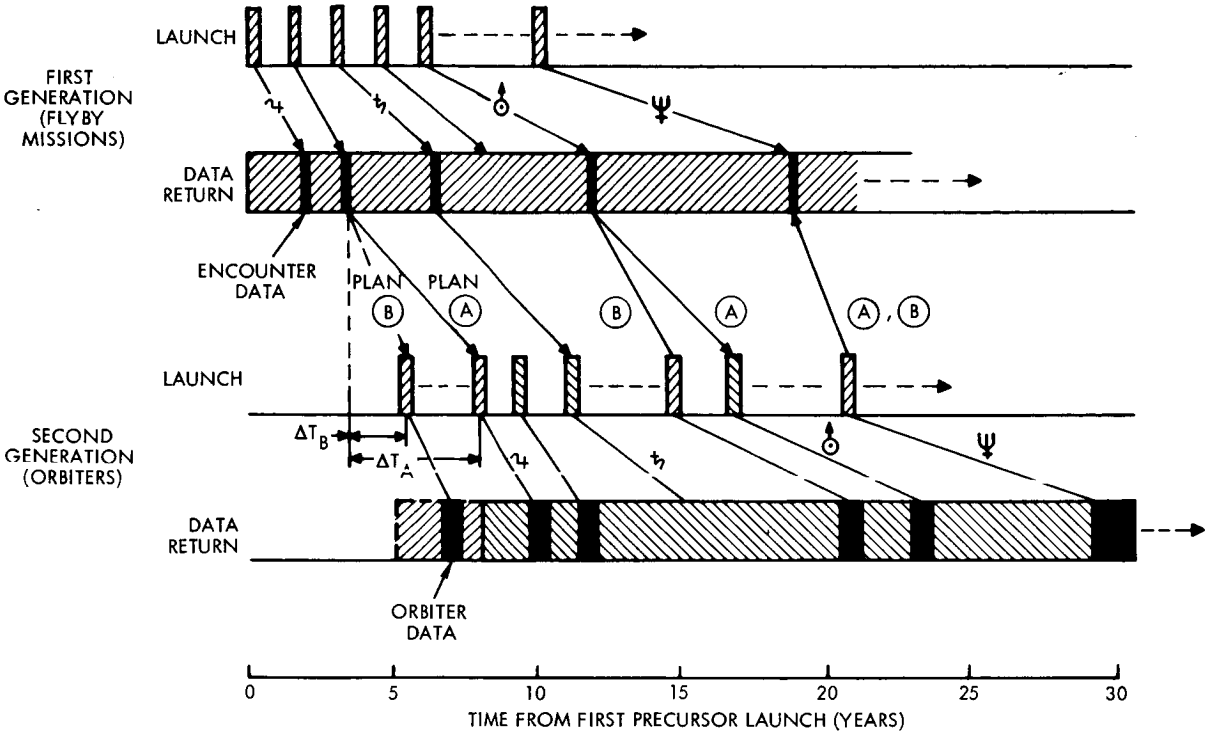

Figure 112. Typical Mission Evolution Programs

events at the various launch opportunities beginning with the first Jupiter flyby mission of a precursor probe. Assuming successful mission performance in each case a sequence of data acquisition periods will develop as shown in the chart in relation to the sequence of launch events. Interplanetary data return will start immediately with the first Jupiter mission. After approximately two years the first data on planetary environment will be received. Since it is assumed that several flyby missions to Jupiter and to the outer planets will be in progress simultaneously, a continuous sequence of data acquisition events will occur, punctuated by planetary encounter data, which are represented in the chart by blocks in darker shading. Periods of eight or nine years will elapse between the launch date of a Neptune flyby probe via Jupiter swingby and the reception of planetary data.

The diagram shows a major time interval for system development between the reception of first Jupiter data and the first launch of a Jupiter orbiter mission. As previously discussed this interval will be larger in program plan A associated with the Atlas/Centaur to Saturn IB/

Centaur transition than in the more gradual program plan B associated with the Titan/Centaur. Under most favorable circumstances the gradual evolution approach (plan B) aiming at a less complex final orbiter design can gain several years in the achievement of the second generation missions compared to program A.

It is anticipated that orbiter missions to Jupiter will be under way before data from the flyby missions to the more distant planets have been returned. Thus, in either program plan A or B any unforeseen engineering and science data relating to the interplanetary and planetary environment will be reflected in subsequent orbiter designs. In accordance with typical schedule dates presented in the diagram, the completion of the flyby operations will occur 10 to 15 years after inception of the program, whereas orbiter missions can be expected to be performed for at least another 10 years. In the light of these extremely long-term developments the potential gain of a few years which may be achieved by the less ambitious program plan B is not considered as decisive. The flexibility of program plan A resulting from the greater performance margin available in the Saturn IB/Centaur promises to be better suited for coping with the uncertainties of program development and with unforeseen environmental findings.

An alternate program plan is conceivable which starts with the simplest spacecraft configuration and lowest payload weight as in plan A but adopts the less ambitious program objectives achievable with the augmented Titan/Centaur as in plan B is such a decision appears most appropriate when the first planetary flyby data are evaluated.

9. ALTERNATE SPACECRAFT CONFIGURATIONS

This section presents the drawings for a number of alternate configurations which were studied in the process of developing recommended ones. These are briefly described here and their advantages and disadvantages reviewed.

Figure 113 shows a spin-stabilized Jupiter flyby spacecraft mounted on the SLV3X/Centaur/HEKS booster with a standard fairing. As can be seen, without a fairing extension the deployed RTG's are close to the spacecraft, requiring thermal shields and presenting considerable problems with respect to radiation interference with particle experiments. However, if a fairing extension of even 20 inches is used the RTG location is no longer a problem.

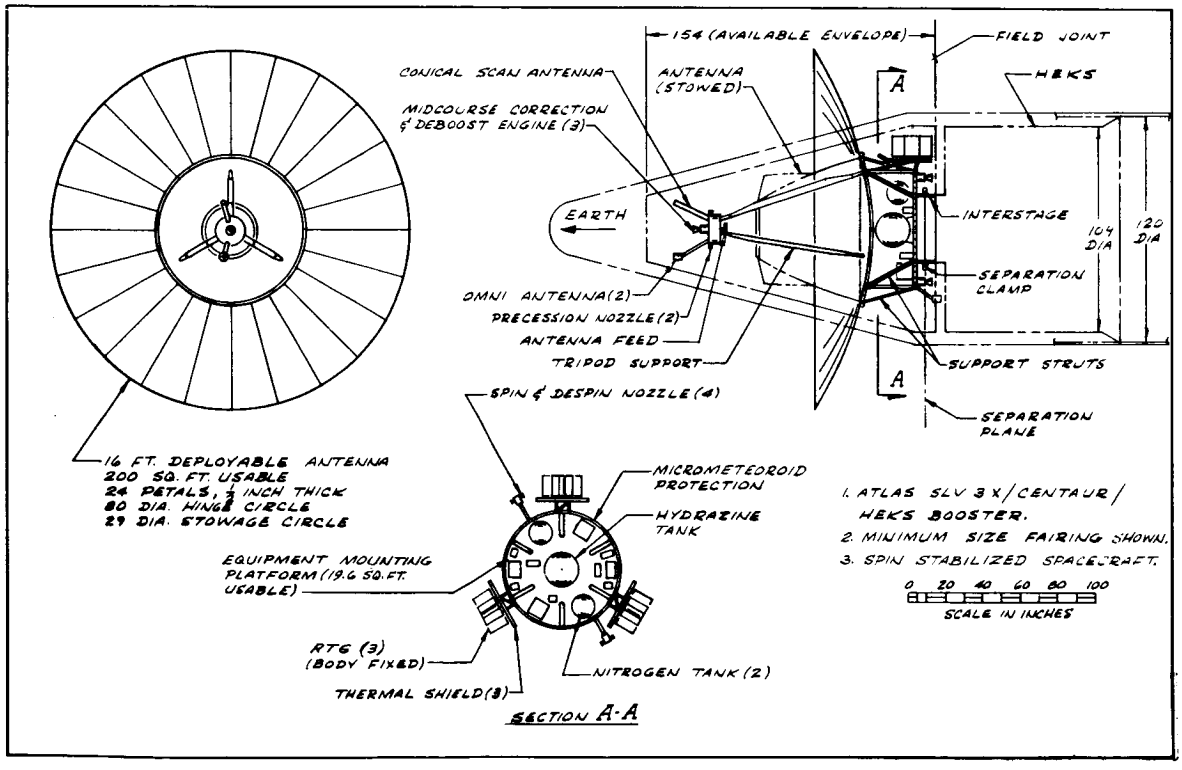

Figure 113. Inboard Profile - Jupiter Orbiter No. 2

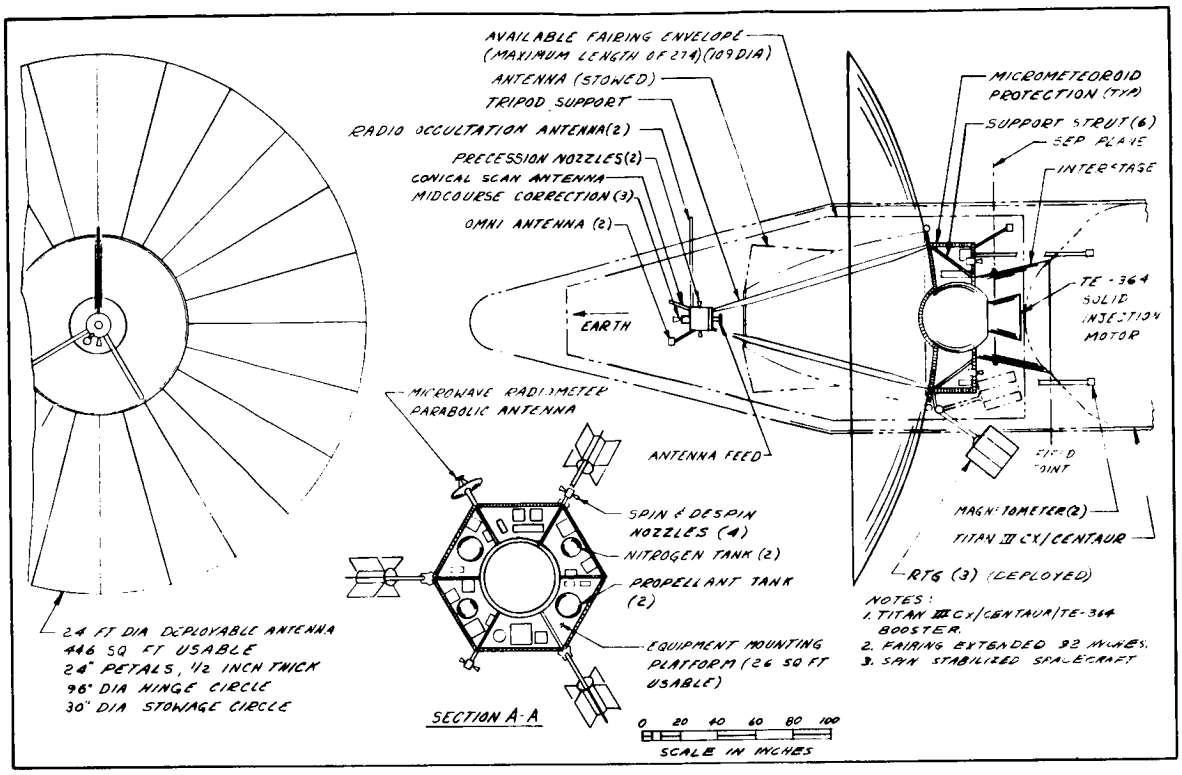

Figure 114. Inboard Profile - Jupiter Flyby No. 3

Figure 114 shows another spin-stabilized Jupiter flyby spacecraft mounted on the Titan IIICX/Centaur. This configuration has the TE-364 injection motor buried within the spacecraft structure. This arrangement permits considerable growth potential since it allows a central mounting structure either for capsules or for deboost propellant and engine for the orbiter. However, such a configuration is not compatible with the minimum weight precursor spacecraft and was there not recommended.

Figure 115 shows a 3-axis Jupiter flyby spacecraft mounted on the SLV3X/Centaur/HEKS booster. In this case the fairing has been extended 60 inches to permit the use of a 20-foot antenna and to deploy the RTG's well away from the spacecraft compartment. A large planetary scan platform is carried for accurate planetary observations.

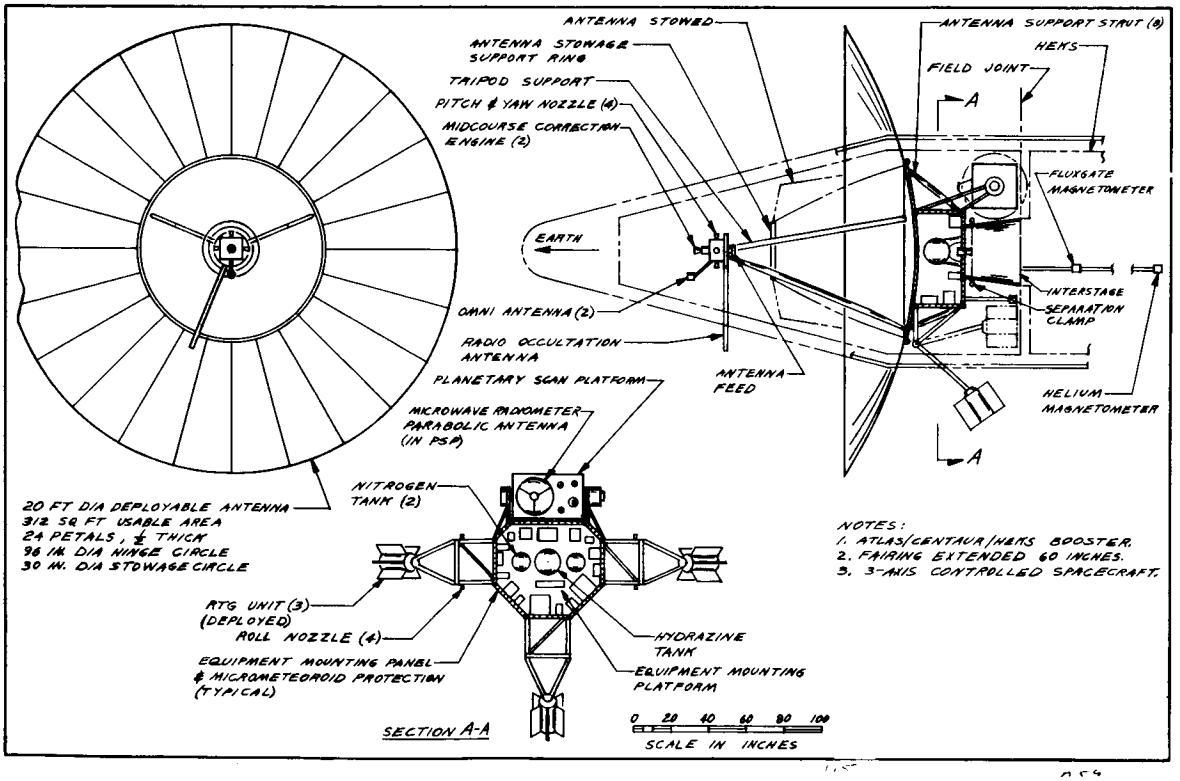

Figure 115. Inboard Profile - Jupiter Flyby No. 4

Figure 116 shows still another version of the spin-stabilized Jupiter flyby spacecraft using the SLV3X/Centaur/TE-364 booster. This configuration is much like the recommended one, except that there is less free space in the main compartment because the propellant and nitrogen tanks are not integrated with the top of the compartment.

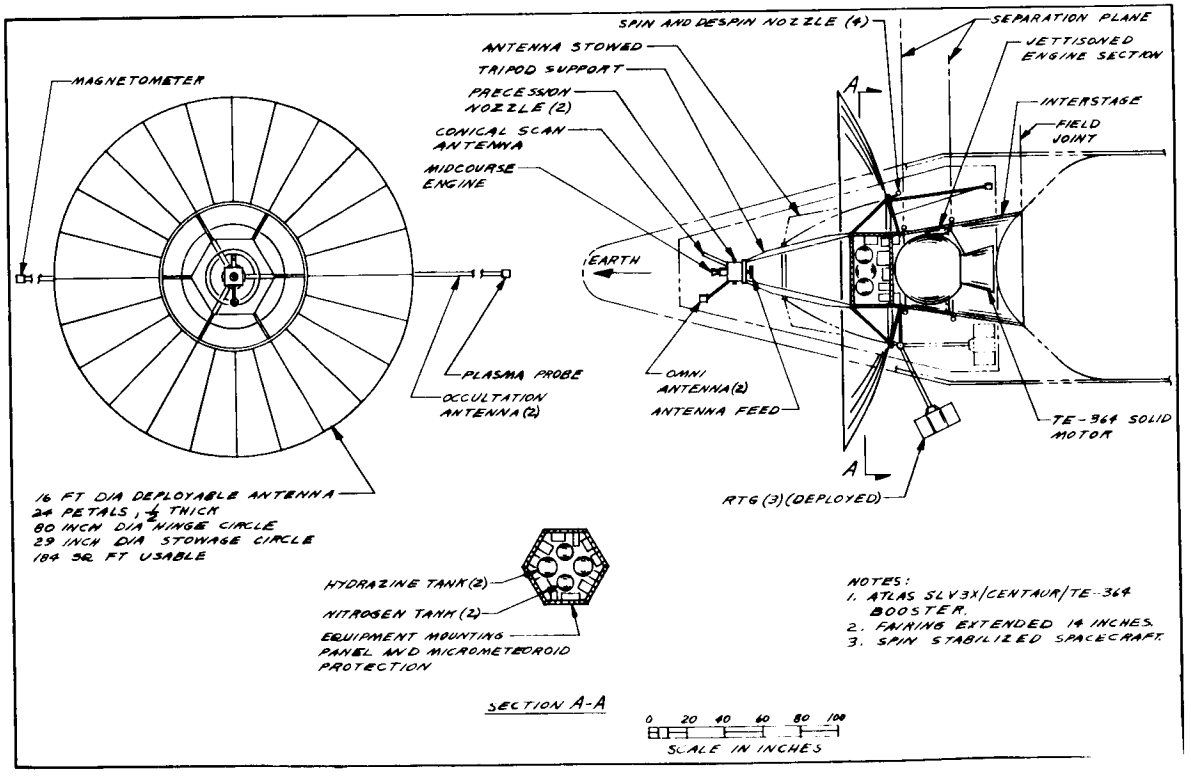

Figure 116. Inboard Profile - Jupiter Flyby No. 5

Figure 117 shows a spacecraft configuration using a cassegrain antenna configuration. The advantage of this approach is that the feed can be made a part of the main compartment, thus minimizing line losses.

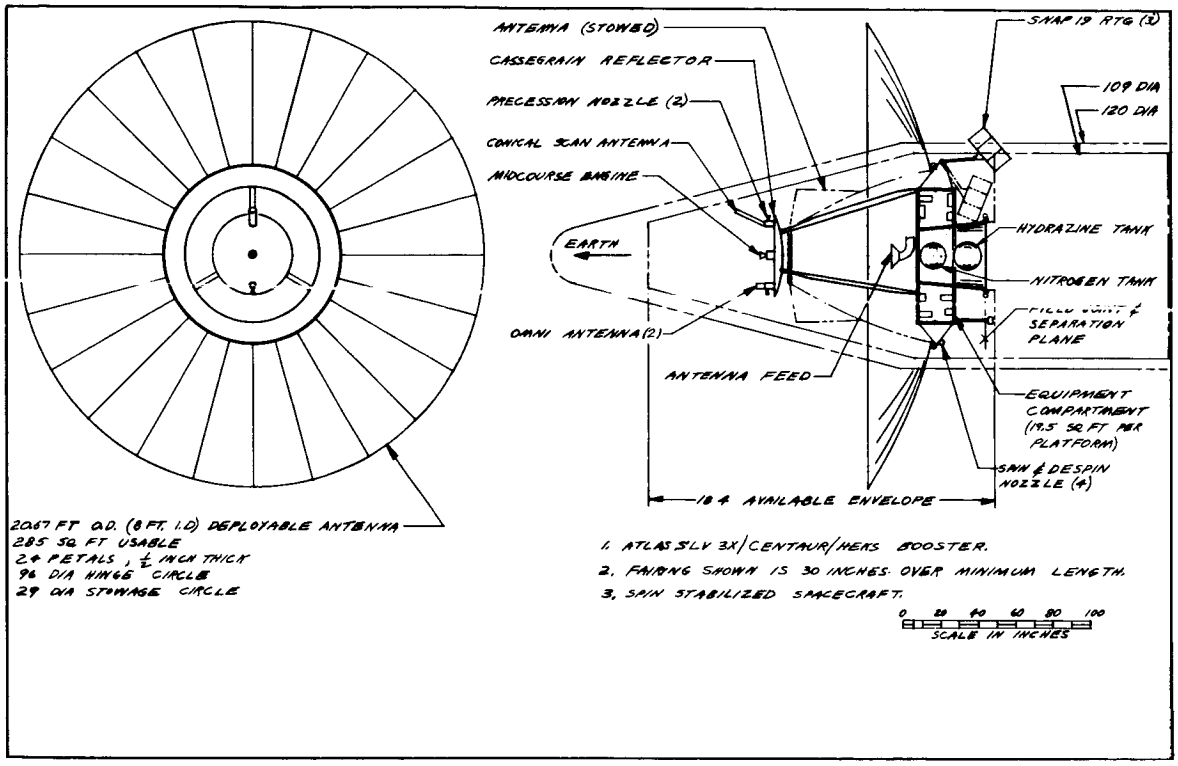

Figure 117. Inboard Profile - Saturn Flyby No. 1

Figure 118 shows a Jupiter orbiter configuration using the TE-364 motor as the deboost engine. The booster is the Titan IIIX/Centaur. The solid motor forms an integral part of the main compartment, and this configuration could be an excellent orbiter. However, the use of an existing solid for deboost means that the propellant weight is to a large extend fixed and flexibility of design is difficult. For this reason the liquid bipropellant system is recommended. Figure 119 shows the same configuration but mounted on the Saturn III/HEKS booster. This is essentially the same configuration recommended in the report but with the solid propellant deboost engine.

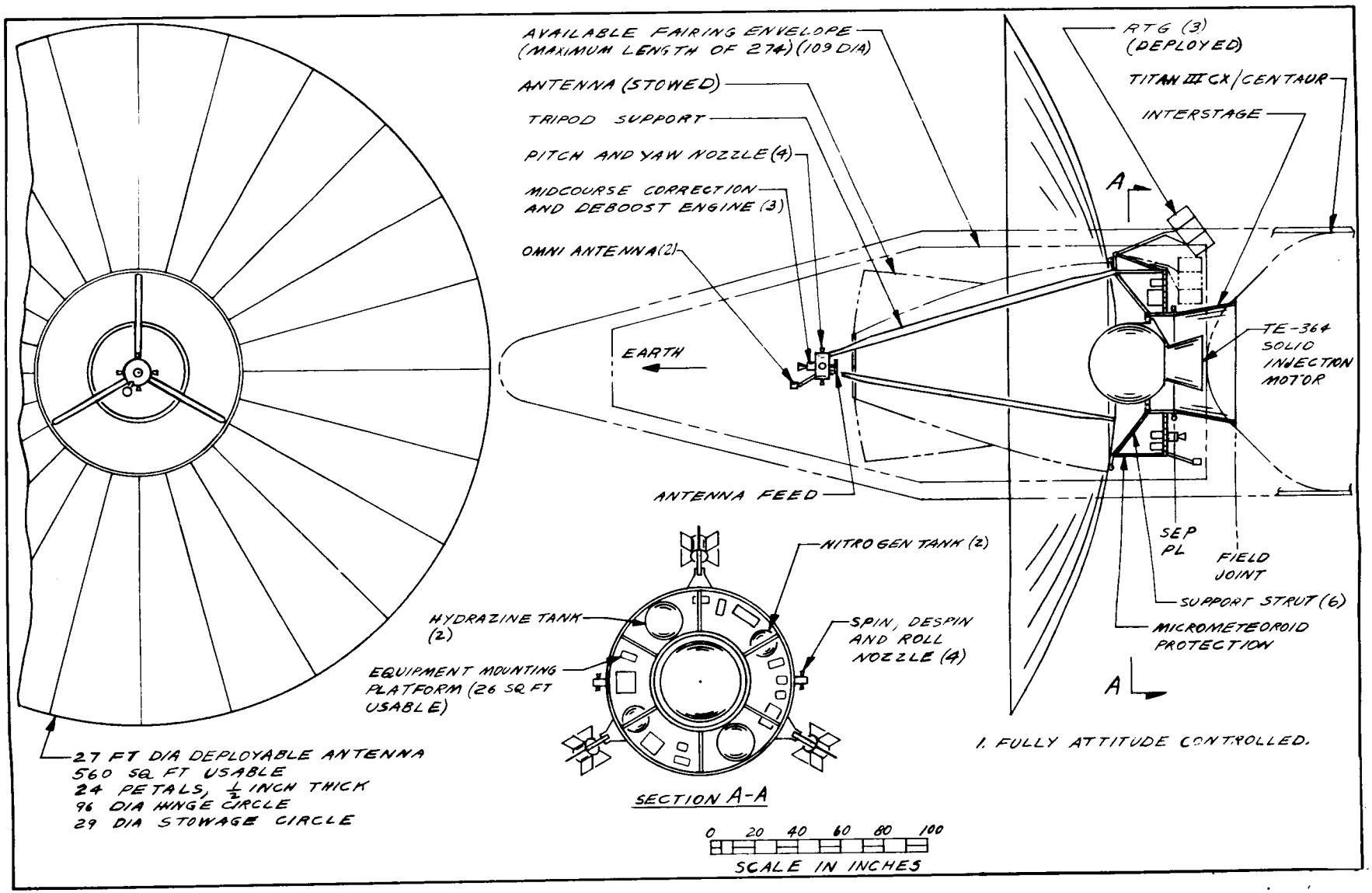

Figure 118. Inboard Profile - Jupiter Orbiter No. 1

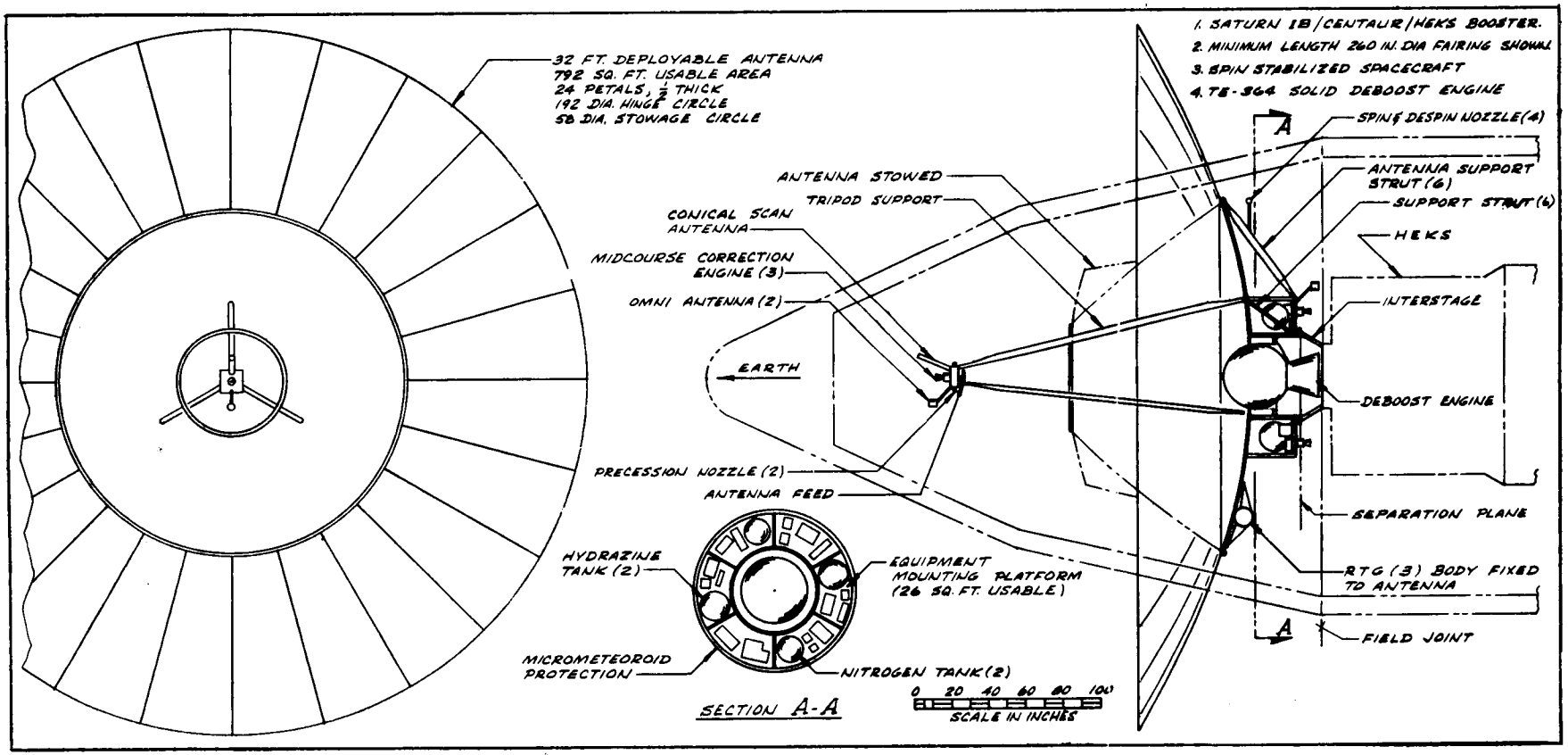

Figure 119. Inboard Profile - Jupiter Orbiter No. 3

Figure 120 shows another orbiter configuration mounted on the Saturn 1B/Centaur/HEKS booster. This configuration is again similar to the one recommended except that a hydrazine monopropellant deboost propulsion system is used. The effect of the monopropellant specific impulse of 230 seconds as compared with the bipropellant specific impulse of 300 seconds can readily be seen in the great propellant tank volume shown. For this reason, it was not recommended.

Figure 121 shows a Jupiter flyby spacecraft with a light-weight spherical capsule attached. Although such a configuration is entirely feasible, the merit of this type of capsule entry package appears dubious.

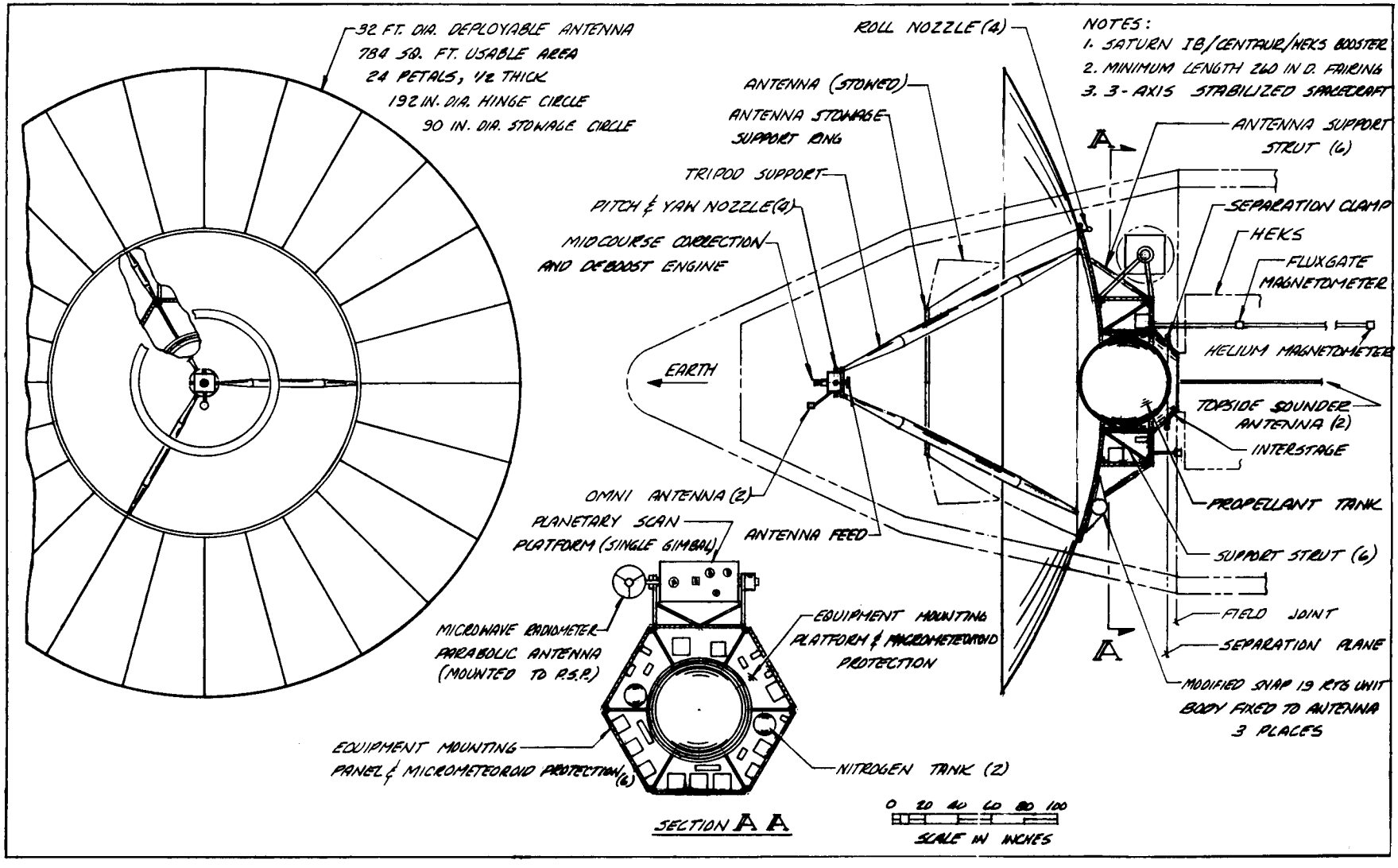

Figure 120. Inboard Profile - Jupiter Orbiter No. 4

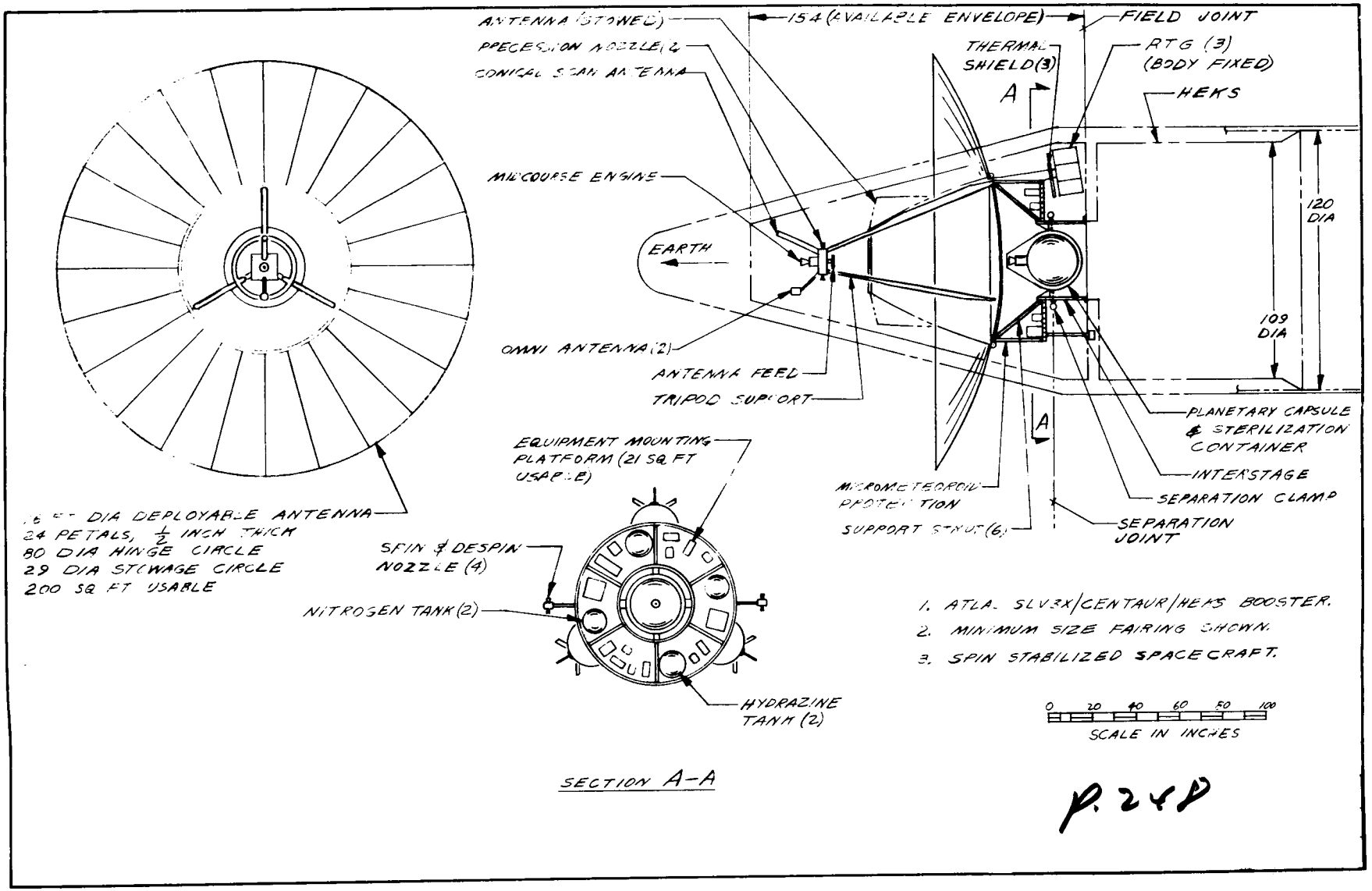

Figure 121. Inboard Profile - Jupiter Flyby, Planetary Capsule No. 1